University of Nottingham

Division of Regenerative Medicine and Cellular Therapies

Université catholique de Louvain, UCLouvain

Louvain Drug Research Institute

MODULATION OF MACROPHAGE PHENOTYPE FOR SPINAL CORD INJURY REPAIR

Natalija Tatić

Supervisors: Dr Lisa White, Prof Anne des Rieux

Co-supervisor: Prof Felicity Rose

2019

Abstract

Upon traumatic injury (SCI), spinal cord capacity for regeneration is limited and one of the main reasons may be the chronic inflammation. It can be then hypothesized that strategies aiming to resolve inflammation would contribute to spinal cord repair. Among different options to achieve that goal, mesenchymal stem cells (MSC) and ECM-based hydrogels have been both described as being immunomodulatory. The aim of this thesis then was to explore the potential of stem cells of dental apical papilla (SCAP) and extracellular matrix (ECM) hydrogels to mitigate SCI inflammation. SCAP had previously been shown to reduce tumour necrosis factor alpha (TNFα) gene (*Tnf*) expression *in vitro*, whilst ECM hydrogels had been shown to induce the M2-like phenotype in naïve monocytes. First, rheological properties of spinal cord and bone ECM hydrogels of 8mg/mL (S8 and B8) were measured. To increase S8 gelation rate and modulus fibrin was added to S8 pre-gel solutions at a 75/25 ratio (S/F). To investigate anti-inflammatory properties of hydrogels and SCAP, a mouse microglia cell line was used (BV2 cells). S8 solubilised, i.e. dispersed in medium before hydrogel formation is completed, reduced LPS-induced increase in inducible nitric oxide synthetase and arginase 1 gene expression ratio (*Nos2*/*Arg1*). Solubilised B8 reduced *Tnf* expression. SCAP reduced *Nos2*/*Arg1* ratio and *Tnf* expression. S8+SCAP reduced *Nos2*/*Arg1*, whilst B8+SCAP reduced *Nos2*/*Arg1* ratio and *Tnf* expression. To get a better understanding of how SCAP metabolism, free or incorporated in S8 ECM hydrogels, could be influenced by pro-inflammatory cytokines, a metabolomic analysis of cell supernatants was performed. SCAP stimulated with TNFα and interferon gamma (IFNγ) activated kynurenine pathway. Anti-inflammatory lipids were detected in scECM. SCAP+scECM had altered antioxidative amino acid and lipid profile. Still, in SCAP+scECM+stimuli the kynurenine pathway was enhanced and anti-inflammatory molecules were more abundant compared to stimulated SCAP alone. Thus, SCAP combined with ECM hydrogels may be considered as a strategy to mitigate SCI inflammation.

List of Presentations

The research done in this thesis was presented at seven national and seven international conferences:

1. NanoFar School, 30/10/2016 Nantes, France, oral presentation
2. Laboratory meeting, 06/11/2016, UCLouvain, Brussels, Belgium, oral presentation
3. NanoFar School, 24-28/04/2017, Nottingham, UK, poster presentation
4. 16th UK Society for Biomaterials (UKSB) annual conference, 20-21/06/2017, Loughborough, UK, oral presentation
5. Tissue Engineering and Regenerative Medicine International Symposium, European chapter (TERMIS-EU) 26-30/06/2017, Davos, Switzerland, oral presentation
6. School of Pharmacy Conference, 04/07/2017, University of Nottingham, Nottingham, UK, poster presentation
7. 17th Annual Meeting of the Tissue and Cell Engineering Society UK (TCES), 05-07/07/2017, Manchester, UK, oral presentation
8. Future Investigators of Regenerative Medicine (FIRM) Symposium, 25-28/09/2017, Platja d'aro, Costa Brava, Spain, oral presentation
9. Divisional research seminar, 14/12/2017, University of Nottingham, Nottingham, UK, oral presentation
10. School of Pharmacy Seminar, 16/05/2018, University of Nottingham, Nottingham, UK, oral presentation
11. NanoFar School, 11-15/06/2018, The University of Modena and Reggio Emilia (UNIMORE), Italy, oral presentation
12. 18th Annual Meeting of the Tissue and Cell Engineering Society UK (TCES), 2-4/7/2018, Keele, UK, oral presentation
13. The 29th Annual Meeting of the European Society for Biomaterials (ESB) 9-13/09/2018, Maastricht, Netherlands, oral presentation
14. 7th Nanofar School, 24-26/06/2019, Angers, France, oral presentation

Acknowledgements

This PhD would not be possible without my thesis supervisors, Dr Lisa White and Prof Anne des Rieux and their invaluable expertise. I have learned so much from them and from my co-supervisor, Prof Felicity Rose. Thank you for helping me focus my research, produce two publications and attend more conferences than I could have imagined. A special thank you is owed to Prof Dong-Hyun Kim and Dr Salah Abdelrazig for collaborating with us on the third chapter. I need to express my gratitude towards the NanoFar, Erasmus Mundus Joint Doctorate program funded by EACEA and the coordinator Prof Frank Boury for the opportunity to do PhD research at the University of Nottingham in UK and UCLouvain in Belgium. I am especially grateful to my evaluation committee, Prof Giulio Muccioli, Prof Françoise Van Bambeke and Prof Christine Dupont, my internal assessor Dr Frankie Rawson and my external assessor Dr James Phillips. I was lucky to have all their suggestions and constructive criticism. I am grateful for the kind-hearted help and support that all of my Regenerative Medicine and Cellular Therapies (RMCT), Advanced Drug Delivery and Biomaterials (ADDB) and NanoFar colleagues gave me. I greatly appreciate Bernard Ucakar and Kevin Vanvarenberg who were always willing to help me, often urgently and sometimes at 6am. Thanks to Teresa Marshall and Ann Williams for keeping the laboratories running. I have to thank Marion Toucheteau, Sandrine Wollanders, Murielle Callier and Anannya Chatterjee for their help with the overwhelming administrative tasks.

I am the most fortunate to have my brother Mihailo, who is always there to offer me the wisest council and make me laugh. I am immensely grateful for the untiring support that my mum and dad, Snezana and Bratislav, gave me. Finally, there are my friends, who now live all around the world, but care about me nevertheless and are always happy to distract me from work.

Foreword

This research was conducted in the field of spinal cord injury (SCI). SCI results in immobility and internal organ dysfunction and yet the standard treatment is still palliative. SCI creates a progressively deteriorating microenvironment sustained by chronic inflammation, unsuitable for regeneration and unsupportive of native or implanted cell viability. A biomaterial may shield the cells from implantation stress improving the viability and actively influence the microenvironment, whilst mesenchymal stem cells (MSC) have immunoregulatory and reparative properties.

MSC of dental apical papilla (SCAP) are accessible, expandable and have been shown to have immunoregulatory and neuro-reparative properties. Extracellular matrix (ECM) hydrogels have been shown to contain active biomolecules (growth factors, matricryptic peptides) and to promote constructive remodelling and immunoregulation in homologous and heterologous organs and species. Previous studies have shown that spinal cord ECM hydrogels (scECM) can stimulate neuronal marker expression in SCAP. However, little is known about their respective and combined anti-inflammatory properties or their interaction in the context of immunoregulation. Therefore, we hypothesised that MSC of dental apical papilla (SCAP) and scECM or bone derived extracellular matrix hydrogels (bECM) have potential to be used in the scope of SCI to mitigate the inflammatory microenvironment and hence to promote repair.

This thesis aims to: i) determine whether scECM and bECM have mechanical properties compatible with SCAP implantation to SCI and how they can be optimised, ii) determine SCAP, scECM and bECM influence on the activation of residential macrophages of the central nervous system (microglia) and whether this changes when SCAP are embedded in the hydrogels, and iii) explore SCAP-ECM hydrogel interactions and elucidate the impact of pro-inflammatory environment upon SCAP potential for immunoregulation in the presence and absence of ECM hydrogel.

List of Acronyms

5-HETE	5-hydroxyeicosatetraenoic acid
AD-MSC	adipose tissue-derived mesenchymal stem cells
ApC	antigen presenting cell
Arg1	arginase 1 gene (murine)
ASTM	American Society for Testing and Materials
ATP	adenosine triphosphate
ATPase	enzyme that catalyses the hydrolysis of a phosphate bond in ATP
AXL	Axl receptor tyrosine kinase
bFGF	basic fibroblast growth factor (FGF 2)
BM-MSC	bone marrow- derived MSC
BMSC	bone marrow stromal cells
cAMP	cyclic adenosine monophosphate
CCL	chemokine (C-C motif) ligand
CD	cluster of differentiation
cGMP	cyclic guanosine monophosphate
CNPase	2′, 3′-cyclic nucleotide 3′-phosphodiesterase
CXCL	chemokine (C-X-C motif) ligand
DBM	demineralised bone matrix
DPSC	dental pulp stem cells
ECM	extracellular matrix
FDA	Food and Drug Administration
FGF	fibroblast growth factor
FIZZ1	resistin-like molecule alpha (Relm-alpha)
GC	granulocytes

GM-CSF	granulocyte-macrophage colony-stimulating factor
GR	glucocorticoid receptor
IC	immune complex
IDO	indoleamine 2,3-deoxygenase
IFNβ	interferon beta
IFNγ	interferon gamma
IL	Interleukin
IL-1ra	IL-1 receptor antagonist
iNOS	inducible nitric oxide synthetase
LC-MS	liquid chromatography-mass spectrometry
LIF	leukaemia inhibitory factor
LPS	bacteria lipopolysaccharide
MCP-1	monocyte chemoattractant protein 1
MERTK	Mer receptor tyrosine kinase
MGL-1	macrophage galactose-type lectin 1
MHC II	major histocompatibility complex II
MMP	matrix metalloproteinase
MSC	mesenchymal stem cells
Nos2	inducible nitric oxide synthetase gene (murine)
PPAR	peroxisome proliferator-activated receptor
RNA	ribonucleic acid
Rpl19	ribosomal protein L19 gene
RXR	retinoid X receptor
SCAP	stem cells of dental apical papilla
SCI	spinal cord injury
SD	standard deviation
SOCS	suppressor of cytokine signalling

SR	scavenger receptor
STRO-1	protein marker of mesenchymal stem cells
TGFβ	tumour/transforming growth factor β
TGF-βR	tumour/transforming growth factor β receptor
TGM 2	Transglutaminase 2
TLR	Toll-like receptor
Tnf	tumour necrosis factor alpha gene (murine)
TNFα	tumour necrosis factor alpha
UC-SC	umbilical cord derived stem cells
WJ-SC	Wharton's jelly stem cells
Ym1	chitinase-3-like protein-3 (Chi3l3)

Table of Contents

MODULATION OF MACROPHAGE PHENOTYPE FOR SPINAL CORD INJURY REPAIR 1

Abstract 2

List of Presentations 3

Acknowledgements 4

Foreword 5

List of Acronyms 6

Table of Contents 9

1 General Introduction 13

1.1 Spinal Cord Injury 14

1.1.1 Spinal Cord Injury Classifications 16

1.1.2 Inflammation and the Macrophage Phenotype in Normal Injury 20

1.1.3 Cellular Events and Immunopathology of Spinal Cord Injury 25

1.1.3.1 Generation of Inflammatory Stimuli- The Vicious Cycle 25

1.1.3.2 Phases of Cellular Response at Spinal Cord Lesion 27

1.1.3.3 Axonal Regrowth 29

1.1.4 Spinal Cord Injury Treatment 30

1.1.4.1 Spinal Cord Injury Pre-Clinical and Clinical Trials 31

1.2 Stem Cells of the Dental Apical Papilla (SCAP) 37

1.2.1 SCAP versus BM-MSC 40

1.2.2 SCAP versus DPSC 41

1.2.3 Impact of the Microenvironment on SCAP Secretome 43

1.2.4 Immunoregulatory Properties of SCAP 44

1.2.5 SCAP for Spinal Cord Injury 47

1.2.6 Strategies to Improve Stem Cell Efficacy for Spinal Cord Repair 48

1.3 Tissue- Derived Extracellular Matrix (ECM) Hydrogels 52

1.3.1 ECM Hydrogels 56

1.3.2 ECM Hydrogel Downstream Modifications 59

1.3.3 ECM Hydrogel Efficacy in Regeneration 61

1.3.4 ECM Hydrogel Immunoregulatory Properties 62

1.3.5 ECM Hydrogels for Spinal Cord Injury Repair 64

1.3.6 Spinal Cord and Bone Derived ECM Hydrogels 65

1.4 Aim of the Thesis 69

1.4.1 Global Hypothesis 69

1.4.2 Specific Aims and Objectives 69

1.5 References 72

2 Stem Cells from the Dental Apical Papilla in Extracellular Matrix Hydrogels Mitigate Inflammation of Microglial Cells 100

2.1 Preface 101

2.1.1 References 105

2.2 Abstract 109

2.3 Introduction 110

2.4 Materials and Methods 113

2.4.1 Chemicals and Reagents 113

2.4.2 Tissue Decellularization 113

2.4.3 Preparation of ECM Hydrogels 113

2.4.4 Mechanical Characterisation of ECM Hydrogels 114

2.4.5 SCAP Culture 115

2.4.6 SCAP Viability in ECM Hydrogel Combinations 115

2.4.7 ECM Hydrogels and SCAP Impact on LPS-Stimulated BV2 cells 116

2.4.7.1 BV2 Cell Culture 116

2.4.7.2 BV2 Stimulation and Treatment 116

2.4.7.3 TNFα Quantification 117

2.4.7.4 BV2 Gene Expression Analysis 117

2.4.8 Statistical Analysis 117

2.5 Results 118

2.5.1 Impact of ECM Origin, Concentration and Composition upon Mechanical Properties 118

2.5.2 Impact of SCAP Encapsulation in ECM Hydrogels upon LPS-Stimulated BV2 Cells 119

2.5.2.1 Impact of ECM Hydrogels upon LPS-Stimulated BV2 Cells 120

2.5.2.2 Impact of SCAP upon LPS-Stimulated BV2 Cells 122

2.5.2.3 Impact of SCAP encapsulated ECM hydrogels upon LPS-Stimulated BV2 Cells 123

2.6 Discussion 126

2.7 References 130

2.8 Supplementary Data 137

3 Interplay Between Stem Cells of the Apical Papilla (SCAP) and Spinal Cord-Derived Extracellular Matrix Hydrogel (scECM) in the Midst of Inflammation- a Metabolomics Approach 140

3.1 Preface 141

3.3.1 References 144

3.2 Abstract 145

3.3 Introduction 146

3.4 Materials and Methods 148

3.4.1 Materials and Reagents 148

3.4.2 Spinal Cord Decellularisation and Preparation of Solubilised Hydrogels 148

3.4.3 SCAP Culture 149

3.4.4 SCAP Stimulation 149

3.4.5 IDO Quantification 150

3.4.6 TGF-β1 and MCP-1 / CCL2 Quantification 150

3.4.7 Metabolites Extraction 150

3.4.8 LC-MS Analytical Methodologies 151

3.4.9 Data Processing and Statistical Analysis 151

3.5 Results and Discussion 154

3.5.1 Impact of the Stimulus on SCAP Metabolism 155

3.5.2 Molecular Profile of scECM 157

3.5.2.1 scECM Molecules Involvement in Immunoregulation 158

3.5.2.2 scECM Molecules Involvement in Spinal Cord Regeneration 159

3.5.3 Interplay between SCAP and scECM in Basal State 160

3.5.4 Interplay between SCAP and scECM in the Presence of the Stimulus 164

3.5.4.1 SCAP Response to the Stimulus in the Presence of scECM 164

3.5.4.2 SCAP Response to scECM in the Presence of the Stimulus 165

3.6 Conclusion 170

3.7 References 172

3.8 Supplementary Data 181

4 Discussion 202

4.1 Discussion 203

4.1.1 Hydrogel Mechanical Properties Seemed Suitable for SCAP Delivery in the Scope of SCI 203

4.1.1.1 Hydrogels Supported SCAP Viability 208

4.1.2 ECM hydrogels, SCAP and SCAP Incorporated in ECM Hydrogels Demonstrated LPS-Activation Mitigating Properties 210

4.1.3 SCAP - scECM Interaction Modified, Possibly Enhanced, the Potential Effects of SCAP and scECM Combination on "Th1 – like" Inflammation 216

4.2 Main Achievements of the Thesis 226

4.3 Thesis Limitations and Future Work 229

4.4 Conclusion 231

4.5 References 232

1 General Introduction

1.1 Spinal Cord Injury

The spinal cord is a part of the central nervous system, positioned inside of the vertebral column. It connects the peripheral nervous system to the brain and transfers sensory (tactile, thermoceptive, nociceptive) and motor (muscle movement) signals participating in voluntary control of the body movement and reflexes. The spinal cord is also a part of the autonomic nervous system that regulates the work of internal organs (smooth muscle and secretory cells) initiating “fight or flight” sympathetic and “rest and digest” parasympathetic responses (Figure 1.1).

SCI is mostly traumatic and a consequence of motor vehicle accidents, work, sport or leisure activity accidents, falls, violence or self-harm. It occurs in 250000-500000 new cases each year worldwide [1]. The incidence of SCI is similar in every part of the world but the cause, severity and life expectancy differ [2]. After the injury, neuronal pathways are partially or completely damaged causing the loss of sensation, paralysis (inability to move muscles) and organ malfunction to a various degree.

There is a correlation between the injury localisation along the spinal cord and the loss of function: if the nerves innervating specific body part connect to the spinal cord above the injury level, the body part will not suffer the loss of function (as a direct consequence of the injury) (Figure 1.2) [3]. Due to the damaged neuronal pathways, patients with SCI further suffer respiratory, cardiovascular, urinary and bowel complications, spasticity, osteoporosis and bone fractures, pain syndrome (nociceptive pain, neuropathic pain) and pressure ulcers which impact their psychology and social behaviour and increase the risk of mortality by 2-5 fold compared to general population [1], [4].

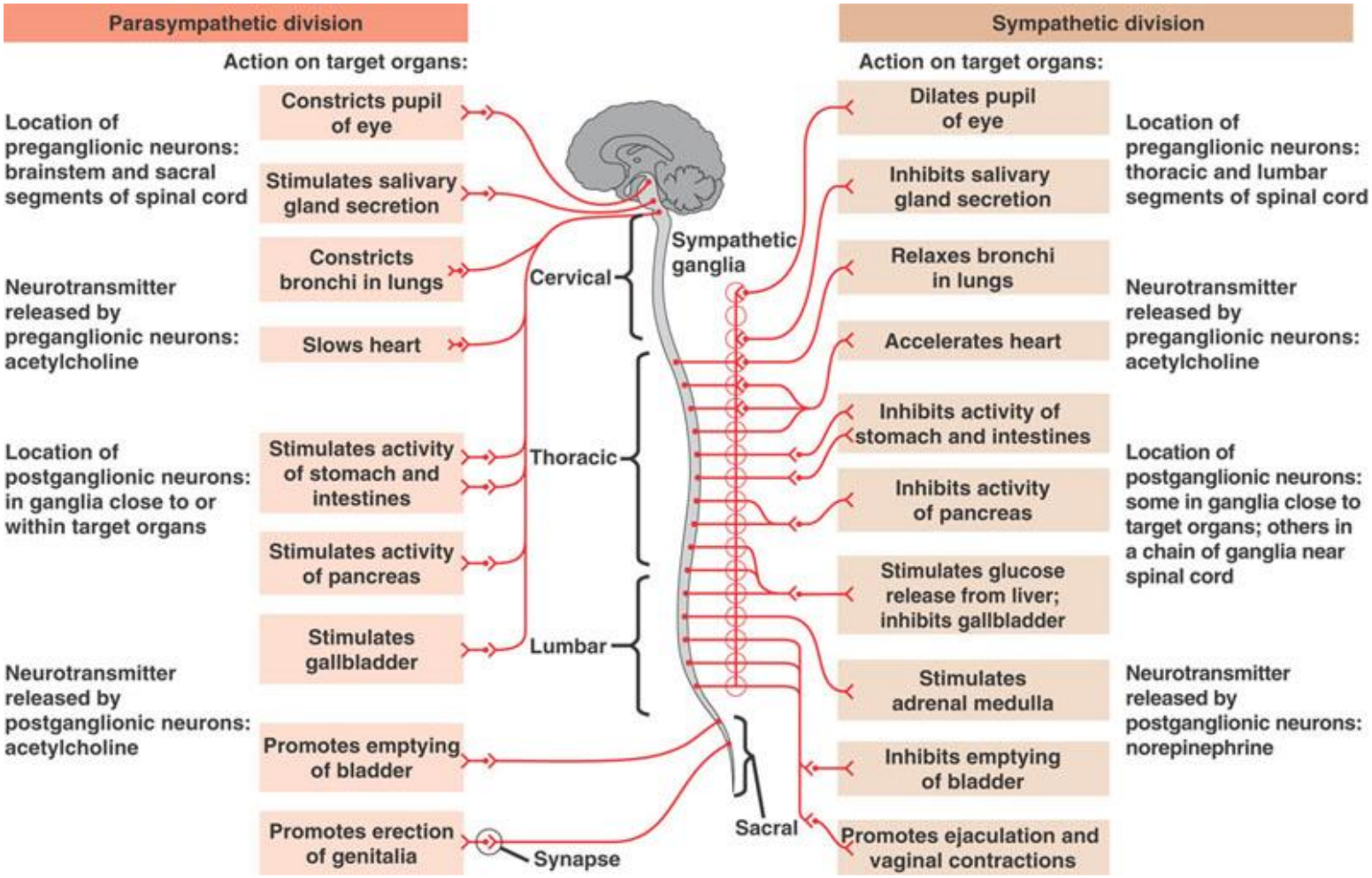


Figure 1.1 Division, location and function of autonomic nervous system (Reproduced from [5])

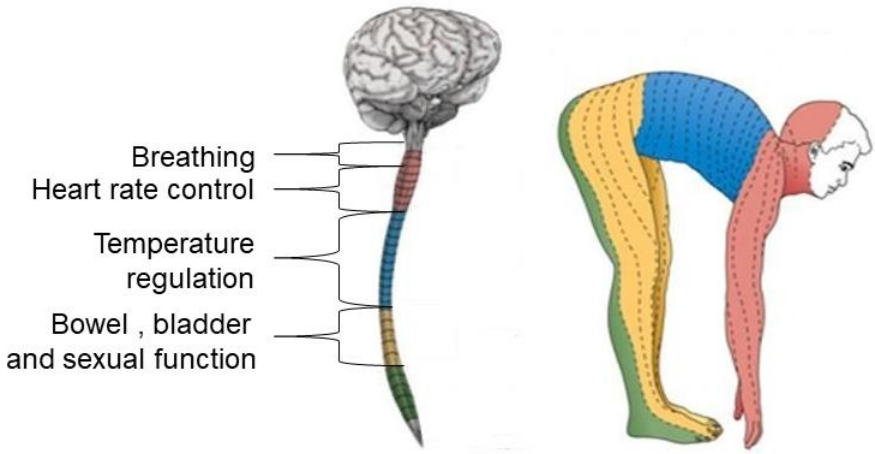


Figure 1.2 Spinal cord injury chart, simplified, shows connection between the injury level and the body parts likely to remain paralysed and desensitised (colour coded) and organs likely to suffer malfunction (Reproduced from [6])

1.1.1 Spinal Cord Injury Classifications

Traumatic SCI is classified in four categories, based on the post injury macroscopic structure: i) solid cord injury, the least common type, where the spinal cord still appears normal; ii) contusion/cavity, the most common type, associated with the areas of haemorrhage, expanding necrosis and cavitation, but with no disruption of the surface of the spinal cord; iii) laceration, which is a clear-cut disruption of the spinal cord; and iv) massive compression, where the spinal cord is mashed to varying degrees [7], [8]. Any of the four types cause progressive deterioration of neuronal function. The functional loss correlates to the intensity of changes within the zones of injury.

Individual SCI macro- and microscopy is not uniform. Therefore, SCI is divided in zones. Size and shape of the zones vary between patients. Zones expand over time and take up more and more tissue. Zonal distribution of injury (Figure 1.3) can be detected immunohistochemically as soon as four hours after the injury. Zone 1 is described as

the area of necrosis or cystic change. Zone 1 is surrounded by neutrophils and macrophages [9]. Zone 2 is associated with axonal injury, Wallerian degradation, neutrophils and activated microglia in the first one to three days post injury. Further axonal degradation, progressive gliosis and macrophages occur after day three. Zone 3 is characterised as macro- and microscopically intact zone. With time, zone 1 progressively expands into the zone 2 and zone 2 into the zone 3 [9].

Post injury pathophysiological response of the patients also changes with time and is therefore divided into phases. Phases are classified as acute, subacute and chronic (Figure 1.4). However immunological response does not follow the same distinctive pattern and timeline. On immunological level acute phase overlaps with acute and subacute physiological phases and subacute immunological response has elements of chronicity [8].

Damage to spinal cord can be classified as primary injury, that is neuronal damage as a consequence of mechanical trauma and secondary injury, that is a result of the following cascade of pathological events that further expands and progresses the primary injury (Figure 1.4).

Secondary events include: vascular damage (rupture of blood vessels and loss of blood brain barrier, haemorrhage, vasospasm, thrombosis, loss of autoregulation) that leads to oedema, ischemia and necrosis; free radical formation and lipid peroxidation that lead to cell death (by membrane peroxidation), loss of excitability and death of neurons by impairment of sodium/potassium ATPase and disruption of potassium, sodium and calcium ion (K^+, Na^+ and Ca^{2+}, respectively) ionic balance and increase of intracellular Ca^{2+}; apoptosis and inflammation [3] (Figure 1.4).

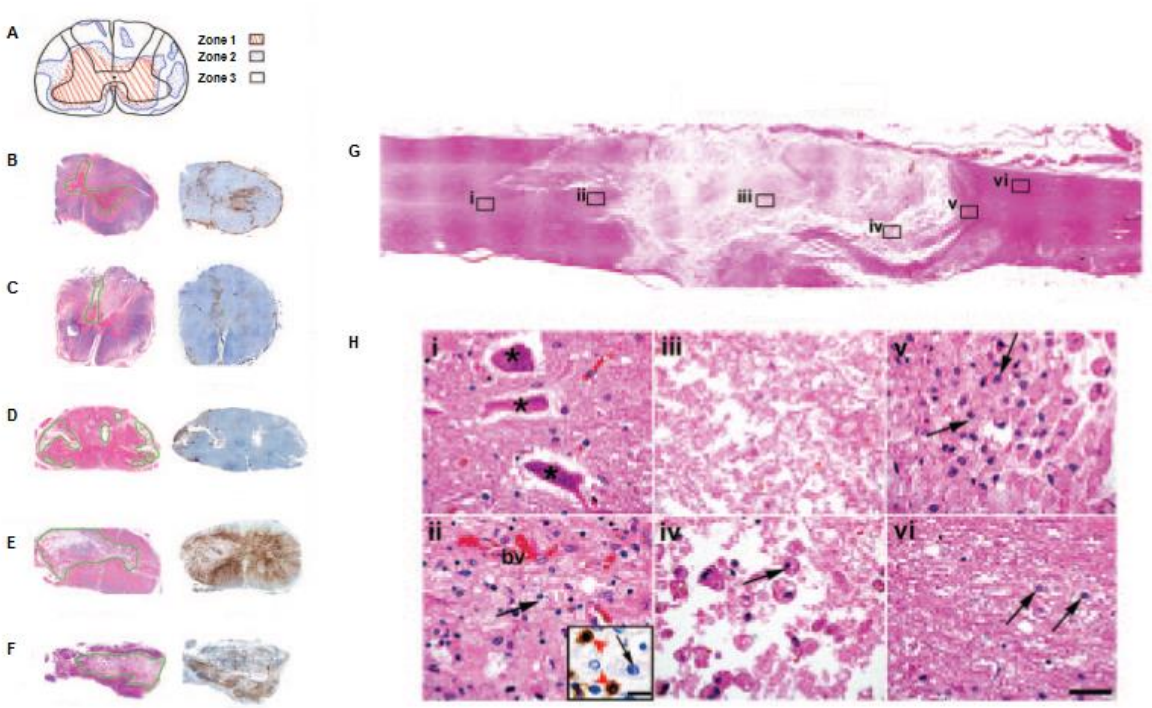


Figure 1.3 Zonal distribution of histopathological changes in human spinal cord after the injury A) A scheme of typical zonal distribution; B-F) Photomontages of spinal cord sections stained with haematoxylin-eosin to visualise zone 1 outlined with green (left column) and adjacent sections stained for defensin (B) and CD68 (C-F) to visualise neutrophils (B) and macrophages (C-F). Area of necrosis is pervaded with neutrophils/macrophages in less than 10 day surviving cases (B-C). Area of cystic cavity (zone 1) is surrounded by macrophages (zone 2) in longer surviving cases (weeks, months) (D-F). Zone 3 lay adjacent to zone 2. G) Longitudinal section of a human contusion injury stained with haematoxylin-eosin with different injury areas labelled i-vi. H) Photomicrographs of the labelled injury areas: i) Intact motor neurons (asterix) on the rostral side of the injury (zone 3); ii) Macrophages (arrows), $CD8^+$ cells, presumably lymphocytes (arrowheads) and intact blood vessels (bv) in zone 2; iii) lesion epicentre contains no intact cells (zone 1); iv) Caudal margin of the lesion is fragmented and contains macrophages (arrows) (zone 1); v) Abundant foamy (type 1) macrophages in zone 2; vi) mostly normal tissue with rare macrophages (arrows) (zone 2-3) (Reproduced from [9])

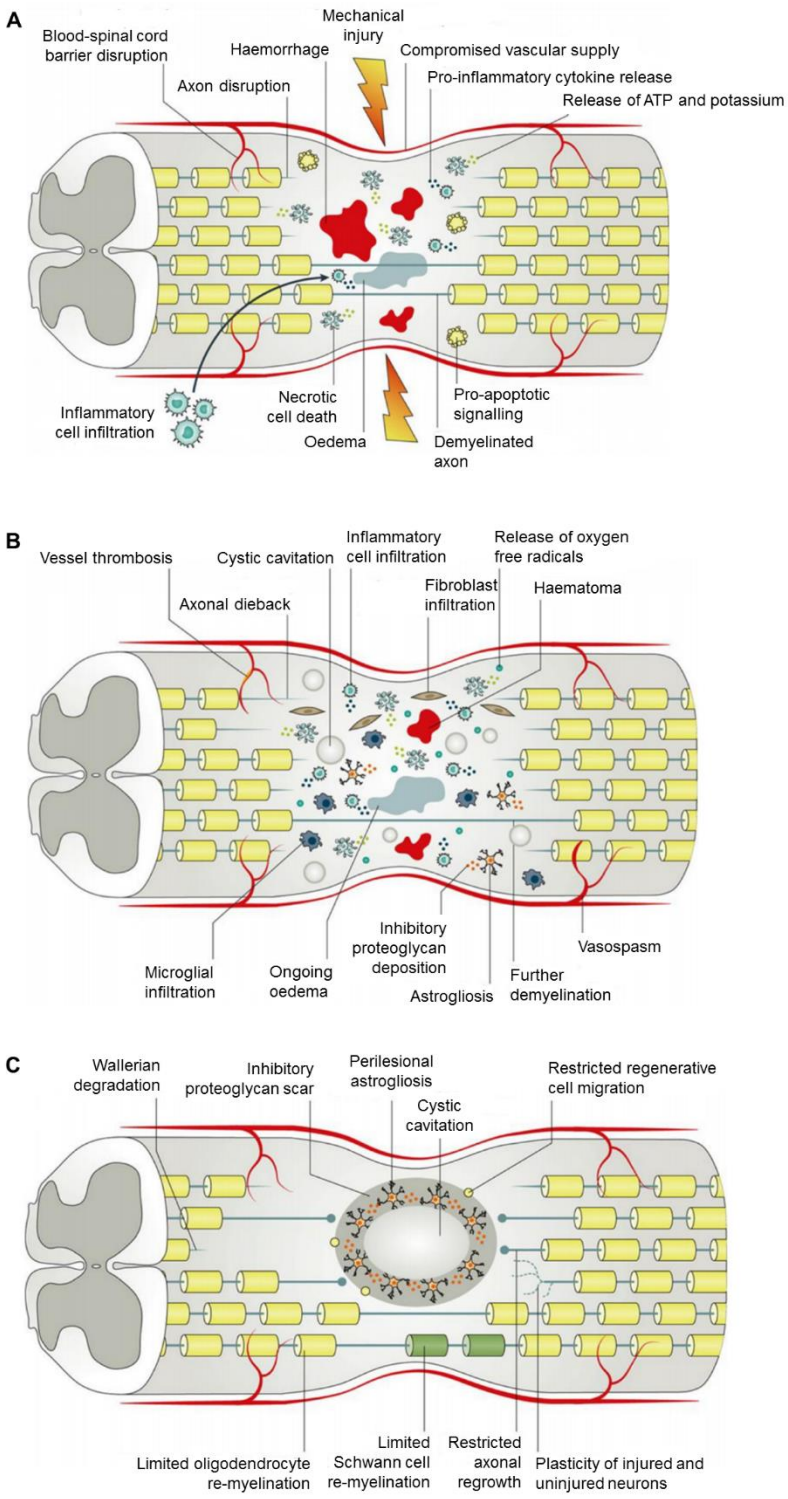


Figure 1.4 Phases of pathophysiological response to spinal cord injury A) Initial response, i.e. acute phase, 0-48h and the development of secondary injury; B) Subacute phase, 2-4 days and chronic inflammation; C) Chronic phase, 2 - 27 weeks, limited regeneration (Reproduced from [10], [11])

1.1.2 Inflammation and the Macrophage Phenotype in Normal Injury

Macrophage and other immune cell activation is different in every individual and depends on the injured tissue, age and general health of the individual and the severity of an injury [12], [13], but it can usually be separated in three phases [12] (Figure 1.5). The first, inflammatory phase, lasts for one to two days [12], [14]. It appears as a response to IFNγ, TNFα and LPS [15]. IFNγ and TNFα are secreted by the antigen-presenting cells (in damaged spinal cord these are astrocytes, microglia, vascular endothelial cells, dendritic cells, monocytes, polymorphonuclear cells, natural killer (NK)-cells and T-lymphocytes) upon encountering antigens from the damaged cells [16]. LPS may come from microorganism infiltration if the wound is open.

This initial phase is characterised by the pro-inflammatory macrophage phenotype (usually labelled as “M1”). Increased production of oxygen free radical species is typical for the phase. Representative secreted markers include pro-inflammatory cytokines interleukin (IL) - 12, IL-1β, TNFα, IL-6 and chemokine (C-C motif) ligand 2 (CCL2) or monocyte chemoattractant protein-1 (MCP-1) along with an upregulated enzyme, indoleamine 2,3-deoxygenase (IDO). Expressed markers of the pro-inflammatory phase are CD16, CD32, CD86 (or B7-2) and macrophage receptor with collagenous structure. Signalling pathways involve nuclear factor κB, signal transducer and activator of transcription 1, interferon regulatory factor 5, activator protein 1. Low IL-10 levels are also typical [17], [18].

During this first pro-inflammatory phase, “M1” macrophages are necessary. Their function is to remove the potential microorganisms and apoptotic cells, their parts and products, apoptotic cells, cellular debris and initiation of fibroblasts, platelets and endothelial cell healing response (Figure 1.6) [19]. Only when that function gets out of

hand and start creating more toxic products and involving healthy tissue, does it become destructive. In the inflammatory phase, a subtype of alternatively activated (other than with IFNγ, LPS and TNFα) macrophages, “M2”, with wound-healing phenotype, “M2a”, are present as well [12], [20].

“M2a” phenotype appears in response to IL-4 or IL-13, it is characterised by upregulated expression of liver arginase 1, mannose receptor CD206, triggering receptor expressed on myeloid cells 2, insulin-like growth factor 1, IL-1 receptor antagonist (IL-1ra) genes and signalling factors signal transducer and activator of transcription 6, Krüppel-like Factor 2, interferon regulatory factor 4, peroxisome proliferator-activated receptors (PPAR) [18], [20]. The function of the wound-healing M2a macrophages is inflammation mitigation, cell proliferation and migration, secretion of growth factors and removal of apoptotic cells [20].

In SCI, macrophages of the wound-healing phenotype stimulate re-myelination and axon regeneration [21]. In the early proliferative phase of immune response, macrophages secrete both pro-inflammatory and anti-inflammatory factors. This phenotype is referred to as immunoregulatory or “M2b”. It is a response to TLR or immune complexes activation, characterised by decrease in IL-12 and increase in IL-10 secretion, markers IL-6, vascular endothelial growth factor, insulin-like growth factor 1, TNF-α, CD86 and Fc receptor CD64. Immunoregulatory macrophages encourage cell maturation, tissue stabilization, angiogenesis and ECM synthesis [12], [14], [20].

As the level of IL-10 increases, macrophage phenotype changes to immunosuppressive, i.e. “M2c”. Immunosuppressive phenotype is characterised by tumour/transforming growth factor beta (TGF-β) and CD206, haemoglobin- haptoglobin scavenger receptor CD163, signalling lymphocytic activation molecule, sphingosine kinase 1,

thrombospondin 1, haem oxygenase 1 gene, signal transducer and activator of transcription 3 signalling and decreased levels of Arg-1. “M2c” macrophages promote the remodelling phase of the immune response, which function is inflammation resolution, tissue repair, growth factors and ECM synthesis (Figure 1.7) [12], [20]. In a matter of weeks, the wound heals and macrophage levels return to normal (Figure 1.5).

If a wound does not heal in three months it is considered chronic and has constant macrophage activation [12], [14]. Macrophage marker expression and cytokine secretion constantly changes in response to the environment, so that new macrophages continuously populate the wound and present macrophages die. Therefore, the tissue-specific macrophage phenotype cannot be so strictly defined and is said to be plastic. Inadequate macrophage activation leads to disrupted transition between the healing phases and to irregular immune response, which is the case after a SCI.

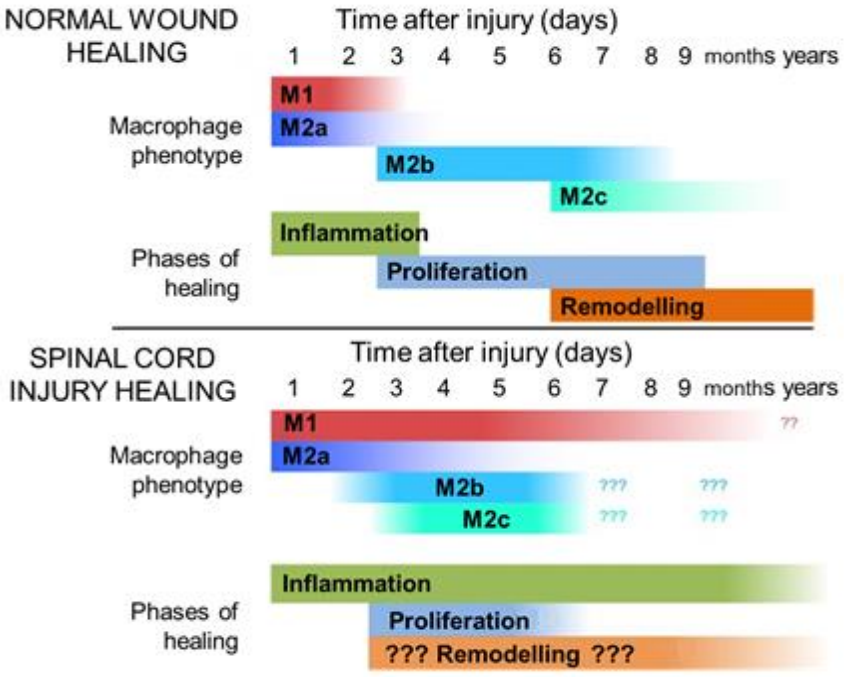


Figure 1.5 Immunopathology of spinal cord injury (Reproduced from [12])

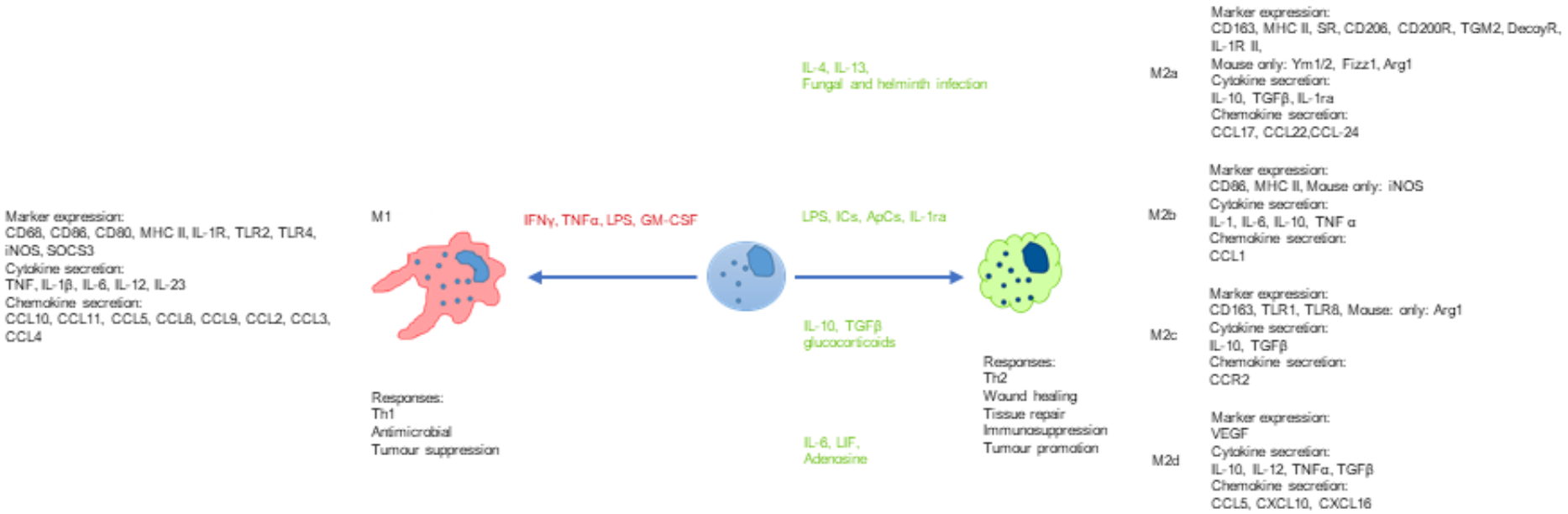


Figure 1.6 Representation of macrophage polarisation, i.e. monocyte differentiation into the two phenotypically distinct macrophage phenotypes, M1 and M2, upon encountering different stimuli. In case of tissue injury and repair, “M1” macrophages promoted inflammation and tissue destruction and “M2” macrophages promoted immunoregulation and regeneration. Abbreviations: ApC - antigen presenting cells, FIZZ1 - resistin-like molecule-alpha (Relm-alpha), GM-CSF - granulocyte-macrophage colony-stimulating factor, IC - immune complex, iNOS - inducible nitric oxide synthetase, LIF – leukaemia inhibitory factor, MHC II – major histocompatibility complex II, TGM2 - transglutaminase 2, TLR - Toll-like receptor, SOCS3 - suppressor of cytokine signalling 3, SR - scavenger receptor, Ym1 - chitinase-3-like protein-3 (Chi3l3) (Adapted from [19], [22])

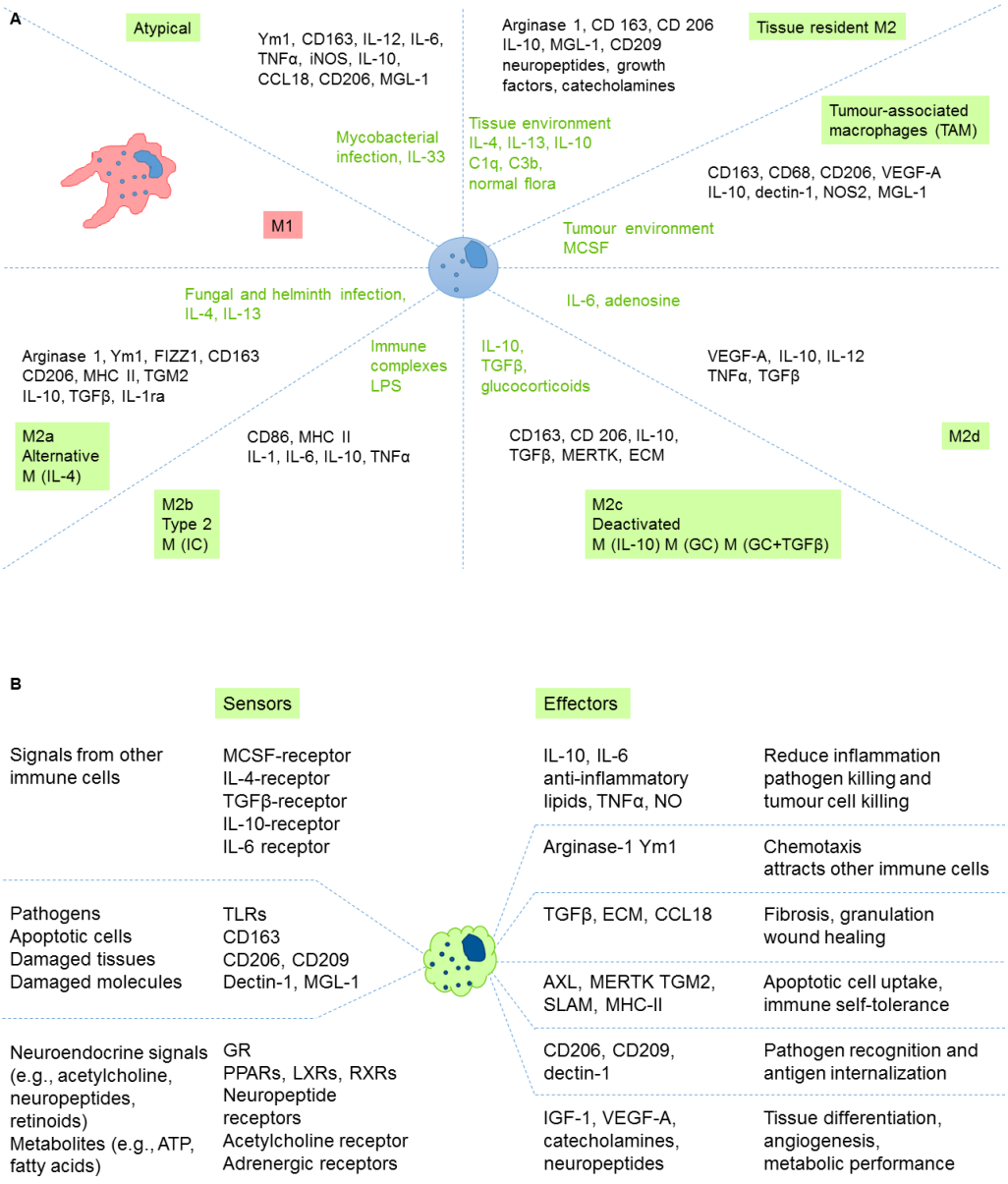


Figure 1.7 Detailed overview of “M2” macrophage activation and the diversity of A) the subpopulation phenotype (human and murine) and B) functional responses. Abbreviations: AXL- Axl receptor tyrosine kinase, GC – granulocytes, GR – glucocorticoid receptor, LXRs - liver X receptors, MCSF – macrophage colony stimulating factor, MERTK – Mer receptor tyrosine kinase, MGL-1 – macrophage galactose-type lectin 1, MHC II – major histocompatibility complex II, NO – nitrogen monoxide, RXRs - retinoid X receptors (Adapted from [20])

1.1.3 Cellular Events and Immunopathology of Spinal Cord Injury

1.1.3.1 Generation of Inflammatory Stimuli- The Vicious Cycle

Trauma to the spinal cord causes direct mechanical damage to the cells and cell death. Immune cells respond to endogenously derived damage associated signalling patterns, also known as alarmins, such as IL-1α, IL-33, high- mobility group protein box 1 (amphoterin), S100 class of proteins, nucleic acid derivates, mitochondrial deoxyribonucleic acid, ATP and uric acid. Alarmins are expressed within the cell and released into the interstitial space after the cell had been injured [23]. Microglia cells have been shown to be particularly sensitive to the increase of extracellular ATP (which leaks out of the damaged cell) [24]. Alarmins bind to the specific (e.g. IL-33 receptor) and pattern recognition receptors (e.g. nod-like receptors and interferon-inducible protein absent in melanoma 2 on the immune cells that respond early to the inflammation (microglia, astrocytes, neutrophils). Alarmins realize their effector functions (that is starting inflammation) directly, through the system of kinases and mostly nuclear factor κB, e.g. amphoterin stimulates release of chemokines from astrocytes [23]. But pattern recognition receptors can also be a part of a protein complex inflammasome, together with pro-caspase 1. After alarmins bind to the receptors, an active form of caspase-1 form within the protein complex and start a cascade of inflammatory reactions, such as proteolytic cleavage of pro-IL-1β into IL1β and pro-IL-18 into IL-18 [25] and natural killer cell activation, IFN-γ [26] and pro-IL-1α secretion [27].

Trauma also induces secondary cell death by causing the rupture of blood vessels (and damage of blood brain barrier) that leads to haemorrhage and ischemia. Low oxygen concentration triggers anaerobic metabolism leading to local metabolic acidosis that maximises vasodilatation, causing leakage of blood components and toxic products to

the injury site. Oedema increases interstitial pressure causing cell death and further ischemia. Thrombin, plasmin, fibrinogen and circulating antibodies leaking from the blood vessels also promote cellular activation, inflammation and scar formation. Hypoxia triggers wound healing at first, promoting endothelial and fibroblast proliferation and the excretion of immune and antigenic growth factors, but on a longer term leads to free radical generation, inflammation and cell death. Cellular debris are not cleared efficiently, providing persistent inflammatory signals [3], [7] (Figure 1.5).

Hypoxia also hinders adenosine triphosphate (ATP) synthesis which initiates cellular damage and promotes inflammation through mechanisms specific for ATP rich neural tissue. Depletion of ATP leads to dysfunction of sodium/potassium ATPase, enzymatic pump that maintains neuron polarisation. Without the enzyme function, passive ionic gradients prevail causing influx of Na^+ and Ca^{2+} ions and swelling of neurons which increases oedema and leads to cell rupture. Increase in intracellular Ca^{2+} concentration triggers release of excitatory amino acids from vesicles and the decrease in their reuptake. Their accumulation leads to additional depolarisation and neurotoxicity. Their binding to the specific receptors further increases intracellular Ca^{2+} triggering generation of free radicals, further depletion of ATP through activation of calcium-dependant ATPase, activation of phospholipase A2 that disrupts membrane phospholipids, modification of cytoskeleton, impairment of mitochondrial phosphorylation and further ATP depletion, activation of lytic enzymes (phosphatases, proteases, endonucleases) and axonal degradation. These mechanisms cause cell death and generation of inflammatory signals. In this vicious cycle insufficient neovascularisation increases hypoxia that causes more neuronal damage, promotes pro-inflammatory immune response and scaring [3], [8], [28].

These pathological events resemble a chronic wound state in which the inflammatory signals are constantly accumulating, residential and myeloid-derived cells (neutrophils, monocytes, lymphocytes) are actively responding and macrophages do not facilitate transition between the phases of immune response.

1.1.3.2 Phases of Cellular Response at Spinal Cord Lesion

Residential cells, such as microglia, astrocytes, oligodendrocytes, neurons and endothelial cells respond first to the injury. Microglia become activated within the first 0.5h and their protrusions meet in the initial attempt to isolate the injury. Further, microglia migrate to the lesion. Microglia and endothelial cells function as antigen-presenting cells and secrete pro-inflammatory cytokines and chemoattractants, such as IL-1α, IL-1β, IL-6, TNF-a, MCSF, and LIF 5h post injury. Local neurons express TNFα as soon as 0.5h post injury. Secretion of pro-inflammatory factors sharply declines to baseline in two days. Due to the high levels of pro-inflammatory cytokines at the lesion (and the disruption of the blood-brain barrier), around 12h post injury 90% of the infiltrating cells are neutrophils. Neutrophils are activated in the first 24h, after which their number sharply declined at day three, which is when monocytes migrate to the lesion. Activated microglia, neutrophils and macrophages have “M1-like” phenotype. After day one their number progressively increases and reaches the pick at 7-10 days post injury. In the meantime, neural/glial antigen 2 (chondroitin sulphate proteoglycan 4) positive oligodendrocyte progenitor/precursor cells and neural stem cells migrate to the injury site. Astrocytes swell osmotically and die or activate [8], [9], [12], [21], [29], [30].

The proliferative phase of inflammatory response starts 2-4 days post injury, peaks at day 5 and decreases after 10- 12 days. It is initiated by “M2a-like” cells secreting IL-4 and expressing CD206 (that can also be found in the pro-inflammatory phase) and

characterised by “M2b-like” immunoregulatory macrophages secreting IL-10 and tissue stabilisation.

Activated endothelial cells, ependymal cells, astrocytes, and fibroblasts proliferate trying to form an organised scar to stabilise the injury, protect intact parenchyma and restore blood brain barrier. This scar consists of deposed extracellular matrix, mostly collagen and chondroitin sulphate proteoglycans: aggrecan, brevican, neurocan, versican, phosphacan and neural/glial antigen 2) and semi-granulation tissue containing macrophages/microglia, astrocytes, capillaries, pericytes. The scar tissue represents a physical boundary for axonal growth and chondroitin sulphate proteoglycan bind to neural receptors blocking regeneration. Chondroitin sulphate proteoglycan may also inhibit axonal outgrowth as their structure and concentration gradient is similar to the molecules guiding central nervous system formation during development (the concentration gradient of those molecules makes a “mould” within which the central nervous system grows). Apart from secreting chondroitin sulphate proteoglycans, activated astrocytes in the pro-inflammatory lesion microenvironment (presence of activated microglia, IL-1α, TNFα and complement subcomponent C1q) lose their ability to promote synaptic formations and phagocytosis and start secreting neurotoxic molecules. Neural progenitors and glia proliferate and oligodendrocyte precursor cells differentiate trying to reduce Wallerian degeneration (progressive degeneration of axon distal to the injury) and axonal dieback (retrograde axonal degeneration) caused in the initial phases [7]–[9], [12], [21], [29], [31]–[34].

IL-10 in high concentrations stimulates transition to “M2c” phenotype and remodelling phase. However significant decrease in genes associated to IL-10 secreting, proliferative, “M2b” phenotype has been detected between three to seven days after SCI (from initiation until after the peak of proliferative phase) and IL-10 gene expression

decreased by day six, when it should peak at day 5 [14], [35]. The timeline in which different phases of immune response appear after SCI compared to the normal wound healing is presented in Figure 1.8.

Lymphocytes

While in rats both T and B lymphocytes are found at the spinal cord lesion 7 days post injury, followed by the second peak of TNFα and IL-1β, in humans only a few $CD8^+$ T lymphocyte could be detected extravascularly at the time. Only months after the injury $CD8^+$ T lymphocytes are detected in damaged regions randomly distributed among the macrophages. $CD4^+$ lymphocytes follow the similar pattern but are fewer [9], [12]. B-lymphocytes were not found at the lesion site even though they may be activated by the previously hidden endogenous antigens that leaked into the circulation or self-antigens in high concentration (higher than during negative selection) and memory B-lymphocytes may cross-react (poly-specificity/molecular mimicry) [36] and were shown to contribute to the SCI pathology in mice [37].

1.1.3.3 Axonal Regrowth

A few factors have been shown to make axonal regrowth difficult. One is a group of proteins released upon myelin damage (neurite outgrowth inhibitor, myelin-associated glycoprotein, oligodendrocyte myelin glycoprotein, the transmembrane semaphorin 4D and ephrin B3, released upon myelin damage), called myelin-associated inhibitors [38]. Activated astrocytes and the glial scar negatively influence axonal re-growth (as described in section 1.5.2). Progressive damage (described in section 1.5.1) may also make axonal regrowth difficult.

Anti-inflammatory cytokines are small proteins (5–20 kDa), such as IL-10, IL-13, TGFβ and LIF, that resolve classical, type-1 (as after SCI) and other types of immune responses [39]. These cytokines are secreted in immunoregulatory and immunosuppressive phases. Anti-inflammatory cytokines have been shown to promote axonal regrowth by regulating Ca^{2+} concentration, increasing the concentration of neurotrophic factors such as brain derived neurotrophic factor, nerve growth factor, neurotrophin 3 and 4, Rho-GTPases and cyclic nucleotides cAMP and cGMP and decreasing the concentration of fibrotic and glial scar components such as tenascin, fibronectin, myelin binding protein, myelin-associated glycoprotein and oligodendrocyte myelin glycoprotein [40], [41]. The connection between these pro-resolutive phases of immune response and axonal growth is also reflected by the immunological functions of neural growth regulators [40]. For instance, netrin-1 was shown to suppress leukocyte infiltration, cytokine and chemokine production after kidney or lung injury, nerve growth factor may induce angiogenesis, brain derived neurotrophic factor, nerve growth factor, neurotrophin 3 or 4 may increase eosinophils' viability, tenascin–C inhibits T-lymphocyte migration and fibronectin was shown to increase endocytic ability of dendritic cells [40].

However, the pro-resolutive phases that stimulate remodelling, neuronal outgrowth and re-myelination do not seem to occur after the SCI. Instead, predominant pro-inflammatory macrophage phenotype causes neurotoxicity [42] and orchestrates constantly progressing inflammation that deteriorates the tissue, preventing regeneration.

1.1.4 Spinal Cord Injury Treatment

Current SCI treatments reduce the symptoms and control secondary damage. Rather than having a specialised treatment, a cocktail of drugs registered for other indications

is administered (Table 1.1). Surgery is required to stabilise the spinal column and prevent future deformities, remove fragments of bone and foreign objects from the lesion and remove/fix anything that is compressing the spinal cord, e.g. broken vertebra. Surgeries that happened early after the injury are related to better outcomes in patients. Specific medications are used for chronic pain and depression and systemic complications such as heart conditions, orthostatic hypotension and autonomic hyperreflexia, urinary tract infections, urinary incontinence, bowel incontinence, swelling of the extremities, thrombosis, pressure sores, pneumonia, muscle spasms and the improvement of sexual function [43].

1.1.4.1 Spinal Cord Injury Pre-Clinical and Clinical Trials

SCI pre-clinical trials are mainly focused on cell-biomaterial strategies and drugs/growth factors with controlled release. Cells have been delivered locally, with the support of biomaterials to enhance their viability. For instance, poly(lactic-co-glycolic acid) alginate and fibrin scaffolds, chitosan-based channels coated with laminin and gellan gum modified with GRGDS (Glycine-Arginine-Glycine-Aspartate-Serine) peptide have been shown to increase survival of transplanted neural stem cells [48]. Local administration of individual cell types, for instance dental [49], [50] or neural stem cells [51], neural precursor cells [52], non-neural cell types such as glial cells, olfactory ensheathing cells, Schwann cells and fibroblasts of different origin [53] have had notable success, as well as simultaneous transplantation of multiple cell types, e.g. oligodendrocytes and motoneuron progenitors [54] or simultaneous local and intravenous administration of MSC [55].

Systemic administration of some individual biomolecules such as anti-CD20 antibody for depletion of B lymphocytes and anti-CXCL10 antibody to reduce T lymphocyte infiltration

seemed to have had more success compared to others such as IL-4, immunoglobulin G and fingolimod (targets sphingosine 1-phosphate receptor) [56]–[58]. Still, the therapeutic potential as well as the engineering challenge appeared to be lying in the more rounded approach of multiple growth factor delivery, especially if their release is continuous, or matched with the timeline of immunopathological events [59]. The growth factor combinations often contained epidermal growth factor and bFGF (basic fibroblast growth factor) as they have been shown to promote functional recovery after SCI in humans [60]. The timed release was achieved using the minipump technology or combining various macroparticles and hydrogels for encapsulation [61]–[64]. Drugs and growth factors incorporated in the supportive biomaterials, such as glial-derived neurotrophic factor-loaded alginate, vascular endothelial growth factor -loaded fibrin, different sizes of Chicago sky blue-loaded liposomes and neurotrophin-3-loaded polymeric nanoparticles incorporated in hyaluronan/methyl cellulose hydrogel had improved local retention, reduced degradation and prolonged release [65]–[68].

Biomaterials in pre-clinical trials had specifically designed formation and degradation rate to best support cell and growth factor delivery and effectiveness. Mechanical properties, topography and porosity can also be altered to influence cell migration, immune response and axonal regrowth [69]–[73]. Some of the tested biomaterials, for instance functionalised with laminin or derived from decelularised tissue had intrinsic bioactivity [74]–[77].

However, lasers [78], gene/enzyme/receptor/growth factor blocking [58], [79], [80], nanovectors [81], [82], exosomes [83], [84], inflammasomes [58] and tissue grafts [35], [85] have also had measurable success in pre-clinical trials, mostly on rat models. Due to the complexity of the problem, plenty of scientists in the field of SCI repair now

advocate a multifaceted approach [86]–[88] and only a few strategies progressed to the clinical trials.

Clinical trials are commonly categorised as neuroprotective and neuro-reparative, according to their action [44]. According to the type of intervention, they mostly fall under one of the following categories:

- Systemic [89] and local administration of drugs [90] and growth factors [91],
- Rehabilitation/physiotherapy [92],
- Assistive devices [93], [94],
- Neural bypasses [95] and
- Cellular therapies.

Drugs such as riluzole, minocycline and cethrin improved motor score in patients with cervical SCI and granulocyte colony stimulation factor in all patients, by limiting excitotoxicity, reducing inflammation, inhibiting axonal dieback and promoting angio- and neurogenesis, respectively. Anti- neurite outgrowth inhibitor A antibody showed no adverse effects and promoted neural sprouting, but had no influence on pain or mobility [96]. Short-term bFGF therapy did not have significant short-term effect [97], but it caused functional improvement after 2-4 years [60]. Gacyclidine and GM-Ganglioside showed no significant effects in clinical trials [97]. Phase I/II glibenclamide and hepatocyte growth factor clinical trials are ongoing [10].

Rehabilitation therapies, such as motor and sensory trainings are known to contribute to locomotor improvement in combination with other treatments [98], however virtual patient engagement in, for example, sailing simulator is a currently being tested in clinical trial [99]. Currently recruiting clinical trials for assistive devices are evaluating various neuroprostetic systems [100] and robotic exoskeletons [94]. Prosthetics with

brain-machine interface [101] and a microelectrode array brain implant that may bridge the SCI and restore motoric [95] are being tested as a proof of concept.

Cellular therapies represent a strategy to deliver multiple growth factors, nanovesicles and metabolites through paracrine signalling to regenerate the microenvironment. The cells are autologously derived or taken from an allogenic or engineered phenotype (e.g. iPSC-derived) stock. Treatment designs depend on the cell type, time and route of delivery (e.g. intravenous, intrathecal, intraparenchymal) [10]. Cell types studied in phase I/II clinical trials are Schwann cells [102], olfactory ensheathing cells [103], oligodendrocyte progenitor cells [104], macrophages [105], neural stem cells [106], bone marrow mesenchymal stem cells (BM-MSC) [107], adipose-tissue derived mesenchymal stem cells (AD-MSC) [108] and UC-SC [109].

Cellular therapies were shown to be safe [107]. However, only oligodendrocyte progenitor cells seem to be notably effective in only few patients. Oligodendrocyte progenitor cells are hypothesised to produce myelin and restore conductivity after the SCI in humans. The success may have occurred due to the clinical trial exclusion criteria. The study accepted only “clean” injuries occurring due to penetrating trauma, traumatic anatomical transection or laceration and excluded “messy” or “rough” SCI, which increased the possibility of recovery. Another reason for the notable success may be administration of the immunosuppressive therapy at the subacute phase of the injury. Due to the inter-individual differences in the strength and tendencies of immune response, in some cases inflammation was decreased enough to allow repair [104].

Only one phase I/II clinical trial studied the transplantation of cells and scaffold combination. NeuroRegen™ scaffold, derived from decelularised bovine aponeurosis and UC-SC evoked changes of sensation level, motor function or marker expression in

seven out of eight patients [110]. Only one phase I clinical trial studies the safety of collagen scaffold in acute SCI and the results are not yet available [111].

Less than 10% of SCI clinical trials study cellular therapy, out of which 92.5% involve stem cells. Only three clinical trials of cellular therapy progressed to the phase III (expanded studies of safety and effectiveness) and all three involve MSC. The first investigated effectiveness of UC-SC versus rehabilitation therapy and the results were not accessible. The second is recruiting and the third is not yet recruiting, to investigate safety/efficacy of autologous BM-MSC and neural stem cells, respectively [112].

Success of cellular therapies for SCI is limited [87], presumably as over 90% of the injected cells die or migrate away [113]. Multiple factors may contribute to the cell retention upon transplantation. For instance, the stress that cells suffer during the preparation and injection (e.g. shear stress) [114]. Cell survival and retention at the lesion may also be affected by the time of injection, number of injected cells, variations between injury types and between patients. However, these factors limit the effectiveness of cellular therapies in general and in most cases they have been overcome [115]. Typical for SCI and therefore the probable main reason for the high cell death and low retention at the lesion is deteriorating lesion microenvironment [116]. More specifically, the microenvironment that has high concentrations of toxic products of the chronic inflammation, enhanced free radical synthesis and phagocytotic activity, ionic imbalance, the necrotic/cystic cavity that does not provide ligands for cellular attachment and other factors explained in section 1.1.5.

Table 1.1 Pharmacotherapy of acute spinal cord injury and mechanisms of action [43]–[45]

Methylprednisolone*	Inhibits lipid peroxidation, has anti-oxidative and anti-inflammatory properties, decreases ischemia, supports energy metabolism, inhibits neurofilament degradation, decreases intracellular Ca^{2+}, decreases prostaglandin F, increases spinal neuron excitability, decreases oedema
Ganglioside GM-1	Stimulates neurite regrowth/regeneration
Opioid receptor antagonists	Antagonize the increase in endogenous opioid levels; opioid receptor activation can contribute to excitotoxicity
Thyrotropin-releasing hormone and its analogues	Reduce excitotoxicity by antagonizing endogenous opioids and excitatory amino acids; reduce inflammation by antagonising platelet-activating factor and peptido-leukotrienes
Nimodipine	Decreases intracellular Ca^{2+} accumulation to preserve neuronal viability and prevent release of excitotoxic amino acids; modulates ischemic damage by attenuating vasospasm
Gacyclidine	Antagonises glutamate receptors to prevent excitotoxicity
Magnesium	Reduces Mg^{2+} depletion, diminishes intracellular Ca^{2+} accumulation and blocks N-methyl-D-aspartate receptor ion channel which reduces neuronal damage (neural membrane disruption and excitotoxicity); modulates binding of endogenous opioids which reduces excitotoxicity
Hypothermia	Reduces extracellular glutamate (which reduces excitotoxicity), vasogenic oedema (which reduces ischemia, cell death and cystic formation), apoptosis, neutrophil and macrophage invasion and activation and oxidative stress
Minocycline	Inhibits microglial activation and cytochrome c release (indicates mitochondrial and cellular damage)
Erythropoietin	Reduced apoptosis and lipid peroxidation
Oestrogen	Increases expression of the anti-apoptotic factor bcl-2
Progesterone	Reduces inflammation by reducing the production of inflammatory cytokines
Cyclooxygenase inhibitors	Reduces inflammation by antagonising effects of arachidonic acid metabolites, e.g. decreased blood flow and platelet aggregation
Riluzole	Reduces excitotoxicity by blocking voltage-sensitive Na^{+} channels and antagonising presynaptic Ca^{2+}-dependent glutamate release
Atorvastatin	Prevents neuronal and oligodendrocyte apoptosis
Antioxidants	Antagonize deleterious effects of free radicals such as lipid peroxidation and reperfusion injury

* Conflicting research debates whether the potential side effects of methylprednisolone, such as blood clots and pneumonia outweigh the benefits [46], [47]. Recommendations for the use of methylprednisolone after SCI differ.

1.2 Stem Cells of the Dental Apical Papilla (SCAP)

MSC are capable of self-renewal and multi-lineage differentiation (can give rise to the tissues of mesenchymal and non-mesenchymal origin) under appropriate conditions [117], [118]. By the definition of Mesenchymal and Tissue Stem Cell Committee of the International Society for Cellular Therapy, MSC are adherent, $CD105^+$, $CD73^+$, $CD90^+$ and $CD45^-$, $CD34^-$, $CD14^-$ or $CD11b^-$, $CD79\alpha^-$ or $CD19^-$ and $HLA\text{-}DR^-$ and able to differentiate into osteoblasts, chondroblasts and adipocytes *in vitro* [119]. They have low immunogenicity [120], [121] and well reported *in vitro* and *in vivo* immunoregulatory properties (expressed against different types of immune cells in various immunological conditions) [121], [122]. MSC remain present in the adulthood and can be isolated from a number of different tissues [118]. MSC have few ethical and legal problems associated with their use [122]. The most well-known and studied MSC are BM-MSC but due to some limitations (discussed in section 1.1.1), alternatives, such as AD-MSC and dental stem cells are being investigated.

Dental stem cells are advantageous due to their accessibility (easy isolation) and expandability (high proliferative capacity). They are especially promising for neural regeneration due to the high potential for neuro-differentiation (Table 1.2). Dental stem cells express neural markers (neurotrophins and their receptors) without neurogenic stimulation (Table 1.2), presumably as they derive from the same part of embryo as neural stem cells- ectomesenchyme [49], [123]. Dental MSC include dental pulp stem cells (DPSC), stem cells from the dental apical papilla (SCAP), dental follicle precursor stem cells, stem cells from human exfoliated deciduous teeth, periodontal ligament stem cells and tooth germ progenitor cells. SCAP are easy to access and isolate and have high proliferation capacity and therapeutic potential.

SCAP are isolated from healthy third molar teeth in the immature stage of development when apices are open, of patients between the age of 16 and 25. After the standard surgical procedure for tooth extraction the tooth is washed in antibiotics solution. Apical papilla (the soft tissue at the apex) is cut out from the surface of the root (Figure 1.9) and cultured within 24h. Two methods are described and compared for obtaining SCAP primary culture: outgrowth and enzymatic dispersal [124], [125]. In the outgrowth method a piece cut from the apical papilla tissue is put into the Petri dish. Cells that grow out of the piece are more than 95% SCAP (Figure 1.10). In the enzymatic dispersal method apical papilla is minced, digested and single-cell suspensions are added to Petri dish. 70-90% of the cells adhered to the bottom are SCAP [121]. Enzymatic dispersal method is faster, but SCAP have the same properties regardless of the isolation method.

SCAP expressed mesenchymal, endothelial and embryonic stem cell markers [124], [126] and maintained their expression up to the passage twenty (P20), even though their individual levels rose or declined [125]. Under appropriate conditions, they were capable of multi-lineage differentiation [126], [127]. They had high capacity for proliferation (correlating with high telomerase activity), *in vivo* migration and tissue regeneration [123], [128].

Table 1.2 Neuronal and glial markers detected on SCAP regarding the neurogenic stimulation

Culturing condition	Neuronal and glial markers detected on SCAP
Normal culturing condition-prior to any stimulation	Low-affinity nerve growth factor receptor, CD49d (alpha4-integrin), neural cell adhesion molecule, neuroblast differentiation-associated protein, nestin, musashi1 and neuro-filament L (NFL) [115], [126] neuron-specific enolase, glial markers, 2′, 3′-cyclic nucleotide 3′-phosphodiesterase (CNPase), midkine, pleiotrophin, mesencephalic astrocyte-derived neurotrophic factor, Neurophilin 2 [129]
Incubation in neurogenic medium	Glutamic acid decarboxylase, βIII-tubulin, neuronal nuclear antigen, neuro-filament M (NFM), NSE, glial fibrillary acidic protein, and CNPase, DCX, chondroitin sulphate proteoglycans [109], [127].
Secreted by SCAP *ex vivo*	Nerve growth factor, brain derived neurotrophic factor, and glial cell-derived neurotrophic factor, mesencephalic astrocyte-derived neurotrophic factor, neuropilin 2, neuregulin 1, pleiotrophin or neurite growth-promoting factor 1 or 2 (midikine) [126], [130]

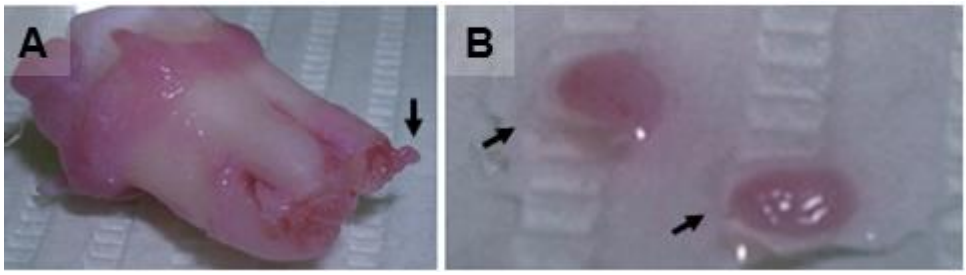


Figure 1.9 A) Apical papilla cut off from a molar B) Apical papilla tissue (Reproduced from [123])

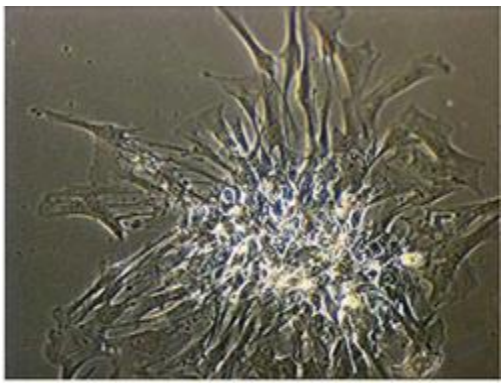


Figure 1.10 SCAP primary culture (Reproduced from [131])

1.2.1 SCAP versus BM-MSC

BM-MSC are currently the focus of most clinical studies, including SCI [132]. Contrary to the isolation of SCAP, isolation of BM-MSC is described as cumbersome, painful and invasive [133]. Assuming it is autologous, it may damage the endogenous pool of MSC and monocytes, lowering the capacity of spinal cord to heal.

Utilisation of autologous SCAP, unlike autologous BM-MSC, may be challenging as they are available only during approximately nine years of early adulthood. However, this can be overcome by using tissue banks, which accessibility and technology grow continuously [134]. Autologous cells may be favoured over allogenic to avoid the immune reaction, even though stem cells were found to supress the immune system activation [135], [136]. The opposite may be advised in case the autologous cells' health is compromised in the same way as the patient's [137], [138]. Allogenic cells are also easier to obtain in large numbers on demand [134].

Yu at al. compared the properties of SCAP and BM-MSC at the same passage numbers under normal culturing conditions [139]. SCAP had higher proliferation capacity then BM-MSC, meaning that the higher number of cells can be obtained faster and by using less resources. SCAP secreted the higher amounts of some specific proteins, such as immunomodulatory IL-6, macrophage colony-stimulating factor 1, follistatin-related protein 1, pentraxin-related protein PTX3, TGFβ1, TGFβ2, macrophage migration inhibitory factor, galectin 1 and 3; antiapoptotic MMP inhibitor 1, 2 and 4, insulin-like growth factor-binding protein 2 and 4-7, insulin-like growth factor II, hepatocyte growth factor, mitochondrial stress-70 protein, heat shock 70 kDa protein 4 and protein HSP 90-beta; transcription factors such as KH domain-containing, ribonucleic acid (RNA)-binding, signal transduction-associated protein 1/Src-associated substrate in mitosis of

68 kDa, Rho GDP-dissociation inhibitor 1, eukaryotic translation initiation factors and heat shock proteins and other factors, such as retinol-binding protein 1, dickkopf-related protein 1 and 3, bone morphogenetic protein 1, mimecan, annexin A2, thrombospondin 1 and 2, signal transducer and activator of transcription 3 and tumor suprpresor p53-binding protein 1.

Even though no significant differences were found for immunomodulatory and anti-apoptotic factors on the whole, production of chemokines and neurotrophins, such as stromal cell-derived factor 1, midkine, pleiotrophin, mesencephalic astrocyte-derived neurotrophic factor, neuroblast differentiation-associated protein and neuropilin 2 was significantly higher in SCAP. In the context of the acute SCI, these advantages may contribute to downscaling the inflammation (by influencing phenotype of a larger cell number) and neural damage (by promoting growth). Significantly lower overall production of extracellular matrix proteins by SCAP (apart from collagen alpha 1(I), 2(I), 1(III), 1(V), 2(V), 2(VI), 3(VI) chains, laminin subunit alpha 1 and gamma 1) may also be favourable after SCI, as it is presumably disorganised and may contribute to scar formation. However, the overall production of angiogenic factors (necessary for neovascularisation) was significantly lower in SCAP (except for the vascular endothelial growth factor C, platelet-derived growth factor receptor beta, angiopoietin-related protein 1, 2 and 4, angiopoietin 1, FGF 7, hepatocyte growth factor, 72 kDa type IV collagenase, MMP-14 and 19, interstitial collagenase, vascular cell adhesion protein 1 and integrin beta-1) and it may be a disadvantage[139].

1.2.2 SCAP versus DPSC

Although both give rise to odontoblasts, SCAP and DPSC come from two anatomically distinctive areas separated by layers of mature cells. DPSC were discovered earlier and

are the most well-characterised dental stem cells [140]. SCAP have higher proliferative and dental tissue regeneration capacity (entire tooth) [123], [129], [140], even though both cell types have similar potential for osteogenic, odontogenic, chondrogenic and adipogenic differentiation *in vitro*. SCAP appear to have higher potential for neuro-differentiation than DPSC [141] and they promote neurite outgrowth in a concentration-dependant manner [130], [142]. Myogenic differentiation was shown only for DPSC [140].

SCAP and DPSC secretion and marker expression also differs (Table 1.3). However, both cell types have STRO-1^{+} melanoma cell adhesion molecule positive subpopulations that are thought to be more immature adult MSC or pluripotent embryonic stem cells retained into adulthood. The CD34/c-Kit and STRO-1 co-expression in both cell types is thought to confirm neural crest origin. Even though MSC are supposed to be CD34^{-} by definition, it was shown that CD34 may be expressed in primitive pluripotent stromal stem cells but is progressively eliminated during cell culturing [123], [129], [142].

Higher expression of surviving and telomerase in SCAP (normal culturing conditions) [129], [140] confirms the higher proliferation capacity but also suggests higher resilience towards apoptosis [143], [144], which may be important for the SCI microenvironment. DPSC secrete higher amount of extracellular matrix proteins (as do BM-MSC described in section 1.1.1), such as dentin sialoprotein, matrix extracellular phosphoglycoprotein, which may also be advantageous after SCI (as described in section 1.1.1). DPSC also secrete higher amount of angiogenic factors compared to SCAP in normal culturing conditions (as do BM-MSC described in section 1.1.1). However, the secretion of angiogenic factors changes under various stress conditions and both SCAP and DPSC show proangiogenic effect *in vitro* and *in vivo* [129].

Table 1.3 Differences in SCAP and DPSC marker expression

Comparison between SCAP and DPSC in the same normal culturing conditions	Molecule name
Expressed in SCAP but not DPSC	NSE, keratin sulphate antigens (TRA-1-60, TRA-1-81), insulin-like growth factor-binding protein 1 and 2, activin A, hepatocyte growth factor, fibroblast growth factor 7, TGFβ, CXCL-16, persephin, neuregulin 1-b1 [127], vascular cell adhesion molecule 1 (CD106), survivin, microtubule-associated protein 2, glutamic acid decarboxylase, neurofilament M [140]
Higher expression in SCAP	Neuronal nuclear antigen, telomerase reverse transcriptase [140]
Similar expression	Endoglin (CD105), thymocyte differentiation antigen, 1, 5'-nucleotidase/ecto-5'-nucleotidase (CD73), integrin beta-1 (CD29), cell-surface glycoprotein CD44, alanyl aminopeptidase (CD13), endostatin, bFGF [140]
Higher expression in DPSC	Dentin sialoprotein, matrix extracellular phosphoglycoprotein, TGFβ receptor II (TGF βRII), FGF receptor 3, vascular endothelial growth factor receptor (Flt) 1, filaggrin and melanoma cell adhesion molecule (CD146), βIII-tubulin [123], FGF receptor 1, desmoplakin, alkaline phosphatase [140]
Expressed in DPSC but not SCAP	DCX, glial fibrillary acidic protein, S-100, cell surface ganglioside A2B5 [145] MAC-inhibitory protein (CD59), Collagen type I Collagen type III, Scleraxis, Osteonectin [140]

1.2.3 Impact of the Microenvironment on SCAP Secretome

SCAP secretome changes under various stress conditions. Previous studies have shown that hypoxia caused significant increase of neurogenic and osteogenic gene expression, had no influence on SCAP proliferation, allowed osteogenic but not adipogenic differentiation and promoted neuro-differentiation [146]. Hypoxia, hypoglycaemia and absence of serum increased angiogenic potential of SCAP and their secretome [126]. These results allowed further exploration of SCAP utility in spinal cord repair, as SCI causes a severe hypoxic microenvironment (more detailed description in section 1.1.5).

1.2.4 Immunoregulatory Properties of SCAP

While quite extensively explored and reported for BM-MSC and AD-MSC, SCAP immunoregulatory properties have not been thoroughly investigated [139], [147]. Given the immunoregulatory properties of other MSC, SCAP are expected to express and secrete molecules involved in immunoregulation and reparation mechanisms, such as major histocompatibility complex class 1, G5, IL-10, IL-6, TGFβ, LIF, prostaglandin E2, IDO and other (Table 1.4) [148]–[153]. SCAP are also expected to have direct and indirect immunosuppressive effect on the immune cells, as observed for other types of MSC *in vitro* (Table 1.5) [149], [154]–[156].

In vivo, BM-MSC administered in animal model of multiple sclerosis, characterised by “Th17” inflammation, decreased IFNγ and IL-17 production and increased the numbers of IL-4 producing “Th2” lymphocytes [149]. Administered in “Th2” mediated allergic airways inflammation, BM-MSC inhibited hyper-reactivity, mitigated the increase in specific IgG1 and IgE production and even though it did not reduce the number of antigen-specific T-lymphocytes, it promoted the “Th1” phenotype [150]. That is why SCAP, applied to SCI model, are hypothesised to suppress the “Th1” inflammation.

Table 1.4 Summarised immunoregulatory and reparative factors reported for other types of MSC and expected for SCAP at spinal cord lesion [148]–[153]

Secretion of chemokines	Monocyte chemoattractant protein 1 and 3 (CCL2/MCP-1 and CCL7/MCP-3), macrophage inflammatory protein 1α, 1β, and 3α (CCL3, CCL4 and CCL20), RANTES (CCL5), eotaxin-3 (CCL26), growth-regulated oncogene α, β and γ (CXCL1, CXCL2 and CXCL3), epithelial-neutrophil activating peptide (CXCL5), CXCL8/IL-8, monokine induced by IFNγ (CXCL-9), IFNγ -induced protein 10 (CXCL10), interferon-inducible T-cell alpha chemoattractant (CXCL11), stromal cell-derived factor 1 (CXCL12), fractalkine (CX3CL1), semaphorin-3A, TNF-stimulated gene 6 protein
Secretion of growth factors	Vascular endothelial growth factor, hepatocyte growth factor, epidermal growth factor, platelet-derived growth factor, FGF, keratinocyte growth factor, GM-CSF, insulin-like growth factor 1, angiopoetin 1, erythropoietin, glial cell-derived neurotrophic factor, FMS-related tyrosine kinase 3 ligand, stem cell factor, IL-7, IL-11, IL-12, IL-14 and IL-15, oncostatin M, bone morphogenetic protein 4
Expression of adhesion molecules for cells and extracellular matrix	Intercellular adhesion molecules 1, 2 and 3, very late antigen α1, α2, α3, α5, α6, and β chain, β4 integrin, vascular cell adhesion molecule 1, programmed cell death ligand 1 and 2, Fas ligand, V-set domain-containing T-cell activation inhibitor 1 (B7-H4), homing cell adhesion molecule (CD44), activated leucocyte cell adhesion molecule (CD166), neural cell adhesion molecule, platelet endothelial cell adhesion molecule, L-selectin, P-selectin, E-selectin, CD40, lymphocyte function-associated antigen 1α, 1β and 3 (CD58), thymocyte differentiation antigen 1, bone marrow stromal cell antigen 1, vitronectin receptor β chain, galectin 1 and 9, cadherin 5, hyaluronate receptor
Expression of cytokine and growth factor receptors	IL-1αR, IL-1βR, IL-3R, IL-4R, IL-6R, IL-7R, IFNγ receptor, TNFα receptor 1 and 2, TGF β receptor 1 and 2, FGF receptor, epidermal growth factor receptor and platelet-derived growth factor receptor, transferrin receptor
Exosome secretion	microRNA-320 (downregulated matrix metalloproteinase 13 gene expression), microRNA-22 (inhibited IL-1β expression and suppressed matrix metalloproteinase 13 gene expression), microRNA-25 (lowered IL-1 β and TNFα levels, regulated oxidative stress, improved the reperfusion and reduced tissue damage after SCI)

Table 1.5 Summarised MSC influence on immune cells [149], [154]–[156]

Immune cell type	Reported mesenchymal stem cell actions
T-lymphocytes	Inhibited response to antigens, expression of activation markers and antigen specific proliferation of naïve and memory T-lymphocytes, through programmed cell death protein 1 and adenosine secretion Prevented the differentiation of naïve T-cells into Th17 and acted directly on Th17 cells promoting their differentiation to regulatory T cells through CCR6 and adenosine Inhibited the formation of cytotoxic T-lymphocytes Inhibited the production of IFNγ by “Th1” and IL-4 by “Th2” lymphocytes Recruited, regulated, and maintained regulatory T-lymphocytes phenotype and function over time using jagged1, jagged2, delta-like 1, 3, and 4 ligands, producing, among above mentioned factors, haem oxygenase 1 and modifying CD69 expression by T-lymphocytes
B-lymphocytes	Inhibited B-lymphocyte activation and proliferation, not by inducing apoptosis, but through the arrest in the G0/G1 phase of the cell cycle Impaired IgM, IgG and IgA production and differentiation to plasma cells Impaired CXCR4, CXCR5, and CCR7 expression and the chemotaxis of B-cell towards CXCL12 and CXCL13, respective CXCR4 and CXCR5 ligands
Natural killer cells	Inhibited IL-2 and IL-15-driven NK-cell proliferation Modified cytokine secretion Remained resistant to non-activated allogenic NK cell cytolysis
Dendritic cells (DC)	Inhibited activation and differentiation of monocytes to DC and DC maturation by downregulating their expression of CD1a, CD86, HLA-DR, costimulatory molecules, CD83, CD11c and the production of IL-12 upon TLR-mediated DC activation Decreased the TNFα production by myeloid and increased IL-10 production by plasmacytoid DC

1.2.5 SCAP for Spinal Cord Injury

It is expected that, after the local injection to spinal cord lesion, grafted MSC will be able to stimulate regeneration by releasing neurotrophic factors, modifying extracellular matrix and downregulating axonal growth inhibitors. MSC will also be stimulating endogenous neurogenesis and angiogenesis, through secretion of exosomes and activation of endogenous stem cell proliferation, migration and differentiation toward neurons. It is not excluded that the implanted MSC may differentiate into neural and glial progenitors and mature cells, repairing specific connections and promoting re-myelination. By filling small cavities upon implantation, MSC will have a physical function of a scaffold, supporting axonal outgrowth between the interrupted ends and stimulates revascularization [157], [158].

In an experiments done by De Berdt *et al*, an entire apical papilla tissue improved rat locomotor recovery after SCI [85]. Also, SCAP applied to LPS-stimulated murine microglia cell line (BV2 cells) reduced inflammation (reducing TNFα and increasing *Arg1*). Equally SCAP applied to spinal cord organotypic slices with oligodendrocyte precursor cells improved regeneration (improving oligodendrocyte maturation and myelination by increasing myelin basic protein, CC1, activin A and galactocerebrosidase synthesis) [147]. However, there are no records of SCAP mitigating inflammation or improving tissue repair after SCI *in vivo*. The reasons, apart from the previously described influence of the microenvironment, may be the SCAP delivery system (fibrin hydrogel) or a fast cellular turnover in rats [159].

Overall, SCAP characterisation *in vitro* is promising: high proliferative capacity [132], high passage index [125], high potential for neuro-differentiation [142], potential to

stimulate neuro-regeneration [85] and possibly decrease inflammation [160]. Therefore, more studies showing SCAP efficacy are warranted.

1.2.6 Strategies to Improve Stem Cell Efficacy for Spinal Cord Repair

The success of cellular therapies in the SCI is limited [61]. That may be due to the harsh microenvironment that the injury creates and the ongoing tissue deterioration that creates the secondary injury (as described in section 1.1.5). It has also been shown that over 90% of MSC transplanted in damaged spinal cord die or migrate away [6]. Thus, finding ways to increase their survival and utility is paramount (as described in section 1.1.5 and 1.2.3).

Specialising MSC to have a particular activity such as IL-4 [161] or brain-derived neurotrophic factor secretion [162], or enhancing MSC immunoregulatory activity by priming them with pro-inflammatory cytokines (Table 1.6 and 1.7), or genetic engineering of MSC to prolong their survival [163] are some of the options. Good results may also be obtained after priming MSC in microglia/ macrophage co-culture (with the possibility to control the system and regulate the application). However, to maximise the influence on the pathological immune response, the post-injury injection time needs to be considered [74]. Thus, an optimal solution may be a multicellular MSC therapy where the injection time is optimised for each specialised MSC type to steer the immune response.

Another way to overcome a problem of MSC viability is by using MSC secretome instead of the cells [164]. The main influence of the cells injected to SCI is considered a consequence of the short-term paracrine signalling, which is the cell secretome. The signalling is short-termed, due to the short retention of the cells at the injection site [87],

[113]. Therefore, there may be little difference between the injection of cells and their secretome with prolonged release. The paracrine signalling is a response to the local microenvironment and may therefore be considered individualised therapy. However, he secretome can also be optimised in similar ways, such as genetic engineering or priming the MSC with pro-inflammatory cytokines [161], [162] (Table 1.6 and 1.7).

A way to increase the stem cell survival and their retention at the injection site could be the utilisation of a biomaterial (described in section 1.3). An adequate biomaterial would be the one that can reduce the shear stress the MSC withstand during the injection (that significantly impairs their survival [114]), serve as a scaffold keeping the cells from migrating away from the injury site (and provides the support for neuronal outgrowth) and shields the cells from deterioration whilst not influencing their secretion and interaction with the microenvironment.

Table 1.6 Summary of the results achieved by exposing MSC to the cytokines leading the immune response at SCI microenvironment

Cytokine	Concentration	Stem cell type	Action
TNFα	5, 10, 20 ng/mL	UC-SC	Induced IL-6 and MCP-1 production in a hyperbolic dose-response curve: TNFα, 5ng/mL, caused significantly lower IL-6 and MCP-1 secretion compared to 20ng/mL, whilst the difference in between 5 and 10 and 10 and 20 ng/mL was not significant. TNFα caused cell death only in combination with IFNγ, up to 23% after 48h [165].
	10 ng/mL	UC-SC	Nuclear translocation of nuclear factor κB. IL-8 upregulated after 24h.
		BM-MSC	Nuclear translocation of nuclear factor κB. IL-8 upregulated after 8h [166].
	6 ng/mL	BM-MSC	With 3ng/mL of IL-1β and 200 mmol/L of sodium nitroprusside (NO donor) increased bFGF, vascular endothelial growth factor, insulin-like growth factor 1 and TGFβ1. Conditioned medium achieved significant improvements *in vivo* [164]. Increased secretion of proangiogenic cytokines, IL-6 and IL-8 upon 48h incubation.
	10 ng/mL	AD-MSC	Conditioned medium achieved significantly better results *in vivo* upon priming with TNFα [167].
	20 ng/mL	BMSC	With IL-1β, 20ng/mL, upon 24h incubation in serum-free medium increased bFGF, hepatocyte growth factor, heparin binding epidermal growth factor-like growth factor, IL-6 and amphiregulin [168].
	50 ng/mL		Increased vascular endothelial growth factor, bFGF, hepatocyte growth factor and insulin-like growth factor 1 upon 24h incubation [169].
IFNγ	50 ng/mL	UC-SC	With IL-1β, 10 ng/mL, caused faster IL-6 production and with TNFα 5, 10 or 20 ng/mL significantly higher IL-6 and MCP-1 production, upon 24 or 48h incubation [165].
	5, 50, 500 U	AD-MSC, WJ-SC	MSC treated with 500U significantly prevented graft versus host disease (ED_{50} ≤ 0.2 ng/mL corresponding to $5x10^6$ units/mg) [170].
	200 IU/mL	BM-MSC	24h incubation increased Janus kinase- signal transducer and activator of transcription 1 signalling pathway activation, IDO expression and graft versus host disease survival ± 10 ng/mL TNFα [171].
	6.5 ng/mL	BMSC	With 1.5 ng/mL TNFα, 48h incubation.
	65 ng/mL		With 15 ng/mL TNF-α, 48h incubation. "Th1" chemoattractant molecules (e.g. CCL5, CXCL9, CXCL10, CXCL11) and the immunosuppressive molecules (e.g. IDO1, programmed cell death ligand 1, HLA-G) were strongly upregulated in all stimulated single cells. cyclooxygenase 2 and prostaglandin E2 expression was upregulated by both IFNγ and TNFα [172].
	10, 200 ng/mL	BM-MSC	With or without TNFα, 10 ng/mL, after 6h incubation, programmed cell death ligand 1 and IDO expression was induced by IFNγ but not TNFα. cyclooxygenase 2, prostaglandin E2 and hepatocyte growth factor increased, TGFβ1 decreased [173].
	30 ng/mL	BMSCs	Overnight incubation increased: IDO-1, programmed cell death ligand 1 expression; 3rd party T lymphocyte proliferation; inhibition of IFNγ producing T-lymphocyte development; promotion of regulatory T-cell expansion and upregulation of 232 proteins including IDO-1, programmed cell death ligand 1, prostaglandin E2, galectin-9, intercellular adhesion molecule 1, vascular cell adhesion molecule 1, CCL9, bone marrow stromal cell antigen 2 [174].
	500 U/mL (25ng/mL)	BM-MSC	Upregulated MHC II related molecules, IDO and CXCL9 upon five- day incubation [175].
	30ng/mL	BMSC	Increased concentration of 75 and decreased the concentration of 40 proteins detected by liquid chromatography-double mass spectrometry proteomics after 20h. bone marrow stromal cell antigen 2, Intercellular adhesion molecule 1, programmed cell death ligand 1 and IDO were also increased [174].
	10, 50 ng/mL	BM-MSC	Cell elongation after 24h incubation correlated with the increased immunomodulatory behaviour. 10 and 50ng/mL gave statistically similar results, different to control [176].
	200 ng/mL		TGFβ1, IDO, hepatocyte growth factor increased after 24h incubation [177].

Abbreviations: BMSC- bone marrow stromal cells, ED50- the dose causing 50% of the effect, UC-SC- umbilical cord derived stem cells, WJ-SC- Wharton's jelly stem cells

Table 1.7 Summary of the results achieved by exposing MSC to other factors that lead to different types of immune response

Factor	Concentration	Stem cell type	Action
LPS	200 ng/mL	UC-SC, BM-MSC	Significantly increased IL-8 production after 24h, compared to 0, 4 and 8h [166].
	200 ng/mL	BM-MSC	Increased MSC vascular endothelial growth factor, bFGF, hepatocyte and insulin-like growth factor after 24h incubation [169].
	0.1, 1 μg/mL		Stimulated viability. Pre-treatment, especially with 1 μg/mL, inhibited 50 μg/mL LPS induced apoptosis.
	10, 20 μg/mL		Decreased viability, not significantly. Pre-treatment did not inhibit 50 μg/mL LPS induced apoptosis.
	40, 50 μg/mL		Significantly reduced viability (MTT) after 12, 24 and 48h.
			Increased TLR dependant IL-6 and IL-1β production [178].
	20 mg/mL		Increased CXCL1, IL-6, IL-8 and CCL2 [179].
IL-1β	10 ng/mL	UC-SC	Induced IL-6 and MCP-1 production, hyperbolic dose-response curve [165].
			48h incubation increased efficacy of cell transplantation *in vivo* [180].
IL-4	10 ng/mL	AD-MSC	In osteogenic medium decreased runt-related transcription factor 2 and increased osteocalcin [181].
			Increased adipogenic proteins and lipogenesis after 6h incubation [182].
IL-10, IFNβ	Secreted from T-cells	BM-MSC	IFNβ upregulated signal transducer and activator of transcription 1 and IDO expression.
			IL-10 and IFNβ upregulated IFNβ, signal transducer and activator of transcription 1 and IDO [183].
IL-17A	50 ng/mL	BM-MSC	Upregulated MMP13, LPS binding protein, IL-6, CCL2, MMP1, CCL8 upon 1, 2 or 5 day incubation [175].
rIL-17B	100/200 ng/mL	UC-SC	IL-6, IL-8, TGFβ, CCL5, octamer binding transcription factor 4, Sal-like protein 4 increased after 48h incubation with 100 and 200 and Nanog after the incubation with 200 ng/mL [184].
IL-6 +	40 ng/mL	BM-MSC	CD45, TGFβ expression and differentiation increased, whilst IL-4 decreased and costimulatory
IL-1b +	20 ng/mL	AD-MSC	molecules, stem and apoptotic markers, morphology, IFNγ, TNFα, IL-10 and mixed leukocyte
IL-23	20 ng/mL		reaction did not change [185].
Abbreviations: IFNβ- interferon beta, MMP-matrix metalloproteinase, MTT- colorimetric assay for assessing cell metabolic activity			

1.3 Tissue- Derived Extracellular Matrix (ECM) Hydrogels

A biomaterial is a material that can be used in a living organism for medical purposes [186]. Biomaterials can be bio- derived, i.e. completely or partially come from a living organism, or synthetic, i.e. produced in a laboratory. Based on their mechanical (e.g. ductility, tensile strength, yield strength, compression strength and fatigue, friction and wear debris), physical (e.g. hydrophilicity, swelling, surface charge and surface topography) and chemical properties (e.g. stability in regard to hydrolysis, oxidation, free-radical reactions and biochemical reactivity in general), biomaterials may have different functions. For instance, stiff and durable biomaterials, such as titanium alloys, cobalt-chromium alloy and ceramics are suitable for hip replacement; biodegradable biomaterials with various degradation rates are used for controlled/ prolonged drug delivery and to guide tissue regeneration, such as poly (lactic-co-glycolic acid) used for LUPRON DEPOT® and poly(lactic-co-glycolic acid)-collagen matrix used for CYTOPLAST Resorb® [187]. All the biomaterials however must not be toxic or cause adverse immune response.

An ideal material for application to spinal cord lesion may be a fast-forming biodegradable hydrogel injected into the subdural space above the lesion (Figure 1.11). Injectability implies minimally invasive delivery while biodegradability eliminates the need for removal. Both may prevent additional inflammation and tissue damage. An intrathecal injection through a needle/ catheter [188], so that material occupies subdural space above the lesion, brings material into the contact with the tissue, but causes less damage (possible subtle pressure) then injection into the lesion. For the intrathecal injection or the injection into the lesion cavity the anatomy of spinal cord, that is “a cylinder inside a tube” and the irregular shape of the lesion should be considered. Therefore, the material should mould in real time to occupy the given space upon

injection, e.g. be a gel, foam or a sponge. Gels may be a compromise between the immense variety of designs and modifications and the ease of design and production. A hydrogel, rather than aero- or oleo-gel, would be advantageous for the diffusion of biomolecules.

As cerebrospinal fluid (volume: 90 - 150 mL in adults) constantly flows through the subdural space (flow rate: 0.3 - 0.4 mL/min) [189], the hydrogel would need to gel quickly to avoid dissolution. In addition, high doses of therapeutic molecules need to be constantly released from the hydrogel due to washout from the cerebrospinal fluid. Using a continuous material/drug injection with pumps to provide the constant release was shown to lead to tissue damage, infection and pump blockage [190]. However, design of every drug/biological product not injected intraparenchymally faces this obstacle. Therefore, hydrogels designed to express and secrete bioactive molecules may overcome the obstacle and have increased efficacy. Hydrogel stiffness similar to spinal cord tissue and a non-rigid, dynamical micro topography may avoid cell polarisation and glial scar formation and ensure the absence of adverse immune reaction [191]. Size, concentration and alignment of hydrogel pores should allow cell inhabitation and axonal ingrowth [192]. This hydrogel also needs to have adequate molecular makeup and scalable manufacturing according to the quality and safety standards.

In tissue engineering, hydrogels are mostly used as a vehicle for local delivery and slow release of drugs, or the local delivery and mechanical support of cells. Similar strategies were applied in spinal cord repair pre-clinical research [132], [192]. Another strategy, typical for damaged nerve regeneration, is the use of hydrogels, mostly their pore orientation, for nerve guidance and bridge through injury-induced cavitation [69].

Hydrogels that have been used for cell delivery to SCI have largely been synthetic materials [69]. For instance, implantation of MSC in microporous poly[N-(2-hydroxypropyl) methacrylamide]-arginylglycylaspartate, poly(2-hydroxyethyl methacrylate) and serotonin-modified poly(2-hydroxyethyl methacrylate) hydrogels to rat SCI resulted in significant functional improvement, axonal ingrowth into the hydrogel and increased survival of MSC, respectively [193]–[196]. Neural stem cells in poly(caprolactone) with chondroitinase and complex architecture poly(lactic-co-glicolic acid) hydrogels enhanced axonal regeneration and caused significant functional improvement after rat spinal cord hemisection [197], [198], whilst peroxynitrite scavengers in poly(lactic-co-glicolic acid) hydrogel improved neural stem cell viability [199]. Schwann cells in poly(lactic-co-glicolic acid) multichannel scaffolds or poly-(β-hydroxybutyrate) tubular conduit promoted axonal regeneration, whilst combined with poly(acrylonitrile-co-vinylchloride) guidance channels improved axonal re-myelination, regeneration and growth across the lesion and Basso, Beattie and Bresnahan locomotor score after rat SCI [200]–[207]. Schwann cells were also compared to and combined with neural stem cells in different types of scaffolding material [192]. However, tissue derived ECM hydrogels may be able to fulfil all the mentioned requirements and strategies, whilst also actively stimulating immunoregulation and the constructive remodelling of the injured tissue [187].

ECM hydrogels have been shown to promote immunomodulatory macrophage phenotype and constructive tissue remodelling [208]. This reparative potential derives from the retained growth factors, such as bFGF and TGFβ1 in porcine small intestine submucosa-derived hydrogel [209] and revealed cryptic peptides and chemotactic motifs, as described for porcine urinary bladder matrix hydrogel [210]. ECM hydrogels are presumed to contain matrix-bound nanovesicles that are released upon digestion. Matrix-bound nanovesicles are RNA-rich vesicles similar to exosomes. These vesicles

were found in freshly made digests (digest is a step in material processing, presented in Figure 1.12 and described in section 1.3.1) but their stability during to standard digest handling has not been thoroughly explored [211], [212]. Investigated structural elements of the ECM hydrogels are mostly collagen and sulphated glycosaminoglycans, as they are the principal components of the ECM [213]. However, the exact composition, the mechanism of action and origin-related differences of ECM hydrogels remained largely unknown. Regardless, their sourcing and production can be standardised for clinical use, as shown in the example of Ventrigel^{TM}, porcine myocardium derived ECM hydrogel. This ECM hydrogel passed the safety studies (phase I) and is currently in phase II clinical trials [214].

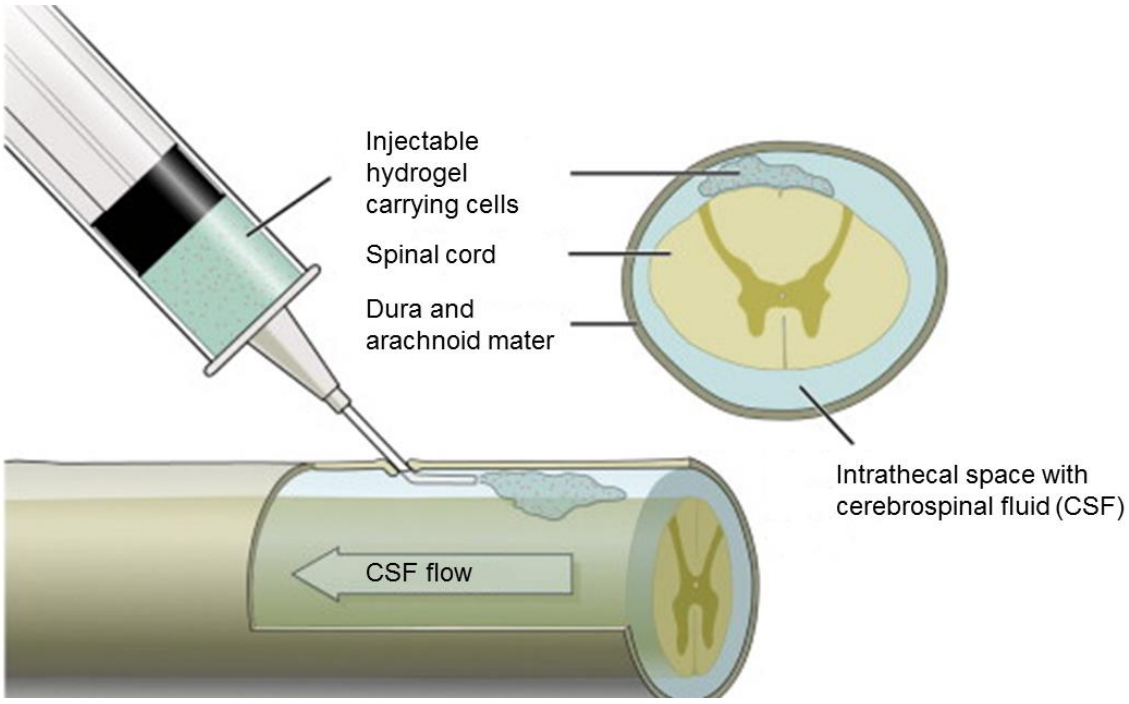


Figure 1.11 Schematic of the hydrogel intrathecal injection. The hydrogel may carry active molecules (drugs, cytokines, growth factors etc.), loaded nano/microparticles (with drugs, cytokines, growth factors etc.) and/or cells (Reproduced from [215])

1.3.1 ECM Hydrogels

ECM hydrogels can be made from almost any tissue, including kidney cortex [216], liver [217], pancreas [218], lung [219], placenta [220], blood vessel [221], aortic valve [222], skeletal muscle [223], nerve [75]. First, the tissue decellularisation process is optimised to obtain the ECM. Tissue decellularisation step involves different reagents and methods that can be chemical, enzymatic or mechanical [203] (Figure 1.12). The methods are combined for different time periods so that a balance between the efficient decellularisation and the preservation of tissue ultrastructure and the biochemical composition is achieved. The balance is important as cellular remains contain antigens and ECM biochemical composition affects hydrogel functionality [204]. Novel methods, such as supercritical carbon dioxide or apoptosis assisted decellularisation are being developed to eliminate the use of chemicals and retain the three-dimensional fibre micro-structure as close to the original as possible [205], [206]. Residual chemical detergents may influence ECM material safety and efficacy [207]. In addition, limiting the use of chemicals may decrease the cost and environmental impact of the large scale decellularisation. If necessary, the tissue specific steps, such as bone demineralisation [196] may be included.

ECM can be mechanically shaped to obtain an ECM scaffold. Oasis®, porcine small intestine submucosa scaffold, have been in use for 19 years (Food and Drug Administration (FDA)- approved in 2000th) for the management of wounds (apart from the third-degree burns). Over 50 different porcine, bovine or horse ECM scaffolds have been commercialised [224] and have not caused an adverse immune reaction in humans, presumably due to the similarity of ECM proteins (e.g. collagen, laminin, fibronectin domains) between the species.

When a hydrogel is desired scaffolds are processed further. First, ECM is translated into the ECM digest, for which there are several common methods. One is incubation with pepsin and 0.01 M hydrochloric acid [208] (Figure 1.12). But other digestion enzymes, such as collagenase or proteinase K, or high salt buffer solution containing protease inhibitors are also used. Centrifugation and dialysis have also been researched, so instead of digestion the step is sometimes referred to as solubilisation [209], [210]. Regardless of the chosen method, the digestion step breaks the organisation of ECM protein fibres and the three-dimensional structure of ECM proteins (collagen, elastin, proteoglycans).

Following digestion, the digest ionic strength and pH are brought to physiological values to obtain the pre-gel. To regulate ionic strength of the digest, phosphate buffer saline is used. If pepsin and 0.01 M hydrochloric acid were used for digestion, the pH is neutralised with sodium hydroxide. Pre-gel is incubated at 37 °C to obtain ECM hydrogel [187]. ECM proteins start self-assembling upon neutralisation and during the incubation make a new gel network.

To date, the exact and absolute structure of the gel network has not been determined due to the lack of suitable methods and sample preparation techniques. For instance, the ECM hydrogel protein structure cannot be efficiently imaged with regular, “cryo” or environmental scan electron microscopy, as the sample preparation requires water removal/snap freezing which distorts the hydrogel pores [211]. ECM hydrogel dyeing and imaging under a light/fluorescent/confocal microscope has also been proven inefficient [212], [213].

It is however evident that decellularisation and digestion break down the structural network of ECM proteins such as collagen, elastine, proteoglycans, sulphated

glycosaminoglycans, transforming the solid tissue into the viscous digest [208]. Upon neutralisation, van der Waals, hydrophobic and polar π interactions between collagen, sulphated glycosaminoglycans and possibly other ECM proteins lead to self-assembly and formation of a hydrogel [208]. The re-grouped structure is different and less stiff compared to the tissue of origin, as most of the proteins and protein binding sites are dismantled (even though some new binding sites may be built/uncovered) and the new protein structures and bonds are less complex. Therefore, longer digestion times decrease the stiffness and gelation time of the hydrogels. Neutralisation step may also influence hydrogel mechanical properties by decreasing ECM protein concentration. However, the temperature-dependant time window for collagen and sulphated glycosaminoglycans self-assembly, i.e. gelation time, during which the pre-gel is viscous, allows for hydrogel manipulation, passing through the syringe and injection. Lower viscosity means easier pre-gel passage through the syringe, but also the lower post-gelation stiffness.

Processes of decellularisation and digestion lead to the disruption of proteins and therefore also to the loss of functional elements (cytokines, growth factors, receptors) present in the native tissue. The digestion step alone has been demonstrated to decrease the growth factor content by 10-50% [209]. However, quantifiable amounts remain, contributing to the ECM hydrogel potential for repair and immunoregulation. The disruption and the re-assembly of protein structures during the decellularisation, digestion and gelation may also lead to the formation or exposure of new protein structures, recognised as hostile by the immune system. Yet it has been suggested that digestion is the reason for the lack of ECM hydrogel immunocompatibility issues as it may also be breaking down the immunogenic proteins [199], [214]. Further, it was demonstrated that the digestion in fact released the previously mentioned exosome-like matrix-bound nanovesicles and unravelled the fibres and exposed the matricryptic

peptides and bioactive motifs [210], [211]. Matrix-bound nanovesicles micro RNA cargo was related to inflammation mitigation [212] and matricryptic peptides induced cell migration *in vitro* [210].

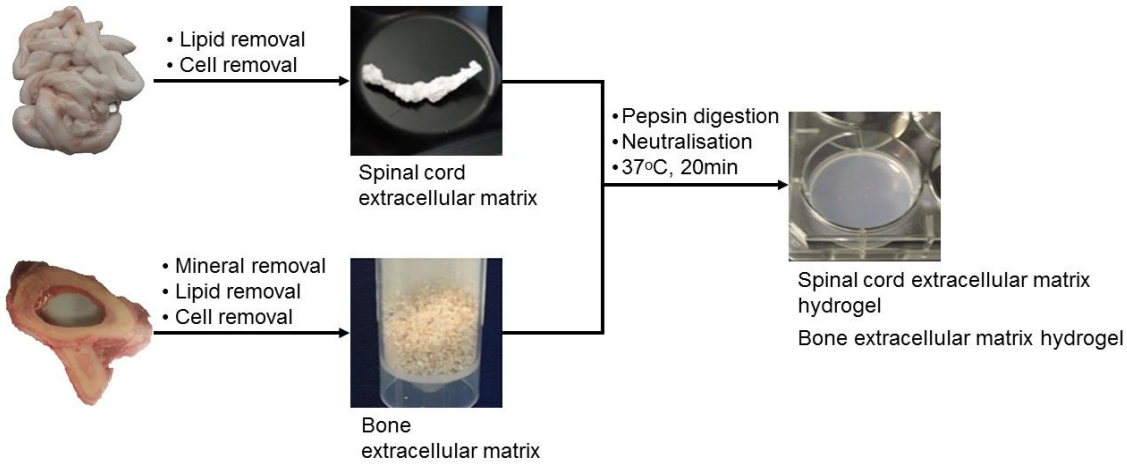


Figure 1.12 Diagram of spinal cord and bone extracellular matrix hydrogels (scECM and bECM, respectively) generation

1.3.2 ECM Hydrogel Downstream Modifications

Due to their naturally predetermined properties, bioderived hydrogels sometimes require optimisation, e.g. to gel faster, withstand higher stress or degrade slower, for the best *in vivo* results. Such optimisations are usually achieved by hydrogel combinations and crosslinking [71]. In the case of ECM hydrogels (or other protein-based hydrogels), crosslinking may change protein composition and conformation, altering the cellular ligands and revealing antigen epitopes [225] which may lead to an adverse immune response, as shown for ECM scaffolds [226]–[228].

Interestingly, crosslinking of myocardial ECM hydrogel with chitosan and genipin was non-immunogenic *in vitro* and *in vivo* [229]. That may be explained by the fact that each crosslinker produces different crosslinking structures, as described in comparison

between genipin and 1-ethyl-3-(3-dimethyl aminopropyl)carbodiimide [230], [231] or by lower cytotoxicity of genipin compared to other crosslinkers, such as glutaraldehyde [232]. As increased stiffness is related to the increased adverse immune response [191], the absence of immune response in genipin-crosslinked myocardial ECM may also be related to its lower stiffness compared to the glutaraldehyde, 1-ethyl-3-(3-dimethyl aminopropyl)carbodiimide and microbial transglutaminase crosslinked hydrogels [231], [233].

An FDA- approved and therefore possibly safer crosslinkers, such as fibrin, transglutaminase and calcium ions (catalyst) were also used with myocardial ECM hydrogels [234]. The process of binding fibrinogen to collagen with transglutaminase in the presence of calcium ions occurs during blood coagulation [234]. This process has been used to bind fibrin to ECM hydrogels that contain collagen. This crosslinking method improved stiffness and lowered degradation rate of the hydrogel composite. The composite retained the benefits of myocardial ECM hydrogel, enabled optimisation of mechanical properties to match the myocardium and enabled previously impossible cell encapsulation and targeted delivery [234]. Myocardial ECM hydrogel seemed to be stiffer upon crosslinking with fibrin/transglutaminase than with genipin. However, the fibrin/transglutaminase method requires high percentage of fibrin to myocardial ECM, 90:10. This is disadvantageous, as with the lower ECM concentration, the content of its active components, growth factors, matricryptic peptides and matrix bound nanovesicles is also lower [234]. Myocardial ECM hydrogel in clinical trials is unmodified [235]. The functionality of the successfully crosslinked ECM hydrogels, i.e. of the newly formed protein structures, has not been tested in clinical trials.

Seeing that ECM hydrogel has high collagen content (Table 1.8) [213], ECM hydrogel-fibrin combination, without the crosslinker, may be similar to the previously studied

collagen-fibrin hydrogel composites [236]–[238]. Lai et al. used mathematical modelling to predict the network and the resulting mechanical behaviour of the collagen-fibrin hydrogel composite [237], [239]. Then they demonstrated the mechanical behaviour and supported the network descriptions by scan electron microscopy imaging [237], [239]. They found that if the concentration of collagen in the composite is low, collagen and fibrin form a single network of randomly interacting fibres. As the collagen concentration increases, the networks become parallel, i.e. fibrin intertwines with collagen fibres but does not bind to them [237], [239]. Reyhani et al. further showed that fibrin does not bind to the denatured collagen, as the binding sites are discretely present in the native triple helix [240]. Therefore, just by the addition of fibrin, ECM hydrogel mechanical properties may be reinforced, whilst the collagen conformation (related to the presentation of antigens, cryptic motives and other bioactive sites) may remain intact. Fibrin has also been shown to support angiogenesis [241]–[243] and peripheral nerve regeneration [244] and has been widely used in regenerative medicine as a delivery vehicle [85], [245].

1.3.3 ECM Hydrogel Efficacy in Regeneration

ECM hydrogels have been tested for their efficacy for over 20 years [246] and have been shown to provide both tissue-specific and general cues for regeneration *in vitro* and *in vivo* [247]–[251]. For example, oesophageal ECM hydrogel induced migration of oesophageal stem cells and three-dimensional organoid formation, unlike the porcine urinary bladder matrix and small intestine submucosa hydrogels tested in parallel. However there were no significant differences in the hydrogel influence on oesophageal mucosa remodelling [252]. Rothrauff *et al*. have linked the tissue-specific effects of tendon and cartilage hydrogels on BM-MSC to the solubilisation method: Urea-extracted hydrogels promoted specific differentiation in 2D and 3D cultures, whilst pepsin digested

did not [248]. Another example of tissue specificity is *in vitro* studies demonstrating that even though both porcine urinary bladder matrix and brain ECM hydrogel supported cell survival and promoted three-dimensional neurite outgrowth, only brain derived hydrogel increased neurite length and acted as a chemoattractant [249], [250]. Bible *et al.* have measured the ability of porcine urinary bladder matrix and brain ECM hydrogel mixtures to deliver neural stem cells into the brain cavity [251]. Further to that, Badylak group showed that porcine urinary bladder matrix hydrogel improve neurobehavioral recovery after the traumatic brain injury, specifically, vestibular motor/sensorimotor function in the foot fault test and beam-walking task and cognitive function via Morris water maze in rat controlled cortical impact model) [253], [254], whilst *in vivo* experiments with brain ECM hydrogel have not yet been done. Ghuman *et al.* did a 12-week follow up study of porcine urinary bladder matrix hydrogel effects on stroke cavity and showed a reduction in cavity size but the findings were no different compared to untreated group [255].

1.3.4 ECM Hydrogel Immunoregulatory Properties

Some ECM hydrogels, including porcine urinary bladder matrix, small intestine submucosa, oesophagus and colon derived, have induced expression of the anti-inflammatory markers *in vitro*. However, this effect is specific to the tissue of origin, as skeletal muscle, dermal and liver hydrogels did not. All of the tested ECM hydrogels had antimicrobial activity [256]. However, differential results were obtained for brain ECM in two separate studies with different conditions. Dziki *et al.* [256] showed that treatment of naïve mice macrophages with brain ECM hydrogel at a concentration of 0.2 mg/mL reduced the expression of a pro-inflammatory marker iNOS, whereas Meng *et al.* [257] found that treatment of rat bone marrow derived macrophages with higher concentrations of brain ECM hydrogels (0.5 and 1 mg/mL) resulted in increased secretion of the pro-inflammatory markers TNFα and NO. These results suggest that

ECM hydrogels, derived from different tissues and applied at different concentrations, may induce different anti-inflammatory gene expression patterns in macrophages.

In vivo, porcine urinary bladder matrix injected into rat stroke cavity induced significant cell infiltration, predominantly on the tissue- porcine urinary bladder matrix border, with the majority of the cells being macrophage-like and polarised towards the anti-inflammatory “M2” phenotype [258]. A shift in cellular immune response from the predominantly cytotoxic to almost exclusively Th2-helper was observed between the day 3 and 7 after acellular porcine small intestine submucosa and myocardial ECM hydrogel xenograft transplantation [259], [260]. Porcine small intestine submucosa hydrogel was shown to promote regeneration, immunoregulatory macrophage phenotype and decrease concentration of TNFα in the rat model of chemically induced ulcerative colitis [245].

Wang *at al.* took into account the inadequacies of rodent model and to improve, tested human and porcine myocardial matrix hydrogel in humanized, i.e. immunocompromised mice with transplanted human immune cells and wild type mice [261]. Human hydrogel was considered allogeneic to the humanized model. Due to predominantly present “type 2” immune cells in human and porcine hydrogel regardless of the mouse model, Wang *et al*. concluded that both allogenic and xenogeneic ECM hydrogel promoted the immune response that enables the tissue remodelling [261]. Due to the higher density of human T-cell and macrophage infiltrate within the porcine, compared to human hydrogel in humanized mice, Wang *et al.* concluded that the response to xenogeneic hydrogel was higher compared to allogenic [261].

Overall, ECM hydrogels have promoted regulatory and pro-regenerative immune response *in vivo*, however the exact actions and their mechanisms remained unclear. It

would be beneficial if the *in vivo* performance of hydrogels could be related to the generation protocol [247], tissue of origin or the concentration of the specific constituents, however that has not been done to date. The promoted regeneration seems to be a consequence of the mechanical scaffolding, evolutionary conserved protein patterns as well as the presumed active elements. So far, the only way to find out whether the hydrogels of heterologous origin or those corresponding to the injured tissue would have the higher capacity for immunoregulation and regeneration is to test them in the specific scenario that is in question.

1.3.5 ECM Hydrogels for Spinal Cord Injury Repair

Porcine spinal cord ECM hydrogel (scECM) [74], nerve derived [75] and porcine urinary bladder matrix hydrogels [74] have been investigated in SCI along with acellular spinal cord [262] sciatic nerve [263] and muscle scaffolds [264].

Tukmachev *et al.* compared the performance of scECM to porcine urinary bladder matrix hydrogel in spinal cord lesions [74]. Both of the hydrogels entirely filled the lesion cavity, prevented pseudocyst formation, grouped astrocytes (glial fibrillary acidic protein positive) and “M1” ($CD68^+$, $CD86^+$) macrophages around the border and “M2” ($CD68^+$, $CD206^+$) macrophages within [74]. Both scECM and porcine urinary bladder matrix hydrogel were mostly degraded after two weeks, which is when downregulated pro-inflammatory gene expression (bFGF gene, haemoglobin-haptoglobin complex scavenger receptor CD163 gene, interferon regulatory factor 5 gene, CCL5 gene and growth associated protein 43 (Gap43) was detected [74]. scECM-specific effects were found after 8 weeks (when the hydrogel degraded) in the upregulation of neurotrophin 3, but also the pro-inflammatory genes bFGF, interferon regulatory factor 5 and caspase 3. No difference in axonal ingrowth (neurofilament 160 positive area) or neo-

vascularisation (protein essential for the repair and maintenance of deoxyribonucleic acid positive area) was found between the hydrogels or the hydrogels carrying human WJ-SC, probably as very few of the cells (mitochondrially encoded cytochrome c oxidase II positive) survived [74]. In SCI, as in other conditions, the xenogeneic non-tissue-specific hydrogel did not seem to have different efficacy compared to the tissue-specific, i.e. the tissue-specific effects were not observed *in vivo*.

Cornelison *et al.* tested peripheral nerve ECM available for clinical use solubilised into a hydrogel [75]. This hydrogel increased the number of "M2" ($CD68^+$, $CD206^+$) macrophages at the spinal cord lesion, whilst the number of "M1" ($CD68^+$, $CCR7^+$) macrophages as well as the locomotor and respiratory recovery remained unchanged [75].

Tukmachev *at al.* and Cornelison *et al.* considered the specificity of the SCI anatomy and found that ECM hydrogels gelled filling in the lesion cavity, whether injected immediately or one week after contusion [74], [75]. All tested ECM hydrogels appeared to degrade quickly [74], [75]. Within one to two weeks, before the complete degradation, ECM hydrogels started influencing the immune response, compared to sham groups, but had very little influence on tissue remodelling [74], [75].

1.3.6 Spinal Cord and Bone Derived ECM Hydrogels

None of the previous studies have investigated anti-inflammatory properties of bone ECM hydrogel (bECM) and scECM. However, there is data on their mechanical properties (Table 1.8), concentration of some structural (Table 1.8) and functional elements and the tissue-specific *in vitro* response they initiated [213], [249], [250], [265].

Mechanical properties of ECM hydrogels depended on the tissue of origin and concentration, even though the results between the authors varied due to the differences in the obtained tissue and instrumentation, regardless of the standardised protocols for scECM and bECM generation and rheological measurement (Table 1.8).

The quantities of vascular endothelial growth factor and bFGF retained in scECM hydrogel after processing were similar to those in porcine urinary bladder matrix, brain ECM and optic nerve ECM hydrogel [249]. However, scECM did not retain nerve growth factor, even though optic nerve ECM hydrogel did [249].

scECM and bECM have previously been shown to be cytocompatible. Mouse primary calvarial cell proliferation was significantly higher on top of bECM (two-dimensional, 2D culture) compared to demineralised bone matrix (DBM) on day 3 [266]. scECM increased pheochromocytoma-derived PC12 cell mitogenesis (1.5 fold) and differentiation (up to 20%), but only the induced chemotactic migration (1.5 fold) was different compared to porcine urinary bladder matrix hydrogel [249]. About 20% more N1E-115 mouse neuroblastoma cells extended neurites (differentiated) in contact with solubilised, i.e. 100 mg ECM/mL cell culture medium, scECM hydrogel, compared to the brain or porcine urinary bladder matrix derived, however only brain derived ECM hydrogel increased the neurite length. In three-dimensional (3D) cell culture, brain derived ECM hydrogels demonstrated stronger tissue-specific effects compared to scECM, as the N1E-115 cells gained extensions sooner, at day 2, whereas it took until day 7 for scECM and porcine urinary bladder matrix hydrogel [250]. The influence of scECM and porcine urinary bladder matrix hydrogels on the extension of dorsal root ganglia neurites did not differ either after 7 days in 2D culture [74].

Previously, the impact of incorporation in ECM-based hydrogels on SCAP was investigated [213]. In bECM 3D culture, SCAP viability seemed higher, whilst in scECM, a higher percentage of SCAP showed elongated morphology [213]. Strong expression of glial cell-derived neurotrophic factor and glyceraldehyde 3-phosphate dehydrogenase (GAPDH) at day 2 and zinc finger protein SNAIL, βIII tubulin, platelet-derived growth factor receptor polypeptide α, vascular endothelial growth factor alpha at day 7 and 14 was detected in SCAP in scECM, whilst routinely cultured SCAP expressed glial cell-derived neurotrophic factor and platelet-derived growth factor receptor polypeptide α at day 2 and SCAP in bECM expressed platelet-derived growth factor receptor polypeptide α and GADPH at day 2 and SNAIL, βIII tubulin, glial cell-derived neurotrophic factor and vascular endothelial growth factor alpha at day 14. In this work scECM seemed to support SCAP neuro-differentiation more than bECM [213]. This potential of scECM to promote neuro-differentiation correlates with the previously mentioned work of Crapo *et al.* [249] and Medberry *at al.* [250].

Table 1.8 Investigated mechanical properties and self-assembly fibre content of bone and spinal cord derived ECM hydrogels

	DBM 3mg/mL [266]	DBM 6mg/mL [266]	bECM 3mg/mL [266]	bECM 6mg/mL [266]	bECM 8mg/mL [213]	scECM 8mg/mL [213]	scECM 8mg/mL [250]	scECM 6mg/mL [250]	scECM 4mg/mL [250]
Mean ± standard deviation (SD) ($p<0.05$)									
Gelation kinetics (turbidimetry)									
Lag phase (t_{lag}, min)					11.25± 1.40	12.00± 1.90		3.60± 5.60	
50% gelation ($t_{1/2}$, min)					21.06± 3.20	20.58± 2.42		8.20± 5.10	
95% gelation (t_{95}, min)					36.00± 0.00	30.25± 2.91		12.20± 4.60	
Speed (S, min^{-1})					0.06± 0.00	0.07± 0.009		0.11± 0.02	
Gelation kinetics (rheometry)									
Storage modulus (G', Pa)	58.70± 4.30	313.00± 31.20	32.50± 3.80	143.70± 7.60	287.17± 8.43	19.35± 1.16	757.00± 74.90	235.50± 63.10	138.50± 33.80
Loss modulus (G", Pa)					42.61± 3.72	2.40± 0.38	93.60± 10.90	37.50± 11.40	16.30± 4.90
Complete gelation (T, min)							28.97± 4.70	7.00± 3.60	11.70± 5.63
Strain stiffening (amplitude %, G' Pa)	43.80, 507.30± 76.40	20.50, 604.30± 133.70	29.20, 202.30± 14.20	20.50, 274.30± 36.30					
Hydrogel composition									
Collagen content	0.93 ± 0.06 mg in digest/ mg of initial dry weight		0.92 ± 0.06 mg in digest/ mg of initial dry weight		84.28± 10.20%	67.41± 23.16%	703.20 ± 47.30 µg /mg dry weight		
Sulphated glycosaminoglycan content					0.30% of dry weight	0.65% of dry weight	1.30 ± 0.90 µg /mg dry weight		

1.4 Aim of the Thesis

1.4.1 Global Hypothesis

Recovery and repair in SCI are hampered by chronic inflammation. A cell-biomaterial strategy may support inflammation resolution, as MSC express and secrete numerous immunoregulatory and reparative molecules and as biomaterials may preserve cell viability and retention at the lesion. Specifically, my hypothesis is that delivery of SCAP with immunoregulatory and regenerative properties, in ECM hydrogels, that have been separately shown to promote immunoregulation and constructive tissue remodelling, may provide a suitable strategy to mitigate inflammation and promote a reparative microenvironment in SCI (Figure 1.13).

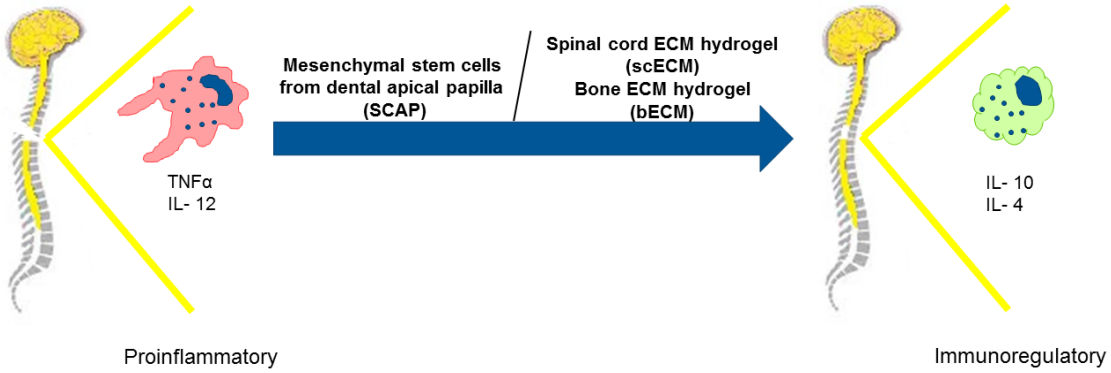


Figure 1.13 General hypothesis: SCAP delivered in scECM or bECM can modulate inflammation in the scope of SCI

1.4.2 Specific Aims and Objectives

A part of the overall hypothesis was that scECM and bECM can be used for SCAP delivery in the scope of SCI. Therefore, the first specific aim was to determine if i) scECM and bECM mechanical properties would be suitable for SCAP incorporation,

experimental manipulation, being in close contact with spinal cord tissue without causing stiffness-related gliosis and maintaining SCAP viability and ii) whether scECM/bECM mechanical properties can be optimised. The first specific objective was then to asses scECM/bECM mechanical properties using rheology, to incorporate SCAP in the hydrogels and to assess SCAP viability. Another part of the same objective was to combine ECM hydrogels with fibrin to improve ECM handling and thus to evaluate the impact of the addition of fibrin on the resulting hydrogel mechanical properties and on SCAP viability.

The second part of the general hypothesis was that scECM, bECM and SCAP have anti-inflammatory properties. Therefore, the second specific aim was to investigate the scECM, bECM and SCAP intrinsic potentials to mitigate microglia activation and whether they are preserved when SCAP are incorporated in ECM hydrogels. The second specific objective was then to assess the changes in inflammatory marker expression in the culture of microglial cells after they were treated with scECM, bECM, SCAP and SCAP incorporated in scECM and bECM (Figure 1.14). Another part of this objective was to assess the marker expression upon the addition of fibrin to ECM hydrogels and ECM hydrogels with SCAP. As different physical forms of ECM hydrogels may expose/release different ligands and active molecules, the third part of this objective was to compare scECM and bECM effect as a solid and a solubilised form on the expression of selected markers (Figure 1.14). A solid form was necessary to incorporate SCAP whilst ECM hydrogels have previously been tested in solubilised form. Moreover, our hypothesis was that a part of ECM hydrogel will gel upon the injection, i.e. take solid form and a part will dissolute and take solubilised form.

According to the general hypothesis, SCAP will be in direct contact with the ECM hydrogel and Th1 pro-inflammatory cytokines at spinal cord lesion. Therefore, the third specific aim was to focus on the hydrogel homologous to the lesion site, scECM and

investigate the differences in the individual and combined impact of Th1 pro-inflammatory cytokines and scECM on SCAP. Another part of this aim was to gain information on SCAP - scECM interplay and further characterise SCAP and scECM. The third specific objective was then to detect and compare the changes in the following conditions: SCAP with pro-inflammatory stimulus (IFNγ, TNFα), scECM, SCAP with scECM and SCAP with scECM and the stimulus, after incubation, using liquid chromatography coupled with mass spectrometry (LC-MS) and metabolomics approach (Figure 1.15).

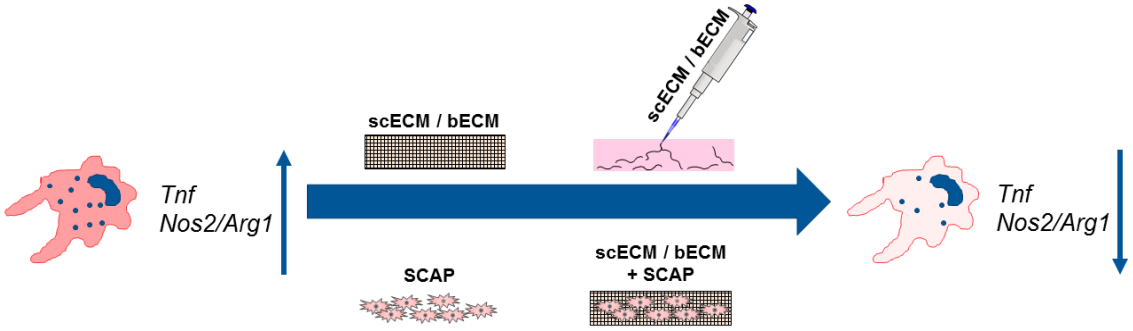


Figure 1.14 Specific hypothesis 2: SCAP alone, ECM hydrogel (solid or solubilised) or SCAP embedded within ECM hydrogel would reduce expression of pro-inflammatory markers in microglial cells

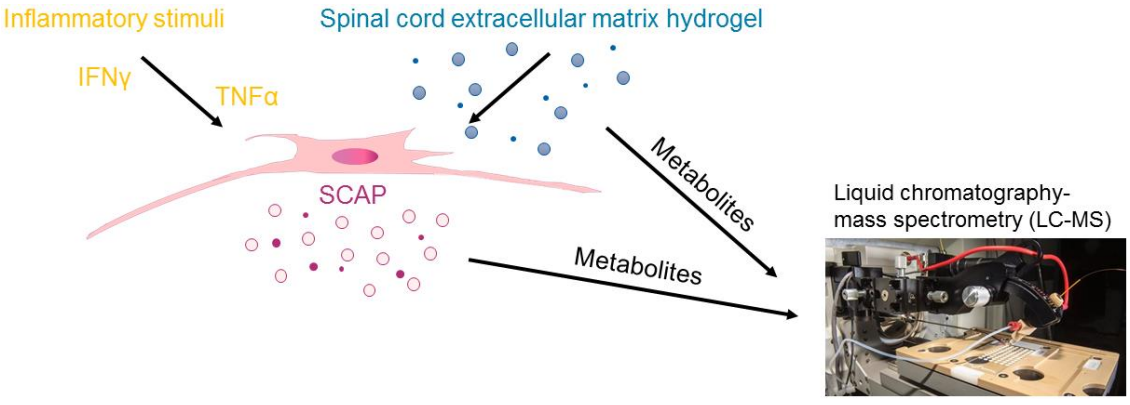


Figure 1.15 Specific hypothesis 3: When SCAP are encapsulated in ECM hydrogel, specifically scECM, the interplay between SCAP and ECM hydrogel would alter the immunoregulative potential of the SCAP and/or ECM hydrogel. The interplay would be reflected in changes in the metabolic footprint of SCAP

1.5 References

[1] World Health Organisation, “Spinal cord injury,” *Fact sheet N°384*, 2013.

[2] B. B. Lee, R. A. Cripps, M. Fitzharris, and P. C. Wing, “The global map for traumatic spinal cord injury epidemiology: Update 2011, global incidence rate,” *Spinal Cord*, vol. 52, no. 2, pp. 110–116, 2014.

[3] N. A. Silva, N. Sousa, R. L. Reis, and A. J. Salgado, “From basics to clinical: A comprehensive review on spinal cord injury,” *Prog. Neurobiol.*, vol. 114, pp. 25–57, 2014.

[4] N. Sezer, “Chronic complications of spinal cord injury,” *World J. Orthop.*, vol. 6, no. 1, p. 24, 2015.

[5] “anatomybody101.com/parasympathetic-vs-sympathetic-nervous-system-pictures.”

[6] “newkunci.co.” http://newkunci.co/dermatomes-chart-and-locations-on-the-skin/.

[7] M. D. Norenberg, J. Smith, and A. Marcillo, “The Pathology of Human Spinal Cord Injury: Defining the Problems,” *J. Neurotrauma*, vol. 21, no. 4, pp. 429–440, 2004.

[8] M. M. Mortazavi *et al.*, “The microanatomy of spinal cord injury: A review.,” *Clin. Anat.*, vol. 00, no. June, pp. 27–36, 2014.

[9] J. C. Fleming *et al.*, “The cellular inflammatory response in human spinal cords after injury,” *Brain*, vol. 129, no. 12, pp. 3249–3269, 2006.

[10] J. H. Badhiwala, C. S. Ahuja, and M. G. Fehlings, “Time is spine: a review of translational advances in spinal cord injury,” *J. Neurosurg. Spine*, vol. 30, no. 1, pp. 1–18, 2019.

[11] C. S. Ahuja *et al.*, “Traumatic spinal cord injury - Repair and regeneration,” *Clin. Neurosurg.*, vol. 80, no. 3, pp. S22–S90, 2017.

[12] J. C. Gensel and B. Zhang, “Macrophage activation and its role in repair and pathology after spinal cord injury,” *Brain Res.*, vol. 1619, pp. 1–11, 2015.

[13] G. Natoli and S. Monticelli, “Macrophage Activation: Glancing into Diversity,” *Immunity*, vol. 40, no. 2, pp. 175–177, 2014.

[14] M. L. Novak and T. J. Koh, “Phenotypic transitions of macrophages orchestrate tissue repair,” *Am. J. Pathol.*, vol. 183, no. 5, pp. 1352–1363, 2013.

[15] F. O. Martinez and S. Gordon, “The M1 and M2 paradigm of macrophage activation: time for reassessment.,” *F1000Prime Rep.*, vol. 6, no. March, p. 13, 2014.

[16] N. Koning, J. Ilarregui, J. García-Vallejo, and Y. van Kooyk, “Antigen-Presenting Cells in the Central Nervous System,” in *Multiple Sclerosis Immunology*, T. Yamamura and B. Gran, Eds. New York: Springer US, 2013.

[17] S. J. Galli, N. Borregaard, and T. A. Wynn, “Phenotypic and functional plasticity of cells of innate immunity: macrophages, mast cells and neutrophils,” *Nat. Immunol.*, vol. 12, no. 11, pp. 1035–1044, 2012.

[18] F. O. Martinez, S. Gordon, M. Locati, and A. Mantovani, “Transcriptional profiling of the human monocyte-to-macrophage differentiation and polarization: new molecules and patterns of gene expression,” *J. Immunol.*, vol. 177, no. 10, pp. 7303–7311, 2006.

[19] G. A. Duque and A. Descoteaux, “Macrophage cytokines: Involvement in immunity and infectious diseases,” *Front. Immunol.*, vol. 5, no. OCT, pp. 1–12, 2014.

[20] T. Rőszer, “Understanding the Mysterious M2 Macrophage through Activation Markers and Effector Mechanisms,” *Mediators Inflamm.*, vol. 2015, pp. 1–16, 2015.

[21] K. A. Kigerl, J. C. Gensel, D. P. Ankeny, J. K. Alexander, D. J. Donnelly, and P. G. Popovich, “Identification of two distinct macrophage subsets with divergent effects causing either neurotoxicity or regeneration in the injured mouse spinal cord.,” *J. Neurosci.*, vol. 29, no. 43, pp. 13435–44, 2009.

[22] I. Metchnikoff and N. Prize, “Mini - review : Macrophage Polarization,” *Biorad*,

vol. 2, pp. 1–8, 2015.

[23] S. P. Gadani, J. T. Walsh, J. R. Lukens, J. Kipnis, and S. T. Program, “Dealing with Danger in the CNS: The Response of the Immune System to Injury,” *Neuron*, vol. 87, no. 1, pp. 47–62, 2015.

[24] D. Davalos *et al.*, “ATP mediates rapid microglial response to local brain injury in vivo,” *Nat. Neurosci.*, vol. 8, no. 6, pp. 752–758, 2005.

[25] F. Martinon, K. Burns, and J. Tschopp, “The Inflammasome: A molecular platform triggering activation of inflammatory caspases and processing of proIL-β,” *Mol. Cell*, vol. 10, no. 2, pp. 417–426, 2002.

[26] Y. Gu *et al.*, “Activation of Interferon-γ Inducing Factor Mediated by Interleukin-1β Converting Enzyme Published by : American Association for the Advancement of Science Stable URL : http://www.jstor.org/stable/2891903 Mediated by Interleukin-1 , Converting Enzyme Activ,” 2016.

[27] M. Keller, A. Rüegg, S. Werner, and H. D. Beer, “Active Caspase-1 Is a Regulator of Unconventional Protein Secretion,” *Cell*, vol. 132, no. 5, pp. 818–831, 2008.

[28] J. E. Burda and M. V. Sofroniew, “Reactive gliosis and the multicellular response to CNS damage and disease,” *Neuron*, vol. 81, no. 2. pp. 229–248, 2014.

[29] J. E. Burda and M. V. Sofroniew, “Reactive gliosis and the multicellular response to CNS damage and disease,” *Neuron*, vol. 81, no. 2, pp. 229–248, 2014.

[30] R. Orihuela, C. A. McPherson, and G. J. Harry, “Microglial M1/M2 polarization and metabolic states,” *Br. J. Pharmacol.*, vol. 173, no. 4, pp. 649–665, 2016.

[31] G. Yiu and Z. He, “Glial inhibition of CNS axon regeneration,” *Nat. Rev. Neurosci.*, vol. 7, no. 8, pp. 617–627, 2006.

[32] H. Wang *et al.*, “Effect of glial cells on remyelination after spinal cord injury,” *Neural Regen. Res.*, vol. 12, no. 10, p. 1724, 2017.

[33] S. A. Liddelow *et al.*, “Neurotoxic reactive astrocytes are induced by activated microglia,” *Nature*, vol. 541, no. 7638, pp. 481–487, 2017.

[34] R. J. McKeon, R. C. Schreiber, J. S. Rudge, and J. Silver, “Reduction of neurite outgrowth in a model of glial scarring following CNS injury is correlated with the expression of inhibitory molecules on reactive astrocytes,” *J. Neurosci.*, vol. 11, no. 11, pp. 3398–3411, 1991.

[35] H.-S. Kuo *et al.*, “Acid Fibroblast Growth Factor and Peripheral Nerve Grafts Regulate Th2 Cytokine Expression, Macrophage Activation, Polyamine Synthesis, and Neurotrophin Expression in Transected Rat Spinal Cords,” *J. Neurosci.*, vol. 31, no. 11, pp. 4137–4147, 2011.

[36] D. P. Ankeny and P. G. Popovich, “B cells and Autoantibodies: Complex Roles in CNS Injury Daniel,” *Trends Immunol.*, vol. 31, no. 9, pp. 332–338, 2010.

[37] D. P. Ankeny, Z. Guan, and P. G. Popovich, “B cells produce pathogenic antibodies and impair recovery after spinal cord injury in mice,” *J. Clin. Invest.*, vol. 119, no. 10, 2009.

[38] G. Yiu and Z. He, “Glial inhibition of CNS axon regeneration,” *Nat. Rev. Neurosci.*, vol. 7, no. 8, pp. 617–627, 2006.

[39] T. P. Monie, “A Snapshot of the Innate Immune System,” in *The Innate Immune System*, Academic Press, 2017, pp. 1–40.

[40] P. M. Vidal, E. Lemmens, D. Dooley, and S. Hendrix, “The role of ‘ anti-inflammatory’ cytokines in axon regeneration,” *Cytokine Growth Factor Rev.*, vol. 24, no. 1, pp. 1–12, 2013.

[41] I. Bollaerts, J. Van Houcke, L. Andries, L. De Groef, and L. Moons, “Neuroinflammation as Fuel for Axonal Regeneration in the Injured Vertebrate Central Nervous System,” *Mediators Inflamm.*, vol. 2017, 2017.

[42] K. A. Kigerl, J. C. Gensel, D. P. Ankeny, J. K. Alexander, D. J. Donnelly, and P. G. Popovich, “Identification of two distinct macrophage subsets with divergent effects causing either neurotoxocity or regeneration in th einjured mouse spinal

cord," *J Neurosci.*, vol. 29, no. 43, pp. 13435–13444, 2010.

[43] T. Yılmaz and E. Kaptanoğlu, "Current and future therapeutic strategies for functional repair of spinal cord injury," *World J. Orthop.*, vol. 6, no. 1, pp. 42–55, 2015.

[44] Y. H. Kim, K. Y. Ha, and S. Il Kim, "Spinal cord injury and related clinical trials," *CiOS Clin. Orthop. Surg.*, vol. 9, no. 1, pp. 1–9, 2017.

[45] T. Eleftheriadis, G. Pissas, V. Liakopoulos, and I. Stefanidis, "Cytochrome c as a potentially clinical useful marker of mitochondrial and cellular damage," *Frontiers in Immunology*, vol. 7, no. JUL. Frontiers Research Foundation, 20-Jul-2016.

[46] C. A. Bowers, B. Kundu, and G. W. J. Hawryluk, "Methylprednisolone for acute spinal cord injury: An increasingly philosophical debate," *Neural Regen. Res.*, vol. 11, no. 6, pp. 882–885, 2016.

[47] V. Cheung, R. Hoshide, V. Bansal, E. Kasper, and C. C. Chen, "Methylprednisolone in the management of spinal cord injuries: Lessons from randomized, controlled trials.," *Surg. Neurol. Int.*, vol. 6, no. 2, p. 142, 2015.

[48] R. C. Assuncao-Silva, E. D. Gomes, N. Sousa, N. A. Silva, and A. J. Salgado, "Hydrogels and Cell Based Therapies in Spinal Cord Injury Regeneration," *Stem Cells Int*, vol. 2015, p. 948040, 2015.

[49] W. Martens, A. Bronckaers, C. Politis, R. Jacobs, and I. Lambrichts, "Dental stem cells and their promising role in neural regeneration: An update," *Clin. Oral Investig.*, vol. 17, no. 9, pp. 1969–1983, 2013.

[50] A. Yamamoto, K. Sakai, K. Matsubara, F. Kano, and M. Ueda, "Multifaceted neuro-regenerative activities of human dental pulp stem cells for functional recovery after spinal cord injury," *Neuroscience Research*, vol. 78, no. 1. pp. 16–20, 2014.

[51] Z. Cheng *et al.*, "Anti-inflammatory mechanism of neural stem cell transplantation in spinal cord injury," *Int. J. Mol. Sci.*, vol. 17, no. 9, pp. 1–16,

2016.

[52] S. Karimi-Abdolrezaee, E. Eftekharpour, J. Wang, C. M. Morshead, and M. G. Fehlings, “Delayed Transplantation of Adult Neural Precursor Cells Promotes Remyelination and Functional Neurological Recovery after Spinal Cord Injury,” *J. Neurosci.*, vol. 26, no. 13, pp. 3377–3389, 2006.

[53] A. Toft, M. Tome, S. C. Barnett, and J. S. Riddell, “A comparative study of glial and non-neural cell properties for transplant-mediated repair of the injured spinal cord,” *Glia*, vol. 61, no. 4, 2013.

[54] S. Erceg *et al.*, “Transplanted oligodendrocytes and motoneuron progenitors generated from human embryonic stem cells promote locomotor recovery after spinal cord transection,” *Stem Cells*, vol. 28, no. 9, pp. 1541–1549, 2010.

[55] S. H. Lee *et al.*, “Impact of local injection of brain-derived neurotrophic factor–expressing mesenchymal stromal cells (MSCs) combined with intravenous MSC delivery in a canine model of chronic spinal cord injury,” *Cytotherapy*, vol. 19, no. 1, pp. 75–87, 2017.

[56] R. B. Shultz, Z. Wang, J. Nong, Z. Zhang, and Y. Zhong, “Local delivery of thyroid hormone enhances oligodendrogenesis and myelination after spinal cord injury,” *J. Neural Eng.*, 2017.

[57] R. Lima *et al.*, “Systemic interleukin-4 administration after spinal cord injury modulates inflammation and promotes neuroprotection,” *Pharmaceuticals*, vol. 10, no. 4, pp. 1–16, 2017.

[58] R. Putatunda, J. R. Bethea, and W. Hu, “Potential immunotherapies for traumatic brain and spinal cord injury,” *Chinese J. Traumatol.*, vol. 21, no. 3, pp. 125–136, 2018.

[59] A. R. Harvey, S. J. Lovett, B. T. Majda, J. H. Yoon, L. P. G. Wheeler, and S. I. Hodgetts, “Neurotrophic factors for spinal cord repair : Which , where , how and when to apply , and for what period of time ?,” *Brain Res.*, vol. 1619, pp. 36–71, 2015.

[60] C. C. Ko *et al.*, “Functional improvement in chronic human spinal cord injury: Four years after acidic fibroblast growth factor,” *Sci. Rep.*, vol. 8, no. 1, Dec. 2018.

[61] M. C. Jimenez Hamann, C. H. Tator, and M. S. Shoichet, “Injectable intrathecal delivery system for localized administration of EGF and FGF-2 to the injured rat spinal cord,” *Exp. Neurol.*, vol. 194, no. 1, pp. 106–119, 2005.

[62] M. A. Anderson *et al.*, “Required growth facilitators propel axon regeneration across complete spinal cord injury,” *Nature*, vol. 561, no. 7723, pp. 396–400, 2018.

[63] A. R. Harvey, S. J. Lovett, B. T. Majda, J. H. Yoon, L. P. G. Wheeler, and S. I. Hodgetts, “Neurotrophic factors for spinal cord repair: Which, where, how and when to apply, and for what period of time?,” *Brain Res.*, vol. 1619, pp. 36–71, 2015.

[64] M. D. Baumann *et al.*, “An injectable drug delivery platform for sustained combination therapy,” *J. Control. Release*, vol. 138, no. 3, pp. 205–213, 2009.

[65] T. Saxena *et al.*, “Nanocarrier-mediated inhibition of macrophage migration inhibitory factor attenuates secondary injury after spinal cord injury,” *ACS Nano*, 2015.

[66] E. Ansorena *et al.*, “Injectable alginate hydrogel loaded with GDNF promotes functional recovery in a hemisection model of spinal cord injury,” *Int. J. Pharm.*, vol. 455, no. 1–2, pp. 148–158, 2013.

[67] A. Des Rieux *et al.*, “Vascular endothelial growth factor-loaded injectable hydrogel enhances plasticity in the injured spinal cord,” *J. Biomed. Mater. Res. - Part A*, vol. 102, no. 7, pp. 2345–2355, 2014.

[68] I. Elliott Donaghue, C. H. Tator, and M. S. Shoichet, “Sustained delivery of bioactive neurotrophin-3 to the injured spinal cord,” *Biomater. Sci.*, 2015.

[69] J. R. Siebert, A. M. Eade, and D. J. Osterhout, “Biomaterial Approaches to Enhancing Neurorestoration after Spinal Cord Injury: Strategies for Overcoming

Inherent Biological Obstacles," *Biomed Res. Int.*, vol. 2015, pp. 1–20, 2015.

[70] M. C. Jimenez Hamann, E. C. Tsai, C. H. Tator, and M. S. Shoichet, "Novel intrathecal delivery system for treatment of spinal cord injury," *Exp. Neurol.*, vol. 182, no. 2, pp. 300–309, 2003.

[71] D. Macaya and M. Spector, "Injectable hydrogel materials for spinal cord regeneration: A review," *Biomed. Mater.*, vol. 7, no. 1, 2012.

[72] G. Perale *et al.*, "Multiple drug delivery hydrogel system for spinal cord injury repair strategies," *J. Control. Release*, 2012.

[73] T. Führmann, P. N. Anandakumaran, and M. S. Shoichet, "Combinatorial Therapies After Spinal Cord Injury: How Can Biomaterials Help?," *Adv. Healthc. Mater.*, vol. 6, no. 10, pp. 1–21, 2017.

[74] D. Tukmachev *et al.*, "Injectable Extracellular Matrix Hydrogels as Scaffolds for Spinal Cord Injury Repair.," *Tissue Eng. Part A*, vol. 22, no. 3–4, pp. 306–17, 2016.

[75] R. C. Cornelison, E. J. Gonzalez-rothi, S. L. Porvasnik, S. M. Wellman, and J. H. Park, "Injectable hydrogels of optimized acellular nerve for injection in the injured spinal cord," 2018.

[76] A. E. Haggerty, M. M. Marlow, and M. Oudega, "Extracellular matrix components as therapeutics for spinal cord injury," *Neurosci. Lett.*, vol. 652, pp. 50–55, 2017.

[77] P. M. Crapo, S. Tottey, P. F. Slivka, and S. F. Badylak, "Effects of biologic scaffolds on human stem cells and implications for CNS tissue engineering.," *Tissue Eng Part A*, vol. 20, no. 1–2, 2013.

[78] J. W. Song *et al.*, "Low-level laser facilitates alternatively activated macrophage/microglia polarization and promotes functional recovery after crush spinal cord injury in rats," *Sci. Rep.*, vol. 7, no. 1, pp. 1–13, 2017.

[79] C.-W. Chiu *et al.*, "The immunomodulator decoy receptor 3 improves locomotor functional recovery after spinal cord injury," *J. Neuroinflammation*, vol. 13, pp.

1–12, 2016.

[80] T. Kuboyama *et al.*, “HDAC3 inhibition ameliorates spinal cord injury by immunomodulation,” *Sci. Rep.*, vol. 7, no. 1, pp. 1–13, 2017.

[81] W. Gao and J. Li, “Targeted siRNA delivery reduces nitric oxide mediated cell death after spinal cord injury,” *J. Nanobiotechnology*, vol. 15, no. 1, pp. 1–11, 2017.

[82] S. Papa *et al.*, “Selective nanovector mediated treatment of activated proinflammatory microglia/macrophages in spinal cord injury,” *ACS Nano*, 2013.

[83] L. Zhao *et al.*, “Exosomes derived from bone marrow mesenchymal stem cells overexpressing microRNA-25 protect spinal cords against transient ischemia,” *J. Thorac. Cardiovasc. Surg.*, vol. 157, no. 2, pp. 508–517, 2019.

[84] G. Sun *et al.*, “hucMSC derived exosomes promote functional recovery in spinal cord injury mice via attenuating inflammation,” *Mater. Sci. Eng. C*, vol. 89, no. January, pp. 194–204, 2018.

[85] P. De Berdt *et al.*, “Dental Apical Papilla as Therapy for Spinal Cord Injury.,” *J. Dent. Res.*, vol. 94, no. 11, pp. 1575–81, 2015.

[86] D. A. McCreedy and S. E. Sakiyama-Elbert, “Combination therapies in the CNS: Engineering the environment,” *Neurosci. Lett.*, vol. 519, no. 2, pp. 115–121, 2012.

[87] E. J. Bradbury and S. B. McMahon, “Spinal cord repair strategies: Why do they work?,” *Nat. Rev. Neurosci.*, vol. 7, no. 8, pp. 644–653, 2006.

[88] S. Thuret, L. D. F. Moon, and F. H. Gage, “Therapeutic interventions after spinal cord injury,” *Nat. Rev. Neurosci.*, vol. 7, no. 8, pp. 628–643, 2006.

[89] Niguarda Hospital, “Evaluation of Tolerability and Efficacy of Erythropoietin (EPO) Treatment in Spinal Shock : Comparative Study Versus Methylprednisolone (MP),” *ClinicalTrials.gov Identifier: NCT00561067*, 2019.

[90] BioAxone BioSciences Inc., “Cethrin in Acute Cervical Spinal Cord Injury,” *ClinicalTrials.gov Identifier: NCT02053883*, 2014.

[91] BioArctic AB, “Safety and Efficacy of SC0806 (Fibroblast Growth Factor 1 and a Device) in Traumatic Spinal Cord Injury Subjects,” *ClinicalTrials.gov Identifier: NCT02490501*, 2019.

[92] General Hospital of Chinese Armed Police Forces, “Different Efficacy Between Rehabilitation Therapy and Stem Cells Transplantation in Patients With SCI in China (SCI-III),” *ClinicalTrials.gov Identifier: NCT01873547*, 2018.

[93] S. R. AbilityLab, “Motor Learning in a Customized Body-Machine Interface (BMI),” *ClinicalTrials.gov Identifier: NCT01608438*, 2018.

[94] Shirley Ryan AbilityLab, “EKSO Trial : Powered Exoskeleton for Ambulation in Subjects With Spinal Cord Injury (SCI) (EKSO),” *ClinicalTrials.gov Identifier: NCT01701388*, 2019.

[95] C. Bouton, “Restoring Motor and Sensory Hand Function in Tetraplegia Using a Neural Bypass System,” *ClinicalTrials.gov Identifier: NCT03680872*, 2018.

[96] M. G. Fehlings, A. Ulndreaj, and A. Badner, “Promising neuroprotective strategies for traumatic spinal cord injury with a focus on the differential effects among anatomical levels of injury,” *F1000Research*, vol. 6. Faculty of 1000 Ltd, 2017.

[97] J. Donovan and S. Kirshblum, “Clinical Trials in Traumatic Spinal Cord Injury,” *Neurotherapeutics*, vol. 15, no. 3. Springer New York LLC, pp. 654–668, 01-Jul-2018.

[98] M. P. Côté, M. Murray, and M. A. Lemay, “Rehabilitation Strategies after Spinal Cord Injury: Inquiry into the Mechanisms of Success and Failure,” *Journal of Neurotrauma*, vol. 34, no. 10. Mary Ann Liebert Inc., pp. 1841–1857, 15-May-2017.

[99] “Virtual Sailing Simulator in Individuals With Spinal Cord Injury - Full Text View - ClinicalTrials.gov.”

[100] “Multi-functional Neuroprosthetic System for Restoration of Motor Function in Spinal Cord Injury - Full Text View - ClinicalTrials.gov.”

[101] “Brain Machine Interface (BMI) in Subjects Living With Quadriplegia | Clinical Research Trial Listing (Spinal Cord Injury) (NCT02564419).”

[102] W. Dalton Dietrich, “Safety of Autologous Human Schwann Cells (ahSC) in Subjects With Subacute SCI,” *ClinicalTrials.gov Identifier: NCT01739023*, 2019.

[103] Wroclaw Medical University, “Autologous Bulbar Olfactory Ensheathing Cells and Nerve Grafts for Treatment of Patients With Spinal Cord Transection,” *ClinicalTrials.gov Identifier: NCT03933072*, 2019.

[104] I. Asterias Biotherapeutics and Information, “Dose Escalation Study of AST-OPC1 in Spinal Cord Injury,” *ClinicalTrials.gov Identifier: NCT02302157*, 2019.

[105] Proneuron Biotechnologies, “Autologous Incubated Macrophages for Patients With Complete Spinal Cord Injuries,” *ClinicalTrials.gov Identifier: NCT00073853*, 2009.

[106] E. Curtis, J. R. Martin, B. Gabel, C. Jamieson, M. Marsala, and J. D. Ciacci, “A First-in-Human, Phase I Study of Neural Stem Cell Transplantation for Chronic Spinal Cord Injury,” *Cell Stem Cell*, vol. 22, pp. 941–950, 2018.

[107] X. C. Li, C. F. Zhong, G. Bin Deng, R. W. Liang, and C. M. Huang, “Efficacy and safety of bone marrow-derived cell transplantation for spinal cord injury: A systematic review and meta-analysis of clinical trials,” *Clin. Transplant.*, vol. 29, no. 9, pp. 786–795, 2015.

[108] J. W. Hur, T.-H. Cho, D.-H. Park, J.-B. Lee, J.-Y. Park, and Y.-G. Chung, “Intrathecal transplantation of autologous adipose-derived mesenchymal stem cells for treating spinal cord injury: A human trial,” *J. Spinal Cord Med.*, vol. 39, no. 6, pp. 655–664, 2016.

[109] H. Zhu *et al.*, “Phase I–II clinical trial assessing safety and efficacy of umbilical cord blood mononuclear cell transplant therapy of chronic complete spinal cord injury,” *Cell Transplant.*, vol. 25, no. 11, pp. 1925–1943, 2016.

[110] Y. Zhao *et al.*, “Clinical study of neuroregen scaffold combined with human mesenchymal stem cells for the repair of chronic complete spinal cord injury,”

Cell Transplant., vol. 26, no. 5, pp. 891–900, 2017.

[111] “Functional Neural Regeneration Collagen Scaffold Transplantation in Acute Spinal Cord Injury Patients - Full Text View - ClinicalTrials.gov.” https://clinicaltrials.gov/ct2/show/NCT02510365. [Accessed: 10-Dec-2019].

[112] “Search of: cell | Spinal Cord Injuries | Phase 3 - List Results - ClinicalTrials.gov.” [https://clinicaltrials.gov/ct2/results?term=cell&cond=Spinal+Cord+Injuries&Search=Apply&age_v=&gndr=&type=&rslt=&phase=2. [Accessed: 10-Dec-2019].

[113] C. Paul, A. F. Samdani, R. R. Betz, I. Fischer, and B. Neuhuber, “Grafting of human bone marrow stromal cells into spinal cord injury: A comparison of delivery methods,” *Spine (Phila. Pa. 1976).*, vol. 34, no. 4, pp. 328–334, 2009.

[114] M. H. Amer, F. R. A. J. Rose, K. M. Shakesheff, and L. J. White, “A biomaterials approach to influence stem cell fate in injectable cell-based therapies,” *Stem Cell Res. Ther.*, vol. 9, no. 1, pp. 1–15, 2018.

[115] I. Kim, “A brief overview of cell therapy and its product,” *J. Korean Assoc. Oral Maxillofac. Surg.*, vol. 39, no. 5, p. 201, 2013.

[116] R. C. Assunção-Silva, E. D. Gomes, N. Sousa, N. A. Silva, and A. J. Salgado, “Hydrogels and Cell Based Therapies in Spinal Cord Injury Regeneration,” *Stem Cells International*, vol. 2015. 2015.

[117] M. Krampera, A. Pasini, G. Pizzolo, L. Cosmi, S. Romagnani, and F. Annunziato, “Regenerative and immunomodulatory potential of mesenchymal stem cells.”

[118] M. Krampera *et al.*, “Induction of neural-like differentiation in human mesenchymal stem cells derived from bone marrow , fat , spleen and thymus,” vol. 40, pp. 382–390, 2007.

[119] M. Dominici *et al.*, “Minimal criteria for defining multipotent mesenchymal stromal cells. The International Society for Cellular Therapy position statement.,” *Cytotherapy*, vol. 8, no. 4, pp. 315–317, 2006.

[120] K. Le Blanc, C. Tammik, K. Rosendahl, E. Zetterberg, and O. Ringdén, “HLA expression and immunologic properties of differentiated and undifferentiated mesenchymal stem cells,” *Exp. Hematol.*, vol. 31, no. 10, pp. 890–896, 2003.

[121] M. J. Hoogduijn *et al.*, “The immunomodulatory properties of mesenchymal stem cells and their use for immunotherapy,” *Int. Immunopharmacol.*, vol. 10, no. 12, pp. 1496–1500, 2010.

[122] K. Le Blanc *et al.*, “Mesenchymal stem cells for treatment of steroid-resistant , severe , acute graft-versus-host disease : a phase II study,” pp. 1579–1586.

[123] G. T.-J. H. Wataru Sonoyama, Yi Liu, Takayoshi Yamaza, Rocky S. Tuan, Songlin Wang, Songtao Shi, “Characterization of Apical Papilla and its Residing Stem Cells from Human Immaturer Permanent Teeth-A Pilot Study,” vol. 34, no. 2, pp. 166–171, 2009.

[124] T. Ha Le Bao, T. Thi Huyen Dinh, and N. Hao Thi Thu, “Stem cells from apical papilla and their properties in two primary culture methods,” *Int. J. Biomed. Res.*, vol. 5, no. 8, 2014.

[125] N. B. Ruparel, J. F. A. De Almeida, M. A. Henry, and A. Diogenes, “Characterization of a stem cell of apical papilla cell line: Effect of passage on cellular phenotype,” *J. Endod.*, vol. 39, no. 3, pp. 357–363, 2013.

[126] A. Bakopoulou *et al.*, “Angiogenic Potential and Secretome of Human Apical Papilla Mesenchymal Stem Cells in Various Stress Microenvironments,” *Stem Cells Dev.*, vol. 24, no. 21, pp. 2496–2512, 2015.

[127] S. Abe, S. Yamaguchi, and T. Amagasa, “Multilineage Cells from Apical Pulp of Human Tooth with Immature Apex,” *Oral Sci. Int.*, vol. 4, no. 1, pp. 45–58, 2007.

[128] W. Sonoyama *et al.*, “Mesenchymal stem cell-mediated functional tooth regeneration in Swine,” *PLoS One*, vol. 1, no. 1, pp. 1–8, 2006.

[129] A. Bakopoulou and I. About, “Stem Cells of Dental Origin: Current Research Trends and Key Milestones towards Clinical Application,” *Stem Cells International*, vol. 2016. 2016.

[130] J. F. A. de Almeida, P. Chen, M. A. Henry, and A. Diogenes, “Stem Cells of the Apical Papilla Regulate Trigeminal Neurite Outgrowth and Targeting through a BDNF-Dependent Mechanism,” *Tissue Eng. Part A*, vol. 20, no. 23–24, pp. 3089–3100, 2014.

[131] W. Zhang, X. Zhang, J. Ling, X. Wei, and Y. Jian, “Osteo-/odontogenic differentiation of BMP2 and VEGF gene-co-transfected human stem cells from apical papilla,” *Mol. Med. Rep.*, vol. 13, no. 5, pp. 3747–3754, 2016.

[132] A. M. Ziemba and R. J. Gilbert, “Biomaterials for local, controlled drug delivery to the injured spinal cord,” *Front. Pharmacol.*, vol. 8, no. MAY, pp. 1–20, 2017.

[133] R. Secunda, R. Vennila, A. M. Mohanashankar, M. Rajasundari, S. Jeswanth, and R. Surendran, “Isolation, expansion and characterisation of mesenchymal stem cells from human bone marrow, adipose tissue, umbilical cord blood and matrix: a comparative study,” *Cytotechnology*, vol. 67, no. 5, pp. 793–807, 2015.

[134] G. N. Stacey *et al.*, “Preservation and stability of cell therapy products: recommendations from an expert workshop,” *Regen. Med.*, vol. 12, no. 5, pp. 553–564, 2017.

[135] S. Beyth *et al.*, “and induce T-cell unresponsiveness Human mesenchymal stem cells alter antigen-presenting cell maturation and induce T-cell unresponsiveness,” *Blood*, vol. 105, no. 5, pp. 2214–2219, 2010.

[136] K. Le Blanc, “Mesenchymal stromal cells: Tissue repair and immune modulation.,” *Cytotherapy*, vol. 8, no. 6, pp. 559–61, 2006.

[137] T. de Witte *et al.*, “Value of allogeneic versus autologous stem cell transplantation and chemotherapy in patients with myelodysplastic syndromes and secondary acute myeloid leukemia. Final results of a prospective randomized European intergroup trial,” *Haematologica*, vol. 95, no. 10, pp. 1754–1761, 2010.

[138] N. M. Reddy *et al.*, “Comparison of Autologous Vs. Allogeneic Stem Cell Transplantation for Non-Hodgkin Lymphoma,” *Blood*, vol. 120, no. 21, pp. 2036

LP – 2036, Nov. 2012.

[139] S. Yu, Y. Zhao, Y. Ma, and L. Ge, “Profiling the Secretome of Human Stem Cells from Dental Apical Papilla,” *Stem Cells Dev.*, vol. 25, no. 6, pp. 499–508, 2016.

[140] G. T.-J. Huang, S. Gronthos, and S. Shi, “Mesenchymal stem cells derived from dental tissues vs. those from other sources: their biology and role in regenerative medicine.,” *J. Dent. Res.*, vol. 88, no. 9, pp. 792–806, 2009.

[141] A. Bakopoulou, G. Leyhausen, J. Volk, P. Koidis, and W. Geurtsen, “Comparative characterization of STRO-1 neg / stem cells enriched with flow cytometry,” *Arch. Oral Biol.*, vol. 58, no. 10, pp. 1556–1568, 2013.

[142] C. Yang *et al.*, “ The Potential of Dental Stem Cells Differentiating into Neurogenic Cell Lineage after Cultivation in Different Modes In Vitro ,” *Cell. Reprogram.*, vol. 16, no. 5, pp. 379–391, 2014.

[143] M. I. Zvereva, D. M. Shcherbakova, and O. A. Dontsova, “Telomerase: Structure, functions, and activity regulation,” *Biochem.*, vol. 75, no. 13, pp. 1563–1583, 2010.

[144] A. C. Mita, M. M. Mita, S. T. Nawrocki, and F. J. Giles, “Survivin: Key regulator of mitosis and apoptosis and novel target for cancer therapeutics,” *Clin. Cancer Res.*, vol. 14, no. 16, pp. 5000–5005, 2008.

[145] S. Abe, S. Yamaguchi, A. Watanabe, K. Hamada, and T. Amagasa, “Hard tissue regeneration capacity of apical pulp derived cells (APDCs) from human tooth with immature apex,” *Biochem. Biophys. Res. Commun.*, vol. 371, no. 1, pp. 90–93, 2008.

[146] J. Vanacker *et al.*, “Hypoxia modulates the differentiation potential of stem cells of the apical papilla,” *J. Endod.*, vol. 40, no. 9, pp. 1410–1418, 2014.

[147] P. de Berdt *et al.*, “Stem cells from human apical papilla decrease neuro-inflammation and stimulate oligodendrocyte progenitor differentiation via activin-A secretion,” *Cell. Mol. Life Sci.*, no. 0123456789, pp. 1–14, 2018.

[148] D. Kyurkchiev, “Secretion of immunoregulatory cytokines by mesenchymal stem cells,” *World J. Stem Cells*, vol. 6, no. 5, p. 552, 2014.

[149] R. Haddad and F. Saldanha-Araujo, “Mechanisms of T-cell immunosuppression by mesenchymal stromal cells: What do we know so far?,” *Biomed Res. Int.*, vol. 2014, 2014.

[150] X. Chen, M. A. Armstrong, and G. Li, “Mesenchymal stem cells in immunoregulation,” *Immunol. Cell Biol.*, vol. 84, no. 5, pp. 413–421, 2006.

[151] S. Ma, N. Xie, W. Li, B. Yuan, Y. Shi, and Y. Wang, “Immunobiology of mesenchymal stem cells.,” *Cell Death Differ.*, vol. 21, no. 2, pp. 216–25, 2014.

[152] W. Seong Toh, R. Chai Lai, J. Hoi Po Hui, and S. Kiang Lim, “MSC exosome as a cell-free MSC therapy for cartilage regeneration : Implications for osteoarthritis treatment,” *Semin. Cell Dev. Biol.*, vol. 67, pp. 56–64, 2017.

[153] L. Zhao, X. Jiang, J. Shi, S. Gao, and Y. Zhu, “Exosomes derived from bone marrow mesenchymal stem cells overexpressing microRNA-25 protect spinal cords against transient ischemia,” *J. Thorac. Cardiovasc. Surg.*, vol. 157, no. 2, pp. 508–517, 2019.

[154] M. Krampera *et al.*, “Bone marrow mesenchymal stem cells inhibit the response of naive and memory antigen-specific T cells to their cognate peptide,” vol. 101, no. 9, pp. 3722–3729, 2003.

[155] A. Corcione *et al.*, “Human mesenchymal stem cells modulate B-cell functions,” *Mult. Scler.*, vol. 107, no. 1, pp. 367–372, 2006.

[156] A. Uccelli, L. Moretta, and V. Pistoia, “Immunoregulatory function of mesenchymal stem cells,” pp. 2566–2573, 2006.

[157] S. Forostyak, P. Jendelova, and E. Sykova, “The role of mesenchymal stromal cells in spinal cord injury, regenerative medicine and possible clinical applications,” *Biochimie*, vol. 95, no. 12, pp. 2257–2270, 2013.

[158] A. J. Mothe and C. H. Tator, “Science in medicine Advances in stem cell therapy for spinal cord injury,” *J. Clin. Invest.*, vol. 122, no. 11, pp. 3824–3834, 2012.

[159] S. Hornsey, R. Myers, P. G. Coultas, M. A. Rogers, and A. White, “Turnover of proliferative cells in the spinal cord after X irradiation and its relation to time-dependent repair of radiation damage,” *Br. J. Radiol.*, 1981.

[160] P. de Berdt *et al.*, “Stem cells from human apical papilla decrease neuro-inflammation and stimulate oligodendrocyte progenitor differentiation via activin-A secretion,” *Cellular and Molecular Life Sciences*, pp. 1–14, 2018.

[161] T. LIN *et al.*, “Transplanted interleukin-4–secreting mesenchymal stromal cells show extended survival and increased bone mineral density in the murine femur,” *Cytotherapy*, vol. 20, no. 8, pp. 1028–1036, 2018.

[162] S. H. Lee *et al.*, “Impact of local injection of brain-derived neurotrophic factor – expressing mesenchymal stromal cells (MSCs) combined with intravenous MSC delivery in a canine model of chronic spinal cord injury,” *Cytotherapy*, vol. 19, no. 1, pp. 75–87, 2017.

[163] A. Nowakowski, P. Walczak, B. Lukomska, and M. Janowski, “Genetic Engineering of Mesenchymal Stem Cells to Induce Their Migration and Survival,” vol. 2016, 2016.

[164] H. Chen *et al.*, “Pre-activation of mesenchymal stem cells with TNF-α, IL-1β 2 and nitric oxide enhances its paracrine effects on radiation-induced intestinal injury,” *Sci. Rep.*, vol. 5, pp. 1–14, 2015.

[165] X. Li, W. Du, F. X. Ma, X. Feng, F. Bayard, and Z. C. Han, “High concentrations of TNF-α induce cell death during interactions between human umbilical cord mesenchymal stem cells and peripheral blood mononuclear cells,” *PLoS One*, vol. 10, no. 5, pp. 1–13, 2015.

[166] L. C. J. van den Berk *et al.*, “Mesenchymal stem cells respond to TNF but do not produce TNF,” *J. Leukoc. Biol.*, vol. 87, no. 2, pp. 283–289, 2010.

[167] Y. W. Kwon *et al.*, “Tumor necrosis factor-α-activated mesenchymal stem cells promote endothelial progenitor cell homing and angiogenesis,” *Biochim. Biophys. Acta - Mol. Basis Dis.*, vol. 1832, no. 12, pp. 2136–2144, 2013.

[168] W. Broekman *et al.*, “TNF-α and IL-1β-activated human mesenchymal stromal cells increase airway epithelial wound healing in vitro via activation of the epidermal growth factor receptor,” *Respir. Res.*, vol. 17, no. 1, p. 3, 2016.

[169] P. R. Crisostomo, Y. Wang, T. A. Markel, M. Wang, T. Lahm, and D. R. Meldrum, “Human mesenchymal stem cells stimulated by TNF- , LPS, or hypoxia produce growth factors by an NF B- but not JNK-dependent mechanism,” *AJP Cell Physiol.*, vol. 294, no. 3, pp. C675–C682, 2008.

[170] D. Polchert *et al.*, “Prevention of Graft Versus Host Disease,” vol. 38, no. 6, pp. 1745–1755, 2011.

[171] D. S. Kim *et al.*, “Enhanced Immunosuppressive Properties of Human Mesenchymal Stem Cells Primed by Interferon-γ,” *EBioMedicine*, vol. 28, pp. 261–273, 2018.

[172] P. Jin *et al.*, “Interferon-γ and Tumor Necrosis Factor-α Polarize Bone Marrow Stromal Cells Uniformly to a Th1 Phenotype,” *Sci. Rep.*, vol. 6, no. May, pp. 1–11, 2016.

[173] K. English, F. P. Barry, C. P. Field-Corbett, and B. P. Mahon, “IFN-γ and TNF-α differentially regulate immunomodulation by murine mesenchymal stem cells,” *Immunol. Lett.*, vol. 110, no. 2, pp. 91–100, 2007.

[174] Q. Guan, P. Ezzati, V. Spicer, O. Krokhin, D. Wall, and J. A. Wilkins, “Interferon γ induced compositional changes in human bone marrow derived mesenchymal stem/stromal cells,” *Clin. Proteomics*, vol. 14, no. 26, 2017.

[175] K. N. Sivanathan, D. Rojas-Canales, S. T. Grey, S. Gronthos, and P. T. Coates, “Transcriptome Profiling of IL-17A Preactivated Mesenchymal Stem Cells: A Comparative Study to Unmodified and IFN- *γ* Modified Mesenchymal Stem Cells,” *Stem Cells Int.*, vol. 2017, pp. 1–16, 2017.

[176] M. W. Klinker, R. A. Marklein, J. L. Lo Surdo, C.-H. Wei, and S. R. Bauer, “Morphological features of IFN-γ–stimulated mesenchymal stromal cells predict overall immunosuppressive capacity,” *Proc. Natl. Acad. Sci.*, vol. 114, no. 13,

pp. E2598–E2607, 2017.

[177] J. M. Ryan, F. Barry, J. M. Murphy, and B. P. Mahon, “Interferon-γ does not break, but promotes the immunosuppressive capacity of adult human mesenchymal stem cells,” *Clin. Exp. Immunol.*, vol. 149, no. 2, pp. 353–363, 2007.

[178] Y. Sen Hou *et al.*, “Lipopolysaccharide pretreatment inhibits LPS-induced human umbilical cord mesenchymal stem cell apoptosis via upregulating the expression of cellular FLICE-inhibitory protein,” *Mol. Med. Rep.*, vol. 12, no. 2, pp. 2521–2528, 2015.

[179] X. He, H. Wang, T. Jin, Y. Xu, L. Mei, and J. Yang, “TLR4 activation promotes bone marrow MSC proliferation and osteogenic differentiation via wnt3a and wnt5a signaling,” *PLoS One*, vol. 11, no. 3, pp. 1–20, 2016.

[180] H. Fan *et al.*, “Pre-treatment with IL-1β enhances the efficacy of MSC transplantation in DSS-induced colitis,” *Cell. Mol. Immunol.*, vol. 9, no. 6, pp. 473–481, 2012.

[181] A. P. Bastidas-Coral *et al.*, “ Cytokines TNF- α , IL-6, IL-17F, and IL-4 Differentially Affect Osteogenic Differentiation of Human Adipose Stem Cells ,” *Stem Cells Int.*, vol. 2016, pp. 1–9, 2016.

[182] F. Lizcano, D. Vargas, Á. Gómez, and A. Torrado, “Human ADMC-Derived Adipocyte Thermogenic Capacity Is Regulated by IL-4 Receptor,” *Stem Cells Int.*, vol. 2017, pp. 1–10, 2017.

[183] J. Y. Lim *et al.*, “Enhanced immunoregulation of mesenchymal stem cells by IL-10-producing type 1 regulatory T cells in collagen-induced arthritis,” *Sci. Rep.*, vol. 6, no. January, pp. 1–13, 2016.

[184] Q. Bie *et al.*, “IL-17B activated mesenchymal stem cells enhance proliferation and migration of gastric cancer cells,” *Oncotarget*, vol. 8, no. 12, pp. 18914–18923, 2017.

[185] A. Pourgholaminejad, N. Aghdami, H. Baharvand, and S. M. Moazzeni, “The

effect of pro-inflammatory cytokines on immunophenotype, differentiation capacity and immunomodulatory functions of human mesenchymal stem cells," *Cytokine*, vol. 85, pp. 51–60, 2016.

[186] "Biomaterial," *Merriam-Webster*. https://www.merriam-webster.com/dictionary/biomaterial.

[187] L. S. Nair and C. T. Laurencin, "Biodegradable polymers as biomaterials," vol. 32, pp. 762–798, 2007.

[188] A. P. Amar, D. W. Larsen, and G. P. Teitelbaum, "Percutaneous spinal interventions," *Neurosurg. Clin. N. Am.*, vol. 16, no. 3, pp. 561–568, 2005.

[189] T. Brinker, E. Stopa, J. Morrison, and P. Klinge, "A new look at cerebrospinal fluid circulation," *Fluids Barriers CNS*, vol. 11, no. 1, pp. 1–16, 2014.

[190] U. Tutak and D. M. Doleys, "Intrathecal infusion systems for treatment of chronic low back and leg pain of noncancer origin." pp. 295–300, 1996.

[191] R. Sridharan, A. R. Cameron, D. J. Kelly, C. J. Kearney, and F. J. O'Brien, "Biomaterial based modulation of macrophage polarization: A review and suggested design principles," *Mater. Today*, vol. 18, no. 6, pp. 313–325, 2015.

[192] Š. Kubinová and E. Syková, "Biomaterials combined with cell therapy for treatment of spinal cord injury," *Regen. Med.*, vol. 7, no. 2, pp. 207–224, 2012.

[193] J. Růžička *et al.*, "Treating spinal cord injury in rats with a combination of human fetal neural stem cells and hydrogels modified with serotonin.," *Acta Neurobiol. Exp. (Wars).*, vol. 73, no. 1, pp. 102–15, 2013.

[194] E. Syková and P. Jendelová, "Magnetic resonance tracking of implanted adult and embryonic stem cells in injured brain and spinal cord," in *Annals of the New York Academy of Sciences*, 2005, vol. 1049, pp. 146–160.

[195] S. H. Min *et al.*, "Development of complete thoracic spinal cord transection model in rats for delayed transplantation of stem cells," *Spine (Phila. Pa. 1976).*, vol. 36, no. 3, Feb. 2011.

[196] A. Hejčl *et al.*, "HPMA-RGD hydrogels seeded with mesenchymal stem cells

improve functional outcome in chronic spinal cord injury," *Stem Cells Dev.*, vol. 19, no. 10, pp. 1535–1546, Oct. 2010.

[197] D. H. Hwang *et al.*, "Combination of multifaceted strategies to maximize the therapeutic benefits of neural stem cell transplantation for spinal cord repair," *Cell Transplant.*, vol. 20, no. 9, pp. 1361–1379, 2011.

[198] Y. D. Teng *et al.*, "Functional recovery following traumatic spinal cord injury mediated by a unique polymer scaffold seeded with neural stem cells," *Proc. Natl. Acad. Sci. U. S. A.*, vol. 99, no. 5, pp. 3024–3029, Mar. 2002.

[199] D. Yu *et al.*, "Blockade of peroxynitrite-induced neural stem cell death in the acutely injured spinal cord by drug-releasing polymer," *Stem Cells*, vol. 27, no. 5, pp. 1212–1222, 2009.

[200] X. M. Xu, V. Guénard, N. Kleitman, and M. B. Bunge, "Axonal regeneration into Schwann cell-seeded guidance channels grafted into transected adult rat spinal cord," *J. Comp. Neurol.*, vol. 351, no. 1, pp. 145–160, 1995.

[201] J. Y. C. Hsu and X. M. Xu, "Early profiles of axonal growth and astroglial response after spinal cord hemisection and implantation of Schwann cell-seeded guidance channels in adult rats," *J. Neurosci. Res.*, vol. 82, no. 4, pp. 472–483, Nov. 2005.

[202] C. H. Chau *et al.*, "Chondroitinase ABC enhances axonal regrowth through Schwann cell-seeded guidance channels after spinal cord injury.," *FASEB J.*, vol. 18, no. 1, pp. 194–196, 2004.

[203] K. Fouad, L. Schnell, M. B. Bunge, M. E. Schwab, T. Liebscher, and D. D. Pearse, "Combining Schwann cell bridges and olfactory-ensheathing glia grafts with chondroitinase promotes locomotor recovery after complete transection of the spinal cord," *J. Neurosci.*, vol. 25, no. 5, pp. 1169–1178, Feb. 2005.

[204] R. Vavrek, D. D. Pearse, and K. Fouad, "Neuronal populations capable of regeneration following a combined treatment in rats with spinal cord transection," *J. Neurotrauma*, vol. 24, no. 10, pp. 1667–1673, Oct. 2007.

[205] M. J. Moore *et al.*, “Multiple-channel scaffolds to promote spinal cord axon regeneration,” *Biomaterials*, vol. 27, no. 3, pp. 419–429, Jan. 2006.

[206] L. N. Novikova, J. Pettersson, M. Brohlin, M. Wiberg, and L. N. Novikov, “Biodegradable poly-β-hydroxybutyrate scaffold seeded with Schwann cells to promote spinal cord repair,” *Biomaterials*, vol. 29, no. 9, pp. 1198–1206, Mar. 2008.

[207] A. J. Krych *et al.*, “Relationship between scaffold channel diameter and number of regenerating axons in the transected rat spinal cord,” *Acta Biomater.*, vol. 5, no. 7, pp. 2551–2559, Sep. 2009.

[208] L. T. Saldin, M. C. Cramer, S. S. Velankar, L. J. White, and S. F. Badylak, “Extracellular matrix hydrogels from decellularized tissues: Structure and function,” *Acta Biomater.*, vol. 49, pp. 1–15, 2017.

[209] R. Liang *et al.*, “Positive effects of an extracellular matrix hydrogel on rat anterior cruciate ligament fibroblast proliferation and collagen mRNA expression,” *J. Orthop. Transl.*, vol. 3, no. 3, pp. 114–122, 2015.

[210] V. Agrawal, S. Tottey, S. A. Johnson, J. M. Freund, B. F. Siu, and S. F. Badylak, “Recruitment of Progenitor Cells by an Extracellular Matrix Cryptic Peptide in a Mouse Model of Digit Amputation,” *Tissue Eng. Part A*, vol. 17, no. 19–20, pp. 2435–2443, 2011.

[211] L. Huleihel *et al.*, “Matrix-bound nanovesicles within ECM bioscaffolds,” *Sci. Adv.*, vol. 2, no. 6, pp. e1600502–e1600502, 2016.

[212] L. Huleihel *et al.*, “Matrix-Bound Nanovesicles Recapitulate Extracellular Matrix Effects on Macrophage Phenotype,” *Tissue Eng. Part A*, vol. 23, no. 21–22, pp. 1283–1294, 2017.

[213] A. Viswanath *et al.*, “Extracellular Matrix-Derived Hydrogels for Dental Stem Cell Delivery,” *J. Biomed. Mater. Res. Part A*, pp. 1–10, 2016.

[214] Y. Zhu, Y. Matsumura, and W. R. Wagner, “Ventricular wall biomaterial injection therapy after myocardial infarction: Advances in material design, mechanistic

insight and early clinical experiences," *Biomaterials*, vol. 129. Elsevier Ltd, pp. 37–53, 01-Jun-2017.

[215] A. Tuladhar, N. Mitrousis, T. Führmann, and M. S. Shoichet, "Central Nervous System," *Transl. Regen. Med.*, pp. 415–435, Jan. 2015.

[216] R. J. Nagao *et al.*, "Decellularized Human Kidney Cortex Hydrogels Enhance Kidney Microvascular Endothelial Cell Maturation and Quiescence," *Tissue Eng. Part A*, vol. 22, no. 19–20, pp. 1140–1150, 2016.

[217] H. Ijima, S. Nakamura, R. P. Bual, and K. Yoshida, "Liver-specific extracellular matrix hydrogel promotes liver-specific functions of hepatocytes in vitro and survival of transplanted hepatocytes in vivo," *J. Biosci. Bioeng.*, vol. xxx, no. xxx, 2019.

[218] S. D. Sackett *et al.*, "Extracellular matrix scaffold and hydrogel derived from decellularized and delipidized human pancreas," *Sci. Rep.*, vol. 8, no. 1, pp. 1–16, 2018.

[219] R. A. Pouliot *et al.*, "Development and characterization of a naturally derived lung extracellular matrix hydrogel," pp. 1–14, 2016.

[220] M. P. Francis *et al.*, "Human placenta hydrogel reduces scarring in a rat model of cardiac ischemia and enhances cardiomyocyte and stem cell cultures," *Acta Biomater.*, vol. 52, pp. 92–104, 2017.

[221] W. Fu, P. Xu, B. Feng, Y. Lu, and J. Bai, "A hydrogel derived from acellular blood vessel extracellular matrix to promote angiogenesis," 2019.

[222] L. Nehrenheim *et al.*, "Native aortic valve derived extracellular matrix hydrogel for three dimensional culture analyses with improved biomimetic properties," *Biomed. Mater.*, 2019.

[223] Y. Fu *et al.*, "Decellularization of porcine skeletal muscle extracellular matrix for the formulation of a matrix hydrogel: A preliminary study," *J. Cell. Mol. Med.*, vol. 20, no. 4, 2016.

[224] B. N. Brown and S. F. Badylak, "Extracellular matrix as an inductive scaffold for

functional tissue reconstruction," *Transl. Res.*, vol. 163, no. 4, pp. 268–285, 2014.

[225] B. N. Brown *et al.*, "Surface characterization of extracellular matrix scaffolds," *Biomaterials*, vol. 31, no. 3. pp. 428–437, 2010.

[226] J. E. Valentin, J. S. Badylak, G. P. McCabe, and S. F. Badylak, "Extracellular matrix bioscaffolds for orthopaedic applications. A comparative histologic study.," *J. Bone Joint Surg. Am.*, vol. 88, no. 12, pp. 2673–86, 2006.

[227] S. F. Badylak, J. E. Valentin, A. K. Ravindra, G. P. McCabe, and A. M. Stewart-Akers, "Macrophage Phenotype as a Determinant of Biologic Scaffold Remodeling," *Tissue Eng. Part A*, vol. 14, no. 11, pp. 1835–1842, 2008.

[228] H. C. Liang, Y. Chang, C. K. Hsu, M. H. Lee, and H. W. Sung, "Effects of crosslinking degree of an acellular biological tissue on its tissue regeneration pattern," *Biomaterials*, vol. 25, no. 17, pp. 3541–3552, 2004.

[229] Y. Efraim, H. Sarig, N. Cohen, U. Sarig, E. De Berardinis, and S. Chaw, "Biohybrid cardiac ECM-based hydrogels improve long term cardiac function post myocardial infarction," *Acta Biomater.*, vol. 50, pp. 220–233, 2017.

[230] H. W. Sung, W. H. Chang, C. Y. Ma, and M. H. Lee, "Crosslinking of biological tissues using genipin and/or carbodiimide," *J. Biomed. Mater. Res. - Part A*, 2003.

[231] B. Ma, X. Wang, C. Wu, and J. Chang, "Crosslinking strategies for preparation of extracellular matrix-derived cardiovascular scaffolds," pp. 81–89, 2014.

[232] J. Lai, "Biocompatibility of Genipin and Glutaraldehyde Cross-Linked Chitosan Materials in the Anterior Chamber of the Eye," pp. 10970–10985, 2012.

[233] G. Yang, Z. Xiao, H. Long, K. Ma, J. Zhang, and X. Ren, "Assessment of the characteristics and biocompatibility of gelatin sponge scaffolds prepared by various crosslinking methods," *Sci. Rep.*, no. May 2017, pp. 1–13, 2018.

[234] C. Williams *et al.*, "Cardiac extracellular matrix-fibrin hybrid scaffolds with tunable properties for cardiovascular tissue engineering," *Acta Biomater.*, vol.

14, pp. 84–95, 2015.

[235] “A Study of VentriGel in Post-MI Patients - Full Text View - ClinicalTrials.gov,” *NCT02305602*, 2019. https://clinicaltrials.gov/ct2/show/NCT02305602.

[236] Z. Chen, J. Yang, B. Wu, and B. Tawil, “A Novel Three-Dimensional Wound Healing Model,” *J. Dev. Biol.*, vol. 2, no. 4, pp. 198–209, 2014.

[237] V. K. Lai, S. P. Lake, C. R. Frey, R. T. Tranquillo, and V. H. Barocas, “Mechanical Behavior of Collagen-Fibrin Co-Gels Reflects Transition From Series to Parallel Interactions With Increasing Collagen Content,” 2012.

[238] Y.-D. Nien, Y.-P. H. Han, B. Tawil, L. S. Chan, T. Tai-Lan, and W. L. Garner, “Fibrinogen inhibits fibroblast-mediated contraction of collagen,” *Wound Repair Regen.*, vol. 11, no. 5, pp. 380–385, 2003.

[239] V. K. Lai, C. R. Frey, A. M. Kerandi, S. P. Lake, R. T. Tranquillo, and V. H. Barocas, “Microstructural and Mechanical Differences Between Digested Collagen-Fibrin Co-Gels and Pure Collagen and Fibrin Gels,” *Acta Biomater.*, vol. 8, no. 11, pp. 4031–4042, 2012.

[240] V. Reyhani, P. Seddigh, B. Guss, R. Gustafsson, L. Rask, and K. Rubin, “Fibrin binds to collagen and provides a bridge for αVβ3 integrin-dependent contraction of collagen gels,” *Biochem. J.*, vol. 462, no. 1, pp. 113–123, 2014.

[241] K. T. Morin and R. T. Tranquillo, “In vitro models of angiogenesis and vasculogenesis in fibrin gel,” *Exp. Cell Res.*, vol. 319, no. 16, pp. 2409–2417, 2013.

[242] A. Lesman, J. Koffler, R. Atlas, Y. J. Blinder, Z. Kam, and S. Levenberg, “Engineering vessel-like networks within multicellular fibrin-based constructs,” *Biomaterials*, vol. 32, no. 31, pp. 7856–7869, 2011.

[243] M. A. Lafleur, M. M. Handsley, V. Knäuper, G. Murphy, and D. R. Edwards, “Endothelial tubulogenesis within fibrin gels specifically requires the activity of membrane-type-matrix metalloproteinases (MT-MMPs).,” *J. Cell Sci.*, vol. 115, no. Pt 17, pp. 3427–38, 2002.

[244] C. M. A. P. Schuh, A. G. E. Day, H. Redl, and J. Phillips, “An Optimized Collagen-Fibrin Blend Engineered Neural Tissue Promotes Peripheral Nerve Repair,” *Tissue Eng. Part A*, vol. 24, no. 17–18, pp. 1332–1340, 2018.

[245] M. Alonso-Sande *et al.*, “Development of PLGA-mannosamine nanoparticles as oral protein carriers,” *Biomacromolecules*, vol. 14, no. 11, pp. 4046–4052, 2013.

[246] S. L. Voytik-Harbin, A. O. Brightman, B. Z. Waisner, J. P. Robinson, and C. H. Lamar, “Small Intestinal Submucosa: A Tissue-Derived Extracellular Matrix That Promotes Tissue-Specific Growth and Differentiation of Cells in Vitro,” *Tissue Eng.*, vol. 4, no. 2, pp. 157–174, 1998.

[247] T. J. Keane, I. T. Swinehart, and S. F. Badylak, “Methods of tissue decellularization used for preparation of biologic scaffolds and in vivo relevance,” *Methods*, vol. 84. 2015.

[248] B. B. Rothrauff, G. Yang, and R. S. Tuan, “Tissue-specific bioactivity of soluble tendon-derived and cartilage-derived extracellular matrices on adult mesenchymal stem cells,” *Stem Cell Res. Ther.*, vol. 8, no. 1, pp. 1–17, 2017.

[249] P. M. Crapo *et al.*, “Biologic scaffolds composed of central nervous system extracellular matrix,” *Biomaterials*, vol. 33, no. 13, pp. 3539–3547, 2012.

[250] C. J. Medberry *et al.*, “Hydrogels derived from central nervous system extracellular matrix,” *Biomaterials*, vol. 34, no. 4, pp. 1033–1040, 2013.

[251] E. Bible *et al.*, “Biomaterials Non-invasive imaging of transplanted human neural stem cells and ECM scaffold remodeling in the stroke-damaged rat brain by 19 F- and diffusion-MRI,” *Biomaterials*, vol. 33, no. 10, pp. 2858–2871, 2012.

[252] T. J. Keane *et al.*, “Tissue-Specific Effects of Esophageal Extracellular Matrix,” *Tissue Eng. Part A*, vol. 21, no. 17–18, pp. 2293–2300, 2015.

[253] L. Zhang *et al.*, “Effect of an Inductive Hydrogel Composed of Urinary Bladder Matrix Upon Functional Recovery Following Traumatic Brain Injury,” vol. 19, 2013.

[254] J. Y. Wang *et al.*, “Neurorestorative effect of urinary bladder matrix-mediated

neural stem cell transplantation following traumatic brain injury in rats.," *CNS Neurol. Disord. Drug Targets*, vol. 12, no. 3, pp. 413–425, 2013.

[255] H. Ghuman *et al.*, "Acta Biomaterialia Long-term retention of ECM hydrogel after implantation into a sub-acute stroke cavity reduces lesion volume," *Acta Biomater.*, vol. 63, pp. 50–63, 2017.

[256] J. L. Dziki, D. S. Wang, C. Pineda, B. M. Sicari, T. Rausch, and S. F. Badylak, "Solubilized extracellular matrix bioscaffolds derived from diverse source tissues differentially influence macrophage phenotype," pp. 12–15, 2016.

[257] F. W. Meng, P. F. Slivka, C. L. Dearth, and S. F. Badylak, "Solubilized extracellular matrix from brain and urinary bladder elicits distinct functional and phenotypic responses in macrophages," *Biomaterials*, vol. 46, pp. 131–140, 2015.

[258] H. Ghuman *et al.*, "ECM hydrogel for the treatment of stroke: Characterization of the host cell infiltrate," *Biomaterials*, vol. 91, pp. 166–181, 2016.

[259] J. Muhamed, D. Revi, A. Rajan, S. Geetha, and T. V. Anilkumar, "Biocompatibility and Immunophenotypic Characterization of a Porcine Cholecyst–derived Scaffold Implanted in Rats," *Toxicol. Pathol.*, vol. 43, no. 4, pp. 536–545, 2015.

[260] R. M. Wang and K. L. Christman, "Decellularized myocardial matrix hydrogels: In basic research and preclinical studies," *Advanced Drug Delivery Reviews*, vol. 96. 2016.

[261] R. M. Wang and K. L. Christman, "Decellularized myocardial matrix hydrogels: In basic research and preclinical studies," *Adv. Drug Deliv. Rev.*, vol. 96, pp. 77–82, Jan. 2016.

[262] J. Liu *et al.*, "Acellular spinal cord scaffold seeded with mesenchymal stem cells promotes long-distance axon regeneration and functional recovery in spinal cord injured rats," *J. Neurol. Sci.*, vol. 325, no. 1–2, pp. 127–136, 2013.

[263] C. Li *et al.*, "Allografts of the Acellular Sciatic Nerve and Brain-Derived

Neurotrophic Factor Repair Spinal Cord Injury in Adult Rats," *PLoS One*, vol. 7, no. 8, 2012.

[264] X. Y. Zhang, H. Xue, J. M. Liu, and D. Chen, "Chemically extracted acellular muscle: A new potential scaffold for spinal cord injury repair," *J. Biomed. Mater. Res. - Part A*, vol. 100 A, no. 3, pp. 578–587, 2012.

[265] F. Paduano, M. Marrelli, L. J. White, K. M. Shakesheff, and M. Tatullo, "Odontogenic differentiation of human dental pulp stem cells on hydrogel scaffolds derived from decellularized bone extracellular matrix and collagen type I," *PLoS One*, vol. 11, no. 2, 2016.

[266] M. J. Sawkins *et al.*, "Hydrogels derived from demineralized and decellularized bone extracellular matrix," *Acta Biomater.*, vol. 9, no. 8, pp. 7865–7873, 2013.

2 Stem Cells from the Dental Apical Papilla in Extracellular Matrix Hydrogels Mitigate Inflammation of Microglial Cells

Adapted from:

Natalija Tatic, Felicity R. A. J. Rose, Anne des Rieux, Lisa J. White, “Stem cells from the dental apical papilla in extracellular matrix hydrogels mitigate inflammation of microglial cells”, Scientific Reports, 9, 1-9, 2019.

https://doi.org/10.1038/s41598-019-50367-x

2.1 Preface

This chapter describes the first two objectives: measurement and optimization of scECM and bECM mechanical properties and the investigation of the SCAP and their potential to mitigate inflammation.

Mechanical properties, mainly stiffness and gelation kinetics [1] dictate hydrogel ability to incorporate SCAP [2], [3] and protect them from the share stress during injection [4], the length and the forcefulness of hydrogel handling [5], [6], physical form in which they are delivered [7], [8] and further down the line, delivery method [8], [9] and influence on the surrounding tissue [10]–[12]. Therefore, it is also necessary to explore whether and how these properties can be varied.

An instrument that measures the stiffness and the gelation kinetics of a bulk ECM hydrogel is a rheometer [5], [13]. A rheometer measures the plastic flow of the viscoelastic “soft solids”, such as ECM hydrogels, that results from applying the specific dynamic oscillatory stress and strain ECM may suffer during manipulation and delivery. Previously described ECM stiffness and viscosity [6], [14], [15] and the possibility to avoid an additional axial sample stress before the measurement prompted the use of parallel plates. The size of the plates and the gap between them allowed a reasonable use of the material (available at limited amounts) but did not compromise the measurement. The oscillatory frequency and the deformation amplitude were determined experimentally to allow the undisturbed gelation and avoid signal omission for the duration of the measurement.

To modulate ECM hydrogel mechanical properties fibrin was chosen for its fast gelation and stiffness that can be varied by adjusting the concentrations of fibrin components,

fibrinogen and thrombin [16]. Fibrin is also FDA approved as a biological glue for surgical procedures and has been previously used for cell delivery to SCI [2], [16].

In-depth analysis of SCAP viability in scECM and bECM hydrogels of 8mg/mL and fibrin were already available [14], [16]. Still, before testing anti-inflammatory properties of incorporated SCAP, their viability in hydrogel combinations was confirmed with a quick, precise metabolic assay (PrestoBlue) [17].

As PrestoBlue reagent is always used at the same concentration, the incubation time was optimized at 5h to avoid signal saturation. At every time point, 0, 3 and 7 days upon SCAP incorporation, PrestoBlue reagent was added to a new set of samples and incubated for eight hours. Every two hours, the fluorescence was measured in technical and measurement triplicates, i.e. three samples of hydrogel incorporating cells and three PrestoBlue aliquots taken from each sample. The maximal cell concentration that allowed undiminished cell viability without signal saturation was determined to be $1x10^6$ cells/mL. The hydrogel volume was optimized at 150 µL, so the casted thickness of ≈ 1 mm allowed PrestoBlue diffusion. PrestoBlue diffusion in the gel was visually estimated by the colour of the medium inside and above the hydrogel. The volume of PrestoBlue solution was optimized at 1 mL, so that the influence of the medium remaining in the hydrogel pores on the reagent concentration was negligible.

During these experiments the hydrogel formation seemed to be undisrupted by cell incorporation and the hydrogel combinations seemed to be stable for 7 days of culture in the selected conditions. The determined setting, $1x10^6$ cells/mL, 150 µL volume and ≈ 1 mm hydrogel thickness was later used to assess hydrogel/SCAP potential to mitigate inflammation.

To evaluate SCAP and/or ECM hydrogel influence on inflammation, the most commonly used microglia model, LPS-stimulated BV2 cells, was selected. Recent publications have been focused on microglia cells as they initiate SCI inflammation and have a direct relationship with re-myelination and neural regeneration [18]–[24]. Compared to microglia, BV2 cells are more robust, resilient and easily obtainable [25]–[27]. Even though SCI inflammation is sterile and therefore does not involve LPS [28], upon BV2 stimulation with LPS, marker expression is consistent, predictable and overlaps with primary microglia by 90% [29]–[31]. When SCAP and/or ECM hydrogel were added to LPS-stimulated BV2 cells, the changes in the most sensitive markers, *Tnf*, *Nos2* and *Arg1*, were followed. Mannose receptor CD206, typically a marker of immunoregulatory phenotype, was excluded as it may be increased after LPS stimulation [32]. IL-6 and prostaglandin E2 inflammation-induced secretion were excluded, as their role is both pro- and anti- inflammatory, making the concentration changes hard to interpret [33]–[35].

LPS concentration, duration of stimulation, time-point and duration of SCAP/hydrogel treatment were determined experimentally, by following the gene expression as well as the viability of BV2 cells. To establish the ECM hydrogel - BV2 cells co-culture, initially, BV2 cells were incorporated in 3D hydrogel culture or seeded in 2D culture on top of the hydrogel. Further, the hydrogel was formed on top of the BV2 cells or a pre-formed solid hydrogel was placed on top of the BV2 cells. Then, BV2 cells were seeded around the hydrogel pre-formed in the center of the well plate. BV2 cells died in all the conditions, possibly due to their antigen sensitivity. Finally, 150 µL of solid hydrogel in ≈ 1 mm thickness, $1.5x10^5$ SCAP or 150 µL of solid hydrogel containing $1.5x10^5$ SCAP on cell culture inserts were introduced on top of $1.5x10^5$ BV2 cells after 2h to mitigate the 100 ng/mL LPS-induced inflammation (Figure 2.1). The same volume of solubilised hydrogel, 150 µL, for the same volume of medium, 2 mL, was tested in parallel (Figure 2.1) for the same amount of time, 24h, as the additional physical form of hydrogel expected upon

delivery, to bring ECM in direct contact with BV2 cells and compare scECM/bECM to the other ECM hydrogels tested in literature in solubilised form [36], [37].

LPS stimulation may require the change of medium and re-introduction of fresh LPS due to the saturation of the TLR 4. LPS-priming may also influence the magnitude of BV2 response. The complete removal of the stimuli before introducing SCAP/hydrogel was also considered. These options were found unnecessary due to the short duration of the experiment and the introduction of other foreign (human, porcine and bovine) antigens with the SCAP and hydrogels.

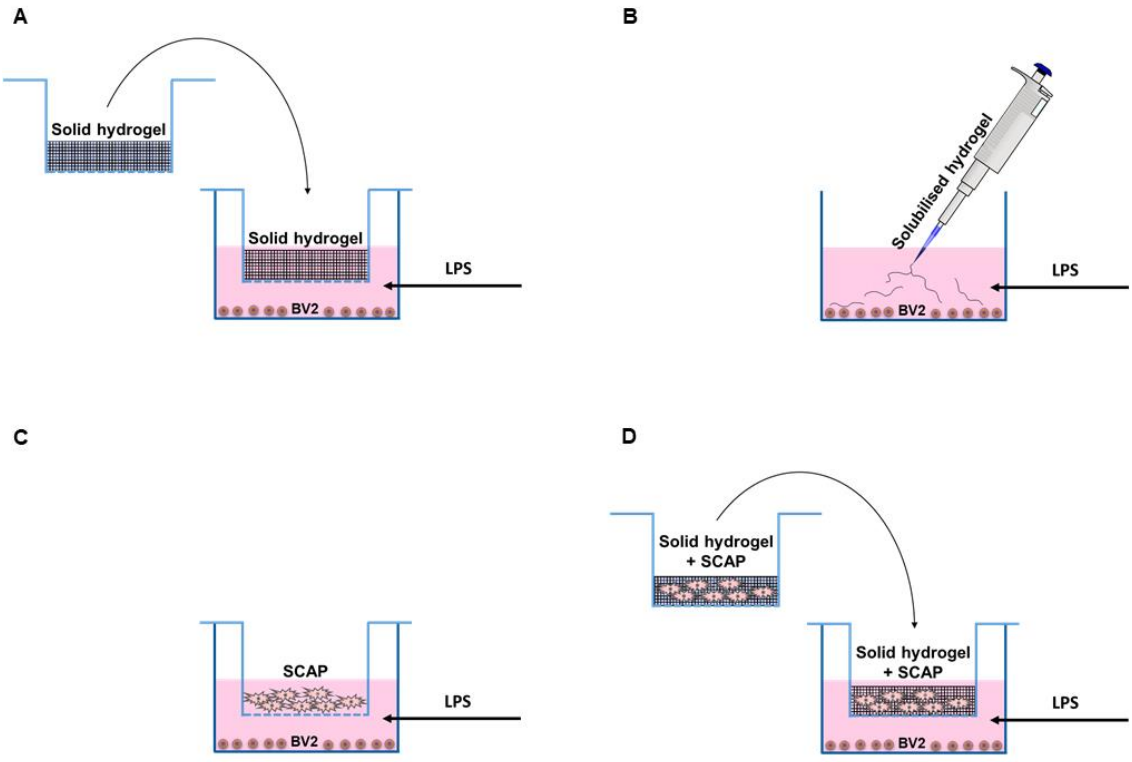


Figure 2.1 Experimental settings used to test the influence of SCAP/ECM hydrogels on LPS-activated microglia: A-B) Settings in which scECM 8mg/mL (also denoted as S8) and bECM 8mg/mL (also denoted as B8) were tested; C) Setting in which SCAP were tested; D) Setting in which scECM 8mg/mL (S8) + SCAP, bECM 8mg/mL (B8) + SCAP and scECM 8mg/mL 75% + Fibrin 25% (S/F) + SCAP were tested

2.1.1 References

[1] D. Gupta, C. H. Tator, and M. S. Shoichet, “Fast-gelling injectable blend of hyaluronan and methylcellulose for intrathecal, localized delivery to the injured spinal cord,” *Biomaterials*, vol. 27, no. 11, pp. 2370–2379, 2006.

[2] C. Williams *et al.*, “Cardiac extracellular matrix-fibrin hybrid scaffolds with tunable properties for cardiovascular tissue engineering,” *Acta Biomater.*, vol. 14, pp. 84–95, 2015.

[3] J. Jokinen *et al.*, “Integrin-mediated Cell Adhesion to Type I Collagen Fibrils*,” 2004.

[4] M. H. Amer, F. R. A. J. Rose, K. M. Shakesheff, and L. J. White, “A biomaterials approach to influence stem cell fate in injectable cell-based therapies,” *Stem Cell Res. Ther.*, vol. 9, no. 1, pp. 1–15, 2018.

[5] A. R. Massensini *et al.*, “Concentration-dependent rheological properties of ECM hydrogel for intracerebral delivery to a stroke cavity,” *Acta Biomater.*, vol. 27, pp. 116–130, 2015.

[6] M. J. Sawkins *et al.*, “Hydrogels derived from demineralized and decellularized bone extracellular matrix,” *Acta Biomater.*, vol. 9, no. 8, pp. 7865–7873, 2013.

[7] T. Brinker, E. Stopa, J. Morrison, and P. Klinge, “A new look at cerebrospinal fluid circulation,” *Fluids Barriers CNS*, vol. 11, no. 1, pp. 1–16, 2014.

[8] M. C. Jimenez Hamann, E. C. Tsai, C. H. Tator, and M. S. Shoichet, “Novel intrathecal delivery system for treatment of spinal cord injury,” *Exp. Neurol.*, vol. 182, no. 2, pp. 300–309, 2003.

[9] P. De Berdt *et al.*, “Dental Apical Papilla as Therapy for Spinal Cord Injury.,” *J. Dent. Res.*, vol. 94, no. 11, pp. 1575–81, 2015.

[10] D. Prodanov and J. Delbeke, “Mechanical and biological interactions of implants with the brain and their impact on implant design,” *Frontiers in Neuroscience*, vol. 10, no. FEB. Frontiers Media S.A., 09-Feb-2016.

[11] K. Franze, “The mechanical control of nervous system development,” *Development*, 2013.

[12] J. Lantoine *et al.*, “Matrix stiffness modulates formation and activity of neuronal networks of controlled architectures,” *Biomaterials*, vol. 89, pp. 14–24, May 2016.

[13] L. T. Saldin, M. C. Cramer, S. S. Velankar, L. J. White, and S. F. Badylak, “Extracellular matrix hydrogels from decellularized tissues: Structure and function,” *Acta Biomater.*, vol. 49, pp. 1–15, 2017.

[14] A. Viswanath *et al.*, “Extracellular Matrix-Derived Hydrogels for Dental Stem Cell Delivery,” *J. Biomed. Mater. Res. Part A*, pp. 1–10, 2016.

[15] C. J. Medberry *et al.*, “Hydrogels derived from central nervous system extracellular matrix,” *Biomaterials*, vol. 34, no. 4, pp. 1033–1040, 2013.

[16] L. Germain *et al.*, “Fibrin hydrogels to deliver dental stem cells of the apical papilla for regenerative medicine,” *Regen. Med.*, vol. 10, no. 2, pp. 153–167, 2015.

[17] T. L. Riss *et al.*, “Cell Viability Assays,” *Assay Guid. Man.*, no. Md, pp. 1–25, 2004.

[18] V. Chhor *et al.*, “Characterization of phenotype markers and neuronotoxic potential of polarised primary microglia In vitro,” *Brain. Behav. Immun.*, vol. 32, pp. 70–85, 2013.

[19] A. F. Lloyd *et al.*, “Central nervous system regeneration is driven by microglia necroptosis and repopulation,” *Nat. Neurosci.*, 2019.

[20] M. Karamita *et al.*, “Therapeutic inhibition of soluble brain TNF promotes remyelination by increasing myelin phagocytosis by microglia,” *JCI Insight*, vol. 2, no. 8, pp. 1–19, 2017.

[21] Z. Li, F. Liu, X. He, X. Yang, F. Shan, and J. Feng, “Exosomes derived from mesenchymal stem cells attenuate inflammation and demyelination of the central nervous system in EAE rats by regulating the polarization of microglia,” *Int. Immunopharmacol.*, vol. 67, no. December 2018, pp. 268–280, 2019.

[22] J. D. Cherry, J. A. Olschowka, and M. O’Banion, “Neuroinflammation and M2 microglia: the good, the bad, and the inflamed,” *J. Neuroinflammation*, vol. 11, no.

1, p. 98, 2014.

[23] X. Jin and T. Yamashita, “Microglia in central nervous system repair after injury,” *Journal of Biochemistry*, vol. 159, no. 5. 2016.

[24] J. C. Gensel and B. Zhang, “Macrophage activation and its role in repair and pathology after spinal cord injury,” *Brain Res.*, vol. 1619, pp. 1–11, 2015.

[25] R. Timmerman, S. M. Burm, and J. J. Bajramovic, “An Overview of in vitro Methods to Study Microglia,” *Front. Cell. Neurosci.*, vol. 12, no. August, pp. 1–12, 2018.

[26] E. Blasi, R. Barluzzi, V. Bocchini, R. Mazzolla, and F. Bistoni, “Immortalization of murine microglial cells by a v-raf / v-myc carrying retrovirus,” *J. Neuroimmunol.*, vol. 27, no. 2–3, pp. 229–237, 1990.

[27] D. Giulian and T. J. Baker, “Characterization of ameboid microglia isolated from developing mammalian brain,” *J. Neurosci.*, vol. 6, no. 8, pp. 2163–2178, 1986.

[28] M. Schwartz and R. Shechter, “Protective autoimmunity functions by intracranial immunosurveillance to support the mind: The missing link between health and disease,” *Molecular Psychiatry*, vol. 15, no. 4. pp. 342–354, 2010.

[29] A. Henn, S. Lund, M. Hedtjärn, A. Schrattenholz, P. Pörzgen, and M. Leist, “The suitability of BV2 cells as alternative model system for primary microglia cultures or for animal experiments examining brain inflammation.,” *ALTEX Altern. zu Tierexperimenten*, vol. 26, no. 2, pp. 83–94, 2009.

[30] W. Chanput, J. J. Mes, and H. J. Wichers, “THP-1 cell line: An in vitro cell model for immune modulation approach,” *Int. Immunopharmacol.*, vol. 23, no. 1, pp. 37–45, 2014.

[31] Y. He, X. Yao, N. Taylor, Y. Bai, T. Lovenberg, and A. Bhattacharya, “RNA sequencing analysis reveals quiescent microglia isolation methods from postnatal mouse brains and limitations of BV2 cells,” *J. Neuroinflammation*, vol. 15, no. 1, pp. 1–13, 2018.

[32] Y. Qin *et al.*, “Lipopolysaccharide Preconditioning Induces an Anti-inflammatory

Phenotype in BV2 Microglia," *Cell. Mol. Neurobiol.*, vol. 36, no. 8, pp. 1269–1277, 2016.

[33] J. Scheller, A. Chalaris, D. Schmidt-Arras, and S. Rose-John, "The pro- and anti-inflammatory properties of the cytokine interleukin-6," *Biochim. Biophys. Acta - Mol. Cell Res.*, vol. 1813, no. 5, pp. 878–888, 2011.

[34] J. R. Silva, B. Burger, C. M. C. Kühl, T. Candreva, M. B. P. Dos Anjos, and H. G. Rodrigues, "Wound Healing and Omega-6 Fatty Acids: From Inflammation to Repair," *Mediators Inflamm.*, vol. 2018, p. 2503950, 2018.

[35] Fritsche, "The Science of Fatty Acids and Inflammation," *Adv. Nutr. An Int. Rev. J.*, vol. 6, no. 3, pp. 293S-301S, 2015.

[36] F. W. Meng, P. F. Slivka, C. L. Dearth, and S. F. Badylak, "Solubilized extracellular matrix from brain and urinary bladder elicits distinct functional and phenotypic responses in macrophages," *Biomaterials*, vol. 46, pp. 131–140, 2015.

[37] J. L. Dziki, D. S. Wang, C. Pineda, B. M. Sicari, T. Rausch, and S. F. Badylak, "Solubilized extracellular matrix bioscaffolds derived from diverse source tissues differentially influence macrophage phenotype," pp. 12–15, 2016.

2.2 Abstract

After SCI chronic inflammation hampers regeneration. Influencing the local microenvironment after SCI may provide a strategy to modulate inflammation and the immune response. The objectives of this work were to determine whether bone or spinal cord derived ECM hydrogels can deliver human MSC from the apical papilla (SCAP) to reduce local inflammation and provide a regenerative microenvironment. Bone hydrogels (8 and 10 mg/mL, B8 and B10) and spinal cord hydrogels (8 mg/mL, S8) supplemented with fibrin possessed a gelation rate and a storage modulus compatible with spinal cord implantation. S8 and B8 impact on the expression of anti and pro-inflammatory genes (*Arg1*, *Nos2*, *Tnf*) in LPS treated microglial cells were assessed using solubilised and solid hydrogel forms. S8 significantly decreased the *Nos2*/*Arg1* ratio and solubilised B8 significantly reduced *Tnf* and increased *Arg1* whereas solid S8 and B8 did not impact inflammation in microglial cells. SCAP incorporation within ECM hydrogels did not impact upon SCAP immunoregulatory properties, with significant decrease of *Nos2/Arg1* ratio observed for all SCAP embedded hydrogels. *Tnf* expression was reduced with SCAP embedded in B8, reflecting the gene expression observed with the innate hydrogel. Thus, ECM hydrogels are suitable vehicles to deliver SCAP due to their physical properties, preservation of SCAP viability and immunomodulatory capacity.

2.3 Introduction

SCI, usually caused by a car crash, fall or violence, drastically influences the quality of life and increases mortality risk by 2-5 times. Spinal cord has a very low capacity for self-regeneration and cannot be fully repaired by any of the current therapies[1].

Regardless of the type or intensity, injuries to the spinal cord create a complex deteriorating microenvironment that is not yet fully understood and is dominated by inadequate immune reaction [2]. Comprehensive studies of cellular response show that the inflammatory and proliferative phases of immune response to SCI start as expected (predominantly “M1” macrophage profile), but difficulties occur in later transitions between the proliferative and immunoregulatory phase (“M2b” profile) [2] and the following remodeling phase (“M2c”) does not seem to occur [3]. Thus, the pro-inflammatory phase, initiated by microglia and led by “M1” macrophages and T-lymphocytes, remains chronically predominant [2]. This contributes to the secondary injury and has a negative effect on regeneration [3].

Attempts to influence immune response in injured spinal cord, e.g. by macrophage depletion [4], local or systemic delivery of anti-inflammatory drugs [5] or immunoregulatory cytokines (related to “Th2” and immunoregulatory immune response) [6], or adoptive transfer of “Th2”/immunoregulatory (IL-4, IL-10 or TGFβ stimulated) macrophages [7] have shown positive effects on regeneration in pre-clinical trials. Influencing microglia polarisation and microglia transfer have also been investigated and reviewed as therapeutic options for “Th1” neuro inflammatory conditions and SCI [8].

Influencing the local microenvironment after SCI may provide another strategy to impact upon immune response. MSC can be used for their immunoregulatory properties [9].

However, over 90% of MSC transplanted in damaged spinal cord die or migrate away [10]. Cellular losses occurring during injection due to shear stress may be reduced by suspending MSC in an injectable hydrogel [11]. Upon injection, the gel network can protect MSC from the immediate influence of the hostile microenvironment and assist in cell localisation and retention at the injection site [12]. To stay in place, filling the irregular geometry of SCI and not be washed off by the flow of cerebrospinal fluid, the window of hydrogel gelation time would have to allow hydrogel manipulation and injection while providing a setting time fast enough to avoid hydrogel wash out (typically a couple of minutes) [13]. Hyaluronan and methyl cellulose, fibrin and various biologically derived and synthetic hydrogels carrying cells or drug loaded particles have been tested in pre-clinical phases [14]. Whilst current clinical studies have focused on the delivery of BM- [15] and AD- MSC [16] for SCI, MSC derived from other tissues may also utilised. Stem cells from the human apical papilla (SCAP) can be easily isolated from adult immature tooth, have high proliferative and migratory potential [17] and due to specific embryonal origin, express neural markers without neurogenic stimulation [18]. We and others have previously shown that SCAP secrete a broad pallet of neurotrophic and regenerative growth factors [19] and possess “Th1” anti-inflammatory properties [20].

Hydrogels, in addition to serving as a vehicle for local delivery of SCAP, may also actively participate in immunoregulation of the local environment. ECM hydrogels can be generated from almost any tissue [21] and have been shown to contain growth factors [22], matrix-bound nanovesicles [23] and exposed cryptic peptides and bioactive motifs [24], [25]. ECM hydrogels provide general and tissue specific cues for regeneration *in vitro* and *in vivo* [26], [27]. ECM hydrogels derived from different tissues previously induced “alternative” or “M2a”-like phenotype in unstimulated bone marrow derived macrophages *in vitro* (urinary bladder matrix and small intestine submucosa hydrogels) [28] and displayed “Th1”-regulating properties *in vivo* (urinary bladder matrix, colonic mucosa and myocardial matrix hydrogels) [27], [29], [30].

Our objective was thus to assess whether ECM derived hydrogels would be suitable for SCAP delivery in the scope of SCI. Since ECM hydrogels derived from both heterologous organs [31] and homologous tissues [32] have shown reparative effects in the central nervous system, we postulated that spinal cord or alternative tissue derived hydrogels, e.g. bone, may be suitable for SCAP delivery. In addition, we hypothesised that spinal cord or bone ECM hydrogels would present appropriate mechanical properties to be administered in a spinal cord lesion and support SCAP viability and functionality. Since “Th1”-regulatory properties have been attributed to ECM-derived hydrogels, we postulated that this intrinsic activity, combined with SCAP, may have a synergistic impact upon mitigation of “Th1” inflammation of microglial cells.

2.4 Materials and Methods

2.4.1 Chemicals and Reagents

RNeasy Mini Kit was from Qiagen (Manchester, UK). Sodium Ethylenediaminetetracetate was from AppliChem Panreac (Darmstadt, Germany). Fibrinogen and Thrombin were from Baxter Innovations GmbH (Vienna, Austria). Forty-eight-well cell-repellent plates and tissue culture inserts (pore size 1 µm) were from Greiner Bio-One (Stonehouse, UK). Triton X-100, sodium deoxycholate, peracetic acid concentrated, sterile apyrogenic 10x phosphate buffer saline, pepsin, sodium hydroxide, Minimum Essential Medium, foetal bovine serum and LPS from *Escherichia coli* 0111: B4 were from Sigma-Aldrich (Poole, UK). All other reagents were purchased from Thermo Fisher Scientific (Loughborough, UK).

2.4.2 Tissue Decellularization

Fresh porcine spinal cord and bovine bone were harvested from market weight animals. Female and male animals were used indiscriminately. Spinal cords and cancellous tibias were fragmented and processed following previously described protocols [34], [40]. The obtained ECM were lyophilised and stored at – 20 °C for further use.

2.4.3 Preparation of ECM Hydrogels

Obtained ECM were ground to form powders and digested with 1 mg/mL pepsin in 0.01 N hydrochloric acid for 48h for spinal cord ECM and 72h for bone ECM. Final solutions of 10 mg spinal cord ECM/mL and 10 and 12.5 mg bone ECM/mL were obtained, as previously described [34] and stored at – 20 °C. Prior to use, ECM digests were thawed, neutralised with 10x phosphate buffer saline and 0.01N sodium hydroxide and diluted to

desired concentrations (8 or 10 mg/mL) using phosphate buffer saline, at 4 °C, as described previously [34]. Obtained pre-gels were incubated for 20 minutes at 37 °C to form gels.

Fibrinogen and thrombin were reconstituted following manufacturer instruction, diluted to 50 mg/mL and 50 IU/mL, respectively, and used in equal final volumes as described previously [36]. Hydrogel combination with fibrin (75:25 ECM:Fibrin ratio) was made by mixing pre-gel solution with thrombin, dispensing the mixture and then adding fibrinogen to the mixture *in situ* before the incubation.

2.4.4 Mechanical Characterisation of ECM Hydrogels

Mechanical characterisation was performed on a rheometer (Anton Paar Physica MCR 301, Austria) according to American Society for Testing and Materials (ASTM) F2900-11 standard using 200 µL of material, 25 mm parallel plates, 0.2 mm gap and a Peltier plate to control the temperature within 0.1°C. Pre-gel solutions were placed on a pre-cooled plate (4 °C). For hydrogels containing fibrin, the pre-gel solution and thrombin was mixed with fibrinogen (12.5% of the total volume) directly on the plate. Equal distribution of material between the plates was ensured by rotating the upper plate (shear rate 1000 s^{-1}) for 20 s at 4 °C. Then an oscillatory time sweep test (1% oscillatory strain, 1 rad/s angular frequency) was conducted to follow the gelation kinetics for 20 min. The temperature rose from 4 to 37 °C, at 0.5 °C/s, the fastest steady heating rate. The rest of the analysis was conducted at 37 °C. Frequency sweep test (1% strain, 0.01-100 rad/s angular frequency) followed by amplitude sweep test (0.01-200% strain, 1 rad/s angular frequency) were conducted in sequence at 37 °C. Analysis was performed in triplicate.

2.4.5 SCAP Culture

Human SCAP were isolated from a healthy donor wisdom tooth and characterised [51]. The experiments were performed in accordance with the UCLouvain local ethical committee (2012/14JUN/283). Human SCAP (RP89 cells) [51] were used between passages 5 and 10. SCAP were grown at 37 °C in 5% CO_2 in growth medium composed of Minimum Essential Medium supplemented by 10% foetal bovine serum, 1% of L-glutamine and 1% of penicillin and streptomycin. SCAP were passaged upon reaching about 80% confluence using StemPro Accutase®.

2.4.6 SCAP Viability in ECM Hydrogel Combinations

SCAP viability in individual hydrogels was determined using PrestoBlue cell viability agent following supplier instructions. SCAP were suspended in pre-gel solutions at $1x10^6$ cells/mL and 150µL was cast in 48-well tissue culture plates at 4 °C. Plates were then incubated at 37 °C for 20 minutes for gelation to occur. Growth medium was added on top and changed every other day up to the desired time point. At each time point, growth medium was removed and cells were incubated for 5 hours in 10x PrestoBlue dilution in medium. Cell viability was evaluated by sampling 100µL from the solution above the gel, measuring sample fluorescence at 560 and 590nm (emission and excitation) following the manufacturer's protocol. Cells were incubated for 3 hours with the PrestoBlue reagent. Cell viability was expressed as a percentage of SCAP viability relative to Day 0. Cell viability experiments were performed in triplicates (N=3, n=3). Each type of hydrogel was used alone as negative control and the absorbance of the PrestoBlue reagent solution was subtracted from the obtained values for corresponding hydrogel with cells.

2.4.7 ECM Hydrogels and SCAP Impact on LPS-Stimulated BV2 cells

2.4.7.1 BV2 Cell Culture

Mouse brain microglia cells (BV2 cells) were used between passages 21 and 31 (ATCC® CRL-2469™). BV2 cells were grown at 37 °C in 5% CO_2 in Dulbecco's Modified Eagle Medium GlutaMAX with 4.5 g/L D-glucose and without pyruvates supplemented by 10% foetal bovine serum and 1% of penicillin and streptomycin. BV2 cells were passaged upon reaching over 90% confluence using StemPro Accutase® BV2 cells challenged by LPS are widely used as a model of neural inflammation [52]. Upon stimulation by LPS, 90% of the markers expressed by BV2 reflect similar trends to that observed in LPS stimulated microglia [53].

2.4.7.2 BV2 Stimulation and Treatment

BV2 cells ($1.5x10^5$ cells/well) were seeded in 12-well tissue culture plates using SCAP growth medium. After 16h, the medium was either replaced with SCAP growth medium containing 100 ng/mL LPS (LPS from Escherichia coli 0111: B4, Sigma- Aldrich) for the LPS-stimulated condition or with fresh SCAP growth medium for the control condition. Hydrogel and/or cell treatments were added 2h after LPS stimulation of BV2 cells and cultured for a further 24h. S8 or B8 were added either as solubilised pre-gel solutions (0.5 mg/mL final concentration) directly into BV2 cell medium or as solid hydrogels in the apical compartment of cell culture inserts (pore size 1 µm) cast above BV2 cells (in the basolateral compartment). SCAP were either directly seeded on the insert membrane or incorporated in solid hydrogels ($1.5x10^5$ SCAP/gel). Cells were stored in RLT buffer (RNeasy Mini Kit) at - 80 °C until further analysis. Each experiment was performed in triplicate (N=3, n=3). Controls were non-activated BV2 cells (M0) and non-treated activated BV2 cells (Control).

2.4.7.3 TNFα Quantification

The concentration of murine TNFα in cell culture medium was determined by a commercially available enzyme-linked immunosorbent assay kit (detection limit 5.0 pg/mL) according to manufacturer's instructions (Invitrogen^{TM}).

2.4.7.4 BV2 Gene Expression Analysis

Total RNA was extracted using RNA Isolation Kit (RNeasy Mini Kit) following the manufacturer's instructions. Qualitative and quantitative analysis of RNA was performed by spectrophotometry (NanoDrop ND- 1000 Spectrophotometer, Labtech, Heathfield, UK). Given the major role that NO has in the neurotoxic effects of microglia the following genes were chosen: "Th1" pro-inflammatory *Nos2* coding iNOS that produces NO from L-arginine; "Th1" immunoregulatory *Arg1* coding liver arginase that also metabolises L-arginine preventing the NO synthesis and "Th1" pro-inflammatory *Tnf* [53]. "M1" (*Tnf*-Mm00443258_m1 and *Nos2*- Mm00440502_m1) and "M2" (*Arg1*- Mm00475988_m1) gene expression was determined relative to ribosomal protein L19 gene (*Rpl19*-Mm02601633_g1) according to the TaqMan gene expression assay protocol using TaqMan primers and probes. Reported PCR efficiency was 100%.

2.4.8 Statistical Analysis

Statistical tests were performed using Prism (GraphPad Prism 7.02 software, CA, USA). Results are expressed as mean +/- standard error of the mean and were considered significant if $p < 0.05$. In figure captions, detailed information about number of replicates, type of statistic test and post-test can be found for each experiment.

2.5 Results

2.5.1 Impact of ECM Origin, Concentration and Composition upon Mechanical Properties

Gelation rate, time and final moduli can greatly influence the handling of hydrogels and their applicability *in vivo*. Rheological assessments of spinal cord-derived ECM hydrogel at 8 mg/mL (S8) and on bone-derived ECM hydrogels at 8 and 10 mg/mL (B8 and B10, respectively) were undertaken. Spinal cord derived hydrogels at 10 mg/mL were not considered due to requiring high amounts of starting material.

Once incubated at 37 °C, storage modulus (G') of pre-gel solutions quickly became higher than loss modulus (G"), reflecting the formation of a solid hydrogel (Table 2.1; Supplementary Figure 2.1). The origin of ECM hydrogel (bone or spinal cord), as well as the concentration in the case of bone-derived ECM hydrogel, significantly impacted hydrogel maximum storage modulus. The highest storage modulus was observed for B10 while the lowest was S8 modulus. All hydrogels had a pre-gel solution around 1 Pa and a final storage modulus lower than 1 kPa. Gelation times were also dependent on hydrogel origin but not on concentration; B8 and B10 gelled faster than S8.

In order to increase storage modulus and to decrease gelation time of S8, fibrin was added to the pre-gel solutions at a 75/25 ratio. Addition of 25% fibrin to S8 (S/F) significantly increased the hydrogel maximum modulus and reduced the time to 50% gelation by 24% (Table 2.1).

Table 2.1 Hydrogel maximal moduli and gelation kinetics

Hydrogel	Storage modulus [G', Pa]	Loss modulus [G", Pa]	Gelation rate [Pa/min]	Time to 50% gelation [t_{50}, min]	Time to 95% gelation [t_{95}, min]
S8	258 ± 17^{A}	37 ± 2^{A}	51 ± 9^{A}	2.05 ± 0.51^{A}	4.02 ± 0.67^{A}
B8	499 ± 10^{B}	60 ± 3^{B}	96 ± 5^{B}	1.36 ± 0.12^{A}	3.48 ± 0.50^{A}
B10	608 ± 9^{C}	66 ± 4^{B}	118 ± 16^{B}	1.44 ± 0.25^{A}	3.65 ± 0.70^{A}
S/F	305 ± 28^{D}	44 ± 14^{B}	65 ± 4^{A}	1.56 ± 0.14^{A}	3.97 ± 0.26^{A}

Mean ± standard deviation (SD), N=3. Temperature rose from 4 to 37 °C at 0.5 °C/s and was kept constant for the rest of the 20-minute measurement. Given the values normality (Kolmogorov-Smirnov test) for each parameter, its significance was evaluated by a One-way ANOVA followed by a Tukey post-hoc test. Conditions not linked by the same letter(s) are statistically different ($p<0.05$). S8 – spinal cord ECM hydrogel 8mg/mL, B8 – bone ECM hydrogel 8mg/mL, B10 – bone ECM hydrogel 10mg/mL, S/F- spinal cord ECM hydrogel 8 mg/mL/fibrin at a 75/25 ratio.

2.5.2 Impact of SCAP Encapsulation in ECM Hydrogels upon LPS-Stimulated BV2 Cells

SCAP co-cultured with activated microglia can mitigate their LPS-induced response [20]. Previously, we and others, have encapsulated SCAP in hydrogels, including alginate and hyaluronic acid [33], ECM derived [34], [35], fibrin [36] and gelatin methacryloyl (GelMA) [37]. Whilst these studies have investigated impact upon SCAP viability, proliferation and differentiation, to date, the impact of encapsulation upon SCAP immunomodulatory properties has not been explored.

2.5.2.1 Impact of ECM Hydrogels upon LPS-Stimulated BV2 Cells

" Th1" immunoregulatory properties have been attributed to ECM hydrogels [28], [29]. Hence the objective herein was to evaluate the potential impact of S8 and B8 hydrogels upon LPS-activated microglial cells (BV2 cells) by considering gene expression of markers known either for their "Th1" anti-inflammatory (*Arg1*) or "Th1" pro-inflammatory properties (*Nos2*, *Tnf*). The expression of *Arg1* and of *Nos2*, respectively "Th1" anti- and proinflammatory markers, was not significantly affected by incubation with solid S8 hydrogel (Figure 2.2A, Supplementary Figure 2.2A). In its solubilised form, S8 significantly increased *Arg1* and *Nos2* expression (Figure 2.2A, Supplementary Figure 2.2A). The resulting *Nos2/Arg1* ratios (commonly used to evaluate the immunomodulatory potential of drugs or cells) [38] were slightly decreased, but only significantly for S8 solubilised gel. Neither forms of spinal cord ECM hydrogel impacted *Tnf* expression. B8 as a solid gel did not impact *Arg1*, *Nos2/Arg1* ratio or *Tnf* expression, although it induced an increased expression of *Nos2* (Figure 2.2B, Supplementary Figure 2.2B). B8 in the solubilised form significantly increased *Arg1* and *Nos2* expression (Figure 2.2B, Supplementary Figure 2.2B). The resulting *Nos2/Arg1* ratio and *Tnf* expression were decreased when LPS-activated BV2 cells were incubated with solubilised B8 compared to solid B8. Neither form of B8 or S8 induced an inflammatory response in unstimulated (naïve) microglia as demonstrated by TNFα secretion (Supplementary Figure 2.3).

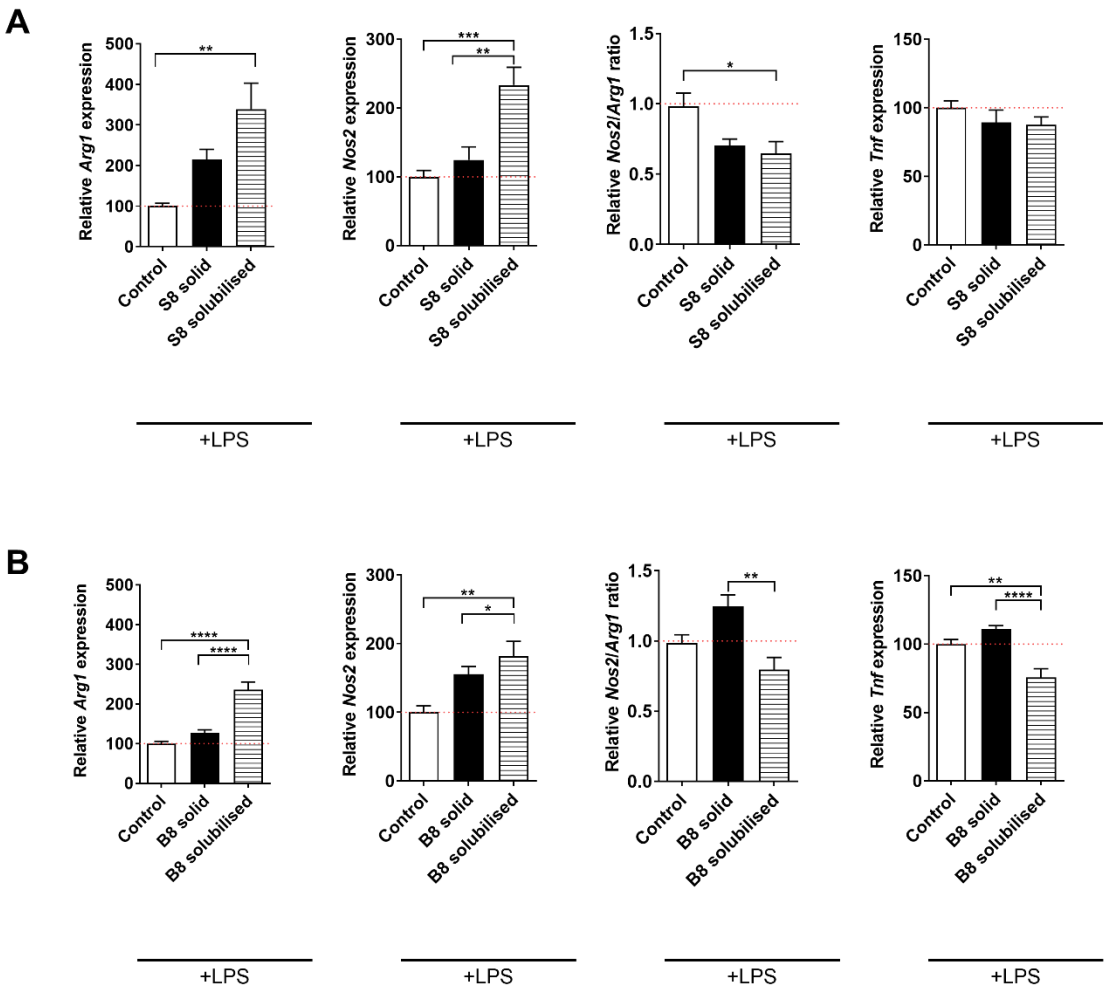


Figure 2.2 Influence of ECM hydrogels on gene expression. After 2h from LPS-activation, BV2 cells were treated for 24h with either solid (cast in an insert) or solubilised S8 and B8 hydrogels (directly added in culture medium) and the gene expression of TNFα (*Tnf*), inducible nitric oxide synthetase gene (*Nos2*) and arginase 1 gene (*Arg1*) was quantified by real time quantitative polymerase chain reaction. *Nos2*/*Arg1* ratio was also calculated. Results were expressed relative to the LPS-activated BV2 cells (control) set at 100% (red dotted bar). Error bars represent the standard error of the mean (N=4, n=3). Values were normally distributed within the columns according to Anderson-Darling, D'Agostino & Pearson, Shapiro-Wilk and Kolmogorov-Smirnov tests. One-way ANOVA with Tukey post-hoc test results were reported as * $p < 0.05$, ** $p < 0.01$, *** $p < 0.001$, **** $p < 0.0001$

2.5.2.2 Impact of SCAP upon LPS-Stimulated BV2 Cells

SCAP can decrease *Tnf* and increase *Arg1* expression of LPS-activated microglia when co-cultured in direct contact for 48h [20]. However, their impact when co-cultured for 24h with no direct contact (seeded on the apical side of an insert) has not been evaluated yet. In the presence of SCAP at the apical side of an insert, LPS-stimulated BV2 cells, seeded in the basolateral compartment, had significantly increased expression of *Arg1* and *Nos2* while the resulting *Nos2/Arg1* ratio and *Tnf* expression significantly decreased (Figure 2.3, Supplementary Figure 2.2C).

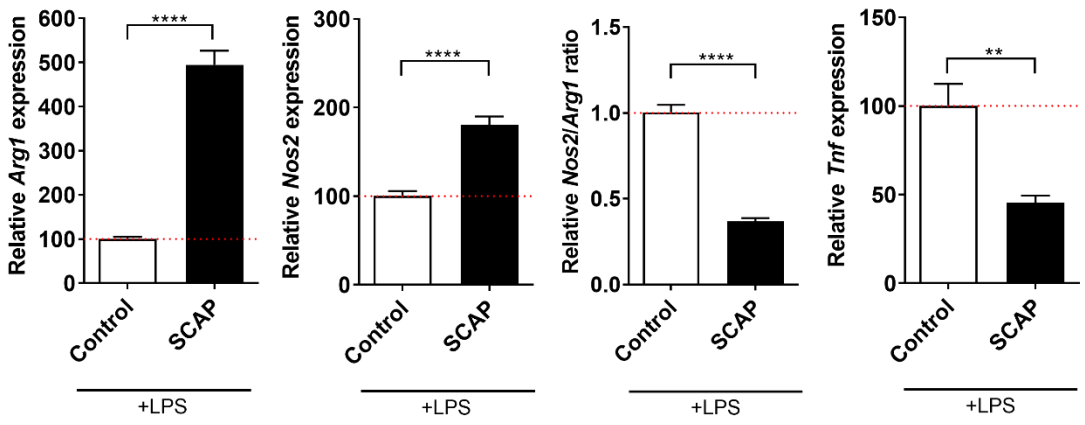


Figure 2.3 Influence of SCAP on BV2 cell inflammatory markers. SCAP seeded on inserts were co-cultured with LPS-activated BV2 cells for 24h (starting 2h post-activation) and the gene expression of tumor necrosis factor alpha (*Tnf*), inducible nitric oxide synthetase gene (*Nos2*) and arginase 1 gene (*Arg1*) were quantified by real time quantitative polymerase chain reaction. *Nos2*/*Arg1* ratio was also calculated. Results were expressed relative to the LPS-activated BV2 cells (control) set at 100% (red dotted bar). Error bars represent the standard error of the mean (N=4, n=3). Values were normally distributed according to Kolmogorov-Smirnov test. An unpaired t test with Welch's correction was performed, * $p < 0.05$, ** $p < 0.01$, *** $p < 0.001$, **** $p < 0.0001$

2.5.2.3 Impact of SCAP encapsulated ECM hydrogels upon LPS-Stimulated BV2 Cells

Prior to investigating the impact of SCAP encapsulation in ECM hydrogels upon their ability to mitigate the LPS-activation, SCAP viability in the hydrogels was first evaluated. SCAP were incorporated in S8, B10 and S/F hydrogels for 3 and 7 days and their metabolic activity was normalized to metabolic activity at encapsulation (day 0). SCAP viability remained above 80% 3 and 7 days after encapsulation except for SCAP encapsulated in B10 at Day 3 (70%) (Figure 2.4).

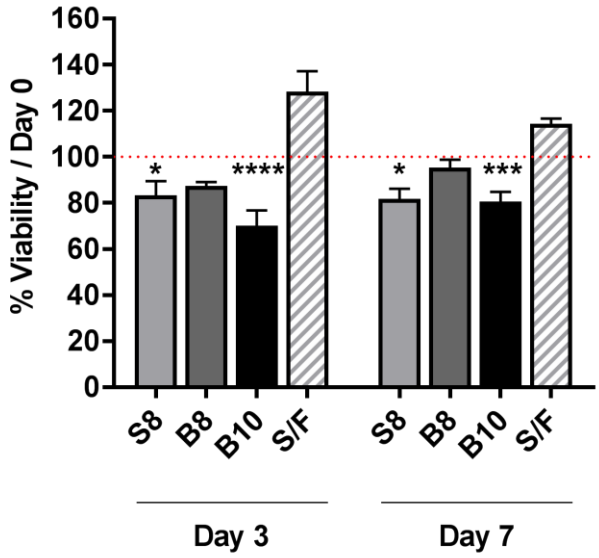


Figure 2.4 Impact of encapsulation in ECM hydrogels upon SCAP viability. SCAP viability in ECM hydrogels was assessed 3 and 7 days after incorporation in different hydrogels: spinal cord at 8 mg/mL (S8) and bone at 8 and 10 mg/mL (B8 and B10) and S8 combined with fibrin (S/F). Results were expressed relative to viability at Day 0 for each condition (red dotted bar). Error bars represent the standard error of the mean (minimum N=2, n=3). Due to the normal distribution within groups of unequal size, mixed effects model with Geisser-Greenhouse correction and Dunnett's post hoc test was performed, * $p < 0.05$, ** $p < 0.01$, *** $p < 0.001$, **** $p < 0.0001$

SCAP were incorporated into S8, B8 or S8 supplemented with fibrin (S/F) at a ratio of 75/25; SCAP incorporated hydrogels were located at the apical side of an insert with LPS stimulated BV2 cells seeded in the basolateral compartment. Incorporation of SCAP into all hydrogel types significantly increased *Arg1* expression relative to control (8 – 10-fold) (Figure 2.5, Supplementary Figure 2.2D). Compared to SCAP alone, incorporation of SCAP into S8 or B8 hydrogels increased *Arg1* expression by 2-fold. *Nos2* expression was significantly increased relative to the control for all SCAP encapsulated hydrogels and significantly increased relative to SCAP alone for SCAP encapsulated in S8 and B8 hydrogels. The *Nos2/Arg1* ratio was significantly decreased relative to the control (> 2-fold) when SCAP were encapsulated in all hydrogels but there was no significant difference observed when compared to SCAP alone. *Tnf* expression was significantly increased relative to SCAP alone when SCAP were encapsulated in S8 and S/F hydrogels. As a corollary to this, *Tnf* expression was significantly reduced by SCAP alone and encapsulated with B8 relative to the control.

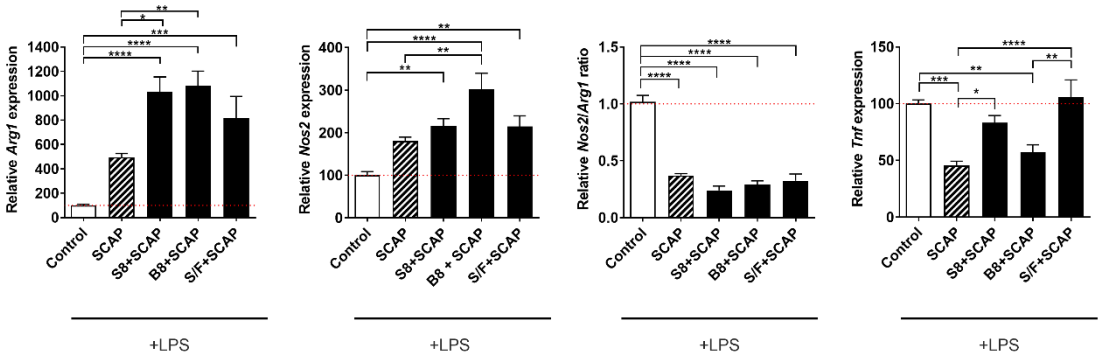


Figure 2.5 Influence of SCAP encapsulation in ECM hydrogels on their LPS-activation modulating properties. SCAP seeded on inserts, alone or encapsulated in S8, B8 or S/F hydrogels, were co-cultured with LPS-activated BV2 cells for 24h (starting 2h post-activation) and the gene expression of tumor necrosis factor alpha (*Tnf*), inducible nitric oxide synthetase gene (*Nos2*) and arginase 1 gene (*Arg1*) was quantified by real time quantitative polymerase chain reaction. *Nos2*/*Arg1* ratio was also calculated. Results were expressed relative to the LPS-activated BV2 cells (control) set at 100% (red dotted bar). Error bars represent the standard error of the mean (N=4, n=3). Values were normally distributed within the columns according to Anderson-Darling, D'Agostino & Pearson, Shapiro-Wilk and Kolmogorov-Smirnov tests. One-way ANOVA with Tukey post-hoc test results were reported as * $p < 0.05$, ** $p < 0.01$, *** $p < 0.001$, **** $p < 0.0001$

2.6 Discussion

Hydrogel application in SCI requires manipulation and injection of the material along with sufficiently quick gelation in the lesion [13]. The thermo-responsive nature of ECM hydrogels provides a potential role for these materials. Rather than being purely dictated by collagen self-assembly, ECM hydrogel formation is regulated by the presence of glycosaminoglycans, proteoglycans and proteins [39]. Thus, polymerization kinetics are influenced by the native biochemical profile of the original tissue and the proteins retained after decellularisation [21]. We have previously shown that the biochemical profiles of bone and spinal cord derived materials are distinctly different with higher collagen and lower sulphated glycosaminoglycan content in bone ECM and lower collagen and higher sulphated glycosaminoglycans in spinal cord [34]. The impact of biochemical profile, i.e. of different tissue origin, was clearly shown in the rheological assessments whereby bone derived ECM gelled faster and had a higher storage modulus than spinal cord ECM. Concentration dependent gelation kinetics has previously been shown at concentrations less than 8 mg/mL for bone [40], dermis [41] and other tissues [21]. Herein a similar dependency was observed with storage moduli of bone hydrogels increasing with concentration, with the highest storage moduli observed at 10 mg/mL.

The low storage moduli of spinal cord derived hydrogels prompted incorporation of fibrin, as a strategy to improve mechanical properties. Fibrin has fast gelation kinetics, an easily tunable strength and concentration and has been used previously to deliver SCAP [36] Whilst the inclusion of fibrin increased the storage moduli and decreased time to gelation, the similarity of S/F to S8 moduli indicated that the S/F hydrogel is an interpenetrating but not interactive network and the mechanical behavior is thus predicated by the dominant entity, i.e. spinal cord ECM. Similar results have been

observed for collagen fibrin co-gels where gels with higher concentrations of collagen acted as two distinct, interpenetrating, but not interacting, networks [42].

It is essential that any tissue engineered therapy for SCI is designed with desirable mechanical characteristics in order to avoid implant-induced damage and to, maximize cellular response, regeneration and functional recovery [43]. Whilst biomechanical studies of spinal cord tissue have reported a range of modulus values (0.12 – 15.2 kPa) [44], depending upon species and measurement methods, low stiffness and viscoelasticity are key parameters in selection of appropriate biomaterials. All the hydrogels assessed in this study had maximum moduli less than 1 kPa and meet these requirements.

Previously, the “M2” phenotype-inducing properties of ECM hydrogels have been investigated *in vitro* with naïve (M0 state) bone marrow derived macrophages from rat and mice and those stimulated to an “M1” –like state [28], [45]. To date, no studies have investigated mitigation of inflammation with bone or spinal cord derived ECM hydrogels nor has the influence upon microglial cells been elucidated. Microglial cells were selected due to their contribution to initiation of inflammation upon SCI [2]. Recent elucidation of the role of “Th1” pro-inflammatory microglia necroptosis in driving microglial repopulation and regeneration has shown that targeting proinflammatory microglia may represent a strategy to dampen central nervous system inflammation [46].

Previous *in vitro* studies have examined “M2” phenotype-inducing properties of ECM hydrogels as solubilised materials, i.e. added directly to the media of stimulated cells [28]. Our desire to use ECM hydrogels to deliver SCAP led us to examine the LPS activation-mitigating properties of both solubilised (direct contact with microglial cells) and solid forms, where the solid hydrogel was cast into a transwell insert placed above stimulated microglial cells (indirect contact). Neither form of these materials induced

"Th1" inflammation in unstimulated (naïve) microglial cells, similar to previous studies of solubilised ECM with unstimulated macrophages [28], [45]. This is due to the similarity of ECM proteins between species [47]. Both allogeneic and xenogeneic ECM hydrogels have been reported to promote immunoregulation and enable tissue remodeling *in vivo* [25], [48].

Only solubilised forms of ECM hydrogels altered LPS-induced gene expression herein: addition of S8 significantly decreased *Nos2*/*Arg1* ratio and addition of B8 significantly decreased *Tnf* expression. Previous studies of ECM materials have shown that changes in the structural form of ECM may alter the presentation and conformation of ligands, thus influencing ligand-receptor interactions [49]. Additionally, different fibre conformations will influence the exposure and release of different molecules, including matricryptic peptides and matrix-bound nanovesicles, which in turn impact upon functional outcomes including cell migration and mitigation of inflammation [23], [24], [50]. Direct addition of solubilised S8 and B8 likely increased presentation of released molecules to stimulated microglial cell surface receptors, compared to the solid forms, resulting in mitigation of inflammation. Whilst it is not currently known why solubilised forms of S8 and B8 differentially impacted *Nos2*, *Arg1* and *Tnf* expression, this is likely predicated by the different biochemical profiles of each tissue as tissue specific induced expression of anti-inflammatory markers has previously been observed [28].

The LPS activation-mitigating properties of SCAP have previously been observed [20] and were further confirmed herein as SCAP decreased both *Nos2/Arg1* ratio and *Tnf e*xpression. Encapsulation in ECM hydrogels did not impede SCAP mitigation of LPS inflammation as demonstrated by a significant decrease of *Nos2/Arg1* ratio observed with all hydrogels. However, encapsulation of SCAP in S8 and S/F hydrogels led to increased *Tnf* expression compared to SCAP alone. Encapsulation of SCAP in B8 significantly reduced *Tnf* expression relative to control and to a similar level of SCAP

alone. The different impacts upon gene expression from SCAP embedded in different source tissue hydrogels mirror the impacts observed with hydrogels alone. S8 alone decreased the *Nos2/Arg1* ratio and whilst not significant, the addition of SCAP to S8 tended to further decrease the *Nos2/Arg1* ratio compared to SCAP alone. Similarly, the decrease in *Tnf* expression was only observed with B8, SCAP alone and SCAP in B8. It appears that the impact of LPS-induced gene expression of SCAP embedded hydrogels reflects not only the innate properties of SCAP but also the specific LPS-activation mitigating properties of the individual ECM hydrogels.

Further investigation of the biochemical profiles of the tissue specific hydrogels is required in order to clearly elucidate the mechanisms by which SCAP and hydrogels in combination modulate inflammation. We intend to use omics analyses to explore the immediate impact of ECM hydrogel composition upon SCAP secretome and downstream regulation of inflammation.

In conclusion, bone hydrogels and spinal cord hydrogels supplemented with fibrin had a gelation rate and storage modulus suitable for delivery of SCAP to SCI and all hydrogels supported SCAP viability. Solubilised S8 and B8 mitigated LPS activation of microglia with differential impacts upon gene expression: S8 significantly decreased *Nos2/Arg1* ratio and solubilised B8 significantly reduced *Tnf* expression. Encapsulation of SCAP within ECM hydrogels did not impede SCAP mitigation of LPS activation, with significant decrease of *Nos2/Arg1* ratio observed with all hydrogels. SCAP embedded ECM hydrogels reflected both the LPS activation-mitigating properties of SCAP and of the individual hydrogel with B8, alone or with SCAP significantly reducing *Tnf* expression. Thus, ECM hydrogels may be suitable vehicles to deliver SCAP for SCI due to their physical properties, preservation of SCAP viability and LPS-activation mitigating capacity.

2.7 References

[1] E. J. Bradbury and S. B. McMahon, "Spinal cord repair strategies: why do they work?," *Nat Rev Neurosci,* vol. 7, pp. 644-53, Aug 2006.

[2] J. C. Gensel and B. Zhang, "Macrophage activation and its role in repair and pathology after spinal cord injury," *Brain Res,* vol. 1619, pp. 1-11, Sep 4 2015.

[3] K. A. Kigerl, J. C. Gensel, D. P. Ankeny, J. K. Alexander, D. J. Donnelly, and P. G. Popovich, "Identification of two distinct macrophage subsets with divergent effects causing either neurotoxicity or regeneration in the injured mouse spinal cord," *J Neurosci,* vol. 29, pp. 13435-44, Oct 28 2009.

[4] P. G. Popovich, Z. Guan, P. Wei, I. Huitinga, N. van Rooijen, and B. T. Stokes, "Depletion of hematogenous macrophages promotes partial hindlimb recovery and neuroanatomical repair after experimental spinal cord injury," *Exp Neurol,* vol. 158, pp. 351-65, Aug 1999.

[5] D. P. Stirling, K. Khodarahmi, J. Liu, L. T. McPhail, C. B. McBride, J. D. Steeves*, et al.*, "Minocycline treatment reduces delayed oligodendrocyte death, attenuates axonal dieback, and improves functional outcome after spinal cord injury," *J Neurosci,* vol. 24, pp. 2182-90, Mar 3 2004.

[6] R. Lima, S. Monteiro, J. P. Lopes, P. Barradas, N. L. Vasconcelos, E. D. Gomes*, et al.*, "Systemic Interleukin-4 Administration after Spinal Cord Injury Modulates Inflammation and Promotes Neuroprotection," *Pharmaceuticals (Basel),* vol. 10, Oct 24 2017.

[7] S. F. Ma, Y. J. Chen, J. X. Zhang, L. Shen, R. Wang, J. S. Zhou*, et al.*, "Adoptive transfer of M2 macrophages promotes locomotor recovery in adult rats after spinal cord injury," *Brain Behav Immun,* vol. 45, pp. 157-70, Mar 2015.

[8] J. D. Cherry, J. A. Olschowka, and M. K. O'Banion, "Neuroinflammation and M2 microglia: the good, the bad, and the inflamed," *J Neuroinflammation,* vol. 11, p. 98, Jun 3 2014.

[9] M. J. Hoogduijn, F. Popp, R. Verbeek, M. Masoodi, A. Nicolaou, C. Baan*, et al.*, "The immunomodulatory properties of mesenchymal stem cells and their use for immunotherapy," *Int Immunopharmacol,* vol. 10, pp. 1496-500, Dec 2010.

[10] C. Paul, A. F. Samdani, R. R. Betz, I. Fischer, and B. Neuhuber, "Grafting of human bone marrow stromal cells into spinal cord injury: a comparison of delivery methods," *Spine (Phila Pa 1976),* vol. 34, pp. 328-34, Feb 15 2009.

[11] M. H. Amer, F. Rose, K. M. Shakesheff, and L. J. White, "A biomaterials approach to influence stem cell fate in injectable cell-based therapies," *Stem Cell Res Ther,* vol. 9, p. 39, Feb 21 2018.

[12] R. C. Assuncao-Silva, E. D. Gomes, N. Sousa, N. A. Silva, and A. J. Salgado, "Hydrogels and Cell Based Therapies in Spinal Cord Injury Regeneration," *Stem Cells Int,* vol. 2015, p. 948040, 2015.

[13] D. Gupta, C. H. Tator, and M. S. Shoichet, "Fast-gelling injectable blend of hyaluronan and methylcellulose for intrathecal, localized delivery to the injured spinal cord," *Biomaterials,* vol. 27, pp. 2370-9, Apr 2006.

[14] A. M. Ziemba and R. J. Gilbert, "Biomaterials for Local, Controlled Drug Delivery to the Injured Spinal Cord," *Front Pharmacol,* vol. 8, p. 245, 2017.

[15] X. C. Li, C. F. Zhong, G. B. Deng, R. W. Liang, and C. M. Huang, "Efficacy and safety of bone marrow-derived cell transplantation for spinal cord injury: a systematic review and meta-analysis of clinical trials," *Clin Transplant,* vol. 29, pp. 786-95, Sep 2015.

[16] J. W. Hur, T. H. Cho, D. H. Park, J. B. Lee, J. Y. Park, and Y. G. Chung, "Intrathecal transplantation of autologous adipose-derived mesenchymal stem cells for treating spinal cord injury: A human trial," *J Spinal Cord Med,* vol. 39, pp. 655-664, Nov 2016.

[17] W. Sonoyama, Y. Liu, D. Fang, T. Yamaza, B. M. Seo, C. Zhang*, et al.*, "Mesenchymal stem cell-mediated functional tooth regeneration in swine," *PLoS One,* vol. 1, p. e79, Dec 20 2006.

[18] S. Y. Abe, S.; Amagasa, T., "Multilineage cells from apical pulp of human tooth with immature apex," *Oral Science International,* vol. 4, pp. 45-58, 2007.

[19] S. Yu, Y. Zhao, Y. Ma, and L. Ge, "Profiling the Secretome of Human Stem Cells from Dental Apical Papilla," *Stem Cells Dev,* vol. 25, pp. 499-508, Mar 15 2016.

[20] P. De Berdt, P. Bottemanne, J. Bianco, M. Alhouayek, A. Diogenes, A. Llyod*, et al.*, "Stem cells from human apical papilla decrease neuro-inflammation and stimulate oligodendrocyte progenitor differentiation via activin-A secretion," *Cell Mol Life Sci,* vol. 75, pp. 2843-2856, Aug 2018.

[21] L. T. Saldin, M. C. Cramer, S. S. Velankar, L. J. White, and S. F. Badylak, "Extracellular matrix hydrogels from decellularized tissues: Structure and function," *Acta Biomater,* vol. 49, pp. 1-15, Feb 2017.

[22] R. Liang, G. Yang, K. E. Kim, A. D'Amore, A. N. Pickering, C. Zhang*, et al.*, "Positive effects of an extracellular matrix hydrogel on rat anterior cruciate ligament fibroblast proliferation and collagen mRNA expression," *J Orthop Translat,* vol. 3, pp. 114-122, Jul 2015.

[23] L. Huleihel, G. S. Hussey, J. D. Naranjo, L. Zhang, J. L. Dziki, N. J. Turner*, et al.*, "Matrix-bound nanovesicles within ECM bioscaffolds," *Sci Adv,* vol. 2, p. e1600502, Jun 2016.

[24] V. Agrawal, S. Tottey, S. A. Johnson, J. M. Freund, B. F. Siu, and S. F. Badylak, "Recruitment of progenitor cells by an extracellular matrix cryptic peptide in a mouse model of digit amputation," *Tissue Eng Part A,* vol. 17, pp. 2435-43, Oct 2011.

[25] G. S. Hussey, M. C. Cramer, and S. F. Badylak, "Extracellular Matrix Bioscaffolds for Building Gastrointestinal Tissue," *Cell Mol Gastroenterol Hepatol,* vol. 5, pp. 1-13, 2018.

[26] P. M. Crapo, C. J. Medberry, J. E. Reing, S. Tottey, Y. van der Merwe, K. E. Jones*, et al.*, "Biologic scaffolds composed of central nervous system extracellular matrix," *Biomaterials,* vol. 33, pp. 3539-47, May 2012.

[27] T. J. Keane, A. DeWard, R. Londono, L. T. Saldin, A. A. Castleton, L. Carey*, et al.*, "Tissue-Specific Effects of Esophageal Extracellular Matrix," *Tissue Eng Part A,* vol. 21, pp. 2293-300, Sep 2015.

[28] J. L. Dziki, D. S. Wang, C. Pineda, B. M. Sicari, T. Rausch, and S. F. Badylak, "Solubilized extracellular matrix bioscaffolds derived from diverse source tissues differentially influence macrophage phenotype," *J Biomed Mater Res A,* vol. 105, pp. 138-147, Jan 2017.

[29] T. J. Keane, J. Dziki, E. Sobieski, A. Smoulder, A. Castleton, N. Turner*, et al.*, "Restoring Mucosal Barrier Function and Modifying Macrophage Phenotype with an Extracellular Matrix Hydrogel: Potential Therapy for Ulcerative Colitis," *J Crohns Colitis,* vol. 11, pp. 360-368, Mar 1 2017.

[30] J. W. Wassenaar, R. Gaetani, J. J. Garcia, R. L. Braden, C. G. Luo, D. Huang*, et al.*, "Evidence for Mechanisms Underlying the Functional Benefits of a Myocardial Matrix Hydrogel for Post-MI Treatment," *J Am Coll Cardiol,* vol. 67, pp. 1074-86, Mar 8 2016.

[31] J. Y. Wang, A. Liou, Z. H. Ren, L. Zhang, B. N. Brown, X. T. Cui*, et al.*, "Neurorestorative effect of urinary bladder matrix-mediated neural stem cell transplantation following traumatic brain injury in rats," *CNS Neurol Disord Drug Targets,* vol. 12, pp. 413-425, May 1 2013.

[32] D. Tukmachev, S. Forostyak, Z. Koci, K. Zaviskova, I. Vackova, K. Vyborny*, et al.*, "Injectable Extracellular Matrix Hydrogels as Scaffolds for Spinal Cord Injury Repair," *Tissue Eng Part A,* vol. 22, pp. 306-17, Feb 2016.

[33] L. Lambricht, P. De Berdt, J. Vanacker, J. Leprince, A. Diogenes, H. Goldansaz*, et al.*, "The type and composition of alginate and hyaluronic-based hydrogels

influence the viability of stem cells of the apical papilla," *Dental Materials,* vol. 30, pp. e349-e361, 2014/12/01/ 2014.

[34] A. Viswanath, J. Vanacker, L. Germain, J. G. Leprince, A. Diogenes, K. M. Shakesheff*, et al.*, "Extracellular matrix-derived hydrogels for dental stem cell delivery," *J Biomed Mater Res A,* vol. 105, pp. 319-328, Jan 2017.

[35] A. Athirasala, A. Tahayeri, G. Thrivikraman, C. M. Franca, N. Monteiro, V. Tran*, et al.*, "A dentin-derived hydrogel bioink for 3D bioprinting of cell laden scaffolds for regenerative dentistry," *Biofabrication,* vol. 10, p. 024101, Jan 10 2018.

[36] L. Germain, P. De Berdt, J. Vanacker, J. Leprince, A. Diogenes, D. Jacobs*, et al.*, "Fibrin hydrogels to deliver dental stem cells of the apical papilla for regenerative medicine," *Regen Med,* vol. 10, pp. 153-67, 2015.

[37] N. Monteiro, W. He, C. M. Franca, A. Athirasala, and L. E. Bertassoni, "Engineering Microvascular Networks in LED Light-Cured Cell-Laden Hydrogels," *ACS Biomaterials Science & Engineering,* vol. 4, pp. 2563-2570, 2018/07/09 2018.

[38] D.-I. Cho, M. R. Kim, H.-y. Jeong, H. C. Jeong, M. H. Jeong, S. H. Yoon*, et al.*, "Mesenchymal stem cells reciprocally regulate the M1/M2 balance in mouse bone marrow-derived macrophages," *Experimental &Amp; Molecular Medicine,* vol. 46, p. e70, 01/10/ 2014.

[39] A. O. Brightman, B. P. Rajwa, J. E. Sturgis, M. E. McCallister, J. P. Robinson, and S. L. Voytik-Harbin, "Time-lapse confocal reflection microscopy of collagen fibrillogenesis and extracellular matrix assembly in vitro," *Biopolymers,* vol. 54, pp. 222-34, Sep 2000.

[40] M. J. Sawkins, W. Bowen, P. Dhadda, H. Markides, L. E. Sidney, A. J. Taylor*, et al.*, "Hydrogels derived from demineralized and decellularized bone extracellular matrix," *Acta Biomater,* vol. 9, pp. 7865-73, Aug 2013.

[41] M. T. Wolf, K. A. Daly, E. P. Brennan-Pierce, S. A. Johnson, C. A. Carruthers, A. D'Amore*, et al.*, "A hydrogel derived from decellularized dermal extracellular matrix," *Biomaterials,* vol. 33, pp. 7028-7038, 2012.

[42] V. K. Lai, S. P. Lake, C. R. Frey, R. T. Tranquillo, and V. H. Barocas, "Mechanical behavior of collagen-fibrin co-gels reflects transition from series to parallel interactions with increasing collagen content," *J Biomech Eng,* vol. 134, p. 011004, Jan 2012.

[43] K. Franze, "The mechanical control of nervous system development," *Development,* vol. 140, pp. 3069-77, Aug 2013.

[44] R. D. Bartlett, D. Choi, and J. B. Phillips, "Biomechanical properties of the spinal cord: implications for tissue engineering and clinical translation," *Regen Med,* vol. 11, pp. 659-73, Oct 2016.

[45] F. W. Meng, P. F. Slivka, C. L. Dearth, and S. F. Badylak, "Solubilized extracellular matrix from brain and urinary bladder elicits distinct functional and phenotypic responses in macrophages," *Biomaterials,* vol. 46, pp. 131-40, Apr 2015.

[46] A. F. Lloyd, C. L. Davies, R. K. Holloway, Y. Labrak, G. Ireland, D. Carradori*, et al.*, "Central nervous system regeneration is driven by microglia necroptosis and repopulation," *Nat Neurosci,* vol. 22, pp. 1046-1052, Jul 2019.

[47] S. B. Seif-Naraghi, J. M. Singelyn, M. A. Salvatore, K. G. Osborn, J. J. Wang, U. Sampat*, et al.*, "Safety and efficacy of an injectable extracellular matrix hydrogel for treating myocardial infarction," *Sci Transl Med,* vol. 5, p. 173ra25, Feb 20 2013.

[48] I. T. Swinehart and S. F. Badylak, "Extracellular matrix bioscaffolds in tissue remodeling and morphogenesis," *Dev Dyn,* vol. 245, pp. 351-60, Mar 2016.

[49] B. N. Brown, C. A. Barnes, R. T. Kasick, R. Michel, T. W. Gilbert, D. Beer-Stolz*, et al.*, "Surface characterization of extracellular matrix scaffolds," *Biomaterials,* vol. 31, pp. 428-37, Jan 2010.

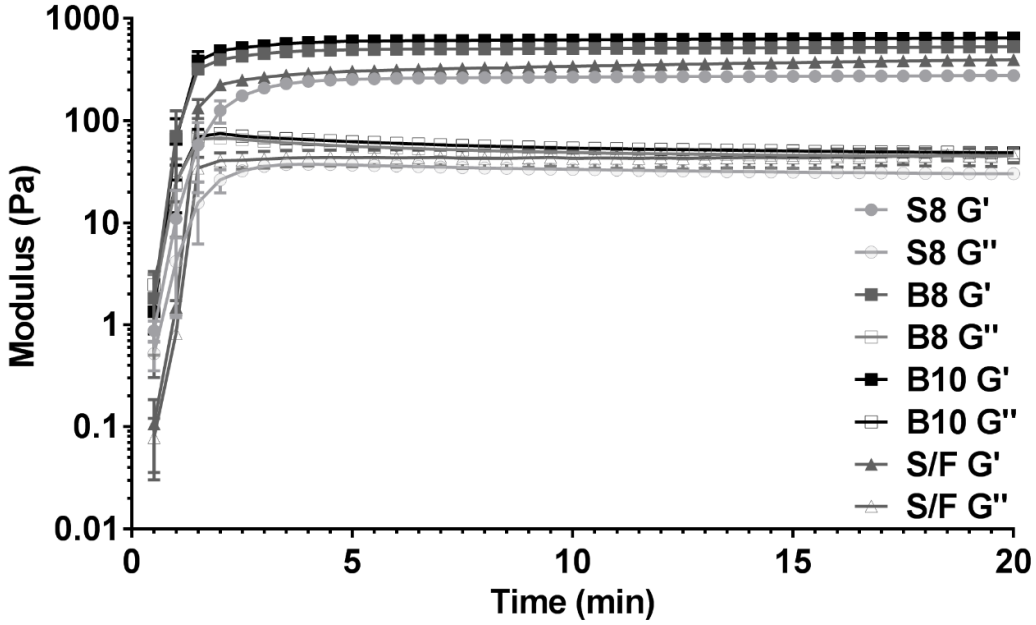
[50] P. F. Slivka, C. L. Dearth, T. J. Keane, F. W. Meng, C. J. Medberry, R. T. Riggio*, et al.*, "Fractionation of an ECM hydrogel into structural and soluble components reveals distinctive roles in regulating macrophage behavior," *Biomater Sci,* vol. 2, pp. 1521-34, Aug 26 2014.

[51] Ruparel, N. B., de Almeida, J. F., Henry, M. A. & Diogenes, A, "Characterization of a stem cell of apical papilla cell line: effect of passage on cellular phenotype," *J Endod*, vol. 39, pp. 357–363, Mar 2013.

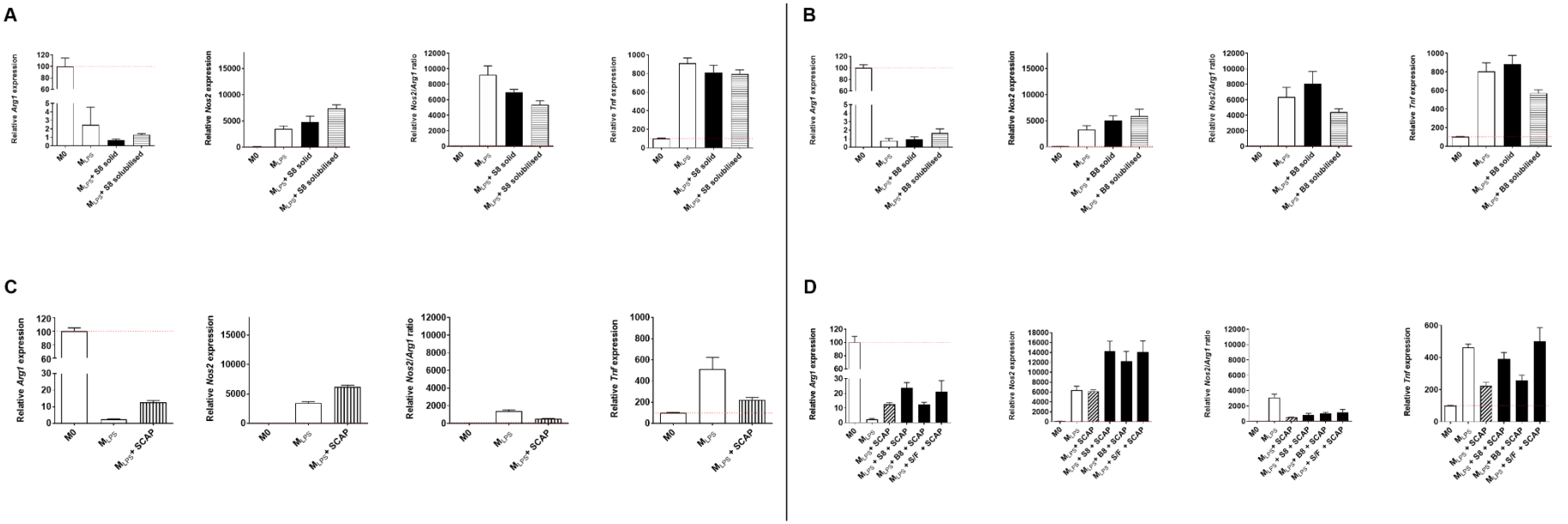
[52] You, M.-M. et al., "Royal Jelly Attenuates LPS-Induced Inflammation in BV-2 Microglial Cells through Modulating NF-κB and p38/JNK Signaling Pathways," *Mediators of Inflammation*, Apr 8 2018.

[53] He, Y. et al., "RNA sequencing analysis reveals quiescent microglia isolation methods from postnatal mouse brains and limitations of BV2 cells," *J Neuroinf,* vol. 15, 2018.

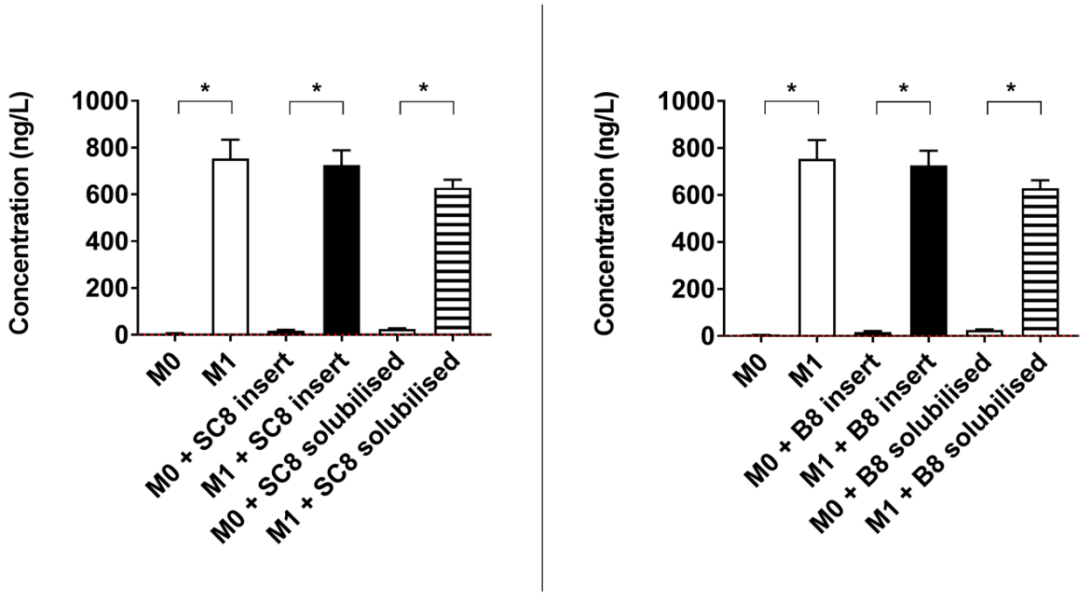
2.8 Supplementary Data



Supplementary Figure 2.1 Rheological characterisation of ECM hydrogels. Oscillatory time sweep curves of mean storage (G') and mean loss (G") moduli of different concentrations (8 and 10 mg/mL) of spinal cord (S8) and bone (B8, B10) derived hydrogels and S8 combined with fibrin (S/F). Error bars represent the standard error of the mean for three replicates (n=3)



Supplementary Figure 2.2 Influence of ECM, SCAP or SCAP encapsulated in ECM hydrogels on BV2 cells. LPS-activated BV2 cells were treated with either solid or solubilised S8 hydrogels (A); solid or solubilised B8 hydrogels (B); SCAP seeded on inserts (C) or SCAP seeded on inserts, alone or encapsulated in S8, B8 or S/F hydrogels (D). The gene expression of *Tnf*, inducible nitric oxide synthetase gene (*Nos2*) and arginase 1 gene (*Arg1*) was quantified by real time quantitative polymerase chain reaction. *Nos2/Arg1* ratio was also calculated. Results were expressed relative to the non-stimulated BV2 cells (M0) set at 100% where appropriate (red dotted bar) and LPS-activated BV2 cells are also shown



Supplementary Figure 2.3 Influence of ECM hydrogels on BV2 TNFα secretion. Non-stimulated (M0) and LPS-activated (M1) BV2 cells were treated with either solid (cast in an insert) or solubilised S8 and B8 hydrogels and secretion of TNFα was quantified by enzyme-linked immunosorbent assay. Error bars represent the standard error of the mean (N=3, n=3). One-way ANOVA with Tukey post-hoc test, * $p < 0.05$

3 Interplay Between Stem Cells of the Apical Papilla (SCAP) and Spinal Cord-Derived Extracellular Matrix Hydrogel (scECM) in the Midst of Inflammation- a Metabolomics Approach

Natalija Tatic, Salah Abdelrazig, Felicity R. A. J. Rose, Dong-Hyun Kim, Anne des Rieux, Lisa J. White

3.1 Preface

This chapter describes the third objective, investigation of “Th1” stimuli and/or scECM effect on SCAP metabolic profile and of SCAP-scECM interplay in basal and stimulated state. To detect molecules expressed by SCAP as well as those contained in the hydrogel, metabolomics, proteomics and NMR spectroscopy can be used. In this study, a metabolomics approach was chosen, specifically: spent medium analysis, due to the complexity of SCAP-scECM interactions and as the technique has previously been used to investigate MSC differentiation [1]. Lead Th1 cytokines driving inflammation at SCI, TNFα and IFNγ [2]–[4] were selected for the stimulation. Tested and compared conditions are specified in Table 3.1.

As detection of the significant differences is conditioned by metabolites concentration, the highest possible number of SCAP was used for the lowest possible volume of medium, $2x10^5$ cells in 1 mL. The volume of medium was also optimised to include the volumes necessary for the performance of molecular assays to support metabolomics investigation. The minimal number of SCAP was estimated by comparing their size and metabolic activity to similar cells whose metabolic footprint detection had been described in published literature. For the reliable detection of the changes in metabolite secretion, the number of cells should not vary by more than 10% between the conditions. Therefore, to have the effect that results in significant differences between the conditions, whilst maintaining SCAP viability according to Live/Dead and PrestoBlue assays combined, the incubation time and TNFα, IFNγ and scECM concentration were optimised at 24h, 35 ng/mL, 35 ng/mL and 1.6 mg/mL, respectively.

SCAP culture medium (containing 10% foetal bovine serum) was incubated and used as a baseline to calculate the changes in metabolite peak intensity. Therefore, freshly

prepared cold SCAP culture medium was also analysed to attest that the incubation at 37 °C did not have an influence on medium content. Due to the sensitivity of the technique, to be able to account for TNFα/IFNγ/scECM- induced differences, one biological and six experimental replicates were analysed. The sextuplicates each represent separate microenvironments with already different metabolic profiles. Introducing more biological replicates into the same experiment would increase the differences within the same condition, making the differences between the conditions either less significant or increasingly more complex.

Molecular assays were selected to confirm and complement metabolomics findings. IDO enzymatic assay was selected to confirm activation of kynurenine pathway [5] and validate LC-MS results. TGFβ secretion was investigated to complement metabolomics findings and investigate immunosuppressor activity of SCAP as a possible result of SCAP activation [6],[7]. MCP-1 enzyme-linked immunosorbent assay was another approach to confirming SCAP activation [8]. These analyses were performed in biological and experimental triplicates (N=3, n=3). After the data distribution was determined to be Normal, a parametric test to determine whether there were differences between the conditions, a One-way ANOVA was performed. To determine what are the separate differences between each condition with equal number of values a Tukey's post-hoc test was used.

Due to the high dimensional and high throughput LC-MS data, where the multiple conditions are connected/overlap, each condition gave data on the hundreds of variables, i.e. metabolites and the variables are strongly interdependent, so multivariate statistical analyses were used. Principal component analysis (PCA) provided data summaries and overviews by using maximum variance method to distribute data into the different groups. SIMCA-P software then used this information for the supervised orthogonal projections to latent structures discriminant analysis (OPLS-DA). OPLS-DA

describes the differences between the groups by using a maximum separation method. OPLS-DA determines the variables with the highest discriminatory power, how variables are correlated and how much is the variation of each variable/correlated set of variables related and not related to group differences/separation. Therefore, OPLS-DA determines which variable/correlated set of variables (i.e. metabolites/set of metabolites) signifies or is relevant to the differences between the conditions.

Table 3.1. Tested conditions and their comparisons were selected to answer the specific objectives

Compared conditions	Purpose of the comparison/ Specific objective
SCAP+stimulus vs SCAP	To investigate influence of the stimulus on SCAP
scECM vs Medium	To investigate scECM constituents detectable by LC-MS using the metabolomics approach
SCAP+scECM vs SCAP	To investigate influence of scECM addition to SCAP on the overall molecular profile in basal state
SCAP+scECM -scECM* vs SCAP	To investigate SCAP-scECM interplay in basal state: Influence of scECM on SCAP Consumption of scECM-derived molecules by SCAP
SCAP+scECM+stimulus vs SCAP+scECM	To investigate SCAP response to the stimulus in the presence of scECM
SCAP+scECM+stimulus vs SCAP+ stimulus	To investigate influence of scECM addition to SCAP on the overall molecular profile in the presence of stimulus
SCAP+scECM+stimulus - scECM* vs SCAP+ stimulus	To investigate SCAP-scECM interplay in the presence of the stimulus: Influence of scECM on SCAP Consumption of scECM-derived molecules by SCAP

Stimulus was TNFα + IFNγ.
* scECM molecular footprint was deducted to discriminate between the scECM influence on SCAP specifically and the scECM contribution to the overall metabolic profile that includes molecules derived from only scECM and SCAP-scECM interaction.

3.3.1 References

[1] A. Surrati, R. Linforth, I. D. Fisk, V. Sottile, and D. H. Kim, “Non-destructive characterisation of mesenchymal stem cell differentiation using LC-MS-based metabolite footprinting,” *Analyst*, vol. 141, no. 12, pp. 3776–3787, 2016.

[2] A. Pourgholaminejad, N. Aghdami, H. Baharvand, and S. M. Moazzeni, “The effect of pro-inflammatory cytokines on immunophenotype, differentiation capacity and immunomodulatory functions of human mesenchymal stem cells,” *Cytokine*, vol. 85, pp. 51–60, 2016.

[3] J. C. Gensel and B. Zhang, “Macrophage activation and its role in repair and pathology after spinal cord injury,” *Brain Res.*, vol. 1619, pp. 1–11, 2015.

[4] A. Berger, “Science commentary: Th1 and Th2 responses: What are they?,” *British Medical Journal*, vol. 321, no. 7258. p. 424, 12-Aug-2000.

[5] F. Hached *et al.*, “Polysaccharide hydrogels support the long-Term viability of encapsulated human mesenchymal stem cells and their ability to secrete immunomodulatory factors,” *Stem Cells Int.*, vol. 2017, pp. 6–8, 2017.

[6] M. Y. Noh *et al.*, “Mesenchymal Stem Cells Modulate the Functional Properties of Microglia via TGF-b Secretion,” *Stem Cells Transl. Med.*, vol. 5, pp. 1538–1549, 2016.

[7] L. Lin and L. Du, “The role of secreted factors in stem cells-mediated immune regulation,” *Cell. Immunol.*, vol. 326, no. February 2017, pp. 24–32, 2018.

[8] X. Li, W. Du, F. X. Ma, X. Feng, F. Bayard, and Z. C. Han, “High concentrations of TNF-α induce cell death during interactions between human umbilical cord mesenchymal stem cells and peripheral blood mononuclear cells,” *PLoS One*, vol. 10, no. 5, pp. 1–13, 2015.

3.2 Abstract

One of the main characteristics of SCI and a hindrance to its repair is chronic “Th1-type” inflammation. MSC and ECM-based hydrogels have been attributed immunomodulatory properties. In a previous work, we reported that human stem cells from the apical papilla (SCAP) were able to modulate the expression of pro- and anti-inflammatory genes in microglia cells subjected to an inflammatory stimulus. The objective of this work was to study the metabolic changes that occur when SCAP were activated by a pro-inflammatory stimulus and to evaluate how the scECM could alter the metabolomics profile of activated SCAP.

LC-MS was used to analyse the metabolite changes in incubation medium and the findings were correlated with kynurenine, TGFβ and MCP-1 assays. First it was shown that TNFα + IFNγ stimulated SCAP responded by activation that may indicate increased immunoregulatory potential. scECM had its own specific metabolic footprint that may have potential for immunoregulation in the scope of SCI. The presence of scECM altered SCAP metabolic profile related to energy, transcription, cellular integrity and stress response, whilst SCAP consumed scECM-derived complex anti-inflammatory lipids and their precursors, presumably for self-regulation. This interaction was more prominent in stimulated compared to basal state. Still, when SCAP exposed to scECM were stimulated, SCAP responded by enhancing the same inherent immunoregulatory pathways. Secreted molecule profiles of SCAP+scECM combined had higher content of anti-inflammatory molecules compared to SCAP in stimulated condition.

3.3 Introduction

SCI results in chronic “Th1-type” inflammation, leading to progressive tissue damage [1] and limited regeneration [2]. MSC, that have well reported immunoregulatory and pro-regenerative properties, have potential as a reparative strategy for SCI. [3], [4]. The majority of MSC in SCI clinical trials are derived from bone marrow [5]. However, dental stem cells may provide an alternative source of MSC mostly due to their ease of accessibility, proliferation rate, basal expression of neural markers and greater potential for neural differentiation [6].

Stem cells of the apical papilla (SCAP) are obtained from the growing tissue at the apex of immature wisdom teeth that gives rise to the roots of the teeth [7], [8]. SCAP present a good compromise between easiness of access, isolation and expansion, and therapeutic potential [9], [10]. SCAP maintain “stemness” in high passages (P20) [11], have high migratory and regenerative capacity [8], secrete high amounts of chemokines and neurotrophins in basal state [12] and their neuro-differentiation and angiogenic potential increase even further in stress microenvironments [9], [13], [14]. We recently showed that SCAP decrease pro- and increase anti-inflammatory marker expression in microglia cells [15] and stimulate oligodendrocyte progenitor cells differentiation [15], important for mitigating inflammation and stimulating re-myelination after SCI [15], [16]. These characteristics are key to SCAP being used as a therapy for SCI.

An ideal system to deliver SCAP to spinal cord lesion may be an injectable hydrogel [17] that could minimize cellular damage during injection and maintain cell viability at the lesion site [18]. As the SCI environment is highly inflammatory, an ideal hydrogel for SCAP delivery will not only support SCAP’s own immunomodulatory effect but may also be able to directly contribute to inflammation modulation. ECM-derived hydrogels may

be a suitable candidate as they are injectable and can modulate inflammation *in vitro* and *in vivo* [19]–[21], presumably as they contain growth factors [22], matrix- bound nanovesicles [23], cryptic peptides and bioactive motifs [24]. We have previously shown that both spinal cord and bone derived hydrogels can reduce inflammation [25], whilst other studies have shown that spinal cord-derived ECM (scECM) hydrogel may promote regeneration [26], [27]. While scECM stimulates neuronal marker expression in SCAP [28], very little is known about scECM immunoregulatory properties or its influence upon the immunoregulatory properties of SCAP.

Thus, the objective of this study was to explore SCAP-scECM interactions by analysing their individual and combined metabolic footprints in a “Th1”-like pro-inflammatory microenvironment, to simulate SCI [29]. We hypothesised that the metabolite profile of SCAP cell culture medium will be affected by both the pro-inflammatory stimuli and the presence of scECM. We aimed to i) study SCAP secreted metabolites in response to the stimulus (IFNγ and TNFα); ii) detect scECM own molecular profile and iii) explore SCAP-scECM interplay through their metabolic profile in a pro-inflammatory environment.

3.4 Materials and Methods

3.4.1 Materials and Reagents

Hydrophilic interaction liquid chromatography column (SeQuant® ZIC®-pHILIC) was from Merck (Feltham, UK). Human recombinant TNFα, human TGF-β1 enzyme - linked immunosorbent assay kit and human monocyte chemoattractant protein-1 (MCP-1/CCL2) enzyme-linked immunosorbent assay kit were from PeproTech (Glassdoor, UK). Triton X-100, sodium deoxycholate, peracetic acid concentrated, sterile apyrogenic 10x phosphate buffer saline, pepsin, sodium hydroxide, minimum essential medium and foetal bovine serum were from Sigma-Aldrich (Poole, UK). All other reagents were purchased from Thermo Fisher Scientific (Loughborough, UK).

3.4.2 Spinal Cord Decellularisation and Preparation of Solubilised Hydrogels

Fresh porcine spinal cords were obtained from market weight animals at a local slaughterhouse (Abattoir d'Anderlecht, Brussels, Belgium). Female and male animals were used indiscriminately. Spinal cords were cleaned, fragmented and processed following previously described protocol for spinal cord decellularisation [28]. The protocol consisted of series of agitated baths, at room temperature and 200 rpm unless stated otherwise: water (overnight, 4 °C, 60 rpm), 0.02% trypsin/0.05% ethylenediaminetetraacetate (60 min, 37 °C), 3.0% Triton X-100 (60 min), water (30 min), 1.0 M sucrose (15 min), water (30 min), 4.0% sodium deoxycholate (60 min), 0.1% peracetic acid in 4.0% ethanol (120 min), phosphate buffer saline (15 min), water (24h). The obtained ECM was lyophilised, fragmented and digested with 1 mg/mL pepsin in 0.01 N hydrochloric acid for 48h to obtain a digest of 10 mg spinal cord ECM/mL. Digest was then centrifuged, aliquoted and stored at – 20 °C. Prior to use, ECM digests were

thawed, neutralised with 10 x phosphate buffer saline and 0.01 N sodium hydroxide and diluted to 8 mg/mL using phosphate buffer saline, at 4 °C, to generate pre-gel solutions as described previously [28].

3.4.3 SCAP Culture

Human wisdom tooth was collected from a healthy individual between 16 and 18 years of age upon obtaining an informed consent (Approved by the Commission d'Ethique Biomédicale Hospitalo-Facultaire of UCL, 2012/14JUN/283). Human SCAP were isolated, characterised [11] and used between passages 5 and 8. SCAP were grown at 37 °C in 5% CO_2 in growth medium composed of Minimum Essential Medium supplemented by 10% foetal bovine serum, 1% of L-glutamine and 1% of penicillin and streptomycin. SCAP were passaged upon reaching 80% confluency using StemPro Accutase®.

3.4.4 SCAP Stimulation

SCAP ($2x10^5$ cells/well) were seeded in 12-well tissue culture plates and incubated for 16h. to allow for cell attachment. SCAP were then incubated for 24h with fresh SCAP growth medium containing either: i) 35 ng/mL IFNγ and 35 ng/mL TNFα (denoted as SCAP+Stimulus); ii) 1.6 mg/mL scECM (denoted as SCAP+scECM); iii) 35 ng/mL IFNγ, 35 ng/mL TNFα and 1.6 mg/mL scECM (denoted as SCAP+scECM+Stimulus) or iv) fresh culture medium. Solubilised hydrogel 1.6 mg/mL was obtained by mixing 200 µL of pre-gel solutions in 1 mL of cell culture medium.

Media were then collected, aliquoted and used directly for metabolite extraction or stored at - 20 °C for other experiments. Each experiment was performed in triplicates (N=3, n=3) for molecular assays and in sextuplicates (N=1, n=6) for metabolic footprinting.

3.4.5 IDO Quantification

IDO enzyme activity was measured by tryptophan-to-kynurenine conversion with photometric determination of kynurenine concentration in the supernatant as previously described [30]. Briefly, 30 µL of 30% trichloroacetic acid solution was added to 60 µL of condition media aliquots (previously stored at – 20 °C) and incubated for 30 min at 50 °C. After centrifugation (10 min, 3000 rpm), 50 µL of supernatant was added to 50 µL of freshly prepared Ehrlich's solution, incubated for 10 min at room temperature and the absorbance was read at 450 nm.

3.4.6 TGF-β1 and MCP-1 / CCL2 Quantification

Concentrations of TGF-β1 and MCP-1 in supernatants (diluted 1:10 for TGF-β1 and 1:5 for MCP-1) were measured by commercially available enzyme-linked immunosorbent assay kits (sensitivity 1 pg/mL) used according to manufacturer's instructions (PeproTech®).

3.4.7 Metabolites Extraction

Freshly collected media from the SCAP stimulation experiments were treated as previously described [29]. Briefly, after the collection, aliquots were centrifuged (5 min, 7378 g) and then ice-cold methanol was added to the supernatant in 3:1 ratio and vortexed for 1 min, incubated at - 20 °C for 20 min, vortexed again for 15 s and centrifuged (10 min, 13200 g, 4 °C). Collected supernatants were stored at - 80 °C until further analysis.

3.4.8 LC-MS Analytical Methodologies

LC-MS was performed on an Accela system coupled to an Orbitrap Exactive MS as described before [29]. Briefly, chromatographic separation was carried out on a ZIC®-pHILIC (150 mm × 4.6 mm, 5 µm) at 45 °C and 300 µL/min flow rate. The mobile phase consisted of 20 mM ammonium carbonate in water (A) and 100% acetonitrile (B) which were eluted with a linear gradient from 80% B to 5% B over 15 min, followed by a 2 min linear gradient from 5% B to 80% B, and 7 min re-equilibration with 80% B. Spectral data was acquired in a full scan mode, m/z range 70 - 1400 and resolution 50000, for both positive and negative electrospray ionisation. The instrument calibration was performed with modified Thermo standard calibration solution (mixture of mases below m/z 1400): $C_2H_6NO_2$ (m/z 76.0393) was included for positive and $C_3H_5O_3$ (m/z 89.0244) for negative ion electrospray ionisation, in order to extend the calibration mass range to small metabolites. Probe and capillary temperatures were maintained at 150 and 275 °C, respectively.

A 10µL aliquot was taken from each sample and combined to make quality control sample pool (QC). QC sample was injected after every five samples for the assessment of instrument performance. The injection volume was 10 µL and samples were maintained at 4 °C.

3.4.9 Data Processing and Statistical Analysis

Normality tests and One-way ANOVA followed by Tukey's correction ($p < 0.05$) for molecular assay data was performed in Prism (7.02, GraphPad, CA, USA). Error bars represent the standard error of the mean in all figures.

LC-MS raw data were obtained in Xcalibur v2.1 software and processed as described before [29], using XCMS for untargeted peak-picking [31], mzMatch for peak matching and annotation of related peaks [32] and IDEOM with standard parameters for noise filtering and putative metabolite identification [33], according to The Metabolomics Standards Initiative (MSI, 2005). Metabolites with masses and retention times matching to authentic standards, run on the same instrument at the same time, were identified with Level 1. If the exact standard was not available, a metabolite was identified according to the predicted retention time. This putative identification is Level 2.

In order to clearly identify the molecular footprint of each condition, baseline values were initially established by analysing metabolites present in basal culture medium, not exposed to SCAP, scECM or stimulus. For instance, scECM molecular footprint was established for scECM in medium compared to medium alone. This scECM molecular footprint was then deducted from SCAP+scECM, to discriminate between the impact of scECM treatment on SCAP and scECM contribution to the overall molecular footprint.

Supervised orthogonal partial least squares discriminant analysis (OPLS-DA) was performed in SIMCA-P (13.0.2, Umetrics AB, Sweden) to analyse the differences in molecular footprint between each condition. T-test followed by Benjamini–Hochberg false discovery rate procedure was performed in Prism (7.02, GraphPad, CA, USA) to analyse the differences in peak intensity of each individual metabolites from each two conditions. If the metabolite was not identified in one of the groups, its peak intensity was estimated at 1000 - the maximum noise level. Significantly different metabolites between each two conditions had variable importance in projection (VIP) score higher than one and adjusted p value (q^2) lower than or equal to 0.05. Significantly different metabolites were matched to Kyoto Encyclopaedia of Genes and Genomes (KEGG) pathways, Human Metabolome Database (HMDB) and PubChem free online databases. If the metabolites were not of human cell origin, such as cell culture antibiotics, or could

not be matched to a KEGG pathway or specific function, such as hydrogel-derived di- and tripeptides, they were removed from further consideration. Metabolites were then matched to pathway groups in MetaboAnalyst - a free online platform. Metabolites that could be related to inflammation were presented in the supplementary tables and their noted peak intensities represented the mean of the sextuplicates. Tables in the main manuscript represented the shortened versions of the supplementary tables and contain only the metabolites with the specifically described relationship to inflammation that are discussed in this manuscript, grouped according to chemical structure.

3.5 Results and Discussion

Principal component analysis (PCA-X) showed distinctive sample distribution (Supplementary Figure 3.1, 3.2) and OPLS-DA analysis a clear separation between the conditions (Figure 3.1), which meant there were significant differences between the conditions. The addition of hydrogel to the stimulated and unstimulated cells (upward shift) had a larger effect on molecular profile compared to the addition of stimulus to SCAP with and without scECM (rightward shift). As the upward shift between the medium and hydrogel was also large, it suggested that the changes in the molecular profile of stimulated and unstimulated cells upon the addition of scECM are largely deriving from the scECM molecules and less from their influence on SCAP (Figure 3.1).

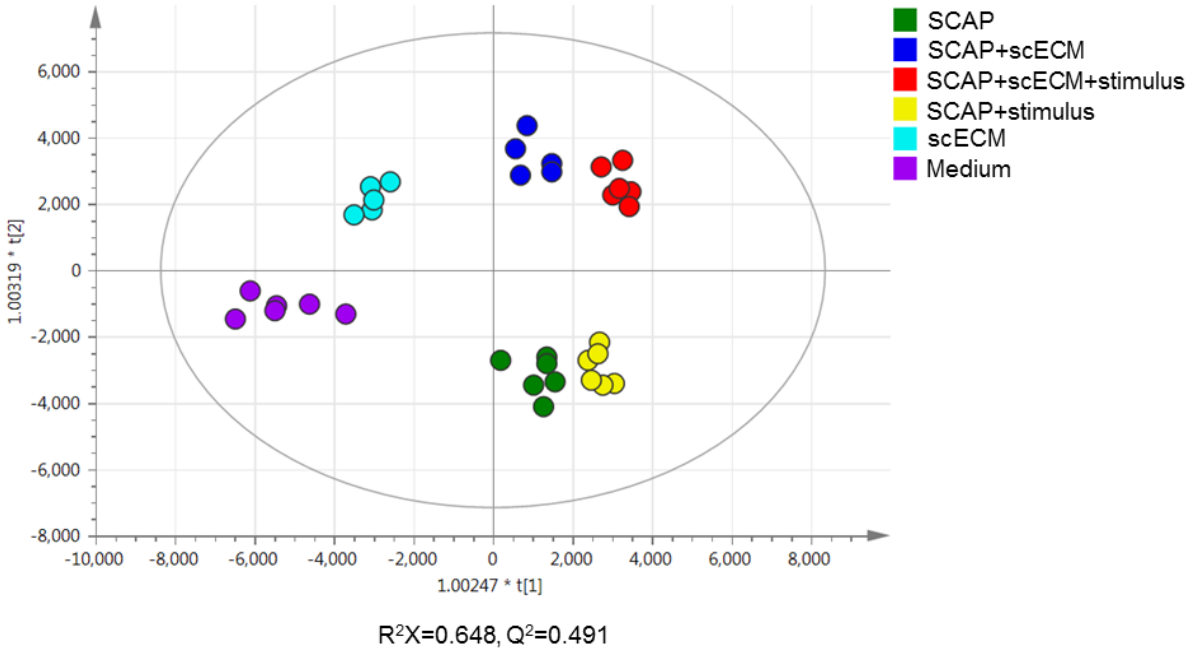


Figure 3.1 OPLS-DA for all sample groups upon 24h of incubation, excluding quality control sample and outliers. Stimulus:TNFα+IFNγ. R^2X and Q^2 are goodness of the fit parameters, 1 equals perfect fit. The addition of scECM caused a clear upward and of stimulus rightward shift

3.5.1 Impact of the Stimulus on SCAP Metabolism

The secreted metabolites of SCAP exposed to an inflammatory stimulus (TNFα and IFNγ) (SCAP+stimuli) were compared to SCAP basal state (SCAP). Out of 15 identified significantly different metabolites (Table 3.2, Supplementary Table 3.1), five belonged to the same tryptophan pathway (Supplementary Figure 3.3). The decrease of tryptophan and increase of formylkynurenine and kynurenine were confirmed by kynurenine quantification assay (reflecting indoleamine 2,3-dioxygenase activity) that showed a significant increase when SCAP were stimulated (Figure 3.2). Increased 8-metoxykynurenate (Table 3.2) has been related to the induction of immune tolerance. The other kynurenine products, that were not detected here, demonstrated neurotoxic effects [79], [80]. Increased expression of indoleamine 2,3-dioxygenase by MSC in the presence of a pro-inflammatory stimulus is a well-known mechanism by which MSC exert immunomodulatory properties [34], i.e. promote regulatory phenotype in macrophages (M2) and regulatory T lymphocytes and induce immune tolerance [35].

Even though TGFβ also supresses T-lymphocytes activation and induces M2 phenotype in macrophages [36], [37], it remained unchanged (around 4 ng/mL) upon SCAP stimulation (Figure 3.2). The increase of MCP-1 secretion (by 310 fold) observed in stimulated SCAP (Figure 3.2), was expected according to literature and suggested that SCAP were activated [38]. Anti-inflammatory effects have been described for octanoic acid [39] that was detected upon stimulation (Table 3.2,). Small decrease (1.7 fold) of docosahexaenoic acid in stimulated condition (Table 3.2) may mean that SCAP used docosahexaenoic acid due to its direct anti-inflammatory effect, or metabolised it into the anti-inflammatory resolvins and protectins [40].

Overall, the results confirmed, this time from the metabolomics perspective, that SCAP primed with an inflammatory stimulus are activated in the similar way to other MSC [41]. As TNFα/IFNγ activated MSC have been shown to have increased immunoregulatory capacity [41], the increased immunoregulatory capacity can be hypothesised for activated SCAP.

Table 3.2 Significant changes in SCAP metabolic footprint detected in response to TNFα and IFNγ after 24h incubation matched to Human Metabolome Database (HMDB) and Kyoto Encyclopaedia of Genes and Genomes (KEGG) pathways, in direct relationship with inflammation

Putative metabolite	IDC	Peak intensity (SCAP+stimulus)	Peak intensity (SCAP)	Fold change
Kynurenine	L1	567339	9809	57.839
5-Hydroxyindoleacetate	L2	179955	5367	33.530
8-Methoxykynurenate	L2	11022	1000	11.022
Octanoic acid	L2	191599	29390	6.519
Formylkynurenine	L2	23872	3844	6.210
Docosahexaenoicacid	L2	9858	16482	0.598
Tryptophan	L1	24614	478310	0.051

Statistical significance was determined with t-test and false discovery rate (FDR) correction using the Benjamini-Hochberg procedure ($q^2 \leq 0.05$), variable importance in projection scores obtained in orthogonal partial least squares discriminant analysis (VIP OPLS-DA > 1) and fold change ≥ 1.5; IDC- metabolite identification level according to the metabolomics standards initiative L1 - Level 1, L2 - Level 2; Colours represent the heat map of the fold change between mean peak intensities in scECM hydrogel and medium: yellow - no change, red - increase, blue – decrease.

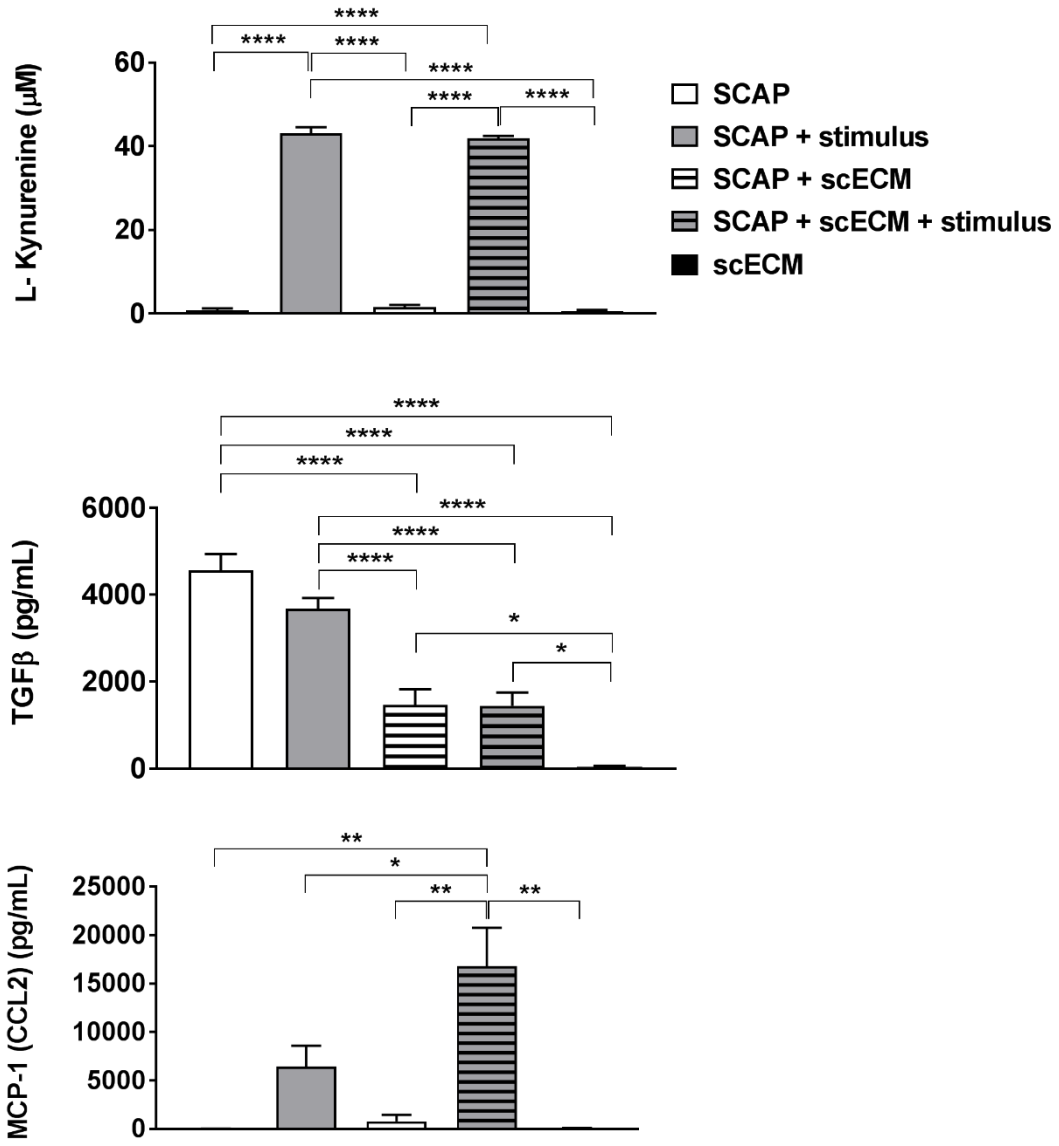


Figure 3.2 L-kynurenine, TGFβ and MCP-1 concentration in cell culture medium of different conditions combining SCAP, scECM and stimuli

3.5.2 Molecular Profile of scECM

Comparing scECM to medium upon 24h incubation, 22 of the significantly different molecules (Table 3.3, Supplementary Table 3.2) were matched to 13 cellular pathways (Supplementary Figure 3.4). Detected unsaturated fatty acids were presumed to be of Z-orientation due to the hydrogel origin [46].

3.5.2.1 scECM Molecules Involvement in Immunoregulation

Choline, choline phosphate, sn-glycero-3-phosphoethanolamine, sn-glycero-3-phosphocholine and various fatty acids may highly effect glycerophospholipid metabolism, arachidonic acid metabolism and fatty acid biosynthesis (Supplementary Figure 3.4) closely related to inflammation [40]. This may be one of the reasons for previously described scECM effects on activated microglia [25].

Furthermore, icosatrienoic (8Z, 11Z, 14Z or 11Z, 14Z, 17Z), 11Z-eicosenoic, 7Z,10Z,13Z,16Z-docosatetraenoic (adrenic), docosapentaenoic (7Z,10Z,13Z,16Z,19Z), docosahexaenoic and 5Z,8Z,11Z,14Z-eicosatetraenoic (arachidonic) acid also directly regulate local inflammatory response, or the metabolism of anti-inflammatory lipids, prostaglandins, leukotrienes, lipoxins, resolvins, protectins and maresins [40], [47]–[50]. Choline has also been shown to directly regulate immune response by attenuating nuclear factor κB [51]. Carnosine has been shown to have a neuroprotective effect, directly metabolise into histidine or with homoanserine, s-glutathionyl-cysteine and methionine-s-oxide, influence oxidative-stress reactions [52], [53]. Gamma-glutamylputrescine also participates in oxidative reactions, spending molecular oxygen [42]. These scECM-derived metabolites may have a specific contribution to inflammation mitigation.

High chenodeoxycholic acid fold change may result from deoxycholate, a detergent used during scECM production. Chenodeoxycholic acid has been shown to be cytotoxic, as it may disrupt cell membranes and induce oxidative stress [44], but also to reduce the release of pro-inflammatory cytokines from macrophages and T-lymphocytes and neutrophils infiltration to the central nervous system in lower concentrations [45].

3.5.2.2 scECM Molecules Involvement in Spinal Cord Regeneration

Molecules released from scECM that may participate in immunoregulation, e.g. arachidonic, docosahexaenoic, chenodeoxycholic and ω-3 fatty acids, may also participate in neuronal differentiation, preservation of neuronal tissue and improved proliferation, differentiation and survival of neural stem cells, [54]–[59]. This may be one of the reasons why scECM has previously been shown to stimulate neural differentiation [60]. Choline, choline phosphate, sn-glycero-3-phosphoethanolamine, sn-glycero-3-phosphocholine and the fatty acids detected in hydrogel have been proven critical for neural membrane integrity [61] and may participate in re-myelination [62].

Table 3.3 Specific molecular footprint of scECM obtained after 24h incubation matched to Human Metabolome Database (HMDB), Kyoto Encyclopaedia of Genes and Genomes (KEGG) pathways and in direct relationship with inflammation

Putative metabolite	IDC	Peak intensity scECM	Peak intensity Medium	Fold change
γ-Glutamylputrescine	L2	122690	1000	122.690
Chenodeoxycholic acid	L1	98294	1000	98.294
Carnosine	L2	79850	1000	79.850
Adrenic acid	L2	8884	1000	8.884
Glycero-3-phosphoethanolamine	L2	30877	3476	8.883
Choline phosphate	L1	8391	1914	4.384
Choline	L2	110293	28021	3.936
Eicosenoic acid	L2	38910	10107	3.850
Glycerophosphocholine	L1	2564584	700026	3.664
Arachidonic acid	L2	37298	10673	3.495
Docosapentaenoic acid	L2	13980	4063	3.441
8,11,14-Eicosatrienoic acid	L2	14671	5759	2.547
Docosahexaenoic acid	L2	23564	9383	2.511
1-acyl-sn-glycero-3-phosphocholines	L2	3546	79328	0.045

Statistical ignificance was determined with t-test and false discovery rate (FDR) correction using the Benjamini-Hochberg procedure ($q^2 \leq 0.05$), variable importance in projection scores obtained in orthogonal partial least squares discriminant analysis (VIP OPLS-DA > 1) and fold change ≥ 1.5; IDC- metabolite identification level according to the metabolomics standards initiative L1 - Level 1, L2 - Level 2; Colours represent the heat map of the fold change between mean peak intensities in scECM hydrogel and medium: yellow - no change, red - increase, blue – decrease.

3.5.3 Interplay between SCAP and scECM in Basal State

When comparing SCAP+scECM with SCAP molecular profile, only one metabolite (glycyl-arginine dipeptide) was significantly increased. Nevertheless, the molecular profile was matched to metabolomics pathways (Supplementary Figure 3.5). To more accurately identify scECM impact on SCAP, the molecule-rich scECM hydrogel baseline was removed from the SCAP+scECM condition and compared again with SCAP alone (SCAP-scECM vs SCAP, Table 3.4, Supplementary Table 3.3). Of the 73 significantly changed molecules, 25 have a fold change with a negative prefix as they were actively

consumed or degraded by SCAP (their concentration in scECM alone was higher than in SCAP-scECM).

Changes in amino acids, nucleotides/nucleosides, lactate, acetoacetate and glucose reflected the changes in SCAP oxidative metabolism and transcription/translation. Changes in methioninsulfone, methionine-S-oxide, serine and asparagine indicated that oxidative stress regulation in SCAP incubated with scECM may be modulated in a way that suggests the existence or increased susceptibility to oxidative stress [53]. Decreased arginine, citruline and other amino acids indicated that nitric oxide metabolism of SCAP in contact with scECM may be reduced. Nitric oxide is involved in oxygen metabolism, free radical neutralisation and regulation of differentiation and apoptosis [66], [67].

Histidine, glutamine, glutamate, nicotinamide, 8-amino-7-oxononanoate, thiamine, choline and sphingolipids are involved in the maintenance of cellular and membrane integrity, response to inflammation, anti-inflammatory lipid synthesis and direct inflammation mitigation [49], [51], [54], [62], [68]–[72]. Therefore, the decrease of these metabolites indicated possible decrease in SCAP cellular integrity and immunoregulatory capacity when combined with scECM.

Decrease of 26,26,26-trifluoro-25-hydroxyvitamin D3 and expenditure of other vitamin D metabolites indicated changes in SCAP vitamin D metabolism. Changes in vitamin D metabolism have been related to altered autocrine and paracrine immunoregulation [73], [74].

Active consumption of anti-inflammatory lipid precursors from scECM, such as phosphatidylethanolamine, acyl-glycerophospho- cholines, fatty acids and amides, but decreased anti-inflammatory lipid production, including prostaglandin E2,

docosahexaenoic and 19,20-dihydroxy-docosapentaenoic acid [40], [47]–[49] implied that SCAP used them for other metabolic processes. These may be the cell membrane regulation, as it is another acyl-glycerophosphocholines and fatty acids metabolic pathway [61], auto-immunoregulation (if scECM elicited an inflammatory response in SCAP), as arachidonic, docosapentaenoic and icosatrienoic acid also have direct immunoregulatory effects [40], [47], [54], or neuro-differentiation, as arachidonic and ω-3 fatty acids are one of the main stimuli [54], [58]. However, the changes in SCAP lipid pathways may also be a result of downregulated synthetic reactions by the presence of lipids in the molecular composition of scECM [75], [76].

Overall, the detected metabolic changes did not inform of SCAP “Th1”- regulatory capacity upon the addition of scECM in basal state. Immunoregulatory cytokine TGFβ concentration was also significantly decreased (2-fold, Figure 3.2) in SCAP+scECM compared to SCAP. However, these changes detected in basal state may not be relevant in the presence of inflammatory stimuli.

Table 3.4 Significantly changed metabolites detected in the interplay between SCAP and scECM in basal state after 24h, matched to Human Metabolome Database (HMDB), Kyoto Encyclopaedia of Genes and Genomes (KEGG) pathways and in direct relationship with inflammation

Putative metabolite	IDC	Peak intensity SCAP-scECM	Peak intensity SCAP	Fold change
Methionine sulfone	L2	3280	1423	2.305
Choline phosphate	L1	24845	13019	1.908
Methionine S-oxide	L2	59807	107585	0.556
Docosahexaenoicacid	L2	7689	16482	0.467
Glutamate 5-semialdehyde	L2	121874	350747	0.347
Thiamin	L2	20684	69918	0.296
Glutamate	L1	291735	1336698	0.218
Creatine	L1	800300	4148851	0.193
Phosphatidylethanolamines	L2	22046	121112	0.182
Histidine	L1	386184	2191530	0.176
Serine	L1	85079	487346	0.175
Arginine	L1	749191	4645452	0.161
Citrulline	L1	41522	263460	0.158
Choline	L2	273490	1861713	0.147
Creatinine	L1	778673	5454315	0.143
Sphinga-di and trienine	L2	129521	1023090	0.142
Prostaglandin E2	L2	15674	224599	0.070
N-Acetylhistidine	L2	46054	729787	0.063
Glutamine	L1	1175806	20000000	0.058
1-acylglycerophosphocholines	L2	2747	69753	0.048
3-Methylhistidine	L1	15113	428680	0.035
19,20-Dihydroxy-docosapentaenoic acid	L2	18377	800136	0.023
8-Amino-7-oxononanoate	L2	3563	342000	0.010
1-Pyrroline-5-carboxylate	L2	-1362	205310	-0.007
Fatty acids and amides	L2	255395	2390050	-0.009
Vitamins D2 and D3	L2	-100694	2039520	-0.043
Asparagine	L1	-20059	354260	-0.057
Docosapentaenoic acid	L2	-971.5	4523	-0.215
Arachidonic acid	L2	-18878	4974	-3.795

Statistical significance was determined with t-test and false discovery rate (FDR) correction using the Benjamini-Hochberg procedure ($q^2 \leq 0.05$), variable importance in projection scores obtained in orthogonal partial least squares discriminant analysis (VIP OPLS-DA > 1) and fold change ≥ 1.5; IDC- metabolite identification level according to the metabolomics standards initiative L1 - Level 1, L2 - Level 2; Colours represent the heat map of the fold change between mean peak intensities in scECM hydrogel and medium: yellow - no change, red - increase, blue - decrease, green - negative values indicating higher peak intensity of scECM compared to SCAP + scECM. Metabolites in the first column are also colour-coded: grey- amino acids directly involved in oxidative stress response, cellular integrity maintenance and regulation of apoptosis, orange- molecules with direct anti-inflammatory activity.

3.5.4 Interplay between SCAP and scECM in the Presence of the Stimulus

Given the chronic “Th1” inflammatory microenvironment after SCI [78] and the idea that MSC primed with “Th1” cytokines may have higher therapeutic efficacy [79], scECM and SCAP interactions were tested in the presence of the “Th1” stimuli, TNFα and IFNγ. Two different scenarios were explored: i) SCAP response to an inflammatory stimulus in the presence of scECM (SCAP+scECM+stimuli compared to SCAP+scECM) and ii) SCAP response to scECM in the presence of an inflammatory stimulus (SCAP+scECM+stimuli compared to SCAP+stimuli).

3.5.4.1 SCAP Response to the Stimulus in the Presence of scECM

When SCAP were subjected to pro-inflammatory cytokines in the presence of scECM, 81% of the metabolites that changed (in SCAP+scECM+stimuli compared to SCAP+scECM) (Table 3.5 Part 1, Supplementary Table 3.4 Part 1) were similar to what was observed without scECM (SCAP+stimuli compared to SCAP) (Table 3.2, Supplementary Table 3.1). Activated tryptophan-kynurenine pathway (Supplementary Figure 3.6) indicated SCAP activation, which has in other MSC been related to the increased ability for immunoregulation [34], [35]. Decrease of docosahexaenoic acid could not be related to SCAP capacity for immunoregulation without performing additional experiments as docosahexaenoic acid may have a direct anti-inflammatory effect or participate in anti-inflammatory lipid synthesis [40].

Significant increase of kynurenine concentration in secreted molecule assay (Figure 3.2) confirmed that upon the stimulation, the tested SCAP activation is similar to that of other MSC [34], regardless of scECM presence. The addition of stimuli to SCAP did not influence TGFβ secretion, whether or not the hydrogel was present (Figure 3.2).

However, increased MCP-1 concentration suggested higher SCAP activation as a response to stimuli in the presence of scECM (Figure 3.2). The increase in MCP-1 concentration may be resulting from the presence of foreign (porcine) antigens in hydrogel. Overall, the presence of scECM did not hinder and may benefit SCAP activation.

3.5.4.2 SCAP Response to scECM in the Presence of the Stimulus

In the comparison between SCAP+scECM+stimuli and SCAP+stimuli, 23 significantly different molecules (Table 3.5 Part 2, Supplementary Table 3.4 Part 2) were matched to 32 specific pathways (Supplementary Figure 3.7). Detected overall metabolic profile contained molecules derived from the influence of scECM on SCAP in the presence of stimulus as well as the scECM-derived molecules.

Carnosine (Table 3.5 Part 2) may have neuroprotective effect or directly metabolise to anti-inflammatory histidine [80]. Carnosine, homoanserine, s-glutathionyl-cysteine, methionine S-oxide, methionine-sulfone and γ-glutamyl-γ-aminobutyraldehyde may influence oxidative stress regulation [52], [53]. Furthermore, adenosine has been directly related to T-lymphocyte suppression [81] and choline and eicosatrienoic acid to inflammation mitigation [40]. However, arachidonic acid may have direct pro-inflammatory effects or be utilised for immunoregulatory lipid synthesis [47]. Significantly increased fold changes of these molecules (Table 3.5 Part 2) indicated that more anti-inflammatory metabolites were detected from SCAP+scECM compared to SCAP in stimulated condition.

To specifically explore the influence of scECM on stimulated SCAP, SCAP-scECM+stimuli was calculated and compared to SCAP+stimuli (Table 3.5 Part 3). Even

though SCAP response to stimuli remained similar in the presence of scECM and most of the detected molecules in SCAP+scECM+stimuli condition were scECM-derived, scECM showed significant impact on SCAP in stimulated condition. The influence of scECM on SCAP overall metabolic response (oxidative/energy metabolism, transcription/translation) was similar to that in basal state (Table 3.4).

Pathways of nitrogen metabolism-related amino acids, such as arginine, ornithine, citruline, asparagine were highly affected (Table 3.5 Part 3), which indicated altered nitrogen oxide synthesis [82], [83]. Changes in these pathways, altered ratios of glutamine, glutamate, creatine and creatinine, increased glutathionyl-cysteine and reduced 1-pyrroline-5-carboxylate and γ-glutamylputrescine indicated that SCAP response to general stress may be altered [65], [84]. Decreased glutamine, glutamate, thiamine, 8-amino-7-oxononanoate, choline, sphingolipid, phospholipid and fatty acid ratios (Table 3.5 Part 3) indicated that SCAP cellular and membrane integrity may be altered [62], [69], [71], [72], [85].

Sphingolipid, glycerophospholipid, phosphatidylethanolamine, fatty acid and fatty acid amide metabolism, closely related to inflammation [40], [50], were also affected by scECM [75], [76]. Indeed, the fold changes of anti-inflammatory molecules, such as nicotinamide [70], choline [51], 19,20-dihydroxydocosapentaenoic acid and other anti-inflammatory lipids [50] were decreased, whilst fold changes of 5-hydroxyeicosatetraenoic acid (5-HETE) di-endoperoxide, 9,10-dihydroxystearicic acid and arachidonic acid indicated uptake from scECM. The complexity of detected lipids, from final stages in cyclooxygenase and lipoxygenase pathways, resolved some of the ambiguity occurring in the analysis of basal state and indicated that SCAP may use these lipids for self-regulation [40], [48], [49] in SCAP+scECM+stimulus condition. Changes in vitamin D metabolism may also be related to altered autocrine and paracrine regulation of SCAP [73], [74].

The addition of scECM to stimulated SCAP decreased secretion of immunoregulatory cytokine TGFβ (Figure 3.2). However, increased MCP-1 secretion in SCAP+scECM+stimuli compared to SCAP+stimuli condition may indicate an increase in SCAP activation [36]. This was in agreement with LC-MS detected molecular patterns (Table 3.5 Part 3). Namely, during 24h SCAP-scECM interaction in stimulated condition, SCAP consumed anti-inflammatory lipids and possibly underwent changes in cellular integrity and response to stress (Table 3.5 Part 3). But the addition of scECM to SCAP+stimulus increased ratios of anti-inflammatory molecules detected in the overall profile (Table 3.5 Part 2). It may be that, even though scECM compromise SCAP adaptability, the overall metabolic profile of SCAP+scECM in stimulated condition seemed to have higher anti-inflammatory potential compared to SCAP+stimuli.

Table 3.5. Significantly changed metabolites detected in the interplay between SCAP and scECM under TNFα and IFNγ stimulation after 24h, matched to Human Metabolome Database (HMDB), Kyoto Encyclopaedia of Genes and Genomes (KEGG) pathways and in direct relationship with inflammation

Putative metabolite	IDC	Peak intensity	Peak intensity	Fold change
Part 1		SCAP+scECM +stimulus	SCAP+scECM	
Kynurenine	L1	665249	15600	42.6
5-Hydroxyindoleacetate	L2	214049	6080	35.2
8-Methoxykynurenate	L2	13389	1000	13.4
Formylkynurenine	L2	24863	2638	9.4
Octanoic acid	L2	176722	29179	6.1
Docosahexaenoicacid	L2	12287	31252	0.4
1-Pyrroline-5-carboxylate	L2	32091	95589	0.3
Tryptophan	L1	10460	497490	0
Part 2		SCAP+scECM +stimulus	SCAP+stimulus	
Carnosine	L2	98021	1745	56.2
Adenosine	L1	31350	666.7	47
Homoanserine	L2	33321	1000	33.3
Icosatrienoic acid	L2	5602	458.8	12.2
Glycero-3-phosphoethanolamine	L1	26398	2721	9.7
Glutathionyl-cysteine	L2	9618	1130	8.5
Methionine sulfone	L2	9225	1618	5.7
γ-Glutamyl-γ-aminobutyraldehyde	L2	7062	1531	4.6
Choline phosphate	L1	32508	7304	4.5
Choline	L2	115421	31859	3.6
Arachidonic acid	L2	11557	3434	3.4
Glycero-3-phosphocholine	L1	2655571	814258	3.3
Methionine S-oxide	L2	256002	107613	2.4
1-Methylnicotinamide	L2	57897	38763	1.5
Tryptophan	L1	10460	24614	0.4
1-acyl-sn-glycero-3-phosphocholines	L2	5470	64177	0.1

Part 3		SCAP-scECM +stimulus	SCAP +stimulus	
Glutathionyl-cysteine	L2	9619	1130	8.512
Choline phosphate	L1	24118	7304	3.302
1-Pyrroline-5-carboxylate	L2	14982	41547	0.361
Thiamin	L2	16771	61987	0.271
Serine	L1	133280	519991	0.256
Glutamate 5-semialdehyde	L2	83068	357232	0.233
Fatty acid amides	L2	665396	3744798	0.227
Citrulline	L1	52232	279843	0.187
Choline	L2	5128	31859	0.161
Sphinga mono-, di- and tri- enine	L2	79818	681425	0.188
Creatine	L1	602600	4458348	0.135
Phosphatidylethanolamines	L2	13675	116031	0.118
Arginine	L1	528562	4688648	0.113
19,20-Dihydroxydocosapentaenoate	L2	75692	738179	0.103
Glutamine	L1	1980515	21000000	0.093
Glutamate	L1	93123	1175296	0.079
Vitamins D2 and D3	L2	81080	2143720	0.069
Dimethyl-arginine	L2	8695	145059	0.060
Histidine derivates	L2	21992	496527	0.040
Creatinine	L1	203593	5428818	0.038
Glycerophospholipides	L2	13243	185581	0.037
8-Amino-7-oxononanoate	L2	11816	395189	0.030
1-Methylnicotinamide	L1	-31509	3114468	-0.010
5-HETE di-endoperoxide	L2	-13175	1136047	-0.012
Fatty acids	L2	-54134	440029	-0.021
Ornithine	L1	-15301	139971	-0.109
Asparagine	L1	-43741	327222	-0.134
9,10-Dihydroxystearicic acid	L2	-87985	576824	-0.153
Arachidonic acid	L2	-25741	3434	-7.496
Tryptophan	L1	-450535	24615	-18.303
Icosatrienoic acid	L2	-9070	458.8	-19.769
γ-Glutamylputrescine	L2	-45453	1000	-45.453

Statistical significance was determined with t-test and false discovery rate (FDR) correction using the Benjamini-Hochberg procedure ($q^2 \leq 0.05$), variable importance in projection scores obtained in orthogonal partial least squares discriminant analysis (VIP OPLS-DA > 1) and fold change ≥ 1.5; IDC- metabolite identification level according to the metabolomics standards initiative L1 - Level 1, L2 - Level 2; Colours represent the heat map of the fold change between mean peak intensities in scECM hydrogel and medium: yellow - no change, red - increase, blue - decrease, green - negative values indicating higher peak intensity of scECM compared to SCAP + scECM + stimulus. Metabolites in the first column are also colour-coded: grey- amino acids directly involved in oxidative stress response, cellular integrity maintenance and regulation of apoptosis, orange- molecules with direct anti-inflammatory activity.

3.6 Conclusion

In this work we sought to understand the interplay between SCAP and scECM in the context of “Th1”-like stimulation. scECM molecular profile was characterised. Detected molecules, for instance choline, docosahexaenoic, arachidonic and other fatty acids, may have immunoregulatory and neuro-reparative activity in the scope of SCI. Nonetheless, when combined with scECM in basal state, SCAP metabolic pathways associated with general metabolism, oxidative stress response and cellular and membrane integrity were altered. SCAP also consumed anti-inflammatory lipids and their precursors from scECM in basal and stimulated state.

We showed that SCAP responded to inflammatory stimulus by activation, which may suggest an increased SCAP immunoregulatory capacity. In the presence of scECM, SCAP responded to inflammatory stimulus by engaging the same intrinsic pathways as in SCAP+stimulus vs SCAP. In stimulated condition, molecular footprint of SCAP and scECM contained more anti-inflammatory molecules compared to SCAP.

However, the addition of scECM to stimulated SCAP modified metabolic pathways associated with energy metabolism, transcription and translation, oxidative and general stress response, cellular integrity and possibly auto-immunoregulation. These modifications were similar to those detected in basal state. SCAP also consumed anti-inflammatory lipids and other molecules from scECM, which decreased their availability in the overall SCAP+scECM molecular profile. It is possible that scECM modified general SCAP metabolism, but not SCAP response to stimuli and thus even though some SCAP susceptibility to oxidative and general stress may be increased in contact with scECM, the immunoregulatory capacity of SCAP+scECM metabolic profile was higher than SCAP in stimulated condition.

Overall, SCAP and scECM separately showed potential for immunoregulation. Even though scECM may hinder SCAP health and SCAP consumed scECM-derived anti-inflammatory lipids, SCAP+scECM were still activated by TNFα/IFNγ and demonstrated higher immunoregulatory potential than SCAP.

3.7 References

[1] J. C. Fleming *et al.*, “The cellular inflammatory response in human spinal cords after injury,” *Brain*, vol. 129, no. 12, pp. 3249–3269, 2006.

[2] E. J. Bradbury and S. B. McMahon, “Spinal cord repair strategies: Why do they work?,” *Nat. Rev. Neurosci.*, vol. 7, no. 8, pp. 644–653, 2006.

[3] M. J. Hoogduijn *et al.*, “The immunomodulatory properties of mesenchymal stem cells and their use for immunotherapy,” *Int. Immunopharmacol.*, vol. 10, no. 12, pp. 1496–1500, 2010.

[4] S. Forostyak, P. Jendelova, and E. Sykova, “The role of mesenchymal stromal cells in spinal cord injury, regenerative medicine and possible clinical applications,” *Biochimie*, vol. 95, no. 12, pp. 2257–2270, 2013.

[5] X. C. Li, C. F. Zhong, G. Bin Deng, R. W. Liang, and C. M. Huang, “Efficacy and safety of bone marrow-derived cell transplantation for spinal cord injury: A systematic review and meta-analysis of clinical trials,” *Clin. Transplant.*, vol. 29, no. 9, pp. 786–795, 2015.

[6] W. Martens, A. Bronckaers, C. Politis, R. Jacobs, and I. Lambrichts, “Dental stem cells and their promising role in neural regeneration: An update,” *Clin. Oral Investig.*, vol. 17, no. 9, pp. 1969–1983, 2013.

[7] W. Martens, A. Bronckaers, C. Politis, R. Jacobs, and I. Lambrichts, “Dental stem cells and their promising role in neural regeneration: An update,” *Clinical Oral Investigations*, vol. 17, no. 9. 2013.

[8] W. Sonoyama *et al.*, “Mesenchymal stem cell-mediated functional tooth regeneration in Swine,” *PLoS One*, vol. 1, no. 1, pp. 1–8, 2006.

[9] G. T.-J. H. Wataru Sonoyama, Yi Liu, Takayoshi Yamaza, Rocky S. Tuan, Songlin Wang, Songtao Shi, “Characterization of Apical Papilla and its Residing Stem

Cells from Human Immaturer Permanent Teeth-A Pilot Study," vol. 34, no. 2, pp. 166–171, 2009.

[10] T. Ha Le Bao, T. Thi Huyen Dinh, and N. Hao Thi Thu, "Stem cells from apical papilla and their properties in two primary culture methods," *Int. J. Biomed. Res.*, vol. 5, no. 8, 2014.

[11] N. B. Ruparel, J. F. A. De Almeida, M. A. Henry, and A. Diogenes, "Characterization of a stem cell of apical papilla cell line: Effect of passage on cellular phenotype," *J. Endod.*, vol. 39, no. 3, pp. 357–363, 2013.

[12] S. Yu, Y. Zhao, Y. Ma, and L. Ge, "Profiling the Secretome of Human Stem Cells from Dental Apical Papilla," *Stem Cells Dev.*, vol. 25, no. 6, pp. 499–508, 2016.

[13] A. Bakopoulou *et al.*, "Angiogenic Potential and Secretome of Human Apical Papilla Mesenchymal Stem Cells in Various Stress Microenvironments," *Stem Cells Dev.*, vol. 24, no. 21, pp. 2496–2512, 2015.

[14] J. Vanacker *et al.*, "Hypoxia modulates the differentiation potential of stem cells of the apical papilla," *J. Endod.*, vol. 40, no. 9, pp. 1410–1418, 2014.

[15] P. de Berdt *et al.*, "Stem cells from human apical papilla decrease neuro-inflammation and stimulate oligodendrocyte progenitor differentiation via activin-A secretion," *Cellular and Molecular Life Sciences*, pp. 1–14, 2018.

[16] A. F. Lloyd *et al.*, "Central nervous system regeneration is driven by microglia necroptosis and repopulation," *Nat. Neurosci.*, 2019.

[17] D. Gupta, C. H. Tator, and M. S. Shoichet, "Fast-gelling injectable blend of hyaluronan and methylcellulose for intrathecal, localized delivery to the injured spinal cord," *Biomaterials*, vol. 27, no. 11, pp. 2370–2379, 2006.

[18] C. Paul, A. F. Samdani, R. R. Betz, I. Fischer, and B. Neuhuber, "Grafting of human bone marrow stromal cells into spinal cord injury: A comparison of delivery methods," *Spine (Phila. Pa. 1976).*, vol. 34, no. 4, pp. 328–334, 2009.

[19] J. L. Dziki, D. S. Wang, C. Pineda, B. M. Sicari, T. Rausch, and S. F. Badylak, “Solubilized extracellular matrix bioscaffolds derived from diverse source tissues differentially influence macrophage phenotype,” pp. 12–15, 2016.

[20] J. W. Wassenaar *et al.*, “Evidence for mechanisms underlying the functional benefits of a myocardial matrix hydrogel for post-MI treatment,” *J. Am. Coll. Cardiol.*, vol. 67, no. 9, 2016.

[21] T. J. Keane *et al.*, “Restoring Mucosal Barrier Function and Modifying Macrophage Phenotype with an Extracellular Matrix Hydrogel: Potential Therapy for Ulcerative Colitis,” *J. Crohn’s Colitis*, p. jjw149, 2016.

[22] R. Liang *et al.*, “Positive effects of an extracellular matrix hydrogel on rat anterior cruciate ligament fibroblast proliferation and collagen mRNA expression,” *J. Orthop. Transl.*, vol. 3, no. 3, pp. 114–122, 2015.

[23] L. Huleihel *et al.*, “Matrix-bound nanovesicles within ECM bioscaffolds,” *Sci. Adv.*, vol. 2, no. 6, pp. e1600502–e1600502, 2016.

[24] V. Agrawal, S. Tottey, S. A. Johnson, J. M. Freund, B. F. Siu, and S. F. Badylak, “Recruitment of Progenitor Cells by an Extracellular Matrix Cryptic Peptide in a Mouse Model of Digit Amputation,” *Tissue Eng. Part A*, vol. 17, no. 19–20, pp. 2435–2443, 2011.

[25] N. Tatic, F. R. A. J. Rose, A. des Rieux, and L. J. White, “Stem cells from the dental apical papilla in extracellular matrix hydrogels mitigate inflammation of microglial cells,” *Sci. Rep.*, 2019.

[26] D. Tukmachev *et al.*, “Injectable Extracellular Matrix Hydrogels as Scaffolds for Spinal Cord Injury Repair.,” *Tissue Eng. Part A*, vol. 22, no. 3–4, pp. 306–17, 2016.

[27] P. M. Crapo *et al.*, “Biologic scaffolds composed of central nervous system extracellular matrix,” *Biomaterials*, vol. 33, no. 13, pp. 3539–3547, 2012.

[28] A. Viswanath *et al.*, “Extracellular Matrix-Derived Hydrogels for Dental Stem Cell Delivery,” *J. Biomed. Mater. Res. Part A*, pp. 1–10, 2016.

[29] A. Surrati, R. Linforth, I. D. Fisk, V. Sottile, and D. H. Kim, “Non-destructive characterisation of mesenchymal stem cell differentiation using LC-MS-based metabolite footprinting,” *Analyst*, vol. 141, no. 12, pp. 3776–3787, 2016.

[30] F. Hached *et al.*, “Polysaccharide hydrogels support the long-Term viability of encapsulated human mesenchymal stem cells and their ability to secrete immunomodulatory factors,” *Stem Cells Int.*, vol. 2017, pp. 6–8, 2017.

[31] R. Tautenhahn, C. Bottcher, and S. Neumann, “Highly sensitive feature detection for high resolution LC/MS,” *BMC Bioinformatics*, vol. 9, pp. 1–16, 2008.

[32] R. A. Scheltema, A. Jankevics, R. C. Jansen, M. A. Swertz, and R. Breitling, “PeakML/mzMatch: A file format, Java library, R library, and tool-chain for mass spectrometry data analysis,” *Anal. Chem.*, vol. 83, no. 7, pp. 2786–2793, 2011.

[33] D. J. Creek, A. Jankevics, K. E. V. Burgess, R. Breitling, and M. P. Barrett, “IDEOM: an Excel interface for analysis of LC-MS-based metabolomic data,” *Oxford Univ. Press*, vol. 28, no. 7, pp. 1048–1049, 2012.

[34] D. S. Kim *et al.*, “Enhanced Immunosuppressive Properties of Human Mesenchymal Stem Cells Primed by Interferon-γ,” *EBioMedicine*, vol. 28, pp. 261–273, 2018.

[35] M. François, R. Romieu-Mourez, M. Li, and J. Galipeau, “Human MSC suppression correlates with cytokine induction of indoleamine 2,3-dioxygenase and bystander M2 macrophage differentiation,” *Mol. Ther.*, vol. 20, no. 1, pp. 187–195, 2012.

[36] M. Y. Noh *et al.*, “Mesenchymal Stem Cells Modulate the Functional Properties of Microglia via TGF-b Secretion,” *Stem Cells Transl. Med.*, vol. 5, pp. 1538–1549, 2016.

[37] L. Lin and L. Du, “The role of secreted factors in stem cells-mediated immune regulation,” *Cell. Immunol.*, vol. 326, no. February 2017, pp. 24–32, 2018.

[38] X. Li, W. Du, F. X. Ma, X. Feng, F. Bayard, and Z. C. Han, “High concentrations of TNF-α induce cell death during interactions between human umbilical cord

mesenchymal stem cells and peripheral blood mononuclear cells," *PLoS One*, vol. 10, no. 5, pp. 1–13, 2015.

[39] A. Hoshimoto, Y. Suzuki, T. Katsuno, H. Nakajima, and Y. Saito, "Caprylic acid and medium-chain triglycerides inhibit IL-8 gene transcription in Caco-2 cells : comparison with the potent histone deacetylase inhibitor trichostatin A," pp. 280–286, 2002.

[40] Fritsche, "The Science of Fatty Acids and Inflammation," *Adv. Nutr. An Int. Rev. J.*, vol. 6, no. 3, pp. 293S-301S, 2015.

[41] D. Kyurkchiev, "Secretion of immunoregulatory cytokines by mesenchymal stem cells," *World J. Stem Cells*, vol. 6, no. 5, p. 552, 2014.

[42] Wishart Research Group University of Alberta, "Gamma-glutamyl-L-putrescine (HMDB0012230)." http://www.hmdb.ca.

[43] L. J. White *et al.*, "The impact of detergents on the tissue decellularization process: A ToF-SIMS study," *Acta Biomater.*, 2017.

[44] Wishart Research Group University of Alberta, "Chenodeoxycholic acid (HMDB0000518)."

[45] C. Zhu, C. D. Fuchs, E. Halilbasic, and M. Trauner, "Bile acids in regulation of inflammation and immunity: Friend or foe?," *Clin. Exp. Rheumatol.*, vol. 34, no. 20, pp. S25–S31, 2016.

[46] A. C. Rustan and C. A. Drevon, "Fatty Acids: Structures and Properties," *Encycl. Life Sci.*, 2005.

[47] J. R. Silva, B. Burger, C. M. C. Kühl, T. Candreva, M. B. P. Dos Anjos, and H. G. Rodrigues, "Wound Healing and Omega-6 Fatty Acids: From Inflammation to Repair," *Mediators Inflamm.*, vol. 2018, p. 2503950, 2018.

[48] C. Morisseau and B. D. Hammock, "Impact of Soluble Epoxide Hydrolase and Epoxyeicosanoids on Human Health," *Annu. Rev. Pharmacol. Toxicol.*, vol. 53, no. 1, pp. 37–58, 2013.

[49] J. U. Scher and M. H. Pillinger, “The anti-inflammatory effects of prostaglandins.,” *J. Investig. Med.*, vol. 57, no. 6, pp. 703–708, Aug. 2009.

[50] G. Drouin, V. Rioux, and P. Legrand, “The n-3 docosapentaenoic acid (DPA): A new player in the n-3 long chain polyunsaturated fatty acid family,” *Biochimie*, vol. 159, pp. 36–48, 2019.

[51] A. K. Mehta, B. P. Singh, N. Arora, and S. N. Gaur, “Choline attenuates immune inflammation and suppresses oxidative stress in patients with asthma,” *Immunobiology*, vol. 215, no. 7, pp. 527–534, 2010.

[52] Y. C. Niu *et al.*, “Histidine and arginine are associated with inflammation and oxidative stress in obese women,” *Br. J. Nutr.*, vol. 108, no. 1, pp. 57–61, 2012.

[53] C. Schöneich, “Methionine oxidation by reactive oxygen species : reaction mechanisms and relevance to Alzheimer ’ s disease,” *Acta Biochim. Biophys.*, vol. 1703, pp. 111–119, 2005.

[54] I. Kan, E. Melamed, D. Offen, and P. Green, “Docosahexaenoic acid and arachidonic acid are fundamental supplements for the induction of neuronal differentiation,” *J. Lipid Res.*, vol. 48, no. 3, pp. 513–517, 2007.

[55] M. Katakura, M. Hashimoto, T. Okui, H. M. Shahdat, K. Matsuzaki, and O. Shido, “Omega-3 polyunsaturated fatty acids enhance neuronal differentiation in cultured rat neural stem cells,” *Stem Cells Int.*, vol. 2013, 2013.

[56] S. P. Yun, J. M. Ryu, M. W. Jang, and H. J. Han, “Interaction of Profilin-1 and F-Actin via a b-Arrestin-1/JNK Mesenchymal Stem Cells Prostaglandin E2-Induced Human Signaling Pathway Involved in Migration and Proliferation,” *J. Cell. Physiol.*, vol. 226, no. 2, pp. 559–571, 2011.

[57] S. J. Park, S. B. Lee, D. S. Lee, Y. J. Ryu, G. Lee, and J. Cho, “Direct effect of chenodeoxycholic acid on differentiation of mouse embryonic stem cells cultured under feeder-free culture conditions,” *Biomed Res. Int.*, vol. 2013, 2013.

[58] N. Sakayori, M. Maekawa, K. Numayama-Tsuruta, T. Katura, T. Moriya, and N. Osumi, “Distinctive effects of arachidonic acid and docosahexaenoic acid on neural stem/progenitor cells,” *Genes to Cells*, vol. 16, no. 7, pp. 778–790, 2011.

[59] R. A. Soares, “Role of a Bile Acid in Improving Survival and Function of Neural Stem Cells,” no. November, pp. 1–10, 2015.

[60] P. M. Crapo, S. Tottey, P. F. Slivka, and S. F. Badylak, “Effects of biologic scaffolds on human stem cells and implications for CNS tissue engineering.,” *Tissue Eng Part A*, vol. 20, no. 1–2, 2013.

[61] L. M. Sanders and S. H. Zeisel, “Choline: Dietary requirements and role in brain development,” *Nutr. Today*, vol. 42, no. 4, pp. 181–186, 2007.

[62] T. Skripuletz, R. A. Linker, and M. Stangel, “The choline pathway as a strategy to promote central nervous system (CNS) remyelination,” *Neural Regen. Res.*, vol. 10, no. 9, pp. 1369–1370, 2015.

[63] A. Wozniacka, M. Wieczorkowska, and J. Gebicki, “Topical application of 1-methylnicotinamide in the treatment of rosacea : a pilot study,” no. May, pp. 632–635, 2005.

[64] M. Yudkoff *et al.*, “Brain Amino Acid Requirements and Toxicity : The Example of Leucine,” *J. Nutr.*, vol. 135, no. 6, pp. 1531S–8S, 2005.

[65] J. Phang, J. Pandhare, and Y. Liu, “The Metabolism of Proline as Microenvironmental Stress Substrate,” *J Nutr*, vol. 138, no. 10, pp. 2008S-2015S, 2008.

[66] A. Beltran-Povea *et al.*, “Role of nitric oxide in the maintenance of pluripotency and regulation of the hypoxia response in stem cells,” vol. 7, no. 3, pp. 605–617, 2015.

[67] H. Chung, H. Pae, B. Choi, T. R. Billiar, and Y. Kim, “Nitric Oxide as a Bioregulator of Apoptosis,” vol. 1079, pp. 1075–1079, 2001.

[68] Z. B. Yagci, E. Esvap, H. A. Ozkara, K. O. Ulgen, and E. Ozkirimli, *Inflammatory response and its relation to sphingolipid metabolism proteins : Chaperones as*

potential indirect anti-inflammatory agents, 1st ed., no. January 2018. Elsevier Inc., 2019.

[69] D. C. De Oliveira *et al.*, “Glutamine metabolism and its effects on immune response : molecular mechanism and gene expression,” *Nutrire*, pp. 1–10, 2016.

[70] J. S. Ungerstedt, M. Blombäck, and S. Sciences, “Nicotinamide is a potent inhibitor of proinflammatory cytokines,” vol. 6, pp. 48–52, 2003.

[71] J. Antenor *et al.*, “The effect of thiamine deficiency on inflammation , oxidative stress and cellular migration in an experimental model of sepsis,” pp. 1–10, 2014.

[72] S. Agrawal, A. Agrawal, and H. M. Said, “Biotin deficiency enhances the inflammatory response of human dendritic cells,” vol. 311, no. 3, pp. 1–12, 2019.

[73] X. Guillot, L. Semerano, N. Saidenberg-kermanac, G. Falgarone, and M. Boissier, “Vitamin D and inflammation,” *Jt. Bone Spine*, vol. 77, no. 6, pp. 552–557, 2010.

[74] K. Yin and D. K. Agrawal, “Vitamin D and inflammatory diseases,” *J. Inflamm. Res.*, pp. 69–87, 2014.

[75] P. Morell and R. H. Quarles, “Characteristic Composition of Myelin,” in *Basic Neurochemistry: Molecular, Cellular and Medical Aspects*, 6th editio., G. Siegel, B. Agranoff, and R. Albers, Eds. Philadelphia: Lippincott-Raven, 1999.

[76] J. M. Berg, J. L. Tymoczko, and L. Stryer, *Biochemistry*, 5th editio. New York: W H Freeman, 2002.

[77] M. Di Nicola *et al.*, “Human bone marrow stromal cells suppress T-lymphocyte proliferation induced by cellular or nonspecific mitogenic stimuli,” *Blood*, vol. 99, no. 10, pp. 3838–3843, 2002.

[78] K. A. Kigerl, J. C. Gensel, D. P. Ankeny, J. K. Alexander, D. J. Donnelly, and P. G. Popovich, “Identification of two distinct macrophage subsets with divergent effects causing either neurotoxicity or regeneration in the injured mouse spinal cord.,” *J. Neurosci.*, vol. 29, no. 43, pp. 13435–44, 2009.

[79] Q. Guan, P. Ezzati, V. Spicer, O. Krokhin, D. Wall, and J. A. Wilkins, “Interferon γ induced compositional changes in human bone marrow derived mesenchymal stem/stromal cells,” *Clin. Proteomics*, vol. 14, no. 26, 2017.

[80] S. Hasegawa *et al.*, “Cysteine , histidine and glycine exhibit anti-inflammatory effects in human coronary arterial endothelial cells,” *Clin. Exp. Immunol.*, no. 167, pp. 269–274, 2012.

[81] F. Saldanha-Araujo *et al.*, “Mesenchymal stromal cells up-regulate CD39 and increase adenosine production to suppress activated T-lymphocytes,” *Stem Cell Res.*, vol. 7, no. 1, pp. 66–74, 2011.

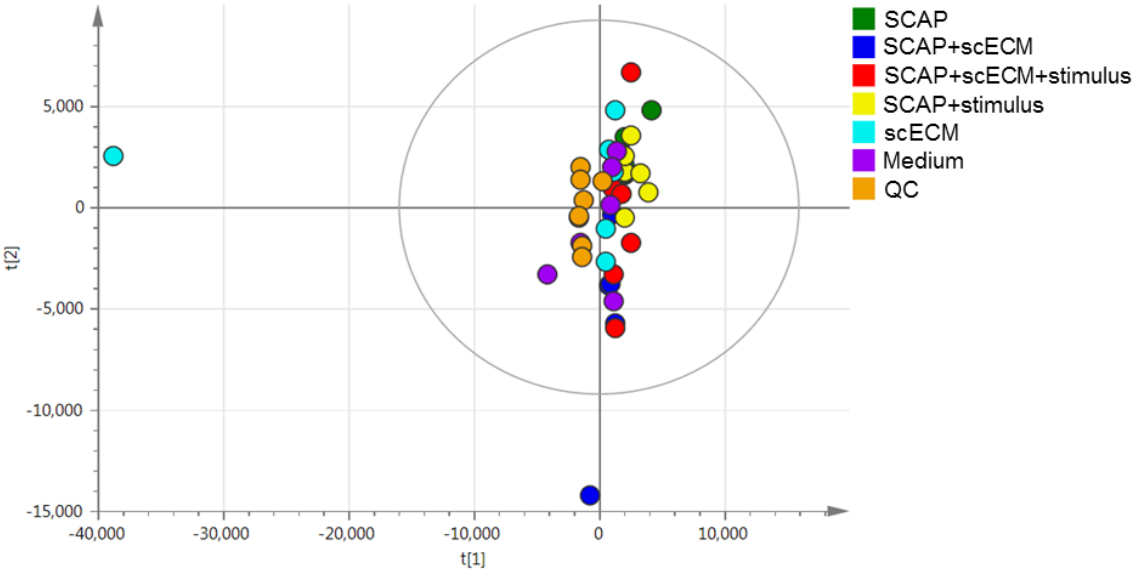
[82] K. A. P. Wijnands, T. M. R. Castermans, M. P. J. Hommen, D. M. Meesters, and M. Poeze, “Arginine and Citrulline and the Immune Response in Sepsis,” pp. 1426–1463, 2015.

[83] L. Sibal, S. C. Agarwal, P. D. Home, and R. H. Boger, “The Role of Asymmetric Dimethylarginine (ADMA) in Endothelial Dysfunction and Cardiovascular Disease,” vol. 2, pp. 82–90, 2010.

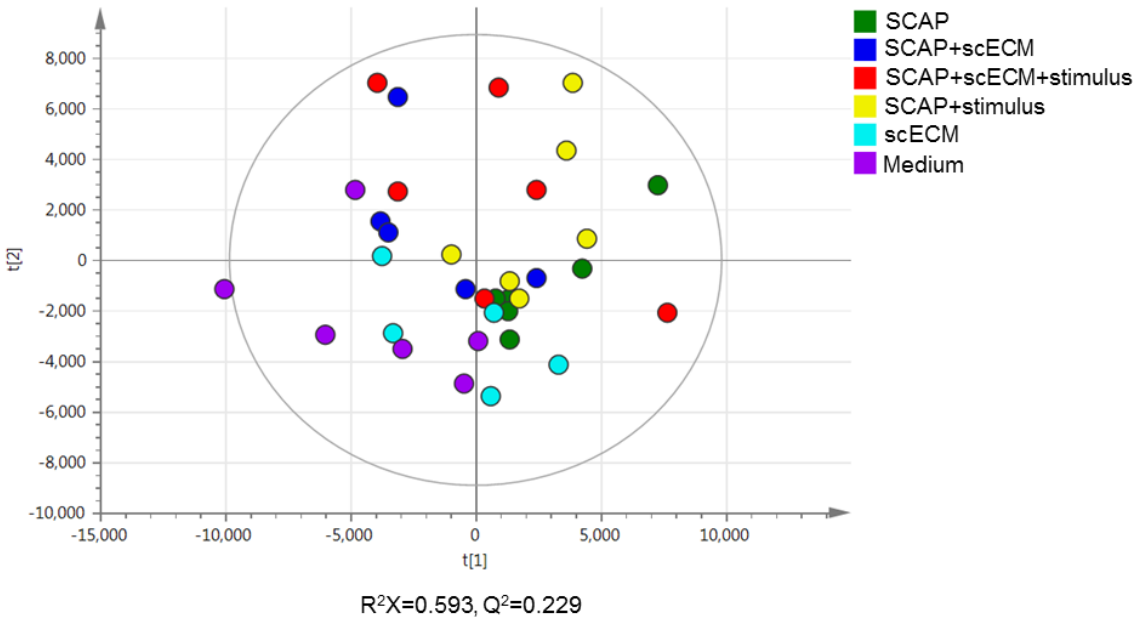
[84] V. S. Andrade *et al.*, “A Possible Anti-Inflammatory Effect of Proline in the Brain Cortex and Cerebellum of Rats,” pp. 4068–4077, 2018.

[85] A. Di Pardo and V. Maglione, “Sphingolipid Metabolism : A New Therapeutic Opportunity for Brain Degenerative Disorders,” vol. 12, no. April, pp. 1–8, 2018.

3.8 Supplementary Data



Supplementary Figure 3.1 Principal component analysis (PCA-X) for all sample groups upon 24h incubation, including QC-quality control sample around the middle of coordinate system and outliers scECM sample number 3 and SCAP+scECM sample number 5. Stimulus- TNFα+IFNγ. R^2X and Q^2 are goodness of the fit parameters, 1 equals perfect fit



Supplementary Figure 3.2 Principal component analysis (PCA-X) for all sample groups upon 24h incubation, excluding quality control sample and outliers scECM sample number 3 and SCAP+scECM sample number 5. Stimulus- TNFα+IFNγ. R^2X and Q^2 are goodness of the fit parameters, 1 equals perfect fit

Supplementary Table 3.1 Significant changes in SCAP metabolic footprint detected in response to TNFα and IFNγ after 24h incubation, matched to Human Metabolome Database (HMDB) and Kyoto Encyclopaedia of Genes and Genomes (KEGG) pathways, in direct relationship with inflammation. RT- retention time; IDC- metabolite identification level according to the metabolomics standards initiative L1 - Level 1, L2 - Level 2; Minimum peak, i.e. background noise intensity was 1000; Colours represent the heat map of the fold change between mean peak intensities in scECM hydrogel and medium: yellow - no change, red - increase, blue – decrease; q^2 value was obtained after t-test and false discovery rate (FDR) correction using the Benjamini-Hochberg procedure; VIP OPLS-DA - variable importance in projection scores obtained in orthogonal partial least squares discriminant analysis

Mass	RT	Formula	Putative metabolite	IDC	Peak intensity SCAP+ stimulus	Peak intensity SCAP	Fold change	q^2 value	VIP OPLS-DA
208.085	8.71462	$C_{10}H_{12}N_2O_3$	Kynurenine	L1	567339	9809	57.839	1.37E-08	14.1
191.058	8.95355	$C_{10}H_9NO_3$	5-Hydroxyindoleacetate	L2	179955	5367	33.530	2.23E-09	7.9
219.052	4.58238	$C_{11}H_9NO_4$	8-Methoxykynurenate	L2	11022	1000	11.022	4.22E-07	2
144.115	4.22791	$C_8H_{16}O_2$	Octanoic acid	L2	191599	29390	6.519	1.35E-09	7.6
236.079	7.66614	$C_{11}H_{12}N_2O_4$	Formylkynurenine	L2	23872	3844	6.210	6.97E-06	2.6
128.058	7.6922	$C_5H_8N_2O_2$	γ-amino-γ-cyanobutanoate	L2	37254	23844	1.562	9.43E-04	2.1
328.239	3.82083	$C_{22}H_{32}O_2$	Docosahexaenoicacid	L2	9858	16482	0.598	1.83E-04	1.5
113.048	5.45472	$C_5H_7NO_2$	1-Pyrroline-2-carboxylate	L2	21573	79711	0.271	8.55E-05	4.5
204.09	9.2631	$C_{11}H_{12}N_2O_2$	Tryptophan	L1	24614	478310	0.051	8.65E-08	12.7

Supplementary Table 3.2 Specific molecular footprint of scECM, matched to Human Metabolome Database (HMDB) and Kyoto Encyclopaedia of Genes and Genomes (KEGG) pathways in direct relationship with inflammation, detected after incubating scECM in medium for 24h. RT- retention time; IDC- metabolite identification level according to the metabolomics standards initiative L1 - Level 1, L2 - Level 2; Minimum peak, i.e. background noise intensity was 1000; Colours represent the heat map of the fold change between mean peak intensities in scECM hydrogel and medium: yellow - no change, red - increase, blue – decrease; q^2 value was obtained after t-test and false discovery rate (FDR) correction using the Benjamini-Hochberg procedure; VIP OPLS-DA - variable importance in projection scores obtained in orthogonal partial least squares discriminant analysis

Mass	RT	Formula	Putative metabolite	IDC	Peak intensity scECM	Peak intensity Medium	Fold change	q^2 value	VIP OPLS-DA
217.142	11.0463	$C_9H_{19}N_3O_3$	γ-Glutamylputrescine	L2	122690	1000	122.690	3.83E-04	4.7
392.292	4.41752	$C_{24}H_{40}O_4$	Chenodeoxycholic acid	L1	98294	1000	98.294	8.27E-04	4.2
226.106	7.64491	$C_9H_{14}N_4O_3$	Carnosine	L2	79850	1000	79.850	2.99E-04	3.8
214.131	5.11067	$C_{10}H_{18}N_2O_3$	Dethiobiotin	L2	41140	1000	41.140	5.18E-03	2.6
254.137	6.86771	$C_{11}H_{18}N_4O_3$	Homoanserine	L2	24613	1000	24.613	6.75E-03	2
214.095	5.13146	$C_9H_{14}N_2O_4$	Pyrimidine nucleoside	L2	8314	751.5	11.063	7.52E-03	1.1
332.27	3.83442	$C_{22}H_{36}O_2$	Adrenic acid	L2	8884	1000	8.884	2.56E-05	1.3

215.055	10.6633	$C_5H_{14}NO_6P$	Glycero-3-phosphoethanolamine	L2	30877	3476	8.883	1.23E-03	2.2
251.101	7.34371	$C_{10}H_{13}N_5O_3$	Deoxyadenosine	L1	7817	1000	7.817	1.07E-03	1.2
183.066	9.9172	$C_5H_{14}NO_4P$	Choline phosphate	L1	8391	1914	4.384	3.67E-04	1.1
103.1	10.0627	$C_5H_{13}NO$	Choline	L2	110293	28021	3.936	1.23E-06	4
310.286	3.83512	$C_{20}H_{38}O_2$	Eicosenoic acid	L2	38910	10107	3.850	2.37E-04	2.3
257.102	10.0631	$C_8H_{20}NO_6P$	Glycerophosphocholine	L1	2564584	700026	3.664	7.69E-06	18.8
304.239	3.87085	$C_{20}H_{32}O_2$	Arachidonic acid	L2	37298	10673	3.495	2.89E-06	2.3
330.255	3.83526	$C_{22}H_{34}O_2$	Docosapentaenoic acid	L2	13980	4063	3.441	6.02E-06	1.4
306.255	3.84513	$C_{20}H_{34}O_2$	8,11,14-Eicosatrienoic acid	L2	14671	5759	2.547	1.55E-04	1.3
328.239	3.82083	$C_{22}H_{32}O_2$	Docosahexaenoic acid	L2	23564	9383	2.511	8.53E-07	1.6
165.046	9.42292	$C_5H_{11}NO_3S$	Methionine S-oxide	L2	177200	108113	1.639	5.90E-03	3.4
523.363	4.70494	$C_{26}H_{54}NO_7P$	1-Octadecanoyl-sn-glycero-3-phosphocholine	L2	3412	68781	0.050	3.22E-06	3.5
495.331	4.79878	$C_{24}H_{50}NO_7P$	1-Palmitoyl-sn-glycero-3-phosphocholine	L2	6584	134720	0.049	2.72E-06	4.9
521.347	4.72729	$C_{26}H_{52}NO_7P$	1-Oleoylglycerophosphocholine	L2	3187	90934	0.035	3.24E-07	4.1
493.316	4.82771	$C_{24}H_{48}NO_7P$	1-(9-Hexadecenoyl)-sn-glycero-3-phosphocholine	L2	1000	22875	0.044	5.57E-07	2.1

Supplementary Table 3.3 Significantly changed metabolites, matched to Human Metabolome Database (HMDB) and Kyoto Encyclopaedia of Genes and Genomes (KEGG) pathways, in direct relationship with inflammation detected in the interplay between SCAP and scECM in basal state after 24h. RT- retention time; IDC- metabolite identification level according to the metabolomics standards initiative L1 - Level 1, L2 - Level 2; Colours represent the heat map of the fold change between mean peak intensities of two conditions: yellow - no change, red - increase, blue – decrease, green – negative values indicating higher peak intensity of scECM compared to SCAP + scECM, i.e. metabolite consumption; q^2 value was obtained after t-test and false discovery rate (FDR) correction using the Benjamini-Hochberg procedure; VIP OPLS-DA - variable importance in projection scores obtained in orthogonal partial least squares discriminant analysis

Mass	RT	Formula	Putative metabolite	IDC	Peak intensity SCAP -scECM	Peak intensity SCAP	Fold change	q^2 value	VIP OPLS-DA
181.041	8.73263	$C_5H_{11}NO_4S$	Methionine sulfone	L2	3280	1423	2.305	4.71E-02	1.1
183.066	9.91719	$C_5H_{14}NO_4P$	Choline phosphate	L1	24845	13019	1.908	2.67E-02	1.8
90.0314	6.86814	$C_3H_6O_3$	Lactate	L1	3385595	5257964	0.644	3.45E-03	3.9
165.046	9.42292	$C_5H_{11}NO_3S$	Methionine S-oxide	L2	59807	107585	0.556	3.19E-02	4.6
328.239	3.82083	$C_{22}H_{32}O_2$	Docosahexaenoicacid	L2	7689	16482	0.467	3.60E-03	1.5
89.0475	10.5829	$C_3H_7NO_2$	Alanine	L1	337499	907135	0.372	1.43E-05	3.9
131.058	10.3736	$C_5H_9NO_3$	Glutamate 5-semialdehyde	L2	121874	350747	0.347	1.81E-05	3.6
264.104	17.3684	$C_{12}H_{16}N_4OS$	Thiamin	L2	20684	69918	0.296	1.90E-06	1.6

184.073	4.17602	$C_9H_{12}O_4$	3-Methoxy-4-hydroxyphenylethyleneglycol	L2	9273	35655	0.260	7.29E-04	1.2
115.063	9.60632	$C_5H_9NO_2$	Proline	L1	5874436	26000000	0.224	5.49E-06	15.7
165.079	8.09144	$C_9H_{11}NO_2$	Phenylalanine	L2	388742	1771731	0.219	6.83E-05	5.6
147.053	9.65589	$C_5H_9NO_4$	Glutamate	L1	291735	1336698	0.218	2.02E-06	1.4
131.069	10.5831	$C_4H_9N_3O_2$	Creatine	L1	800300	4148851	0.193	1.11E-06	3.1
747.576	4.38685	$C_{41}H_{82}NO_8P$	Phosphatidylethanolamine 36:0	L2	22046	121112	0.182	8.92E-05	1.6
155.069	10.411	$C_6H_9N_3O_2$	Histidine	L1	386184	2191530	0.176	1.06E-06	2.5
105.042	10.9408	$C_3H_7NO_3$	Serine	L1	85079	487346	0.175	9.05E-05	2.3
297.266	4.36398	$C_{18}H_{35}NO_2$	Sphinga-4,14-dienine	L2	62370	375152	0.166	1.56E-05	2.6
174.111	17.4697	$C_6H_{14}N_4O_2$	Arginine	L1	749191	4645452	0.161	1.93E-04	2.4
119.058	10.162	$C_4H_9NO_3$	Threonine	L1	343233	2169409	0.158	1.25E-06	3.7
175.095	10.9575	$C_6H_{13}N_3O_3$	Citrulline	L1	41522	263460	0.158	4.45E-04	2.1
181.074	9.79612	$C_9H_{11}NO_3$	Tyrosine	L1	223602	1419074	0.158	2.79E-06	4.4
192.026	11.2005	$C_6H_8O_7$	Citrate	L1	39258	254017	0.155	6.14E-03	2
281.271	4.39638	$C_{18}H_{35}NO$	Oleamide	L2	1695207	11000000	0.150	2.31E-05	2.7
103.099	16.4571	$C_5H_{13}NO$	Choline	L2	273490	1861713	0.147	4.77E-07	6.7
113.059	8.23037	$C_4H_7N_3O$	Creatinine	L1	778673	5454315	0.143	1.19E-06	1.9
146.105	16.4549	$C_6H_{14}N_2O_2$	Lysine	L1	220677	1557988	0.142	2.76E-05	2.7
295.251	4.36308	$C_{18}H_{33}NO_2$	Sphinga-4,8,10-trienine	L2	196671	1671028	0.118	2.24E-05	5.1
219.11	5.11932	$C_9H_{17}NO_5$	Pantothenate	L1	47438	607448	0.078	3.48E-05	4.6
523.363	4.70494	$C_{26}H_{54}NO_7P$	1-Stearoylglycerophosphocholine	L2	4442	59584	0.075	3.53E-07	3.1

328.152	4.13652	$C_{16}H_{24}O_7$	Prostaglandin E2	L2	15674	224599	0.070	3.00E-05	1.2
197.08	5.1603	$C_8H_{11}N_3O_3$	N-Acetylhistidine	L2	46054	729787	0.063	4.09E-05	2.3
146.069	10.4586	$C_5H_{10}N_2O_3$	Glutamine	L1	1175806	20000000	0.058	3.38E-07	6.9
493.316	4.82771	$C_{24}H_{48}NO_7P$	1-Palmitoleylglycerophosphocholine	L2	1000	17929	0.056	1.62E-09	1.8
454.305	4.37926	$C_{27}H_{41}F_3O_2$	26,26,26-Trifluoro-25-hydroxyvitamin D3	L2	25477	470278	0.054	1.02E-05	1.1
521.347	4.72728	$C_{26}H_{52}NO_7P$	1-Oleoylglycerophosphocholine	L2	3147	72696	0.043	2.96E-07	3.5
169.11	5.09727	$C_9H_{12}O_2$	3-Isopropylcatechol	L2	40262	940487	0.043	3.85E-07	3
169.085	9.37818	$C_7H_{11}N_3O_2$	3-Methylhistidine	L1	15113	428680	0.035	4.82E-07	2.8
243.085	9.34803	$C_9H_{13}N_3O_5$	Cytidine	L1	32528	1002657	0.032	1.70E-07	1.6
362.245	4.24001	$C_{22}H_{34}O_4$	19,20-Dihydroxy-docosapentaenoic acid	L2	18377	800136	0.023	2.28E-06	1.1
495.331	4.79878	$C_{24}H_{50}NO_7P$	1-Palmitoylglycerophosphocholine	L2	2397	128802	0.019	8.09E-08	4.7
122.048	6.92711	$C_6H_6N_2O$	Nicotinamide	L1	35119	3064352	0.011	2.80E-06	2.8
187.121	5.09546	$C_9H_{17}NO_3$	8-Amino-7-oxononanoate	L2	3563	342000	0.010	1.42E-06	1.5
284.271	3.85497	$C_{18}H_{36}O_2$	Stearic acid	L1	5157	753561	0.007	7.03E-08	3.4
254.224	3.88379	$C_{16}H_{30}O_2$	Palmitoleic acid	L2	247	89664	0.003	5.79E-08	1.2
474.37	4.11104	$C_{30}H_{50}O_4$	1-Hydroxy-2-(3-hydroxypropoxy)vitamin D3	L2	-1018	379756	-0.003	3.77E-06	2.5
117.079	9.37621	$C_5H_{11}NO_2$	Valine	L1	-11538	3593728	-0.003	9.10E-07	4
113.047	9.55093	$C_5H_7NO_2$	1-Pyrroline-5-carboxylate	L2	-1362	205310	-0.007	2.04E-07	2.8
166.085	6.96124	$C_5H_7N_3O$	5-Methylcytosine	L2	-1828	65184	-0.028	3.17E-04	1.2

460.354	4.12353	$C_{29}H_{48}O_4$	1-Hydroxy-2-(2-hydroxyethoxy)vitamin D3	L2	-275420	6711056	-0.041	1.74E-06	10.9
444.323	4.16202	$C_{28}H_{44}O_4$	1α,25,26-Trihydroxyvitamin D2	L2	-37362	745658	-0.050	1.44E-06	2.5
282.255	3.85915	$C_{18}H_{34}O_2$	Oleic acid	L2	-43233	823062	-0.053	3.04E-08	5.7
446.339	4.14031	$C_{28}H_{46}O_4$	3-dehydroteasterone	L2	-3000000	54000000	-0.055	1.52E-06	26.9
132.053	10.5921	$C_4H_8N_2O_3$	Asparagine	L1	-20059	354260	-0.057	7.63E-09	1.4
418.308	4.14885	$C_{26}H_{42}O_4$	1,24-Dihydroxy-22-oxavitamin D3	L2	-56683	870808	-0.065	1.83E-06	1.9
131.094	8.8289	$C_6H_{13}NO_2$	Leucine	L1	-257844	3925708	-0.066	3.41E-07	8
432.323	4.15459	$C_{27}H_{44}O_4$	6,19-Epidioxy-1-hydroxy-6,19-dihydrovitamin D3	L2	-342224	4960684	-0.069	2.85E-06	5.9
140.156	4.14546	$C_{10}H_{20}$	1-Decene	L2	-85758	1230997	-0.070	1.73E-06	2.4
900.644	4.16154	$C_{57}H_{88}O_8$	1,2-Dilinoleyl-3-(8-(2,4-decadienoyloxy)-5,6-octadienoyl)-glycerol	L2	-52274	712685	-0.073	3.49E-06	3.4
97.9671	11.3212	H_2O_4S	Sulphate	L2	-85956	1049741	-0.082	7.23E-09	2.9
98.1094	4.19261	C_7H_{14}	1-Heptene	L2	-39250	443018	-0.089	6.65E-06	1.4
274.067	8.02721	$C_{10}H_{12}N_4O_4$	Deoxyinosine	L2	-31478	307589	-0.102	3.00E-07	2.2
458.338	4.15385	$C_{29}H_{46}O_4$	18-Acetoxy-1-hydroxyvitamin D3	L2	-17631	138399	-0.127	6.74E-06	1.2
330.255	3.83526	$C_{22}H_{34}O_2$	Docosapentaenoic acid	L2	-971.5	4523	-0.215	8.48E-04	1.2
180.063	10.7088	$C_6H_{12}O_6$	Glucose	L1	-96382	203478	-0.474	1.62E-09	2
114.031	10.6787	$C_5H_6O_3$	2-Hydroxy-2,4-pentadienoate	L2	-38952	78049	-0.499	2.24E-09	1.3
102.031	10.6788	$C_4H_6O_3$	Acetoacetate	L2	-52683	89373	-0.589	3.05E-09	1.4
304.239	3.87085	$C_{20}H_{32}O_2$	Arachidonic acid	L2	-18878	4974	-3.795	8.53E-07	1.5

Supplementary Table 3.4 Significantly changed metabolites, matched to Human Metabolome Database (HMDB) and Kyoto Encyclopaedia of Genes and Genomes (KEGG) pathways, in direct relationship with inflammation, detected in the interplay between SCAP and scECM under TNFα and IFNγ stimulation after 24h. RT- retention time; IDC- metabolite identification level according to the metabolomics standards initiative L1 - Level 1, L2 - Level 2; Colours represent the heat map of the fold change between mean peak intensities of two conditions: yellow - no change, red - increase, blue – decrease, green – negative values indicating higher peak intensity of scECM compared to SCAP + scECM + stimulus condition, i.e. metabolite consumption; q^2 value was obtained after t-test and false discovery rate (FDR) correction using the Benjamini-Hochberg procedure; VIP OPLS-DA - variable importance in projection scores obtained in orthogonal partial least squares discriminant analysis

Mass	RT	Formula	Putative metabolite	IDC	Peak intensity	Peak intensity	Fold change	q^2 value	VIP OPLS-DA
			Part 1		SCAP+ scECM+ stimulus	SCAP+ scECM			
208.085	8.71462	$C_{10}H_{12}N_2O_3$	Kynurenine	L1	665249	15600	42.6	6.83E-07	12.4
191.058	8.95355	$C_{10}H_9NO_3$	5-Hydroxyindoleacetate	L2	214049	6080	35.2	2.75E-06	7
219.052	4.58238	$C_{11}H_9NO_4$	8-Methoxykynurenate	L2	13389	1000	13.4	4.21E-06	1.8
236.079	7.66614	$C_{11}H_{12}N_2O_4$	Formylkynurenine	L2	24863	2638	9.4	8.19E-07	2.3
144.115	4.22791	$C_8H_{16}O_2$	Octanoic acid	L2	176722	29179	6.1	6.56E-08	5.9
328.239	3.82083	$C_{22}H_{32}O_2$	Docosahexaenoicacid	L2	12287	31252	0.4	1.03E-03	2.1
113.048	6.90064	$C_5H_7NO_2$	1-Pyrroline-5-carboxylate	L2	32091	95589	0.3	1.25E-02	3.6

113.048	5.45472	$C_5H_7NO_2$	1-Pyrroline-2-carboxylate	L2	15457	68825	0.2	2.28E-07	3.5
204.09	9.2631	$C_{11}H_{12}N_2O_2$	Tryptophan	L1	10460	497490	0	8.49E-08	10.7
			Part 2		SCAP+ scECM+ stimulus	SCAP+ stimulus			
226.106	7.64491	$C_9H_{14}N_4O_3$	Carnosine	L2	98021	1745	56.2	8.57E-07	5.1
214.131	5.11067	$C_{10}H_{18}N_2O_3$	Dethiobiotin	L2	53473	1000	53.5	1.39E-03	3.7
267.096	7.88517	$C_{10}H_{13}N_5O_4$	Adenosine	L1	31350	666.7	47	2.98E-03	2.7
254.137	6.86771	$C_{11}H_{18}N_4O_3$	Homoanserine	L2	33321	1000	33.3	1.02E-05	3
306.255	3.84513	$C_{20}H_{34}O_2$	Icosatrienoic acid	L2	5602	458.8	12.2	3.12E-04	1.2
214.095	5.13146	$C_9H_{14}N_2O_4$	Pyrimidine nucleoside	L2	11787	1000	11.8	1.49E-06	1.8
215.055	10.6633	$C_5H_{14}NO_6P$	Glycero-3-phosphoethanolamine	L1	26398	2721	9.7	1.46E-07	2.6
426.087	10.5446	$C_{13}H_{22}N_4O_8S_2$	Glutathionyl-cysteine	L2	9618	1130	8.5	3.24E-04	1.5
181.041	8.73263	$C_5H_{11}NO_4S$	Methionine sulfone	L2	9225	1618	5.7	1.00E-03	1.4
216.11	7.79701	$C_9H_{16}N_2O_4$	γ-Glutamyl-γ-aminobutyraldehyde	L2	7062	1531	4.6	5.15E-04	1.2
183.066	9.9172	$C_5H_{14}NO_4P$	Choline phosphate	L1	32508	7304	4.5	4.58E-06	2.6
103.1	10.0627	$C_5H_{13}NO$	Choline	L2	115421	31859	3.6	1.40E-04	4.7
304.239	3.87085	$C_{20}H_{32}O_2$	Arachidonic acid	L2	11557	3434	3.4	5.79E-03	1.4
257.102	10.0631	$C_8H_{20}NO_6P$	Glycero-3-phosphocholine	L1	2655571	814258	3.3	6.77E-05	22.1
174.016	11.0816	$C_6H_6O_6$	Aconitic acid	L2	8191	2544	3.2	1.32E-03	1.2
165.046	9.42292	$C_5H_{11}NO_3S$	Methionine S-oxide	L2	256002	107613	2.4	3.91E-04	6.2
136.064	19.3684	$C_7H_8N_2O$	1-Methylnicotinamide	L2	57897	38763	1.5	1.72E-02	2.1

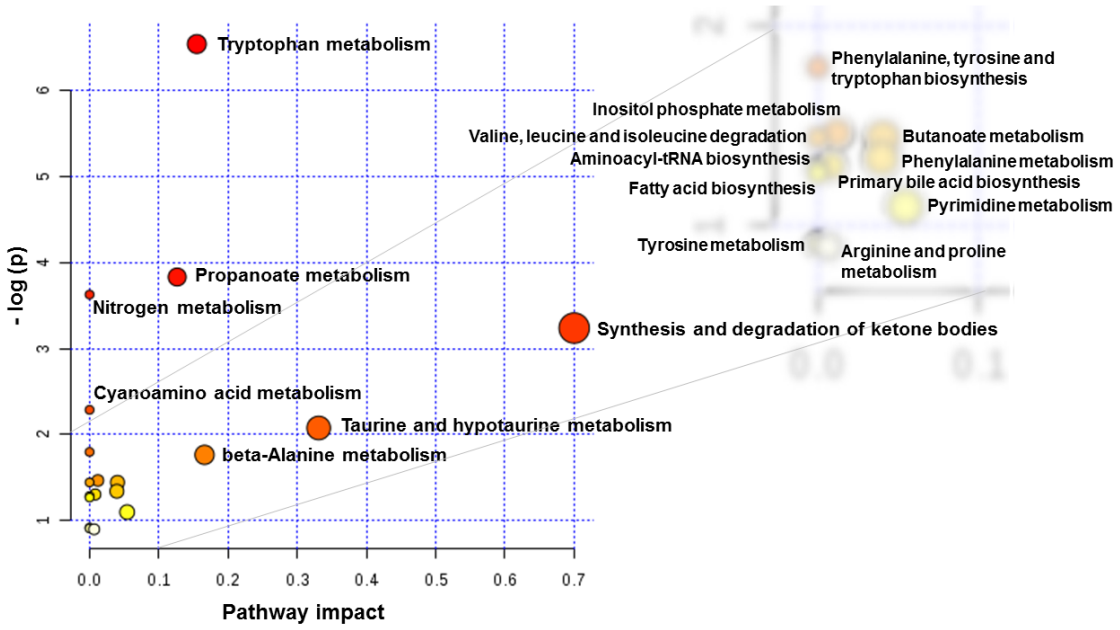
204.09	9.2631	$C_{11}H_{12}N_2O_2$	Tryptophan	L1	10460	24614	0.4	1.97E-04	1.9
523.363	4.70494	$C_{26}H_{54}NO_7P$	1-Octadecanoyl-sn-glycero-3-phosphocholine	L2	9443	52863	0.2	4.41E-03	3.2
521.347	4.72729	$C_{26}H_{52}NO_7P$	1-Oleoylglycerophosphocholine	L2	5412	57567	0.1	1.76E-05	3.7
493.316	4.82771	$C_{24}H_{48}NO_7P$	1-(9-Hexadecenoyl)-sn-glycero-3-phosphocholine	L2	1000	17689	0.1	4.93E-08	2.2
495.331	4.79878	$C_{24}H_{50}NO_7P$	1-Palmitoyl-sn-glycero-3-phosphocholine	L2	6023	128589	0	6.70E-07	5.8
			Part 3		SCAP-scECM+ stimulus	SCAP+ scECM			
426.087	10.5446	$C_{13}H_{22}N_4O_8S_2$	Glutathionyl-cysteine	L2	9619	1130	8.512	1.95E-05	1.5
214.095	5.13146	$C_9H_{14}N_2O_4$	Pyrimidine nucleoside	L2	3473	1000	3.473	4.58E-02	1.8
183.066	9.91719	$C_5H_{14}NO_4P$	Choline phosphate	L1	24118	7304	3.302	1.19E-05	2.6
144.114	4.22791	$C_8H_{16}O_2$	Octanoic acid	L2	125059	191599	0.653	1.38E-02	1.6
113.048	6.90064	$C_5H_7NO_2$	1-Pyrroline-5-carboxylate	L2	14982	41547	0.361	4.17E-03	1.2
315.277	4.54076	$C_{18}H_{37}NO_3$	6-Hydroxysphing-4-enine	L2	16891	54809	0.308	9.86E-04	1.2
89.0475	10.5829	$C_3H_7NO_2$	Alanine	L1	278900	936254	0.298	1.03E-06	2.8
227.225	4.54155	$C_{14}H_{29}NO$	Myristic amide	L2	264186	895057	0.295	5.04E-04	2.1
151.049	9.85939	$C_5H_5N_5O$	Guanine	L1	299262	1041352	0.287	7.07E-07	5.1
253.24	4.48138	$C_{16}H_{31}NO$	Palmitoleamide	L2	420137	1478181	0.284	1.49E-04	2.4
264.104	17.3684	$C_{12}H_{16}N_4OS$	Thiamin	L2	16771	61987	0.271	2.95E-07	1.4
255.256	4.50557	$C_{16}H_{33}NO$	Palmiticamide	L2	329701	1247242	0.264	1.59E-04	2.1
105.042	10.9408	$C_3H_7NO_3$	Serine	L1	133280	519991	0.256	9.23E-05	4.3
131.058	10.3736	$C_5H_9NO_3$	Glutamate 5-semialdehyde	L2	83068	357232	0.233	1.06E-05	2.7
175.095	10.9575	$C_6H_{13}N_3O_3$	Citrulline	L1	52232	279843	0.187	5.88E-04	2.8

440.289	4.37387	$C_{26}H_{39}F_3O_2$	26,26,26-Trifluoro-25-hydroxy-27-norvitamin D3	L2	17673	97928	0.180	1.01E-04	1.2
103.1	10.0627	$C_5H_{13}NO$	Choline	L2	5128	31859	0.161	2.77E-02	4.7
281.271	4.39638	$C_{18}H_{35}NO$	Oleamide	L2	1897368	12000000	0.159	2.18E-05	2.3
297.266	4.36398	$C_{18}H_{35}NO_2$	Sphinga-4,14-dienine	L2	58557	381435	0.154	8.06E-06	2.6
192.026	11.2005	$C_6H_8O_7$	Citrate	L1	38887	269569	0.144	5.25E-03	2.3
131.069	10.5831	$C_4H_9N_3O_2$	Creatine	L1	602600	4458348	0.135	5.66E-07	4.8
279.256	4.40965	$C_{18}H_{33}NO$	Linoleamide	L2	415590	3103509	0.134	6.93E-06	1.6
165.079	8.09144	$C_9H_{11}NO_2$	Phenylalanine	L2	211325	1682784	0.126	6.11E-06	7.8
134.021	10.1901	$C_4H_6O_5$	Malate	L1	13170	110600	0.119	1.57E-06	1.7
747.576	4.38685	$C_{41}H_{82}NO_8P$	Phosphatidylethanolamine 36:0	L2	13675	116031	0.118	5.19E-05	1.3
523.363	4.70494	$C_{26}H_{54}NO_7P$	Stearyl-glycero-3-phosphocholine	L2	6031	52863	0.114	2.16E-04	3.2
174.111	17.4697	$C_6H_{14}N_4O_2$	Arginine	L1	528562	4688648	0.113	1.02E-04	2.2
257.102	10.0631	$C_8H_{20}NO_6P$	Glycero-3-phosphocholine	L1	90987	814258	0.112	1.00E-02	22.1
219.11	5.11932	$C_9H_{17}NO_5$	Pantothenate	L1	61647	592253	0.104	2.25E-05	4.7
454.305	4.37926	$C_{27}H_{41}F_3O_2$	26,26,26-Trifluoro-25-hydroxyvitamin D3	L2	47923	462311	0.104	2.94E-05	2.1
362.245	4.24001	$C_{22}H_{34}O_4$	19,20-Dihydroxydocosapentaenoic acid	L2	75692	738179	0.103	8.65E-06	3.8
295.251	4.36308	$C_{18}H_{33}NO_2$	Sphinga-4,8,10-trienine	L2	164007	1608031	0.102	1.95E-05	7.1
193.074	4.8803	$C_{10}H_{11}NO_3$	Phenylacetylglycine	L1	64749	658816	0.098	1.77E-05	1.8
146.069	10.4586	$C_5H_{10}N_2O_3$	Glutamine	L1	1980515	21000000	0.093	2.05E-07	3.4
119.058	10.162	$C_4H_9NO_3$	Threonine	L1	193048	2163784	0.089	4.94E-07	2.6
280.24	3.93433	$C_{18}H_{32}O_2$	Linoleate	L2	17618	198683	0.089	1.52E-05	1.1
97.9768	9.3477	H_3O_4P	Orthophosphate	L2	7159	82159	0.087	1.59E-03	1.2
147.053	9.65589	$C_5H_9NO_4$	Glutamate	L1	93123	1175296	0.079	2.08E-06	1.2
113.048	5.45472	$C_5H_7NO_2$	1-Pyrroline-2-carboxylate	L2	1602	21573	0.074	2.08E-04	1.2
197.08	6.87142	$C_8H_{11}N_3O_3$	Acetyl-histidine	L2	40366	564065	0.072	7.58E-07	3.1

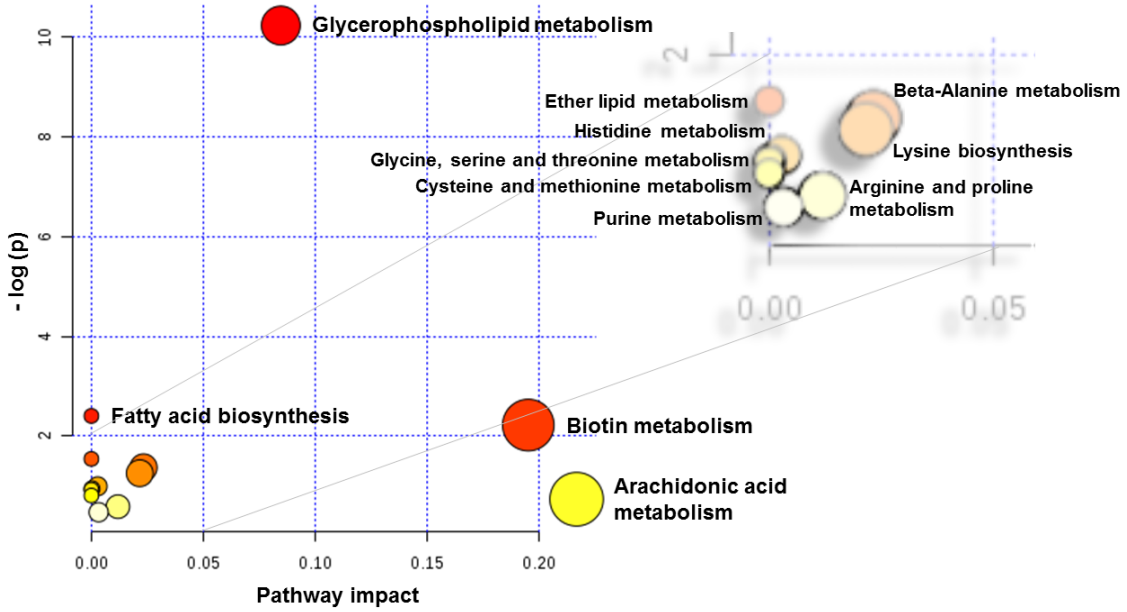
202.143	15.0625	$C_8H_{18}N_4O_2$	Dimethyl-arginine	L2	8695	145059	0.060	4.25E-06	1.2
474.37	4.11104	$C_{30}H_{50}O_4$	1-Hydroxy-2-(3-hydroxypropoxy)vitamin D3	L2	21095	357269	0.059	1.08E-05	1.2
181.074	9.79612	$C_9H_{11}NO_3$	Tyrosine	L1	75632	1296933	0.058	1.93E-07	6.8
493.316	4.82771	$C_{24}H_{48}NO_7P$	1-Palmitoleylglycerophosphocholine	L2	1000	17689	0.057	8.42E-09	2.2
900.644	4.16154	$C_{57}H_{88}O_8$	1,2-Dilinoleyl-3-(8-(2,4-decadienoyloxy)-5,6-octadienoyl)-glycerol	L2	33690	709052	0.048	2.59E-06	2.0
203.115	8.48776	$C_9H_{17}NO_4$	O-Acetylcarnitine	L1	5255	124261	0.042	7.40E-07	1.3
460.354	4.12353	$C_{29}H_{48}O_4$	1-Hydroxy-2-(2-hydroxyethoxy)vitamin D3	L2	256943	6348490	0.040	4.01E-06	4.5
521.347	4.72728	$C_{26}H_{52}NO_7P$	1-Oleoylglycerophosphocholine	L2	2224	57567	0.039	1.76E-06	3.7
113.059	8.23037	$C_4H_7N_3O$	Creatinine	L1	203593	5428818	0.038	3.61E-07	5.0
115.063	9.60632	$C_5H_9NO_2$	Proline	L1	865790	25000000	0.035	2.59E-06	4.3
187.121	5.09546	$C_9H_{17}NO_3$	8-Amino-7-oxononanoate	L2	11816	395189	0.030	5.58E-07	4.2
432.323	4.15459	$C_{27}H_{44}O_4$	6,19-Epidioxy-1-hydroxy-6,19-dihydrovitamin D3	L2	142109	4863262	0.029	2.99E-06	1.2
243.085	9.34803	$C_9H_{13}N_3O_5$	Cytidine	L1	28264	1016587	0.028	7.63E-07	2.5
117.079	9.37621	$C_5H_{11}NO_2$	Valine	L1	94621	3437939	0.028	1.13E-06	1.8
128.058	10.5893	$C_5H_8N_2O_2$	5,6-Dihydrothymine	L2	4487	208928	0.021	1.78E-07	1.3
129.042	7.26008	$C_5H_7NO_3$	1-Pyrroline-3-hydroxy-5-carboxylate	L2	6270	450254	0.014	8.63E-07	2.0
89.995	11.1826	$C_2H_2O_4$	Oxalate	L1	844.7	84634	0.010	1.47E-04	1.7
169.085	9.37818	$C_7H_{11}N_3O_2$	3-Methyl-histidine	L1	3618	428989	0.008	1.60E-07	3.5
444.323	4.16202	$C_{28}H_{44}O_4$	1,25,26-Trihydroxyvitamin D2	L2	735.7	733058	0.001	1.44E-06	1.9
182.079	10.1155	$C_6H_{14}O_6$	Mannitol	L1	307.8	383864	0.001	2.15E-07	1.9
495.331	4.79878	$C_{24}H_{50}NO_7P$	1-Palmytilglycerophosphocholine	L2	-561.3	128589	-0.004	7.53E-08	5.8
179.079	9.9817	$C_6H_{13}NO_5$	Galactosamine	L2	-3525	646803	-0.005	8.03E-06	1.7

122.048	6.92711	$C_6H_6N_2O$	Nicotinamide	L1	-31509	3114468	-0.010	1.37E-06	5.1
402.225	4.14118	$C_{20}H_{34}O_8$	5-HETE di-endoperoxide	L2	-13175	1136047	-0.012	5.33E-06	2.6
98.1094	4.19261	C_7H_{14}	1-Heptene	L2	-5452	455754	-0.012	5.40E-06	1.6
144.042	10.1024	$C_6H_8O_4$	2,3-Dimethylmaleate	L2	-6019	350176	-0.017	4.28E-06	1.8
763.571	4.37288	$C_{41}H_{82}NO_9P$	1-Octadecyl-2-heptadecanoylglycerophosphoserine	L2	-2490	99255	-0.025	1.75E-05	2.0
870.545	4.14071	$C_{50}H_{79}O_{10}P$	Glycerophospholipid (44:0)	L2	-4488	128843	-0.035	1.15E-05	1.5
218.019	10.0164	$C_9H_8O_5$	3-(3,4-Dihydroxyphenyl)pyruvate	L2	-43642	1201380	-0.036	1.11E-06	2.5
161.105	9.63388	$C_7H_{15}NO_3$	Carnitine	L1	-21575	481009	-0.045	2.30E-06	1.9
97.9671	11.3212	H_2O_4S	Sulphate	L2	-69672	1018652	-0.068	2.00E-09	1.5
462.334	4.13715	$C_{28}H_{46}O_5$	3,7,12-Trihydroxyergost-23-en-26-oic acid	L2	-13474	151299	-0.089	8.97E-06	1.2
132.09	15.4051	$C_5H_{12}N_2O_2$	Ornithine	L1	-15301	139971	-0.109	5.05E-06	1.6
132.053	10.5921	$C_4H_8N_2O_3$	Asparagine	L1	-43741	327222	-0.134	2.78E-09	1.1
256.24	3.87802	$C_{16}H_{32}O_2$	Palmitic acid	L2	-148082	1033842	-0.143	1.82E-07	1.3
316.26	3.97464	$C_{18}H_{36}O_4$	9,10-Dihydroxystearicic acid	L2	-87985	576824	-0.153	6.24E-08	2.9
131.094	8.8289	$C_6H_{13}NO_2$	Leucine	L1	-593287	3790634	-0.157	3.51E-07	8.2
254.224	3.88379	$C_{16}H_{30}O_2$	Palmitoleic acid	L2	-14420	78610	-0.183	1.07E-07	1.1
284.271	3.85497	$C_{18}H_{36}O_2$	Stearic acid	L1	-120666	652325	-0.185	1.56E-06	2.3
274.067	8.02721	$C_{10}H_{12}N_4O_4$	Deoxyinosine	L2	-58364	315044	-0.185	1.67E-07	4.1
106.026	8.23591	$C_3H_6O_4$	Glycerate	L1	-11408	60452	-0.189	4.91E-08	1.1
267.096	8.96674	$C_{10}H_{13}N_5O_4$	Deoxyguanosine	L1	-25491	88238	-0.289	1.23E-06	1.2
282.255	3.85915	$C_{18}H_{34}O_2$	Oleic acid	L2	-224975	773846	-0.291	9.98E-08	2.4
283.091	9.8115	$C_{10}H_{13}N_5O_5$	Guanosine	L1	-13369	35579	-0.376	8.06E-07	1.1
180.063	10.7088	$C_6H_{12}O_6$	Glucose	L1	-118075	185935	-0.635	7.50E-10	2.7
114.031	10.6787	$C_5H_6O_3$	2-Hydroxy-2,4-pentadienoate	L2	-49729	67358	-0.738	8.12E-10	1.7
102.031	10.6788	$C_4H_6O_3$	Acetoacetate	L2	-66482	78051	-0.852	1.52E-09	2.0

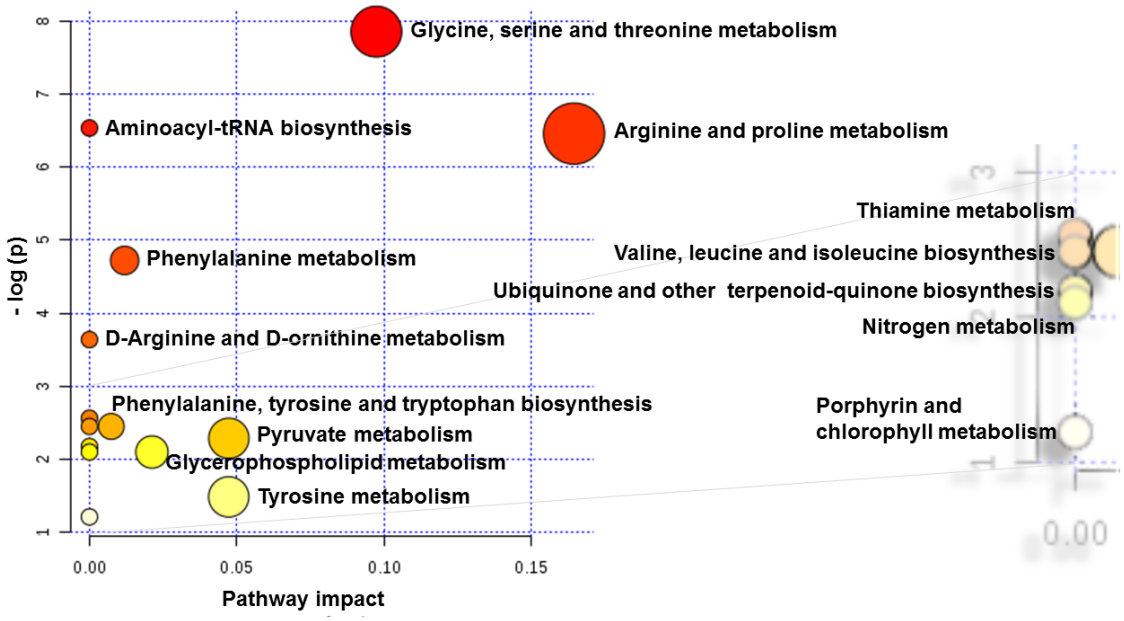
88.0157	6.81772	$C_3H_4O_3$	Malonate semialdehyde	L2	-203450	109473	-1.858	2.41E-09	1.4
304.239	3.87085	$C_{20}H_{32}O_2$	Arachidonic acid	L2	-25741	3434	-7.496	4.58E-07	1.4
204.09	9.2631	$C_{11}H_{12}N_2O_2$	Tryptophan	L1	-450535	24615	-18.303	3.93E-07	1.9
306.255	3.84513	$C_{20}H_{34}O_2$	Icosatrienoic acid	L2	-9070	458.8	-19.769	1.00E-05	1.2
217.142	11.0463	$C_9H_{19}N_3O_3$	γ-Glutamylputrescine	L2	-45453	1000	-45.453	1.97E-02	4.5



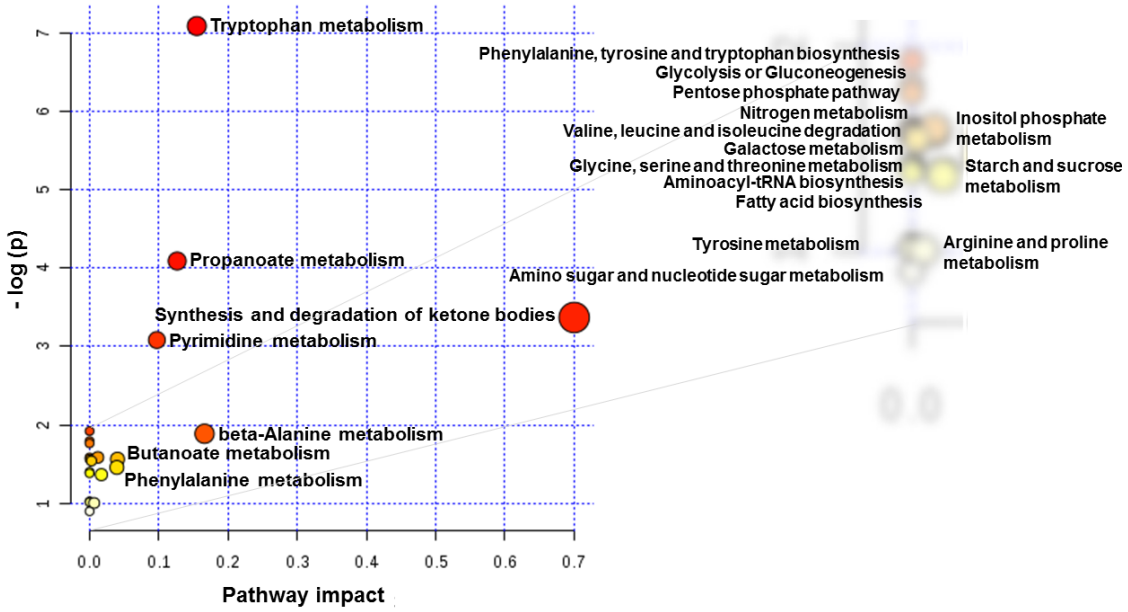
Supplementary Figure 3.3 Node diagram representation of pathways i.e. metabolome view, obtained in MetaboAnalyst, by qualitative (putative metabolite name-based) pathway enrichment, i.e. biological significance of the metabolite and its pathway, (p) and pathway topology, i.e. significance of the metabolite in the pathway (Pathway impact) analysis of significantly different metabolites between SCAP and SCAP+stimulus. A part of the figure at the axes' origin was enlarged and made transparent to allow clear labelling of the pathways



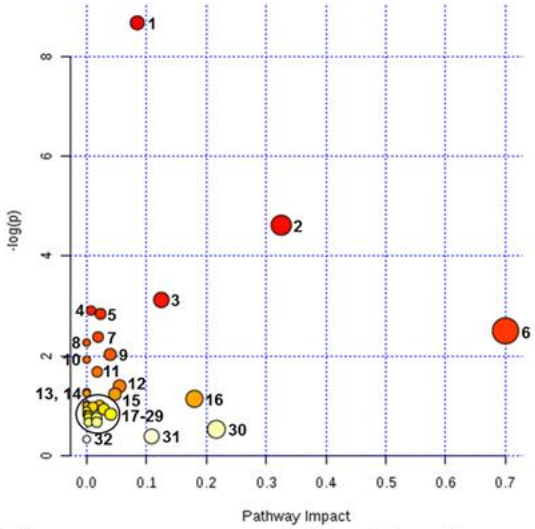
Supplementary Figure 3.4 Node diagram representation of pathways i.e. metabolome view, obtained in MetaboAnalyst, by qualitative (putative metabolite name-based) pathway enrichment, i.e. biological significance of the metabolite and its pathway, (p) and pathway topology, i.e. significance of the metabolite in the pathway (Pathway impact) analysis of significantly different metabolites between scECM and medium. A part of the figure at the axes' origin was enlarged and made transparent to allow clear labelling of the pathways



Supplementary Figure 3.5 Node diagram representation of pathways i.e. metabolome view, obtained in MetaboAnalyst, by qualitative (putative metabolite name-based) pathway enrichment, i.e. biological significance of the metabolite and its pathway, (p) and pathway topology, i.e. significance of the metabolite in the pathway (Pathway impact) analysis of significantly different metabolites between SCAP and SCAP+scECM. A part of the figure at the axes' origin was enlarged and made transparent to allow clear labelling of the pathways



Supplementary Figure 3.6 Node diagram representation of pathways i.e. metabolome view, obtained in MetaboAnalyst, by qualitative (putative metabolite name-based) pathway enrichment, i.e. biological significance of the metabolite and its pathway, (p) and pathway topology, i.e. significance of the metabolite in the pathway (Pathway impact) analysis of significantly different metabolites between SCAP+scECM and SCAP+scECM+stimulus. A part of the figure at the axes' origin was enlarged and made transparent to allow clear labelling of the pathways



1	Glycerophospholipid metabolism	17	Glycolysis or Gluconeogenesis
2	Biotin metabolism	18	Pentose phosphate pathway
3	Thiamine metabolism	19	Lysine biosynthesis
4	Phenylalanine, tyrosine and tryptophan biosynthesis	20	Purine metabolism
5	beta-Alanine metabolism	21	Propanoate metabolism
6	Synthesis and degradation of ketone bodies	22	Ubiquinone and other terpenoid-quinone biosynthesis
7	Arginine and proline metabolism	23	Valine, leucine and isoleucine degradation
8	Nitrogen metabolism	24	Butanoate metabolism
9	Phenylalanine metabolism	25	Galactose metabolism
10	Glycine, serine and threonine metabolism	26	Histidine metabolism
11	Cysteine and methionine metabolism	27	Nicotinate and nicotinamide metabolism
12	Citrate cycle (TCA cycle)	28	Glyoxylate and dicarboxylate metabolism
13	Ether lipid metabolism	29	Starch and sucrose metabolism
14	Aminoacyl-tRNA biosynthesis	30	Arachidonic acid metabolism
15	Tyrosine metabolism	31	Tryptophan metabolism
16	Pantothenate and CoA biosynthesis	32	Amino sugar and nucleotide sugar metabolism

Supplementary Figure 3.7 Node diagram representation of pathways i.e. metabolome view, obtained in MetaboAnalyst, by qualitative (putative metabolite name-based) pathway enrichment, i.e. biological significance of the metabolite and its pathway, (p) and pathway topology, i.e. significance of the metabolite in the pathway (Pathway impact) analysis of significantly different metabolites between SCAP+stimulus and SCAP+scECM+stimulus

4 Discussion

4.1 Discussion

Spinal cord injury induces chronic inflammation limiting regeneration. My hypothesis was that SCAP embedded in ECM hydrogel have anti-inflammatory properties and a potential to be delivered to spinal cord lesions.

Therefore, the specific objectives were to:

1) Determine and optimise mechanical properties of scECM and bECM for the delivery of embedded SCAP

2) Test the anti-inflammatory properties of SCAP and the ECM hydrogels, separately and combined, in the forms they are expected to take upon injection

3) Explore SCAP and ECM hydrogel interaction, whether and how it changes in pro-inflammatory environment and the influence it has on the immunoregulatory potential of SCAP and/or ECM hydrogel

4.1.1 Hydrogel Mechanical Properties Seemed Suitable for SCAP Delivery in the Scope of SCI

Hydrogels are viscoelastic materials, which means that they have mechanical properties of a viscous liquid and an elastic solid, i.e. the ability to flow, to resist deformation and to resume the original shape upon deformation. In ECM hydrogels these properties are temperature-dependant. At 4 °C ECM hydrogels are in the liquid-like pre-gel state, able to flow and their resistance to deformation is described as viscosity. At 37 °C ECM hydrogels are formed and described as “soft solids”, i.e. of low stiffness [1]. The change between these states over time is gelation kinetics. A rheometer was used to measure the storage and loss moduli of the materials, i.e. to obtain information on the physical properties of the hydrogels. Storage modulus is a measure of elastic response that is derived from the relationship between stress and strain. Therefore, the storage modulus

is also interpreted as the stiffness of the hydrogel, i.e. resistance to deformation of a solid. Loss modulus is a measurement of viscosity, i.e. resistance to deformation of a fluid [2].

Atomic force microscopy is another technique that can provide similar measurements of hydrogel elasticity and viscosity. However, due to the sensitivity of this technique, measurements are acquired 'locally', on a microscopical level and results are extrapolated for bulk hydrogel properties. Atomic force microscopy has not been used often with ECM, likely due to the high diversity of the largely unknown ECM proteins and their distribution throughout the hydrogel [1]. A texture analyser can be used to measure stiffness/elasticity under compression/tension, but it may not be adequate for pre-gels and "soft" hydrogels due to their liquid-like properties. ECM hydrogel rheological properties may be measured on texture analyser by using the axial loading with adequate accessories to measure extrusion [3]. However, this may require larger ECM hydrogel volumes compared to those used during parallel plate rheometry. It is also possible to use a spectrophotometer to determine gelation kinetics by measuring the opalescence increase during the phase transition. However, this method was inadequate for scECM as the pre-gel was already cloudy, unlike the more clear bECM [4].

ECM hydrogel mechanical properties depended on the hydrogel origin. As has been reported previously [4], scECM storage/loss moduli and gelation rate were lower than the moduli and gelation rate of bECM of the same concentration. This may be related to the different concentrations of collagen and sGAG in the tested hydrogels, as these are the molecules that have been shown to participate in the creation of the hydrogel network [4]. scECM has been shown to contain higher sGAG and bECM more collagen respectively [4]. Hydrogel concentration also had an influence on the storage modulus (bECM 8mg/mL < bECM 10 mg/mL), as has been reported previously [2], [5], but not

the gelation rate. This may be due to the larger number of molecules making the hydrogel network, as they could take more time to self-assemble. Previously reported maximum storage / loss moduli of scECM 8 mg/mL generated by a similar protocol were 19 ± 1 / 2 ± 0 by Viswanath *et al.* [4] and 757 ± 75 / 94 ± 11 Pa, by Medberry *et al.* [6], whilst scECM moduli in this work had an intermediate value of 258 ± 17 / 37 ± 2. Reported storage / loss moduli for bECM 8 mg/mL are 287 ± 8 / 43 ± 4 [4], which was lower compared to 499 ± 10 / 60 ± 3 Pa obtained in this work. ASTM F2900 - 11 suggested that the variation of the testing parameters or the use of different rheometers may be the reason for obtaining different results, even when the biological variables, operator, hydrogel batch and processing/manipulation are the same [7].

Low hydrogel stiffness at 4 °C (1 Pa) allows hydrogel passage through a syringe and gelation upon reaching 37 °C allows local retention, which makes the tested ECM hydrogels suitable for local injection. Time to scECM, bECM and scECM/fibrin 95% gelation of under 5 minutes allowed preparation of hydrogel combinations, vigorous homogenisation by pipette, cell suspension and casting series of samples onto the well plates.

Stiffness influences ECM hydrogel ability to incorporate cells [5], [8], as it correlates to density of the hydrogel network. The hydrogel network provides mechanical support for the cells expressing focal adhesion points for the cells to attach [4], [9] and stabilising the cell suspension preventing cell precipitation (settling). Therefore, the stiffness (moduli) of 6 mg/mL cardiac ECM hydrogel, even though not specified, it was described by Williams *at al.* as too low to encapsulate cells [8]. Massensini *et al.* determined cardiac ECM hydrogel pre-gel viscosity, 0.084 ± 0.008 to 0.443 ± 0.062 Pas and maximum storage and loss moduli, 77 ± 10 to 460 ± 62 and 11 ± 1 to 66 ± 9 Pa, for the 4 and 8 mg/mL hydrogels, respectively [2]. As the moduli are concentration-dependant, it may be assumed that moduli of the 6mg/mL cardiac ECM hydrogel have intermediate

values [2], [5]. However, scECM and bECM of 8 mg/mL that had significantly lower or intermediate maximum storage/loss moduli values (19 ± 1 / 2 and 287 ± 8 / 43 ± 4 Pa, respectively) were able to support 3D cell culture [4]. This may be due to the influence of hydrogel origin on the cell incorporation. Moduli of scECM, bECM and scECM/fibrin pre-gels and hydrogels obtained in this work had intermediate or higher values compared to the previously mentioned studies [2], [4] and allowed for cell encapsulation and three-dimensional cell culture.

The pre-gel viscosity influences ECM hydrogels' ability to protect the cells from share stress during injection. ECM hydrogel has been shown to reduce the high cell-to-needle wall resistance and form a layer which acts as a lubricant [10]. In previous studies bECM of 1.75 mg/mL concentration (4.6-fold lower than in this work) with a viscosity of around 0.38 Pas, and shear thinning behaviour of around 10^4 Pas during the injection through a low-diameter needle preserved the viability of 60.7 ± 10.1% human MSC. As the reduction of shear stress positively correlates with the concentration of ECM hydrogel, scECM, bECM and scECM/fibrin hydrogels used in this work may give a higher percentage of cell viability post-injection.

.

Stiffness of the injected hydrogel should be similar to the stiffness of the surrounding tissue to avoid damage and an adverse, Th1-like immune response, as to a foreign object [11], [12]. This is especially important for neural tissue, as it is softer (10^2-10^3 Pa), than muscular (10^4 Pa), connective tissue (10^4 Pa), skin (10^4-10^5 Pa) or bone (10^9-10^{10} Pa) [13]. High stiffness and moduli of the cortical neural implants have been positively correlated to the intensity of gliosis and axonal dieback on the meta-analysis level [14]. The maximum storage moduli of scECM, bECM and scECM/fibrin measured in this work (258 - 499 Pa) matched the lower part of the wide range of moduli reported for spinal cord tissue (120 - 15200 Pa) [15] and met the stated requirement.

Hydrogel stiffness upon injection may influence local cell infiltration, axonal ingrowth and synapse formation [16]. This may be more important in the case of intraspinal injection, when hydrogel fills the lesion cavity “bridging the gap” [17], [18], compared to the subdural delivery, by which the additional tissue damage caused by repeated injections may be avoided [19]. Hydrogel gelation rate may influence the local retention upon the subdural injection, as the slow gelling hydrogels may get washed-off by the cerebrospinal fluid flow [20], [21]. scECM hydrogel stiffness and gelation rate can be tuned with different concentrations of fibrinogen and thrombin depending on the technical aspects and the objectives of the delivery strategy.

In this work simple addition of 25% fibrin increased the storage modulus and gelation time of scECM. In the previous studies much more fibrin, 90% of the total volume, and its crosslinking to collagen were necessary to significantly increase the stiffness of cardiac ECM. The resulting stiffness (Young’s modulus of 32000 Pa) however, was much higher than that obtained herein with scECM, bECM and scECM/fibrin [8]. scECM/bECM contain collagen [4] and thus can also be crosslinked with fibrin using transglutaminase to achieve an even higher stiffness. However, crosslinking may alter protein conformation and has been related to the loss of ECM hydrogel effectiveness [22]. For instance, the crosslinked conformation of collagen may block or cause “covering” of ECM components, e.g. matrycriptic peptides and reduce progenitor cell recruitment [23]. We hypothesised, according to the research done on collagen I -fibrin composites, that the addition of fibrin without the crosslinking would not bind the collagen in scECM and that scECM ligands would therefore remain unaltered. Collagen-fibrin networks have been shown to be interpenetrative, i.e. parallel but not interactive, when collagen content is higher than fibrin [24], as it was in scECM/fibrin. Fibrin has been shown to not bind denatured, for instance digested collagen, as in scECM/fibrin. Even the native form has been shown to present only few fibrin binding sites and it is therefore possible that all of them get denaturised [25]. This suggested that the intensity of

digestion, a necessary step in ECM hydrogel production that denaturises the collagen, may also influence the fibrin-collagen binding. Binding of fibrin to ECM hydrogel constituents other than collagen I has not been considered in this work, as collagen I has been shown to be the largest constituent [4].

4.1.1.1 Hydrogels Supported SCAP Viability

High viability of incorporated SCAP was confirmed in scECM and bECM [4] and measured in scECM/fibrin. The results depended on hydrogel origin and concentration, as has been shown in previous research [4], [5], i.e. viability was higher in 8 mg/mL bECM compared to 8mg/mL scECM and 10 mg/mL bECM. Viswanath *et al*. tested SCAP viability in 8 mg/mL scECM and bECM 3D cultures and bECM also performed better [4]. As scECM have been shown to promote neural differentiation [4], [26] and bECM osteodifferentiation [4], [27], an interplay between tissue and cells of the same neural origin, may have led to these results. Specifically, the reduction of viability signal may have been replenished in bECM by SCAP proliferation. However, in scECM, SCAP may have responded to the differentiation signals and therefore stopped proliferating. Therefore, SCAP viability seemed preserved in bECM more than in scECM.

Freytes *et al*. also found that the viability of incorporated cells decreased with increased ECM hydrogel concentration [5]. This suggested that bECM 10mg/mL may be a poor SCAP delivery vehicle. At higher hydrogel concentrations, a denser hydrogel network may have reduced the diffusion of nutrients and waste and therefore affected cellular behaviour [5]. The diffusion of PrestoBlue reagent in the original and reduced form (resazurin and resorufin) may have also been reduced, which can consequently affect the viability measurements.

With the addition of 25% fibrin to scECM, the cells seemed to proliferate. As fibrin has previously been shown to support the viability of incorporated SCAP, this may be a consequence of lowering scECM concentration [5]. Another explanation may come from the fact that PrestoBlue technically measures cell metabolic activity, as the fluorescence is emitted upon the reduction of blue resazurin to red resorufin by cell metabolic products [28]. Reduction of SCAP metabolic activity on day 0 may have occurred due to the additional processing with more mixing and a longer period on ice required to add fibrinogen. This may have given a false negative reading that was normalised to 100%. Thus, SCAP recovery by day 3 and 7 gave the false impression of proliferation. Nonetheless, viability measurements added value to the above discussed suitability of scECM/bECM mechanical properties for SCAP delivery in the scope of SCI.

Another cell viability assay, Live/Dead, was considered as it has lower chance to give a false reading. The ‘Live stain’ calcein AM, can only emit the green fluorescence upon interaction with estherases inside the live cells. Hoechst and DAPI stain all the nuclei blue, giving the total cell number, however DAPI is toxic and may be detrimental to cell viability during prolonged incubation periods. The ‘Dead stain’ propidium iodide, cannot pass the cellular membrane, so it stains only apoptotic, necrotic or dead cells in red. However, Live/Dead assay in 3D culture of SCAP incorporated in ECM hydrogels requires confocal microscopy, prolonged incubation periods and the intrinsic green autofluorescence of the hydrogel may impair the signal measurement or cell counting precision [4]. Therefore, PrestoBlue assay was selected for its precision and low quantification limit.

4.1.2 ECM hydrogels, SCAP and SCAP Incorporated in ECM Hydrogels Demonstrated LPS-Activation Mitigating Properties

As scECM/bECM anti- “Th1” inflammatory properties have not been explored before, they were tested *in vitro* on the types of cells present at the spinal cord lesion that contribute to inflammation. As macrophage-like cells have been shown to orchestrate inflammation and be one of the impediments to its resolution [29], [30], they were prioritised over neurons, endothelial cells, T and B lymphocytes. Results that could be obtained for astrocytes or neutrophils may be complex to interpret, as astrocyte activation is microglia-dependent and incompletely understood [31], [32] and neutrophils have not been explored separately in the context of SCI [30], [33]. Immunomodulatory properties of hydrogels derived from small intestine submucosa, urinary bladder, brain and other tissues have been investigated on monocytes [34], [35]. They are predominantly present at the lesion, so they would be a good, but not typical model of SCI inflammation [29], [36]. Recent publications have been focused on microglia as this cell type initiates inflammation and directly promotes re-myelination and neural regeneration [29], [32], [37]–[42]. Therefore, anti- “Th1” inflammatory properties of SCAP and/or hydrogels were investigated on an LPS-activated microglia cell line: BV2 cells.

LPS-activated BV2 cells are the most commonly used microglia model [43] as they have a robust, predictable and consistent response that predominantly matches microglia in marker expression. BV2 are also much easier to obtain and culture compared to microglia [43]–[48]. However, LPS was not a representative stimulus as SCI is a sterile injury. Meaning that, even if bacteria- caused inflammatory response existed, for instance in the case of penetrating trauma, it would be minor compared to the response of the injured tissue. In order to generate inflammation, TNFα and IFNγ are considered the leading cytokines [49]. However, BV2 response to TNFα and IFNγ is rarely considered, as a stimulation protocol is less well-known and marker expression less

predictable compared to LPS activation [50], [51]. Still, these are the typical problems of a cell line *in vitro* model and using it to commence the investigation of scECM/bECM anti-inflammatory properties was ethically responsible.

The most sensitive and consistent markers of BV2 LPS-activation and its mitigation, *Arg1*, *Nos2* and *Tnf* were assessed by real time quantitative polymerase chain reaction technique. This technique was sensitive as well as cost/effective.

Some ECM hydrogels, such as small intestine submucosa, brain, oesophagus, colon, dermal urinary bladder, skeletal muscle and liver derived, have previously been shown to induce expression of mannose receptor CD206 or *Arg1* and reduce iNOS or TNFα synthesis in naïve macrophage-like cells (primary monocytes or THP1) [34], [35]. Thus, it is crucial to investigate scECM/bECM influence on activated cells, utilising similar markers as reported previously [34], [35]. Pre-activating BV2 was closer to the SCI condition, as microglia activates within 0.5h of injury and before treatment is applied [29], [52]. However, CD206 has been shown to increase upon LPS activation instead of decrease, as a marker of the “M2a” phenotype. This may depend on experimental conditions, such as LPS pre-stimulation of cell sensitisation [53]. Therefore, CD206 expression as well as LPS sensitisation and repeated stimulation were not considered. Other research suggests that LPS stimulation should be repeated before or in parallel with the addition of treatment. That may be to avoid desensitisation of the LPS receptor (Toll-like receptor 4), which may promote alternative BV2 phenotype [54]. Xenogeneic ECM hydrogel proteins originating from different tissues may also contribute to the unpredictability and inconsistency of the results by contributing to BV2 activation, sensitisation as well as “the treatment”. Still, selecting LPS-activated BV2 as a model did not significantly limit the range of investigated markers.

Alongside *Tnf*, *Nos2*/*Arg1* ratio was considered as a single pro- “Th1” inflammatory marker, instead of *Nos2* as a pro- and *Arg1* as an anti-“Th1” inflammatory marker, individually. *Nos2* codes iNOS, that produces citrulline and NO from arginine. NO then has the proinflammatory properties. *Arg1* codes liver arginase, which is an enzyme that hydrolyses arginine to ornithine and urea, so that NO cannot be produced. Therefore, the arginine expenditure and NO generation, i.e. the balance between these 2 enzymes and the expression of their genes is a more robust indicator of inflammation compared to the individual markers.

scECM/bECM LPS-activation mitigating properties were assessed in solid and solubilised form. Due to the possibility of intraparenchymal and intrathecal injection, different forms of scECM/bECM may be required, as they would occupy different space: interstitial and subdural. Upon subdural delivery a portion of the hydrogel molecules may be dissolved by the flow of cerebrospinal fluid before the complete gelation could be achieved. This could result in both solid and solubilised hydrogel form at the lesion. We have hypothesised that depending on the form of hydrogel different molecules will be exposed and released and consequentially, will have different influences on the cells. However, in direct contact with solid scECM/bECM BV2 cells died, probably due to the overstimulation as they were brought into the immediate direct contact with the higher amount of foreign (porcine/bovine) hydrogel proteins. This prompted the use of cell culture inserts and the assessment of solid ECM hydrogels’ indirect influence on BV2 cells. Solid hydrogel effects would be comparable with solubilised in direct contact; however solid hydrogels were presumed to have indirect contact with microglial cells upon subdural delivery [55].

Solubilised hydrogels in direct contact mitigated BV2 activation, whereas solid hydrogels in indirect contact did not. The two forms may express and release different molecules, as hypothesised. Further, the direct contact between the solubilized scECM/bECM and

the cells may bring more diverse molecules in physical proximity to the cell surface receptors, compared to the solid scECM/bECM on the insert, which may result in the observed decrease of inflammation with solubilised ECM. A study by Slivka *et al.* fractionated urinary bladder ECM hydrogels to obtain structural and soluble components [56]. These different components and the original solubilised hydrogel form were added to macrophages derived from a human monocyte cell line, prior to LPS stimulation. Each of the forms of material had different impacts upon LPS stimulated macrophages, including the secretion of different pro-inflammatory and anti-inflammatory molecules but all forms showed potential to reduce inflammation [56]. The lack of positive results for solid hydrogels in this study may be due to the differences in hydrogel origin, the experimental setting, the use of hydrogel as a prevention vs treatment or the lack of direct contact. With a longer incubation period the solid hydrogel may able to mitigate inflammation, as a larger amount of the released molecules would reach the BV2 cells.

Solubilised scECM decreased one (*Nos2*/*Arg1*), whilst solubilised bECM decreased both measured parameters (*Nos2*/*Arg1* and *Tnf*). Hence, hydrogel origin had an impact on the BV2 activation mitigation by solubilised hydrogels. These tissue specific differences in bioactive molecule representation in derived hydrogels have been observed before [34], [35], [57]. However, they also depended on the selection of the tested markers and cell types [34], [35]. For instance, Meng *et al.* demonstrated an upregulation of proinflammatory factors, NO and TNFα [35] whilst Dziki *et al*. showed downregulation of iNOS, that produces NO and upregulation of anti-“Th1”inflammatory markers upon the addition of solubilised brain ECM hydrogel to naïve monocyte cell line or primary monocytes respectively [34]. Contradictory results on brain ECM hydrogel potential to mitigate inflammation may have been the consequence of the different tested concentrations. “Th1”-like activation was caused by 0.5 and 1, but not by 0.2 mg/mL brain ECM hydrogel [34], [35], as alongside anti- “Th1” inflammatory, the hydrogel may have contained more of the pro-“Th1” inflammatory molecules, such as

xenogeneic antigens. In this work, both scECM and bECM demonstrated LPS activation mitigating properties in the solubilised state.

SCAP secretion products from cell culture insert appeared to mitigate LPS-induced inflammation in BV2 cells, based on the measured gene expression. Decrease of *Nos2*/*Arg1* ratio as well as *Tnf* expression is in accordance with previous research [58], [59]. Specifically, de Berdt *et al.* demonstrated SCAP influence on *Arg1* expression and TNFα secretion by direct contact with BV2 cells [58], whilst Yu *et al.* demonstrated anti-"Th1" inflammatory factors in SCAP secretome using proteomics [59]. Hence, this work provides further evidence that SCAP has potential as a strategy for SCI treatment.

SCAP incorporated in scECM, bECM and scECM/fibrin mitigated LPS-activation of BV2, demonstrated by the decrease of *Nos2*/*Arg1* ratio. The addition of fibrin to SCAP and scECM did not influence gene expression. Together with the above-shown ability of fibrin to tune ECM hydrogel rheological properties, this may encourage the further testing of ECM-fibrin hydrogel composites.

However, hydrogel origin had an impact on LPS activation- mitigating properties of the incorporated SCAP. The influence of SCAP in scECM or scECM/fibrin was similar and unlike with SCAP alone and SCAP incorporated in bECM, these combinations did not reduce *Tnf* expression. This may have occurred because SCAP in hydrogels were subjected to the low temperature of pre-gel (4 °C) and took time to recover, which impaired the overall crosstalk between the cells. Furthermore, the increased hydrogel degradation by SCAP may result in the release of a different molecular profile from scECM and bECM, similar to the profile of solubilised hydrogels. In addition, the hydrogel may have hindered the diffusion of cell secretome or bonded some of the molecules, again affecting the crosstalk and causing the difference in BV2 gene expression between the conditions with SCAP only and SCAP in scECM. However, a longer

incubation period may allow for the recovery of SCAP secretion increasing the effect of SCAP secretome and an *in vivo*-like perfusion system may have a different influence on SCAP secretome diffusion. Still SCAP retained their LPS activation- mitigating properties upon incorporation, which makes them a potential strategy for SCI repair.

However, even though not significantly, *Nos2*/*Arg1* ratio in SCAP+scECM condition decreased by 35% further, compared to SCAP alone. This may mean that BV2 activation- mitigating properties of SCAP were altered upon incorporation, not reduced. Firstly, this prompts the re-evaluation of the above-mentioned theories in the way that limits them to scECM and the influence on Tnf expression in BV2. Therefore, SCAP-scECM, but not SCAP-bECM interplay may have diminished the influence of incorporated SCAP on *Tnf* expression, but not *Nos2*/*Arg1* ratio. Furthermore, SCAP secretome diffusion may be impaired in a particular way that affected solely *Tnf* expression in the condition with scECM. However, it may be that LPS had a particular influence on SCAP incorporated in different ECM hydrogels [60]–[63] and their overall influence on BV2 gene expression depended on the intrinsic effects of SCAP and the hydrogel. Therefore, it appears that impacts of SCAP incorporated in different ECM hydrogels mirrored and reflected the specific impacts of those individual hydrogels.

From the investigation of SCAP and/or ECM hydrogel influence on the expression of a few robust markers (*Arg1*, *Nos2*, *Tnf*) in one predictable LPS-activated cell line (BV2 cells) plenty of questions developed. Therefore, their resolution took priority over expanding the investigation of SCAP and/or ECM hydrogel influence on inflammation in the scope of SCI. Further research investigated the specific effects that pro- “Th1” inflammatory stimuli and/or hydrogels form different tissues may have on SCAP biochemical profile and of SCAP-ECM hydrogel interplay in basal and stimulated state. The research herein limited on scECM as it is homologous to the injured spinal cord and of the same neural origin as SCAP.

4.1.3 SCAP - scECM Interaction Modified, Possibly Enhanced, the Potential Effects of SCAP and scECM Combination on “Th1-like” Inflammation

Selection of metabolomics, specifically the spent medium analysis (i.e. molecular footprint) and the limitation to one biological replicate (and experimental sextuplicates) of SCAP and scECM was caused by the sensitivity of analytical instruments, the complexity of the obtainable data and the complexity of research question. One scECM biological replicate, as stated in the materials and methods section, consisted of multiple spinal cords pulled into the six 100 g samples, separately decellularized and digested and then mixed. To mitigate the influence of the singularity of SCAP origin on the intensity of activated pathways the strict statistical discrimination procedure was implemented. After T-test, Benjamini–Hochberg false discovery rate correction was performed against the total number of detected metabolites regardless of their identification or significance (p value). Investigated metabolites had the adjusted p value lower than or equal to 0.05, OPLS-DA variable importance in projection score above 1 and the difference in peak intensity (mean of the sextuplicates) higher that 1.5-fold.

As the inflammation model did not depend on any third-party immune cells, TNFα and IFNγ were selected as the representative stimuli of sterile SCI inflammation. IFNγ has been shown to have stronger influence on MSC phenotype determination, compared to enhancement by TNFα alone [60], [64]–[66]. For instance, programmed cell death ligand 1 and IDO expression was induced by IFNγ but not TNFα in BM-MSC [65]. “Th1” chemoattractant molecules (e.g. CCL5, CXCL9, CXCL10, CXCL11) and the immunosuppressive molecules (e.g. IDO1, programmed cell death ligand 1, human leukocyte antigen G) were strongly upregulated in each stimulated single BMSC after 48h incubation, with or without TNFα [64]. However, TNFα was shown to induce expression of cyclooxygenase 2, prostaglandin E2, IL-6, IL-8, MCP-1, TGFβ1, bFGF,

insulin-like growth factor 1, hepatocyte, heparin binding epidermal growth factor-like and vascular endothelial growth factor in MSC of various tissue origin [60], [61], [64], [67]–[69]. However, 5-20 ng/mL TNFα in combination with 50 ng/mL IFNγ has been shown to cause up to 23% MSC death after 48h [70]. Therefore, the experimental settings were optimised for the highest effect, leading to differences in metabolite secretion and the lowest cell death, leading to false differences in metabolite secretion, both of which positively corelated with TNFα and IFNγ concentration and incubation time.

Upon incubation with TNFα and IFNγ, SCAP tryptophan-kynurenine pathway was activated, reflecting the increased synthesis and activity of IDO, according to both metabolomic and molecular assay results. Previously MSC have been shown to increase IDO activity upon stimulation with TNFα and IFNγ and upregulate a broad pallet of over 200 other anti-"Th1" inflammatory factors, growth factors and chemoattractant molecules, such as programmed cell death ligand 1, prostaglandin E2, galectin-9, intercellular adhesion molecule 1, vascular cell adhesion molecule 1, CCL9, bone marrow stromal cell antigen 2 [66] intercellular adhesion molecule 1 [66], TGFβ1 [65], MCP-1 [70], CXCL9 [71]. These MSC have been shown to supress lymphocyte "Th1"-activation, promote "Th1"- regulatory phenotype and colony expansion of macrophages and T lymphocytes and induce immunomodulation and immune tolerance *in vitro* and *in vivo* [72], [73]. The TNFα/IFNγ- activated MSC increased graft versus host disease survival in mice compared to non-activated MSC [74], [72]. Therefore, the strong activation of tryptophan-kynurenine suggested that "Th1" inflammation mitigating properties of TNFα/IFNγ- activated SCAP should be investigated. Furthermore, kynurenine and its downstream products can be neurotoxic, start free radical reactions and increase inflammation but the only kynurenine product increased upon TNFα/IFNγ-activation of SCAP has been related to immune tolerance [75]–[79]. However, the TNFα/IFNγ- activation did not increase TGFβ secretion in SCAP as in other MSC, even though it has the "Th1"- suppressive function [65]. MCP-1 secretion was increased by

310-fold, even though the increase was not significant it confirmed SCAP activation [70]. Still, SCAP and TNFα/IFNγ- activated SCAP should be researched as a tool for inflammation mitigation in the context of SCI.

To understand SCAP-scECM interaction, investigation of scECM molecular profile was also required and thus the molecular footprint was released from a solubilised hydrogel. This form was chosen over solid as, due to the research above, we hypothesised it would release more active molecules and therefore make for a larger difference between the conditions. Another reason was a hypothesis that some of the molecules released from SCAP incorporated in solid scECM will not diffuse out of the hydrogel. The ratio between the SCAP number and the quantity of scECM proteins remained the same as in previous experiments: $2x10^5$ cells per 200 µL of 8 mg/mL scECM solubilised.

scECM has been shown to contain collagen, sulphated glycosaminoglycans, laminin, myelin, vascular endothelial growth factor and bFGF [80]. However, characterisation of constituents in the size range below 1.5 kDa, detected as metabolites, has not been done. Detected constituents represented hydrogel molecular footprint and were matched to specific pathways and functions in cells as if they were cell derived. The perspective of adding the hydrogel molecules as a potential treatment to influence those specific pathways and functions in cells was interpreted.

Hydrogel molecular footprint, for instance choline, glycerophospholipids, arachidonic, docosahexaenoic and ω-3 fatty acids may directly mitigate “Th1” inflammation. The same molecules may also activate pathways such as glycerophospholipid and arachidonic acid metabolism and fatty acid biosynthesis, that are closely intertwined with “Th1” inflammation regulation [81]–[85]. This may be one of the reasons for scECM effects on LPS-activation mitigation previously demonstrated on BV2 cells [86]. The same detected metabolites may also participate in preservation of neuronal tissue,

neural membrane integrity [87], improved proliferation, differentiation and survival of neural stem cells, [88]–[93] and re-myelination [94]. scECM has shown some of these characteristics *in vitro* and *in vivo* [4], [6], [80], [95] with induced mitogenesis, chemotaxis, differentiation and three-dimensional neurite extensions of neuroblastic cells lines [6], [80]. scECM also stimulated neurogenic marker expression in SCAP [4]. Further, scECM supported axonal ingrowth, blood vessel formation and attracted “M2” macrophages *in vivo* [95]. Therefore, scECM should be further researched as SCI repair strategy.

Even though scECM released a significant number of molecules in the previous comparison with medium, the difference in overall molecular profile was not detected between SCAP+scECM and SCAP. It is possible that in the vast amount of cell derived molecules, the molecules derived from scECM or SCAP-scECM interaction failed to be recognised as significant for the difference between the conditions, due to their dissimilarity.

To discriminate between the scECM-SCAP interaction and the overall molecular footprint of cells and ECM, scECM hydrogel baseline was removed from the SCAP+scECM condition and compared again with SCAP. scECM caused general changes in SCAP oxidative and energy metabolism, transcription and translation. This correlated with the previously shown neurodifferentiation promoting effect of scECM on SCAP and other cells [4], [6], [80]. Still, the specific differentiation pathways were not detected, probably due to the short incubation period of 24h.

However, the 24h incubation was long enough to detect the changes in the levels of amino acids that may alter oxidative stress regulation, free radical neutralisation and nitrogen metabolism. Levels of amino acids that may influence cellular integrity and choline, sphingolipids and glycerophospholipids that may influence the maintenance of

membrane integrity, also changed significantly [94], [96]–[98]. Overall, this may mean that SCAP resilience and response to general and oxidative stress were compromised. This may corelate with the lower viability/metabolic activity signal for SCAP in scECM on day 3 and 7, compared to day 0. Even though scECM molecule conformation and the number of molecules in contact with SCAP in these experiments may be different, biochemical/functional types and the origin of these molecules (xenogeneic antigens, traces of detergents [99]) remained the same. Therefore, regardless of the scECM physical form, some of the scECM constituents may compromise SCAP resilience.

SCAP likely consumed scECM metabolites that may participate in the synthesis of prostaglandins and leukotrienes, as they had a negative prefix after the scECM baseline was subtracted. However, the existing anti-" Th1" inflammatory lipids, such as prostaglandin E2, 19,20-dihydroxy-docosapentaenoic and docosahexaenoic acid were also consumed and the new anti-" Th1" inflammatory lipids were not synthesised. Other than consumed, these lipids may be degraded extracellularly, by SCAP secreted enzymes. A reason for the consumption or degradation of the anti-inflammatory lipids, ω-3 fatty acids, glycerophosphocholines, docosahexaenoic acid and their derivatives may be their use in the restoration of membrane integrity or promotion of neural differentiation [84], [87], [88], [94], [96]–[98]. However, molecules related to the pathways of membrane restoration or neural differentiation were not increased in the footprint. Another reason for prostaglandin E2, docosahexaenoic acid and the other molecules consumption by SCAP may be self-regulation of the integrity and adaptability disturbance upon encountering the hydrogel of xenogeneic origin. As mention above, this is correlated with the decrease of SCAP in scECM PrestoBlue signal after day 0.

TGFβ secretion decreased in SCAP+scECM compared to SCAP and may suggest reduced "Th1" inflammation- regulating capacity [100], [101]. These results may be connected to the altered SCAP secretion upon encapsulation in scECM in the previous

experiment (sections 2.5.2.3 and 4.1.1.2). The altered SCAP secretion was hypothesised based on the altered influence of encapsulated SCAP compared to SCAP only on marker expression in LPS-activated BV2 (further decrease of *Nos2*/*Arg1* and the absence of influence on *Tnf*). Even though the experimental settings differed, for instance, the investigation of solubilised vs solid hydrogel in basal vs LPS-stimulated condition, some of the hydrogel proteins retained the same effects. These effects may be directed at SCAP and may reduce the secretion of anti- "Th1" inflammatory factors such as TGFβ. The retained effects may also be directed at the binding / hydrolysis / "neutralisation" of the already secreted factors. Overall, neither metabolomic nor molecular assays data suggested that SCAP activation altered or that "Th1"-immunoregulatory capacity increased upon the addition of hydrogel in basal state. To better understand scECM influence on SCAP activation and "Th1" inflammation-regulating capacity, SCAP-scECM interaction was assessed in stimulated state.

In the presence of scECM, SCAP responded to pro- "Th1" inflammatory stimulus by activation. As a consequence, SCAP "Th1"- immunoregulatory capacity, such as the secretion of anti-"Th1" inflammatory molecules, chemoattractants, regulation of macrophage and T lymphocyte phenotype and immunosuppression, may be increased [72], [73]. This was concluded based on the activation of the same pathways and secretion of the same molecules, with similar intensity as in the first comparison (SCAP+stimulus vs SCAP), when the hydrogel was not present. For instance, upon the addition of stimulus to SCAP+scECM, tryptophan-kynurenine pathway was activated and IDO activity increased, according to both metabolomic and molecular assay results. Addition of stimuli did not have an influence on the TGFβ secretion, whether or not scECM was present. Moreover, in SCAP+scECM+stimulus, MCP-1 activity significantly increased compared the other tested conditions. This suggested higher SCAP activation as a response to stimuli in the presence of xenogeneic scECM [70]. Overall SCAP response to stimuli and SCAP activation seemed to remain largely unchanged in the

presence of scECM. However, to better understand scECM influence on the “Th1” inflammation- mitigating capacity of the stimulated and activated SCAP, SCAP+scECM+stimulus was compared to SCAP+stimulus.

The overall changes in molecular profile between SCAP+scECM+stimulus and SCAP+stimulus combine the SCAP-scECM interaction- derived and scECM- derived molecules. Upon the addition of scECM to stimulated SCAP, several anti-“Th1” inflammatory molecules, such as adenosine, choline and eicosatrienoic acid increased [82], [102]. Arachidonic acid, that may have direct pro-inflammatory effects or be utilised for immunoregulatory lipid synthesis [81], was also increased. Furthermore, MCP-1 chemoattractant increased. However, secretion of TGFβ that “Th1” inflammation-regulating properties [100], [101] decreased again with the addition of scECM. As some of the “Th1” inflammation-mitigating molecules increased and some decreased with the addition of scECM to stimulated SCAP, it is likely that the SCAP+scECM “Th1” inflammation-mitigating capacity changed compared to SCAP only.

However, the level of amino acids that participate in oxidative stress regulation was also increased, which may mean that SCAP+scECM as a treatment may contribute either to the oxidative stress regulation or to the oxidative damage in pro-“Th1” inflammatory microenvironment. During SCAP-scECM interaction in the basal state, after scECM baseline was subtracted, similar molecules were altered, whilst other detected molecules pointed out the possible changes in SCAP cellular and membrane integrity. This suggested that the detected changes in oxidative stress regulation were probably SCAP-derived and are a consequence of scECM addition. This prompted the closer examination of SCAP-scECM interaction in stimulated state.

To discriminate between the vast amount of hydrogel molecules and the influence they made on SCAP, scECM baseline was deducted from the SCAP+scECM+stimuli. The

influence of scECM on SCAP overall metabolic response (oxidative/energy metabolism, transcription/translation) was similar to that in basal state. Altered levels of molecules that regulate nitrogen metabolism, cellular and membrane integrity confirmed that the above changes in oxidative stress regulation also came from SCAP. Therefore, due to the interaction with scECM, SCAP adaptability may be compromised.

Similarly to basal state, scECM affected sphingolipid, glycerophospholipid, phosphatidylethanolamine, fatty acid, fatty acid amide, arachidonic acid metabolism and consequently, SCAP response to inflammation [82], [85], [103], [104]. However, stimulated SCAP consumed small anti-inflammatory molecules, such as nicotinamide [105] and choline [98], as well as the anti-inflammatory lipids of low (arachidonic acid), medium (19,20-dihydroxydocosapentaenoic acid) [85] and high complexity (5-hydroxyeicosatetraenoic acid (5-HETE) di-endoperoxide, 9,10-dihydroxystearicic acid) from scECM. Therefore, the alternative utilisation of these molecules to restore the membrane integrity or promote neural differentiation [84], [87], [88], [94], [96]–[98] as hypothesised in basal state, seemed less likely compared to the theory that stimulated SCAP used these scECM-derived lipids for self-regulation [82]–[84].

During the 24-hour SCAP-scECM interaction in stimulated, as in basal condition, SCAP consumed scECM anti-inflammatory lipids and possibly suffered changes in cellular integrity and response to stress. A longer follow up and the additional experiments may be needed to confirm the exact outcome of the lipid consumption and level of plausible SCAP damage.

Possible changes in SCAP resilience in combination with scECM correlated with the previous experiments. For instance, SCAP viability/metabolic activity decreased in scECM after day 0, whilst SCAP influence on LPS-activated BV2 marker expression changed upon incorporation in scECM. Even though the experimental setups were

different (SCAP are in 3D culture in contact with solid hydrogel instead of 2D culture and solubilised hydrogel) and SCAP adaptability may be changed due to other factors, such as SCAP suspension in pre-gel at 4 °C, LPS-stimulation and nutrient diffusion through gel network, the shared damage to SCAP may come from potential toxic or antigenic scECM constituents. Except for the detergent residues that were present in negligible amounts [99], the available literature has not investigated that problem. However, chenodeoxycholic acid, discovered in scECM molecular profile may disrupt SCAP membranes and induce oxidative stress [106].

TGFβ decrease was detected with the addition of scECM to SCAP in basal and stimulated state. Even though TGFβ has been shown to play an important role in “Th1”-regulative phenotype induction in macrophages and T lymphocytes [100], [101], plenty of other molecules that were not measured, such as IL-10 and human leukocyte antigen G, have also been proven important in immunoregulation [107], [108]. Furthermore, the addition of scECM did not change the engagement of the activation pathways and metabolites, such as IDO and kynurenine and increased the expression of activation markers, such as MCP-1. It is possible that the same hydrogel antigens that compromise SCAP integrity increase their activation. Therefore, SCAP in the presence of scECM and inflammatory stimuli may still have the increased secretion of “Th1” immunoregulatory factors and the capacity to supress “Th1”- activation, promote “Th1”- regulatory phenotype and colony expansion of macrophages and T lymphocytes and induce immunomodulation and immune tolerance *in vitro* and *in vivo* compared to SCAP only [66], [72]–[74].

Similarly, it was hypothesised in the previous experiment (sections 2.5.2.3 and 4.1.1.2) that the influence of SCAP incorporated in scECM and LPS-activated on gene expression in LPS-activated BV2 was altered, not reduced and depended on both SCAP and scECM. Specifically, *Tnf* expression in LPS-activated BV2 significantly decreased

upon the addition of SCAP only, but not SCAP within scECM. *Nos2*/*Arg1* expression reduced 35% further upon the addition of SCAP and scECM, compared to SCAP only. Molecules released from solid scECM did not influence BV2 activation. Later, metabolic findings demonstrated that scECM plausibly did not hamper but increased SCAP activation by another "Th1" stimulus. Therefore, the molecules deriving form SCAP-scECM interaction may be the reason for the differences in BV2 activation. Even though during SCAP-scECM interaction the availability of anti-inflammatory scECM lipids was decreased, TGFβ secretion reduced and SCAP adaptability in scECM potentially compromised, the addition of scECM to SCAP+stimulus increased the overall levels of detected anti-inflammatory molecules. These experiments suggested that upon the addition of scECM, SCAP potential to regulate "Th1" inflammation is not only altered but possibly increased. The anti- "Th1" inflammatory molecules in scECM profile support this theory.

Therefore, the information obtained for the overall SCAP+scECM+stimuli molecular profile confirms the hypothesis that SCAP incorporated in scECM had different but not hampered influence on LPS-activated BV2 gene expression. Arguably, the difference in "Th1" inflammation mitigation outcome may depend on the scECM physical form (solubilised vs solid). However, it has been discussed in the sections above that ECM hydrogels are presumed to take both solid and solubilised form upon *in vivo* injection. Furthermore, due to the spontaneous and SCAP-caused biodegradation of scECM, showed in the molecular profile of SCAP-scECM interaction, the solid hydrogel will slowly become solubilised-like. Therefore, the further research can demonstrate whether SCAP+scECM potential to mitigate Th1 inflammation increases with time.

Overall, SCAP and scECM may mitigate "Th1" inflammation separately and combined. Therefore, SCAP and ECM may be further researched as a strategy to stimulate SCI repair.

4.2 Main Achievements of the Thesis

This work evaluated SCAP and/or ECM hydrogel, scECM and bECM, as a potential strategy to mitigate inflammation in the scope of SCI.

The first objective was to determine whether scECM/bECM mechanical properties may be suitable for the delivery of embedded SCAP. Rheological characterisation showed scECM and bECM injectability, ability to incorporate cells, a gelation rate that could allow for hydrogel manipulation, but minimise dissolution in body fluids [19], stiffness that could protect the cells form share stress during injection [10] and storage modulus in the range reported for spinal cord tissue [12], [15]. As described previously, differences in gelation time depended on hydrogel origin and final storage modulus depended on hydrogel origin and the concentration [2], [4].

The second objective was to attempt optimisation of ECM hydrogel mechanical properties. The addition of 25% fibrin without crosslinking significantly increased storage modulus and reduced gelation time, whilst the rheological behaviour remained predetermined by scECM. Fibrin is FDA approved, of adjustable strength and applicable for SCAP delivery in the scope of SCI [109], [110], [2]. Low fibrin interaction with ECM hydrogel ligands should be proven in the future work.

Previously, only scECM and bECM influence on SCAP differentiation [4] and scECM influence on regeneration in SCI have been considered [95]. To date, anti-inflammatory properties of scECM and bECM, with and without SCAP, have not been investigated. For the first time ECM hydrogel anti-inflammatory action was tested on inflamed microglia cells (BV2), likely more relevant in the context of SCI [29], [37], than circulating monocytes or THP-1 cells commonly used with ECM hydrogels [34], [35]. Previous *in vitro* studies examined only solubilised hydrogels [1], [34]. We hypothesised that solid

and solubilised form may expose and release different active molecules [56], [111] thus having a different influence on inflammation [56]. Within the 24h experiment scECM/bECM in solid form and indirect contact had no influence on inflammation in microglia, which suggested that a longer time period may be needed for the released molecules [1] to reach BV2 cells. Solubilised scECM and bECM in direct contact mitigated LPS-activation of BV2 cells. The expression of tested markers, as shown previously [34], [35], depended on the hydrogel origin.

SCAP mitigation of BV2 LPS-activation cells was confirmed, even though a different setting (direct contact for 48h vs 24h of indirect exposure) was used [58]. SCAP metabolic activity preservation was confirmed in 8mg/mL scECM and bECM [4] and demonstrated in scECM/fibrin hydrogel.

For the first time MSC and ECM hydrogel have been investigated together *in vitro* in the context of immunoregulation. BV2 LPS activation mitigating properties of SCAP and SCAP incorporated in scECM, scECM/fibrin and bECM differed and seemed to depend on the individual properties of SCAP and ECM hydrogels. The properties depend on the hydrogel origin and did not change with the addition of fibrin.

To further explore the differences between the “Th1” stimuli and/or scECM effect on SCAP metabolic profile and SCAP-scECM interplay in basal and stimulated state spent medium metabolomic analysis was used.

Similar to other MSC [65], [66], SCAP responded to “Th1” stimuli by enhancing the main activation pathways (e.g. tryptophan-kynurenine pathway) and presumably the “Th1”-regulatory capacity. This additional SCAP characterisation was an additional proof of their suitability as SCI repair strategy.

scECM hydrogel molecular footprint was described for the first time. If applied as “treatment”, scECM molecular constituents, such as choline, arachidonic, docosahexaenoic and other fatty acids, may have direct anti- “Th1” inflammatory effect or promote immunoregulatory and neuro-reparative pathways.

Even though MSC and ECM hydrogels have been considered previously in regenerative medicine strategies, including SCI repair [95], for the first time this work investigates the interplay between the MSC and ECM hydrogels in a context other than differentiation. scECM affected SCAP metabolism, increased susceptibility to stress and influenced auto-immunoregulation. SCAP consumed anti-inflammatory lipids from hydrogel. Still, even when combined with scECM, SCAP responded to “Th1” stimulus by activation and presumably the increase of “Th1”-regulatory capacity. The sum of secreted metabolites (that included, for instance, adenosine and arachidonic acid) suggests higher immunoregulatory capacity of SCAP and scECM than SCAP upon the stimulation.

Overall, this work showed that scECM, bECM and scECM/fibrin are suitable for SCAP delivery in the context of SCI due to their mechanical properties, intrinsic anti- “Th1” inflammatory properties and preservation of SCAP viability and anti- “Th1” inflammatory activity. The potential stress and self-regulatory response scECM elicited in SCAP and SCAP consumption of scECM molecules altered but did not reduce SCAP and scECM anti- “Th1” inflammatory potential.

4.3 Thesis Limitations and Future Work

scECM/fibrin and bECM mechanical properties, as well as the strategy of mixing ECM hydrogels with fibrin were proven adequate for SCAP delivery. However, for the future utilisation of ECM hydrogel/fibrin combinations, rheological experiments should be done to determine the concentration of fibrin in the ECM hydrogel and concentrations and ratio of fibrin constituents, fibrinogen and thrombin, for each ECM hydrogel and according to the *in vivo* model. ECM hydrogels injected to spinal cord lesion were mostly degraded after four weeks [95], therefore the influence of the addition of fibrin on the bioavailability [8] of ECM hydrogels should be investigated.

The hypothesis of the interpenetrating but not interactive network in scECM/fibrin was based on previous published work with collagen [112]. Future studies could confirm the type of the network formed between ECM hydrogel and fibrin and explore its effect on the ECM hydrogel ligand presentation.

For its relevance in central nervous system repair [37], a microglial cell line was chosen to test the anti-inflammatory properties of scECM, bECM and SCAP. Due to the time limitations, anti-inflammatory properties of ECM hydrogels and SCAP have not been confirmed on different cell types, for instance primary monocytes or microglia. For the obtained data to be better correlated to the literature [34], immunomodulatory properties of scECM and bECM on unstimulated monocytes and macrophages should also be investigated. Even though solubilised hydrogels mitigated inflammation in microglia and scECM molecular profile was linked to immunoregulation, solid hydrogels did not demonstrate anti-inflammatory properties under the tested conditions. To better detect the difference in anti-inflammatory properties between the solubilised and solid forms, an incubation period longer than 24h should be evaluated, as it may allow molecules to diffuse out of the solid hydrogel and reach microglia.

Based on the expression of tested markers, anti-inflammatory activity of SCAP embedded in bECM seemed to reflect the anti-inflammatory activity of SCAP and bECM, whilst the anti-inflammatory activity of SCAP+scECM was more reflective of the scECM properties. To further explain the outcome of combining SCAP with ECM hydrogel in the context of immunoregulation, bECM molecular footprint and SCAP-bECM interaction will be explored in different inflammatory microenvironments and compared to the results obtained for scECM.

Molecular footprint of scECM and SCAP-scECM interaction was obtained only for solubilised hydrogel due to the limited quantity of scECM. Because of the desire to deliver SCAP, scECM in solid form and SCAP embedded in scECM should also be investigated, as solid scECM may expose different ligands to SCAP and have a different molecular profile. Metabolomic analyses should be repeated with SCAP obtained from other donors and other ECM hydrogels. The immunoregulatory capacity of SCAP primed with “Th1” inflammatory stimulus should be tested on immune cells and compared to unstimulated SCAP. SCAP cellular integrity and susceptibility to oxidative stress in response to scECM should be thoroughly examined. The fate of the scECM-derived lipids consumed by SCAP would be explored. It may have been detected in these experiments if the incubation periods were longer than 24h. Other omics analysis of SCAP activated with inflammatory stimuli and ECM hydrogels would complement this work.

This thesis explored and demonstrated SCAP and scECM/bECM hydrogel separate and combined immunoregulatory properties and potential to be delivered to SCI. Further research on SCAP and ECM hydrogel immunoregulation and neuro-reparation in different microenvironments and *ex vivo* is warranted.

4.4 Conclusion

Delivery of SCAP within scECM or bECM hydrogel is a suitable strategy to mitigate inflammation in the scope of SCI and should be explored further. Specifically, scECM and bECM mechanical properties were suitable for SCAP incorporation, experimental manipulation and maintaining SCAP viability and were unlikely to cause stiffness-related adverse effect upon injection. scECM, bECM and SCAP demonstrated intrinsic potentials to mitigate “Th1” inflammation in two different experimental setups: i) by reducing expression of LPS-activated microglia cells’ activation markers and ii) activating metabolic pathways related to “Th1” immunoregulation and releasing anti-“Th1” inflammatory metabolites. Even though scECM increased SCAP susceptibility to stress and SCAP consumed scECM-derived molecules, SCAP activation by “Th1” stimuli remained unchanged in the presence of scECM hydrogel. Upon SCAP combination with ECM hydrogel, their intrinsic potentials to mitigate “Th1” inflammation were preserved in both experimental setups. “Th1” inflammation mitigation may be altered but not reduced depending on the origin or physical form of ECM hydrogels.

Depending on the technical aspects and the objectives of the delivery strategy, different physical forms of ECM hydrogels, solid and solubilised, may have potential for SCAP delivery and inflammation mitigation in the scope of SCI. The simple addition of fibrin may modify ECM hydrogel mechanical properties, without influencing SCAP viability or the overall anti - “Th1” inflammatory activity.

4.5 References

[1] L. T. Saldin, M. C. Cramer, S. S. Velankar, L. J. White, and S. F. Badylak, “Extracellular matrix hydrogels from decellularized tissues: Structure and function,” *Acta Biomater.*, vol. 49, pp. 1–15, 2017.

[2] A. R. Massensini *et al.*, “Concentration-dependent rheological properties of ECM hydrogel for intracerebral delivery to a stroke cavity,” *Acta Biomater.*, vol. 27, pp. 116–130, 2015.

[3] Y. C. Jao, A. H. Chen, D. Lewandowski, and W. E. Irwin, “Engineering analysis of soy dough rheology in extrusion,” *J. Food Process Eng.*, vol. 2, no. 1, pp. 97–112, Jan. 1978.

[4] A. Viswanath *et al.*, “Extracellular Matrix-Derived Hydrogels for Dental Stem Cell Delivery,” *J. Biomed. Mater. Res. Part A*, pp. 1–10, 2016.

[5] D. O. Freytes, J. Martin, S. S. Velankar, A. S. Lee, and S. F. Badylak, “Preparation and rheological characterization of a gel form of the porcine urinary bladder matrix,” *Biomaterials*, vol. 29, no. 11, pp. 1630–1637, 2008.

[6] C. J. Medberry *et al.*, “Hydrogels derived from central nervous system extracellular matrix,” *Biomaterials*, vol. 34, no. 4, pp. 1033–1040, 2013.

[7] American Society for Testing and Materials, “Standard Guide for Characterization of Hydrogels used in Regenerative Medicine,” *Annu. B. ASTM Stand.*, vol. i, no. C, pp. 1–10, 2011.

[8] C. Williams *et al.*, “Cardiac extracellular matrix-fibrin hybrid scaffolds with tunable properties for cardiovascular tissue engineering,” *Acta Biomater.*, vol. 14, pp. 84–95, 2015.

[9] J. Jokinen *et al.*, “Integrin-mediated Cell Adhesion to Type I Collagen Fibrils*,” 2004.

[10] M. H. Amer, F. R. A. J. Rose, K. M. Shakesheff, and L. J. White, “A biomaterials approach to influence stem cell fate in injectable cell-based therapies,” *Stem Cell Res. Ther.*, vol. 9, no. 1, pp. 1–15, 2018.

[11] D. Prodanov and J. Delbeke, “Mechanical and biological interactions of implants with the brain and their impact on implant design,” *Frontiers in Neuroscience*, vol. 10, no. FEB. Frontiers Media S.A., 09-Feb-2016.

[12] K. Franze, “The mechanical control of nervous system development,” *Development*, 2013.

[13] M. Iwashita *et al.*, “Brain-stiffness-mimicking tilapia collagen gel promotes the induction of dorsal cortical neurons from human pluripotent stem cells,” *Sci. Rep.*, vol. 9, no. 1, Dec. 2019.

[14] A. M. Stiller *et al.*, “A meta-analysis of intracortical device stiffness and its correlation with histological outcomes,” *Micromachines*, vol. 9, no. 9, 2018.

[15] R. D. Bartlett, D. Choi, and J. B. Phillips, “Biomechanical properties of the spinal cord: Implications for tissue engineering and clinical translation,” *Regen. Med.*, vol. 11, no. 7, pp. 659–673, 2016.

[16] J. Lantoine *et al.*, “Matrix stiffness modulates formation and activity of neuronal networks of controlled architectures,” *Biomaterials*, vol. 89, pp. 14–24, May 2016.

[17] J. Liu *et al.*, “Acellular spinal cord scaffold seeded with mesenchymal stem cells promotes long-distance axon regeneration and functional recovery in spinal cord injured rats,” *J. Neurol. Sci.*, vol. 325, no. 1–2, pp. 127–136, 2013.

[18] A. Faccendini *et al.*, “Nanofiber scaffolds as drug delivery systems to bridge spinal cord injury,” *Pharmaceuticals*, vol. 10, no. 3. 2017.

[19] D. Gupta, C. H. Tator, and M. S. Shoichet, “Fast-gelling injectable blend of hyaluronan and methylcellulose for intrathecal, localized delivery to the injured spinal cord,” *Biomaterials*, vol. 27, no. 11, pp. 2370–2379, 2006.

[20] T. Brinker, E. Stopa, J. Morrison, and P. Klinge, “A new look at cerebrospinal fluid circulation,” *Fluids Barriers CNS*, vol. 11, no. 1, pp. 1–16, 2014.

[21] M. C. Jimenez Hamann, E. C. Tsai, C. H. Tator, and M. S. Shoichet, “Novel intrathecal delivery system for treatment of spinal cord injury,” *Exp. Neurol.*, vol. 182, no. 2, pp. 300–309, 2003.

[22] B. N. Brown and S. F. Badylak, *Extracellular matrix as an inductive scaffold for functional tissue reconstruction*, vol. 163, no. 4. Elsevier Inc., 2014.

[23] V. Agrawal, S. Tottey, S. A. Johnson, J. M. Freund, B. F. Siu, and S. F. Badylak, “Recruitment of Progenitor Cells by an Extracellular Matrix Cryptic Peptide in a Mouse Model of Digit Amputation,” *Tissue Eng. Part A*, vol. 17, no. 19–20, pp. 2435–2443, 2011.

[24] V. K. Lai, S. P. Lake, C. R. Frey, R. T. Tranquillo, and V. H. Barocas, “Mechanical Behavior of Collagen-Fibrin Co-Gels Reflects Transition From Series to Parallel Interactions With Increasing Collagen Content,” 2012.

[25] V. Reyhani, P. Seddigh, B. Guss, R. Gustafsson, L. Rask, and K. Rubin, “Fibrin binds to collagen and provides a bridge for αVβ3 integrin-dependent contraction of collagen gels,” *Biochem. J.*, vol. 462, no. 1, pp. 113–123, 2014.

[26] P. M. Crapo, S. Tottey, P. F. Slivka, and S. F. Badylak, “Effects of biologic scaffolds on human stem cells and implications for CNS tissue engineering.,” *Tissue Eng Part A*, vol. 20, no. 1–2, 2013.

[27] F. Paduano, M. Marrelli, L. J. White, K. M. Shakesheff, and M. Tatullo, “Odontogenic differentiation of human dental pulp stem cells on hydrogel scaffolds derived from decellularized bone extracellular matrix and collagen type I,” *PLoS One*, vol. 11, no. 2, 2016.

[28] T. L. Riss *et al.*, “Cell Viability Assays,” *Assay Guid. Man.*, no. Md, pp. 1–25, 2004.

[29] J. C. Gensel and B. Zhang, “Macrophage activation and its role in repair and pathology after spinal cord injury,” *Brain Res.*, vol. 1619, pp. 1–11, 2015.

[30] J. C. Fleming *et al.*, “The cellular inflammatory response in human spinal cords after injury,” *Brain*, vol. 129, no. 12, pp. 3249–3269, 2006.

[31] J. E. Burda and M. V. Sofroniew, “Seducing astrocytes to the dark side,” *Cell Res.*, vol. 27, no. 6, pp. 726–727, 2017.

[32] S. A. Liddelow *et al.*, “Neurotoxic reactive astrocytes are induced by activated microglia,” *Nature*, vol. 541, no. 7638, pp. 481–487, 2017.

[33] M. A. Cassatella, M. Locati, and A. Mantovani, “Never Underestimate the Power of a Neutrophil,” *Immunity*, vol. 31, no. 5, pp. 698–700, 2009.

[34] J. L. Dziki, D. S. Wang, C. Pineda, B. M. Sicari, T. Rausch, and S. F. Badylak, “Solubilized extracellular matrix bioscaffolds derived from diverse source tissues differentially influence macrophage phenotype,” pp. 12–15, 2016.

[35] F. W. Meng, P. F. Slivka, C. L. Dearth, and S. F. Badylak, “Solubilized extracellular matrix from brain and urinary bladder elicits distinct functional and phenotypic responses in macrophages,” *Biomaterials*, vol. 46, pp. 131–140, 2015.

[36] K. A. Kigerl, J. C. Gensel, D. P. Ankeny, J. K. Alexander, D. J. Donnelly, and P. G. Popovich, “Identification of two distinct macrophage subsets with divergent effects causing either neurotoxicity or regeneration in the injured mouse spinal cord.,” *J. Neurosci.*, vol. 29, no. 43, pp. 13435–44, 2009.

[37] A. F. Lloyd *et al.*, “Central nervous system regeneration is driven by microglia necroptosis and repopulation,” *Nat. Neurosci.*, 2019.

[38] X. Jin and T. Yamashita, “Microglia in central nervous system repair after injury,” *Journal of Biochemistry*, vol. 159, no. 5. 2016.

[39] V. Chhor *et al.*, “Characterization of phenotype markers and neuronotoxic potential of polarised primary microglia In vitro,” *Brain. Behav. Immun.*, vol. 32, pp. 70–85, 2013.

[40] M. Karamita *et al.*, “Therapeutic inhibition of soluble brain TNF promotes remyelination by increasing myelin phagocytosis by microglia,” *JCI Insight*, vol. 2, no. 8, pp. 1–19, 2017.

[41] Z. Li, F. Liu, X. He, X. Yang, F. Shan, and J. Feng, “Exosomes derived from mesenchymal stem cells attenuate inflammation and demyelination of the central nervous system in EAE rats by regulating the polarization of microglia,” *Int. Immunopharmacol.*, vol. 67, no. December 2018, pp. 268–280, 2019.

[42] J. D. Cherry, J. A. Olschowka, and M. O’Banion, “Neuroinflammation and M2 microglia: the good, the bad, and the inflamed,” *J. Neuroinflammation*, vol. 11, no. 1, p. 98, 2014.

[43] A. Henn, S. Lund, M. Hedtjärn, A. Schrattenholz, P. Pörzgen, and M. Leist, “The suitability of BV2 cells as alternative model system for primary microglia cultures or for animal experiments examining brain inflammation.,” *ALTEX Altern. zu Tierexperimenten*, vol. 26, no. 2, pp. 83–94, 2009.

[44] R. Timmerman, S. M. Burm, and J. J. Bajramovic, “An Overview of in vitro Methods to Study Microglia,” *Front. Cell. Neurosci.*, vol. 12, no. August, pp. 1–12, 2018.

[45] E. Blasi, R. Barluzzi, V. Bocchini, R. Mazzolla, and F. Bistoni, “Immortalization of murine microglial cells by a v-raf / v-myc carrying retrovirus,” *J. Neuroimmunol.*, vol. 27, no. 2–3, pp. 229–237, 1990.

[46] D. Giulian and T. J. Baker, “Characterization of ameboid microglia isolated from developing mammalian brain,” *J. Neurosci.*, vol. 6, no. 8, pp. 2163–2178, 1986.

[47] W. Chanput, J. J. Mes, and H. J. Wichers, “THP-1 cell line: An in vitro cell model for immune modulation approach,” *Int. Immunopharmacol.*, vol. 23, no. 1, pp. 37–45, 2014.

[48] Y. He, X. Yao, N. Taylor, Y. Bai, T. Lovenberg, and A. Bhattacharya, “RNA sequencing analysis reveals quiescent microglia isolation methods from

postnatal mouse brains and limitations of BV2 cells," *J. Neuroinflammation*, vol. 15, no. 1, pp. 1–13, 2018.

[49] M. Schwartz and R. Shechter, "Protective autoimmunity functions by intracranial immunosurveillance to support the mind: The missing link between health and disease," *Molecular Psychiatry*, vol. 15, no. 4. pp. 342–354, 2010.

[50] U. P. Okorji and O. A. Olajide, "A semi-synthetic derivative of artemisinin, artesunate inhibits prostaglandin E2 production in LPS/IFNgamma-activated BV2 microglia," *Bioorganic Med. Chem.*, vol. 22, no. 17, pp. 4726–4734, 2014.

[51] H.-S. Kim, S.-Y. Whang, M.-S. Woo, J.-S. Park, W.-K. Kim, and I.-O. Han, "Sodium butyrate suppresses interferon-gamma-, but not lipopolysaccharide-mediated induction of nitric oxide and tumor necrosis factor-alpha in microglia.," *J. Neuroimmunol.*, vol. 151, no. 1–2, pp. 85–93, 2004.

[52] A. R. Harvey, S. J. Lovett, B. T. Majda, J. H. Yoon, L. P. G. Wheeler, and S. I. Hodgetts, "Neurotrophic factors for spinal cord repair : Which , where , how and when to apply , and for what period of time ?," *Brain Res.*, vol. 1619, pp. 36–71, 2015.

[53] Y. Qin *et al.*, "Lipopolysaccharide Preconditioning Induces an Anti-inflammatory Phenotype in BV2 Microglia," *Cell. Mol. Neurobiol.*, vol. 36, no. 8, pp. 1269–1277, 2016.

[54] M. Starkhammar *et al.*, "Toll-Like Receptor Ligands LPS and Poly (I:C) Exacerbate Airway Hyperresponsiveness in a Model of Airway Allergy in Mice, Independently of Inflammation," *PLoS One*, vol. 9, no. 8, p. e104114, Aug. 2014.

[55] M. D. Baumann *et al.*, "An injectable drug delivery platform for sustained combination therapy," *J. Control. Release*, vol. 138, no. 3, pp. 205–213, 2009.

[56] P. F. Slivka *et al.*, "Fractionation of an ECM hydrogel into structural and soluble components reveals distinctive roles in regulating macrophage behavior.," *Biomater. Sci.*, vol. 2, no. 10, pp. 1521–34, 2014.

[57] R. Liang *et al.*, “Positive effects of an extracellular matrix hydrogel on rat anterior cruciate ligament fibroblast proliferation and collagen mRNA expression,” *J. Orthop. Transl.*, vol. 3, no. 3, pp. 114–122, 2015.

[58] P. de Berdt *et al.*, “Stem cells from human apical papilla decrease neuro-inflammation and stimulate oligodendrocyte progenitor differentiation via activin-A secretion,” *Cellular and Molecular Life Sciences*, pp. 1–14, 2018.

[59] S. Yu, Y. Zhao, Y. Ma, and L. Ge, “Profiling the Secretome of Human Stem Cells from Dental Apical Papilla,” *Stem Cells Dev.*, vol. 25, no. 6, pp. 499–508, 2016.

[60] L. C. J. van den Berk *et al.*, “Mesenchymal stem cells respond to TNF but do not produce TNF,” *J. Leukoc. Biol.*, vol. 87, no. 2, pp. 283–289, 2010.

[61] P. R. Crisostomo, Y. Wang, T. A. Markel, M. Wang, T. Lahm, and D. R. Meldrum, “Human mesenchymal stem cells stimulated by TNF- , LPS, or hypoxia produce growth factors by an NF B- but not JNK-dependent mechanism,” *AJP Cell Physiol.*, vol. 294, no. 3, pp. C675–C682, 2008.

[62] Y. Sen Hou *et al.*, “Lipopolysaccharide pretreatment inhibits LPS-induced human umbilical cord mesenchymal stem cell apoptosis via upregulating the expression of cellular FLICE-inhibitory protein,” *Mol. Med. Rep.*, vol. 12, no. 2, pp. 2521–2528, 2015.

[63] X. He, H. Wang, T. Jin, Y. Xu, L. Mei, and J. Yang, “TLR4 activation promotes bone marrow MSC proliferation and osteogenic differentiation via wnt3a and wnt5a signaling,” *PLoS One*, vol. 11, no. 3, pp. 1–20, 2016.

[64] P. Jin *et al.*, “Interferon-γ and Tumor Necrosis Factor-α Polarize Bone Marrow Stromal Cells Uniformly to a Th1 Phenotype,” *Sci. Rep.*, vol. 6, no. May, pp. 1–11, 2016.

[65] K. English, F. P. Barry, C. P. Field-Corbett, and B. P. Mahon, “IFN-γ and TNF-α differentially regulate immunomodulation by murine mesenchymal stem cells,” *Immunol. Lett.*, vol. 110, no. 2, pp. 91–100, 2007.

[66] Q. Guan, P. Ezzati, V. Spicer, O. Krokhin, D. Wall, and J. A. Wilkins, “Interferon γ induced compositional changes in human bone marrow derived mesenchymal stem/stromal cells,” *Clin. Proteomics*, vol. 14, no. 26, 2017.

[67] H. Chen *et al.*, “Pre-activation of mesenchymal stem cells with TNF-α, IL-1β 2 and nitric oxide enhances its paracrine effects on radiation-induced intestinal injury,” *Sci. Rep.*, vol. 5, pp. 1–14, 2015.

[68] Y. W. Kwon *et al.*, “Tumor necrosis factor-α-activated mesenchymal stem cells promote endothelial progenitor cell homing and angiogenesis,” *Biochim. Biophys. Acta - Mol. Basis Dis.*, vol. 1832, no. 12, pp. 2136–2144, 2013.

[69] W. Broekman *et al.*, “TNF-α and IL-1β-activated human mesenchymal stromal cells increase airway epithelial wound healing in vitro via activation of the epidermal growth factor receptor,” *Respir. Res.*, vol. 17, no. 1, p. 3, 2016.

[70] X. Li, W. Du, F. X. Ma, X. Feng, F. Bayard, and Z. C. Han, “High concentrations of TNF-α induce cell death during interactions between human umbilical cord mesenchymal stem cells and peripheral blood mononuclear cells,” *PLoS One*, vol. 10, no. 5, pp. 1–13, 2015.

[71] K. N. Sivanathan, D. Rojas-Canales, S. T. Grey, S. Gronthos, and P. T. Coates, “Transcriptome Profiling of IL-17A Preactivated Mesenchymal Stem Cells: A Comparative Study to Unmodified and IFN- *γ* Modified Mesenchymal Stem Cells,” *Stem Cells Int.*, vol. 2017, pp. 1–16, 2017.

[72] D. S. Kim *et al.*, “Enhanced Immunosuppressive Properties of Human Mesenchymal Stem Cells Primed by Interferon-γ,” *EBioMedicine*, vol. 28, pp. 261–273, 2018.

[73] M. François, R. Romieu-Mourez, M. Li, and J. Galipeau, “Human MSC suppression correlates with cytokine induction of indoleamine 2,3-dioxygenase and bystander M2 macrophage differentiation,” *Mol. Ther.*, vol. 20, no. 1, pp. 187–195, 2012.

[74] D. Polchert *et al.*, “Prevention of Graft Versus Host Disease,” vol. 38, no. 6, pp. 1745–1755, 2011.

[75] S. S. Zaher, C. Germain, H. Fu, D. F. P. Larkin, and A. J. T. George, “3-hydroxykynurenine suppresses CD4+ T-cell proliferation, induces T-regulatory-cell development, and prolongs corneal allograft survival,” *Investig. Ophthalmol. Vis. Sci.*, vol. 52, no. 5, pp. 2640–2648, 2011.

[76] S. Trabanelli, D. Ocadlikova, C. Evangelisti, S. Parisi, and A. Curti, “Induction of regulatory T Cells by dendritic cells through indoleamine 2,3-dioxygenase: a potent mechanism of acquired peripheral tolerance.,” *Curr. Med. Chem.*, vol. 18, no. 15, pp. 2234–2239, 2011.

[77] M. Francois, R. Romieu, M. Li, and J. Galipeau, “IDO Expression In Human Mesenchymal Stromal Cells Mediates T Cell Suppression and Leads to Monocyte Differentiation Into IL-10 Secreting Immunosuppressive CD206⁺ M2 Macrophages,” *Blood*, vol. 116, no. 21, pp. 2784 LP – 2784, Nov. 2010.

[78] Q. Wang, D. Liu, P. Song, and M.-H. Zou, “Deregulated tryptophan-kynurenine pathway is linked to inflammation, oxidative stress, and immune activation pathway in cardiovascular diseases,” *Front Biosci*, vol. 20, pp. 1116–1143, 2016.

[79] Y. Chen and G. J. Guillemin, “Kynurenine Pathway Metabolites in Humans : Disease and Healthy States,” vol. 61, no. 02, 2010.

[80] P. M. Crapo *et al.*, “Biologic scaffolds composed of central nervous system extracellular matrix,” *Biomaterials*, vol. 33, no. 13, pp. 3539–3547, 2012.

[81] J. R. Silva, B. Burger, C. M. C. Kühl, T. Candreva, M. B. P. Dos Anjos, and H. G. Rodrigues, “Wound Healing and Omega-6 Fatty Acids: From Inflammation to Repair,” *Mediators Inflamm.*, vol. 2018, p. 2503950, 2018.

[82] Fritsche, “The Science of Fatty Acids and Inflammation,” *Adv. Nutr. An Int. Rev. J.*, vol. 6, no. 3, pp. 293S-301S, 2015.

[83] C. Morisseau and B. D. Hammock, “Impact of Soluble Epoxide Hydrolase and Epoxyeicosanoids on Human Health,” *Annu. Rev. Pharmacol. Toxicol.*, vol. 53, no. 1, pp. 37–58, 2013.

[84] J. U. Scher and M. H. Pillinger, “The anti-inflammatory effects of prostaglandins.,” *J. Investig. Med.*, vol. 57, no. 6, pp. 703–708, Aug. 2009.

[85] G. Drouin, V. Rioux, and P. Legrand, “The n-3 docosapentaenoic acid (DPA): A new player in the n-3 long chain polyunsaturated fatty acid family,” *Biochimie*, vol. 159, pp. 36–48, 2019.

[86] N. Tatic, F. R. A. J. Rose, A. des Rieux, and L. J. White, “Stem cells from the dental apical papilla in extracellular matrix hydrogels mitigate inflammation of microglial cells,” *Sci. Rep.*, 2019.

[87] L. M. Sanders and S. H. Zeisel, “Choline: Dietary requirements and role in brain development,” *Nutr. Today*, vol. 42, no. 4, pp. 181–186, 2007.

[88] I. Kan, E. Melamed, D. Offen, and P. Green, “Docosahexaenoic acid and arachidonic acid are fundamental supplements for the induction of neuronal differentiation,” *J. Lipid Res.*, vol. 48, no. 3, pp. 513–517, 2007.

[89] M. Katakura, M. Hashimoto, T. Okui, H. M. Shahdat, K. Matsuzaki, and O. Shido, “Omega-3 polyunsaturated fatty acids enhance neuronal differentiation in cultured rat neural stem cells,” *Stem Cells Int.*, vol. 2013, 2013.

[90] S. P. Yun, J. M. Ryu, M. W. Jang, and H. J. Han, “Interaction of Profilin-1 and F-Actin via a b-Arrestin-1/JNK Mesenchymal Stem Cells Prostaglandin E2-Induced Human Signaling Pathway Involved in Migration and Proliferation,” *J. Cell. Physiol.*, vol. 226, no. 2, pp. 559–571, 2011.

[91] S. J. Park, S. B. Lee, D. S. Lee, Y. J. Ryu, G. Lee, and J. Cho, “Direct effect of chenodeoxycholic acid on differentiation of mouse embryonic stem cells cultured under feeder-free culture conditions,” *Biomed Res. Int.*, vol. 2013, 2013.

[92] N. Sakayori, M. Maekawa, K. Numayama-Tsuruta, T. Katura, T. Moriya, and N. Osumi, “Distinctive effects of arachidonic acid and docosahexaenoic acid on neural stem/progenitor cells,” *Genes to Cells*, vol. 16, no. 7, pp. 778–790, 2011.

[93] R. A. Soares, “Role of a Bile Acid in Improving Survival and Function of Neural Stem Cells,” no. November, pp. 1–10, 2015.

[94] T. Skripuletz, R. A. Linker, and M. Stangel, “The choline pathway as a strategy to promote central nervous system (CNS) remyelination,” *Neural Regen. Res.*, vol. 10, no. 9, pp. 1369–1370, 2015.

[95] D. Tukmachev *et al.*, “Injectable Extracellular Matrix Hydrogels as Scaffolds for Spinal Cord Injury Repair.,” *Tissue Eng. Part A*, vol. 22, no. 3–4, pp. 306–17, 2016.

[96] Z. B. Yagci, E. Esvap, H. A. Ozkara, K. O. Ulgen, and E. Ozkirimli, *Inflammatory response and its relation to sphingolipid metabolism proteins : Chaperones as potential indirect anti-inflammatory agents*, 1st ed., no. January 2018. Elsevier Inc., 2019.

[97] D. C. De Oliveira *et al.*, “Glutamine metabolism and its effects on immune response : molecular mechanism and gene expression,” *Nutrire*, pp. 1–10, 2016.

[98] A. K. Mehta, B. P. Singh, N. Arora, and S. N. Gaur, “Choline attenuates immune inflammation and suppresses oxidative stress in patients with asthma,” *Immunobiology*, vol. 215, no. 7, pp. 527–534, 2010.

[99] L. J. White *et al.*, “The impact of detergents on the tissue decellularization process: A ToF-SIMS study,” *Acta Biomater.*, 2017.

[100] M. Y. Noh *et al.*, “Mesenchymal Stem Cells Modulate the Functional Properties of Microglia via TGF-b Secretion,” *Stem Cells Transl. Med.*, vol. 5, pp. 1538–1549, 2016.

[101] L. Lin and L. Du, “The role of secreted factors in stem cells-mediated immune regulation,” *Cell. Immunol.*, vol. 326, no. February 2017, pp. 24–32, 2018.

[102] F. Saldanha-Araujo *et al.*, “Mesenchymal stromal cells up-regulate CD39 and increase adenosine production to suppress activated T-lymphocytes,” *Stem Cell Res.*, vol. 7, no. 1, pp. 66–74, 2011.

[103] J. M. Berg, J. L. Tymoczko, and L. Stryer, *Biochemistry*, 5th editio. New York: W H Freeman, 2002.

[104] P. Morell and R. H. Quarles, “Characteristic Composition of Myelin,” in *Basic Neurochemistry: Molecular, Cellular and Medical Aspects*, 6th editio., G. Siegel, B. Agranoff, and R. Albers, Eds. Philadelphia: Lippincott-Raven, 1999.

[105] J. S. Ungerstedt, M. Blombäck, and S. Sciences, “Nicotinamide is a potent inhibitor of proinflammatory cytokines,” vol. 6, pp. 48–52, 2003.

[106] Wishart Research Group University of Alberta, “Chenodeoxycholic acid (HMDB0000518)”

[107] A. Uccelli, L. Moretta, and V. Pistoia, “Immunoregulatory function of mesenchymal stem cells,” pp. 2566–2573, 2006.

[108] X. Chen, M. A. Armstrong, and G. Li, “Mesenchymal stem cells in immunoregulation,” *Immunol. Cell Biol.*, vol. 84, no. 5, pp. 413–421, 2006.

[109] P. De Berdt *et al.*, “Dental Apical Papilla as Therapy for Spinal Cord Injury.,” *J. Dent. Res.*, vol. 94, no. 11, pp. 1575–81, 2015.

[110] L. Germain *et al.*, “Fibrin hydrogels to deliver dental stem cells of the apical papilla for regenerative medicine,” *Regen. Med.*, vol. 10, no. 2, pp. 153–167, 2015.

[111] B. N. Brown *et al.*, “Surface characterization of extracellular matrix scaffolds,” *Biomaterials*, vol. 31, no. 3. pp. 428–437, 2010.

[112] V. K. Lai, C. R. Frey, A. M. Kerandi, S. P. Lake, R. T. Tranquillo, and V. H. Barocas, “Microstructural and Mechanical Differences Between Digested Collagen-Fibrin Co-Gels and Pure Collagen and Fibrin Gels,” *Acta Biomater.*, vol. 8, no. 11, pp. 4031–4042, 2012.